Doctoral Dissertation
Doctoral Program in Chemical Engineering (XXXVII Cycle)

Multimodal Therapies for Pancreatic Ductal Adenocarcinoma: Ultrasound-Stimulated Nanoconstructs based on Lipid-coated Zinc Oxide

Marzia CONTE

Supervisor:
Prof. Valentina Cauda

Politecnico di Torino, 2025

Declaration

I hereby declare that the contents and organisation of this dissertation constitute my own original work and does not compromise in any way the rights of third parties, including those relating to the security of personal data.

The chapters of this dissertation are based on research published in scientific journals and made available through open access:

- Chapter 1: **Conte, M**., Cauda, V., "*Multimodal Therapies against Pancreatic Ductal Adenocarcinoma: A Review on Synergistic Approaches toward Ultimate Nanomedicine Treatments*". Adv. Therap. 2022, 2200079. https://doi.org/10.1002/adtp.202200079.

- Chapter 2: **Conte, M**.; Carofiglio, M.; Rosso, G.; Cauda, V. "*Lipidic Formulations Inspired by COVID Vaccines as Smart Coatings to Enhance Nanoparticle-Based Cancer Therapy*". Nanomaterials 2023, 13, 2250. https://doi.org/10.3390/nano13152250.

- Chapter 3: **Conte, M.**, Carofiglio, M., Vander Pol, R., Wood, A., Hernandez, N., Joubert A., Caffey, C., Chua, C.Y.X., Grattoni, A., Cauda, V. "*Ultrasound-stimulated Zinc Oxide Nanoconstructs as a Pancreatic Cancer Treatment*". ACS Applied Materials & Interfaces, 2025. https://doi.org/10.1021/acsami.4c21975

Turin, February 2025

Marzia Conte

To my family.

Acknowledgment

This PhD dissertation encloses three very different stages of my journey as an aspiring researcher. Bringing them together triggers in me a profound sense of gratitude towards all the people that contributed to my academic and personal development.

First, I want to express my deepest appreciation to my supervisor, Prof. Valentina Cauda, for welcoming me into her lab and for giving me this huge opportunity that completely changed my life. She continuously inspired me with her enthusiasm for research and placed her faith in both me and my ideas, encouraging me to push beyond my limits while being the mentor I needed to regain focus and balance. Working in her dynamic laboratory has taught me that many people can have a huge impact on my life, even if their presence is only temporary. I am truly thankful to all the people that have been part of the TNHLab since my arrival, as well as to those that are its vibrant core today: Luisa, Marta, Bianca, Federica, Veronica, Sugata, Arianna, Nicolò, Giada, Maria Cristina, Giulia M., Giulia C., Alessandro, Giorgia, Giacomo, Elia, Alice.

I spent nearly half of my PhD on the other side of the world, and this experience proved to be one of the hardest and most rewarding periods of my life. I extend my deepest thanks to Prof. Alessandro Grattoni, for inviting me to join his lab, entrusting me with his projects and investing in my own work, and to Corrine Chua. Thanks to his team, Nikita, Simone, Nicola, Robin, Ashley, Anthony, Camden, Ilaria, Tommaso, Nikitha, Jaskirat and Jianhua (James), whose guidance greatly enriched my academic journey and who soon became like family to me, as well as all the visiting students who joined the lab over time: Lorenzo, Eleonora, Paci, Fabiana, Letizia, Martina, Noemi, Alessio, Francesco. I extend my deepest gratitude to the mentors I was fortunate to encounter there: Dr. Yongbin Liu, Dr. Joan E. Nichols and Dr. David Haviland, the scientist who introduced me to the world of flow cytometry and offered invaluable technical and personal support. Thank you Nate, my friend, for the gift of your friendship, wisdom and trust.

Finally, I am and will be forever thankful to the researcher that was my first mentor and kept being my rock despite distance and time zones. He supported every personal and scientific step of my journey and encouraged me to always push forward and find my voice. Marco, I hope to continue growing by your side.

Abstract

In the last decades, extensive research has been carried out on the understanding and treatment of pancreatic cancer. Pancreatic ductal adenocarcinoma (PDAC) is one of the deadliest tumors nowadays, destined to become the second main cause of cancer-related death worldwide by 2030. Its hallmarks are a hypoxic and "cold" tumor microenvironment (TMI) extremely challenging to penetrate and a high chemoresistance, therefore new treatment strategies are urgently needed. Despite the significant progress in medicine and nanotechnology, there is an increasing concern about the lack of a standardized therapy with favourable outcomes for patients affected by this malignant disease, whose survival rates are nowadays far alarmingly low.

Recent advances in nanomedicine have led to the introduction and subsequent establishment of nanoparticles in cancer treatment and diagnosis. Nonetheless, their application is still hindered by a series of challenges mainly related to their biocompatibility and biodistribution. The aim of this PhD thesis is to develop a multimodal and versatile nanoparticle-based therapeutic approach, here specifically applied to pancreatic cancer, able to overcome some of the limitations of conventional therapies.

Starting from an extensive overview on pancreatic cancer, its physiopathology and the state of the art with respect to multimodal therapies, the work here presented focuses on the implementation of a nanoconstruct consisting of a core of iron-doped zinc oxide nanoparticles and a tailored lipidic shell inspired by Covid-19 vaccines. After thorough physico-chemical characterizations and stability studies, the nanoconstructs in object are first tested on a human immortalized cell line of pancreatic cancer, to show the improved cytocompatibility with respect to pristine nanoparticles and the enhanced cell internalization in the presence of a targeting peptide covalently coupled to the lipidic shell.

Encouraged by the promising in vitro results, a combined therapy based on the administration of such nanoconstructs and their following stimulation with an ultrasound transducer is implemented on murine immortalized pancreatic cancer cells, and then a biodistribution study on mice bearing subcutaneous models of pancreatic cancer is conducted. To minimize systemic toxicity and maximize the presence of nanoparticles at the site of interest, intratumoral injection is selected as

the route of administration. After proving a good tumor retention of the nanoparticles and an adequate clearance from the main filtration organs with no sign of toxicity, an efficacy study consisting in the injection of the nanoparticles and the stimulation of the tumor mass with the ultrasound transducer is carried out. A flow cytometry study is performed to prove the immune infiltration caused by the combined therapy, and a survival study is conducted to assess the effectiveness of the combined therapy in prolonging animal survival.

The results here presented pave the way for the implementation of combined therapies featuring nanoparticles and ultrasound stimulation as an effective approach for treating PDAC.

Aim of the Thesis

The aim of this PhD Thesis is to propose the establishment of a novel therapeutic approach based on the remote activation of lipid-coated iron-doped zinc oxide nanoparticles by means of a safe per se ultrasound stimulation.

The dissertation is structured in three chapters focusing on key aspects of the research in object. The aim of the first chapter is to offer a comprehensive view of the pathophysiology of pancreatic cancer: first, a detailed overview on the tumor genesis, progression and resulting intricate microenvironment is presented. Thereafter, an extensive insight into the current treatments and their evolution throughout time, with a major focus on theranostic is proposed. A particular emphasis is given to innovative multimodal treatments involving the combination of different treatments in the context of nanoparticle-based therapies.

To pursue this specific aim, the second chapter is thus focused on the implementation of a lipidic formulation meant to be used as a smart coating of solid-state nanoparticles. The composition of this formulation is finely tuned to ensure efficient and stable shielding of the cargo, in this case iron-coated zinc oxide nanoparticles. The resulting shell is a highly customized tool that enables the possibility of further functionalizations with targeting agents, peptides, antibodies, and fluorescent moieties for future in vitro and in vivo tests and validations. The obtained nanoconstructs are tested in a human pancreatic cancer cell line and the results pave the way towards a potentially promising combined therapy based on the administration of well-tolerated nanoparticles and their successive activation with a remote stimulation.

In the third and final chapter, it is hypothesized that the combined effect of lipid-coated zinc oxide nanoparticles and a local ultrasound stimulation could elicit a tumor response thanks to the generation of radical oxygen species, leading to cancer cell death, and that this effect could be further enhanced by adding a molecular sonosensitizer. Physicochemical characterization of the nanoconstructs demonstrates reproducibility of their synthesis and improved stability obtained with the lipidic coating. In vitro assessment of the sonosensitizer-enhanced nanoconstructs in combination with ultrasound shows potent effects on the viability of a KPC murine PDAC cell line. The nanoconstruct is intratumorally administered in the subcutaneous murine model of PDAC to maximize local bioavailability and

obviate off-target effects of systemic delivery. Antitumor efficacy of the sonosensitizer-enhanced nanoconstructs is demonstrated, particularly in synergy with ultrasound stimulation: increased immune cell infiltration, cancer cell apoptosis and prolonged animal survival are achieved.

These findings support the potential of a synergistic interaction between lipid-coated sonosensitizer-loaded nanoparticles and ultrasound stimulation as an effective approach for treating PDAC.

Table of Contents

List of Figures

List of Tables

Chapter 1

Pancreatic cancer pathophysiology and state of the art of multimodal nanoparticle-based therapies

This first Chapter provides a comprehensive overview of pancreatic cancer pathophysiology and reviews the evolution of current treatment strategies, along with new theranostic approaches and multimodal therapies. It sets the stage for the development of innovative nanoparticle-based therapeutic strategies to address the urgent need for more effective treatments against pancreatic cancer.

1.1 Introduction

Pancreatic cancer (PC) is nowadays among the leading causes of cancer death in the world [1], with the prospect of surpassing breast, prostate and colorectal tumors and thus becoming the second main cause of cancer-related death worldwide by 2030 [2]. In particular, pancreatic ductal adenocarcinoma (PDAC) is the most common pancreatic cancer and represents about 90% of PC cases [3].

Its tumor microenvironment (TME) shows innate and acquired chemoresistance [4], due the presence of a dense tumor stroma, called desmoplasia, made up of many different cellular types [5] and minimal blood flow within the vessels that surround the tumor site [6]. This configuration therefore causes hypoxia and reduces the chances for drugs to reach and successfully treat the cancer [7]. As a direct consequence, chemoresistance and multidrug resistance (MDR) are the major

obstacles to PDAC treatment [8] and must be carefully addressed while designing new therapeutic approaches.

Due to the lack of visible symptoms at early stages, which lead to a very late recognition of the disease, PDAC is often diagnosed when already spread throughout the body and thus not always removable with surgical resection [9]. Nevertheless, surgery preceded and/or followed by systemic treatments remains the only option than can provide a realistic hope for patients [10–12], whose 5-year survival rate is reported to be less than 9% in the case of this malignancy [13]. Other traditional treatments include (I) chemotherapy, in the form of single-agent or multidrug administrations and delivered alone or in combination with other therapies (in this latter case it is called either adjuvant or neoadjuvant chemotherapy [14–16]), or proposed as second-line therapy and palliative treatment [17–19]; (II) radiotherapy and its declinations like chemoradiation [20–22]; (III) local ablative therapies (radiofrequency ablation, irreversible electroporation, stereotactic body radiation therapy and high intensity focused ultrasound amongst many others [23–25]); (IV) immunotherapy and cancer vaccines [26–28]. All these therapies are usually accompanied by severe adverse effects [29]; at late stages and in the presence of recurrence or metastases, curative treatments are typically replaced by palliative care [30] meant to improve patients' quality of life and relieve the pain.

The application of nanotechnology to the medical field, termed nanomedicine [31–33], is enabling novel treatments to enter preclinical and clinical trials, with the aim of overcoming the limitations shown by conventional therapies: to mention but a few, light and ultrasound-triggered minimally invasive techniques such as sonodynamic and photodynamic therapy have recently been applied to PDAC [34,35]. In addition to that, an ever-increasing knowledge of this particularly resistant tumor and its hallmarks has progressively led to the adoption of innovative and smart approaches: targeted therapies to avoid multidrug resistance and systemic toxicity [36,37], stromal therapies aimed at a TME and vessel normalization [38–41], the use of exosomes as nanocarriers for gene therapy [42–44]. Recent advances in nanotechnology are also allowing researchers to develop new platforms, namely nanoparticles, meant to improve drug delivery in the TME surrounding pancreatic cancer cells, while enhancing drug selectivity, providing bigger therapeutic windows, reducing side effects and enabling real time tracking abilities [45].

Indeed, a major contribution is now offered by nanoparticle-based theranostics, a promising area of research that focuses on the manipulation and tuning of surface and bulk properties of some materials that can be synthesized at the nanoscale in

order to create multimodal platforms able to address, diagnose and treat tumors [46–48]. The past thirty years have witnessed increasingly rapid advances in the application of nanomedicine and specifically nanoparticles to pancreatic cancer treatment, and a considerable literature has grown up around this topic [37,49]. The aim of this chapter is to summarize the latest nanomedicine findings concerning PDAC treatment, starting with a thorough preliminary dissertation meant to depict and investigate the plethora of factors influencing tumor pathogenesis and biology, and those contributing to its poor response to current therapies. Afterwards, the main alternatives offered by nanomedicine to overcome some of the limitations related to conventional PDAC treatments are presented, with a special focus on novel multimodal approaches and innovative preclinical models benefiting from the latest nanotechnological advances. Finally, potential concrete and evidence-based future outlooks are proposed, in the light of what has been produced so far and of the ever-evolving nature of bionanotechnology.

1.2 Pancreatic cancer diagnosis

Pancreatic ductal adenocarcinoma (PDAC) is an exocrine cancer that starts mostly (75%) in the head of the organ, from the epithelium of the pancreatic ducts. It takes more than a decade to metastasize, but early stages are largely asymptomatic and thus difficult to be diagnosed [50]. Moreover, current recommended diagnostics [51] such as computed tomography (CT) and magnetic resonance imaging (MRI), together with other more accurate techniques like abdominal and endoscopic ultrasound are costly and invasive, and thus are not used as screening tests on patients who do not show a genetic predisposition [52].

The lack of early symptoms is one of the main challenges related to this type of cancer, and researchers are nowadays focusing on the identification of at-risk populations to better target screenings and prevention measures [30]. In addition, selection and recall bias are very common drawbacks of the studies which have led to the identification of some of the well-established risk factors among the selected patients, such as age [53], sex [54], diabetes mellitus [55], smoking [56], obesity [57], hereditary and recent pancreatitis [58], hereditary pancreatic cancer [59].

1.3 Molecular pathology

There is an urgent need to better understand the molecular pathology of pancreatic cancer, and a 2016 comprehensive integrated genomic analysis of 456 bulk tumor tissues of PDACs detected 32 significantly mutated genes, aggregated

into 10 molecular mechanisms: *KRAS, TGF-β, WNT, NOTCH, ROBO/SLIT* signaling, *G1/S* transition, *SWI-SNF*, chromatin modification, DNA repair and RNA processing.

Expression analyses resolved 4 PC subtypes: squamous, pancreatic progenitor, immunogenic and aberrantly differentiated endocrine exocrine (ADEX), each one associated with specific histological characteristics [60]. These mutations are the drivers of the decline from normal mucosa to invasive malignancy, and thus have been thoroughly analyzed to better understand PDAC pathogenesis from pre-existing non-invasive neoplasia [61]. The most frequent genetic abnormalities are mutational activation of the KRAS oncogene, which in turn engages various downstream effectors [62], inactivation of tumor-suppressor genes including CDKN2A [63], TP53 [64], SMAD4 [65] and BRCA2 [66], telomere shortening [67]. Epigenetic dysregulations such as alterations in DNA methylation and histone modifications, as well as non-coding RNAs were proved to alter gene function in pancreatic cancer [68], and changes in microRNA expression seem to contribute to cancer development [69] and are hence addressed as diagnostic markers for PC detection. [70]

1.4 Precursor lesions

PDAC is thought to develop from precursor lesions, namely pancreatic intraepithelial neoplasia, intraductal papillary mucinous neoplasm and pancreatic mucinous cystic neoplasm, whose early detection could reduce both the incidence of pancreatic cancer and the mortality rate of patients [71].

Pancreatic intraepithelial neoplasia (PanIN) is the most common lesion in elderly population, and it represents a promising target for early detection, since it is usually benign and subjected to predictable morphological changes. It is classified into three grades, PanIN-1, PanIN-2 and PanIN-3, and its detected distinctive genetic changes were shown to occur in a certain order during the lesion grade progression from PanIN-1 to PanIN-3. In fact, KRAS2 mutation and telomere shortening seem to appear first, then the inactivation of p16/CDKN2A takes place and in PanIN-3 lesions the inactivation of TP53 and MAD4/DPC4 is typically detected. An insight of the order of genetic alterations might be useful in developing early gene-based screening tests, as well as in creating more accurate genetically engineered mouse models [72].

Intraductal papillary mucinous neoplasm (IPMN) is a visible mucin-producing neoplasm that develops in the main pancreatic duct or branches and can take years to progress into invasive cancer. There are many similarities but also some

significant differences in the genetic characteristics of IPMN with respect to PDAC, like a lower prevalence of KRAS2 gene mutations. Most patients are cured with surgical resection, and during the hunt for invasive carcinoma in the course of the histological examination it is easy to misdiagnose PDAC from IPMN. [73]

Pancreatic mucinous cystic neoplasm (MCN) is a relatively rare lesion, larger in size compared to PanINs, usually slow growing and non-invasive, with an excellent prognosis and no communication with the main pancreatic ductal system. KRAS mutations are believed to be the main drivers of genetic alterations occurring in low grade MCNs, while alterations in p53 tumor suppressor gene take usually place in invasive MCNs. [74]

Although some of these mechanisms have been well established, the main issue remains the clinical detection of precursor lesions before their degeneration into PDAC, because even modern high-resolution imaging methods lack of the resolution and sensitivity required to detect PanINs smaller than 5 mm and to decipher the diagnostic differentiation of lesions such as IPMN and MCN [75].

1.5 Tumor microenvironment and desmoplasia

The tumor microenvironment (TME) is a pivotal regulator of drug resistance, cancer survival and malignant transformation, and thus it represents a potential target for new therapies against PDAC. In this niche microenvironment, tumor progression is maintained through desmoplasia, namely a fibrous and connective tissue growth in which continuous paracrine signals are exchanged between cells [76], which was recently found to have both tumor promoting and tumor restraining roles in PDAC [77]. Distinctive features of the pancreatic TME are (I) the presence of a dense stroma, which makes up to 90% of the tumor bulk and is characterized by lack of vascularization, intensive fibrosis and poor immune infiltration [78]; (II) the poor perfused vessels which cause hypoxia and prevent drugs from reaching the tumor site [79]; (III) the altered extra cellular matrix (ECM) [80], whose excessive deposition provides solid structural foundation and is responsible for the generation of various chemical signals which regulate tumor progression and desmoplasia [81] and (IV) the continuous molecular crosstalk that takes place between pancreatic cancer cells and pancreatic stellate cells [82]. The altered ECM consists of many non-cellular and cellular components. As regards to non-cellular ones, hyaluronic acid (HA) is excessively produced and deposited [83] and it negatively impacts the vascular compartment of the tumor, by enhancing the interstitial fluid pressure (IFP) and thus compressing blood vessels and hindering drug delivery in the TME [84]; collagen increases solid stress rather than IFP [85] and especially type V was

shown to affect tumor angiogenesis [86]; chemokines, such as CXCL8 and CXCL12 and their corresponding receptors, cooperate to promote angiogenesis and microvessel formation [87,88]; fibronectin is secreted by stellate cells and it has an important role in cell adhesion, migration and differentiation [81].

1.6 Cells in the TME

As regards to cellular constituents, pancreatic stellate cells (PSCs) and cancer-associated fibroblasts (CAFs) are the major components of the TME.

1.6.1 Pancreatic Stellate Cells

Pancreatic stellate cells (PSCs) are activated from their quiescent state by cytokines like interleukins, tumor necrosis factor- α (TNF-α) and growth factors secreted by damaged and tumor cells as a consequence of inflammation [89]. Their transformation into an activated phenotype is assessed by several parameters, such as the loss of vitamin A, proliferation, cytokine release and the synthesis of ECM proteins, and their presence in stromal areas has been proved and pointed out as the main source of stromal collagen [90]. PSCs are believed to closely interact with cancer cells as well as with other stromal cell types such as endothelial and immune cells.

The interaction between PDAC tumor cells and pancreatic stellate cells provokes increased tumor growth and metastases [91], by creating a supporting niche for the tumor cells and by promoting the endothelial-mesenchymal transition (EMT), a developmental process that leads cells to assume an aggressive mesenchymal phenotype with migratory capacity, invasiveness, elevated resistance to apoptosis and increased ECM components production [92]. The loss of epithelial cell markers such as E-cadherin and the increased expression of mesenchymal markers such as vimentin are some of the hallmarks of EMT [93], and this process was proved to contribute to chemoresistance in pancreatic cancer [4] and to be linked with the activation of the Notch signaling pathway [94].

PSCs has also been proved to interact with endothelial cells, inducing proliferation and tube formation of human microvascular endothelial cells, possibly via vascular endothelial growth factor (VEGF) mediation [95]. The process of immune evasion by cancer cells in PDAC is believed to be supported by PSCs, which act a $CD8^+$ T cells sequestration in stromal areas thanks to the PSC-derived chemokine CXCL12, thus reducing their anti-tumor effects [96]. Moreover, various other interplays occur between PSCs and mast cells, whose effect is an increase in

cell proliferation [97], and between PSCs and myeloid derived suppressor cells (MDSCs), whose migration into the tumor suppress immune cell function [98]. Finally, as previously pointed out, PSCs play a fundamental role in hindering drug delivery in the tumor area by producing the thick stroma surrounding cancer cells.

1.6.2 Cancer-Associated Fibroblasts

Cancer-Associated Fibroblasts (CAFs) are a heterogeneous cellular population that can originate from resident fibroblasts, bone marrow derived cells and stellate cells [99]. They lack specific cell surface markers and are therefore mostly identified by their elongated morphology or tissue position [100], they can assume both a tumor supportive or suppressive role, according to the stage of tumorigenesis and many other context-dependent factors [101], and they are responsible for an active remodeling of the desmoplastic stroma through various paracrine mechanisms, while being highly chemotherapy resistant [102] and showing a unique heterogeneity of subpopulations in PDAC. In fact, recent studies identified at first two subtypes of CAFs. One type, called myCAF and located primarily adjacent to cancer cells, expresses high levels of α -smooth muscle actin (α-SMA) and possesses a tumor-suppressing role; the second type, named iCAFs, is located farther from the cancer cells and is believed to exhibit a tumor-promoting behaviour [103].

A later in vivo study identified a third subtype called antigen-presenting (apCAFs), with immune-modulatory capacity that might contribute to the inhibition of optimal T cell response [104,105].

1.6.3 Pancreatic Stem Cells

Pancreatic stem cells are self-renewing, immortal cells derived from the bone marrow which inhabit a hypoxic niche composed of different cells such as endothelial cells, immune cells and cytokines . Their proliferation is increased by the hypoxic environment of the tumor site [107] and influenced by inflammatory cytokines such as interleukins. They show intrinsic chemoresistance, since they are highly resistant to a typically used first-line treatment drug, namely gemcitabine [108], and have been proved to increase their proliferation in the presence of this chemotherapeutic agent [109]. For this reason, many studies have focused on addressing them by other means, like targeting either some signaling pathways such as the Hedgehog (Hh) pathway [110,111] or surface markers which are typically exposed by these cells [112] through treatments with kinase inhibitors, antibodies [113], antibiotics and immunotherapy [7,114].

1.6.4 Other cell types

Other important cell types of the pancreatic cancer TME are (I) T-lymphocytes, which inhabit the site of invasion and the lymphatic system of the tumor and synthesize cytokine interleukins [115] (whose effect is in turn the activation of inflammatory response, proliferation and metastasis); (II) B-lymphocytes, associated with an invasive front of tumors and expressed in lymphoid structures near the TME [116]; (III) tumor-associated macrophages (TAMs), that secrete chemokines and cytokines triggering immune cell recruitment, whose communication with the TME favours the progression of PC [117]; (IV) suppressor cells of myeloid lineage (MDSCs) [118], that downregulate cytotoxic T-lymphocyte activation; (V) dendritic cells (DC), which lose their capacity of processing and presenting antigens in PC [114]; (VI) tumor-associated neutrophils, involved in premetastatic stages pf PC [119]; (VII) vascular endothelial cells and pericytes, activated by growth factors of TME [120,121]; (VIII) natural killer (NK) cells, which are however largely excluded from the tumor tissue and hence mostly present in peripheral blood, but nevertheless support immune evasion mechanisms and contribute to the production of immunoregulatory IL-10 cytokines [122]. **Figure 1** reports a schematization of PDAC TME, which includes all the previously mentioned cell types contributing to its desmoplasia.

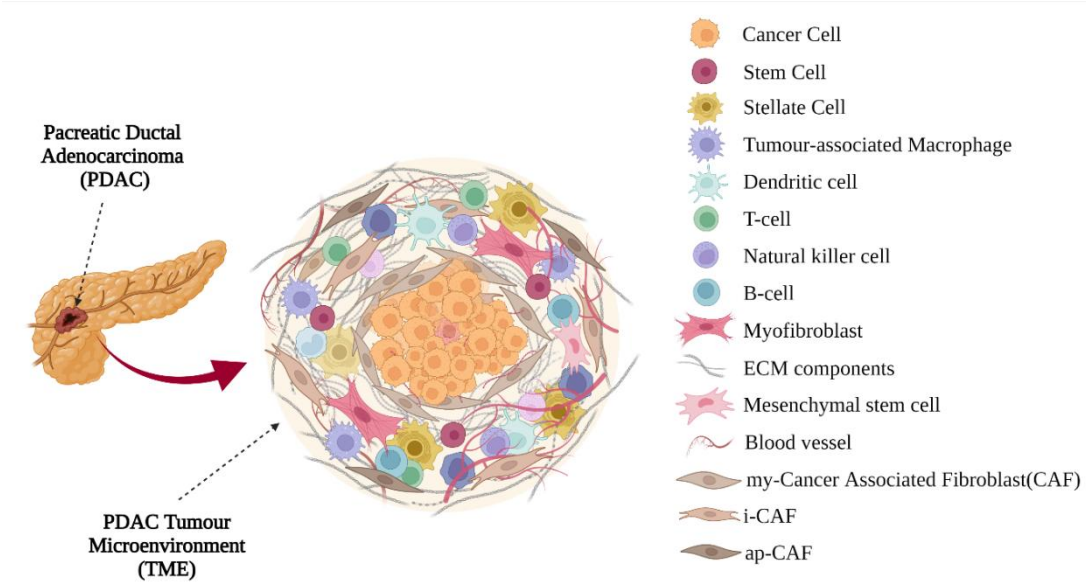

Figure 1. Scheme of the plethora of cells taking part to PDAC TME. Created with Biorender.com

1.7 Molecular markers

Some potential molecular markers have been identified to diagnose and treat PC, and they can be classified into three main classes, based on their biological source: serum markers, tumor markers and cancer stem cell markers. Serum markers like cancer antigen 19.9 (CA19.9) [123], interleukins 6, 8 and 10 (IL-6, IL-8 and IL-10) [124], survivin [125], mesothelin [126] and carcinoembryonic antigen (CEA) are expressed on the surface of PC tumor cells and therefore can be useful for early detection and specific targeting, with the employment of human monoclonal antibodies (mAbs) [127], peptide vaccines [128] or antibody-drug conjugates [129].

Tumor markers include, amongst the others: secreted protein acidic and rich in cysteine (SPARC) [130], which is used to target drugs thanks to its high affinity to albumin; hyaluronic acid [131], abundant in the TME and associated with PDAC pathogenesis, blood vessel collapse and EMT [132], whose depletion proved to improve the tumor condition [133]; mucins, which have a central role in immunosuppression and metastasis [134], can be used to distinguish between PDAC and its precursor lesions [135] and can be targeted by MUC tumor-specific antibodies [136].

Cancer stem cells usually expose several surface markers, which have been proved to be related to stemness and gemcitabine resistance in PC stem cells [137]; for example, CD44 expression is associated with poor prognosis [138], high grade of cancer, radiation therapy resistance and metastasis [139], and it is often exploited for targeted drug delivery as well as for tumor visualization [140].

Other typical markers expressed by PC stem cells are CD133, whose expression is associated with metastasis [141] and whose activity results in a triggering of downstream regulatory signals for stemness properties and EMT [142]; CD24, overexpressed in high-grade PC tumors [143] and advanced PC stages [144]; CXCR4, which promotes cancer development, invasion and metastasis and might be indirectly activated by the hypoxic tumor microenvironment of PC through the expression of CXCL12 by fibroblasts [145,146]; ESA (epithelial cell adhesion molecule, EpCAM), related to shorter survival of patients with advanced pancreatic cancer and overexpressed in PC [147]; Oct4, whose knockdown in a 2013 study by Lu et al. resulted in reduced proliferation, chemoresistance and tumorigenesis in vitro and in vivo [148]. The co-expression of many of these markers has been thoroughly studied over the years, highlighting the considerable complexity of the general framework of pancreatic cancer stem cells markers and of the involved altered molecular pathways [149].

1.8 Signaling pathways

Mutations in the survival pathways involved in PDAC promote tumor progression and resistance against chemotherapeutic drugs. The continuous crosstalk amongst these pathways leads to the formation of interlinked signaling networks [8], whose effect is the increase of tumor aggressiveness.

The Notch signaling pathway is only one of the many implicated in the progression of PDAC and in its distinctive chemoresistance [150]. It has been recently found to contribute to EMT [151] since its activation in endothelial cells results in their mesenchymal transformation: in fact, Notch controls the expression of Snail homologous, implicated in the EMT acquisition [152], and a knockdown of Notch-2, one of its four receptors, in gemcitabine-resistant PC cells resulted in EMT inhibition [153].

KRAS mutation induces the over secretion of transforming growth factor-β and interleukin IL-10 and stimulates various downstream cascades [154]; overexpression of epidermal growth factor receptor (EGFR) and its downstream pathways can result in drug resistance; Hh pathway modulates the stromal environment and is essential for the development of the ECM and the vasculature [155], and its inhibition was proved to have a pro-angiogenic role and thus a positive effect on the delivery of drugs to the tumor site [156]. Signal transducer and activator of transcription 3 (STAT3), a cytoplasmatic transcription factor, is involved in many crucial pathways for tumorigenesis and can be activated by many oncogenes and protooncogenes; it is regulated by cytokines, epidermal and platelet-derived growth factors and contributes to chemoresistance [157]. Phospho-STAT3 (pSTAT3), a risk factor for pancreatic adenocarcinoma prognosis, is abnormally expressed in this type of cancer and related to tumor size [158]; moreover, it may promote tumor angiogenesis via up-regulating the VEGF [159]. Ephrin receptors form the largest known subfamily of receptor tyrosine kinases (RTKs), and together with their ligands they compose an extensive communication system which is involved in many cellular processes along with cancer development and progression. Eph (erythropoietin-producing human hepatocellular) signaling is bidirectional, since ligands are attached to a membrane and can provoke a forward or a reverse response when they bind to receptors, and it is responsible for tumor promotion and suppression according to mechanisms which have not been clarified yet [160]. There are two subfamilies of Eph receptors, EphA and EphB, and in the last decades many studies have correlated their expression in cancers with increased malignancy and poor clinical prognosis; moreover, they appear to be involved in crosstalks with

other signaling networks (Akt, MEK/ERK/RSK, STAT3) and in feedback loops which contribute to the entangled signaling networks featuring in the tumor microenvironment [161]. With regard to pancreatic cancer, EphA2 overexpression has been correlated with increased invasiveness and metastatic abilities for a long time now [162], and highlighted as a possible target for therapies [163]. More recently, EphA2 fragments detected in plasma have been proposed as a possible novel PC biomarker [164], and gemcitabine conjugation with an EphA2 targeting agent has provided encouraging evidence of improved clinical outcomes in xenograft models of pancreatic cancer [165], reinforcing the idea of using Eph receptors as therapeutic targets in PC, lately pursued in a study by Salem et al. [166].

1.9 Tumor vasculature and hypoxia

Angiogenesis plays an important role in tumor development and progression, and in metastasis spreading as well [167]. PDAC vasculature is characterized by high microvascular density and very poorly perfused vessels, which do not allow drugs to reach and treat the tumor site. Moreover, they help tumor growth through mechanisms such as vessel co-option [168], vasculogenic mimicry [169] and vasculogenesis [170]. Pancreatic cancer angiogenesis is activated by genetic and epigenetic alterations, and by the cells and the stromal components of the TME. Moreover, PDAC desmoplasia leads to high IFP, which in turn causes the vasculature collapse and therefore a low drug penetration and uptake [171], that contributes to cancer resistance to targeting therapies.

Microvessel density (MVD) measurements in pancreatic cancers with respect to normal tissues suggested the existence of an active angiogenic process in the central tumor [172], while other evidences [6] highlighted the presence of hypovascular tumor stroma and hypervascular normal pancreas tissue, suggesting the existence of a vast heterogeneity of vascular distribution within PDAC. According to Hexige et al. the presence of basal microvilli, hairy-like microvasculature detected in aggressive and metastatic PDAC, could be exploited as a promising therapeutic target for treatment since they are correlated with high glucose uptake in pathological conditions [173].

The role of pericytes was thoroughly studied and reviewed due to their effect in maintaining impaired microvessel integrity [174], and their poor presence in tumor vessels was highlighted in different studies [175]. For example, Gilles et al. proved that an increase of pericyte coverage resulted in enhanced tumor perfusion and reduced hypoxic area in PDAC [176].

Overall, these studies agreed on the importance of a normalization of the tumor vasculature as a potentially effective therapeutic approach, to both relieve hypoxia and enhance drug delivery [177].

1.10 Mouse models

Over the course of the last decades, several experimental mouse models have been generated in order to faithfully reproduce and thus better understand PDAC tumor. The currently available mouse models of pancreatic cancer include cancer cell line-based heterotopic and orthotopic xenograft in immunocompromised mice, patient-derived xenografts, transgenic mice (genetically engineered mouse models, GEMMs) and organoid models. They are generally classified according to the manner or tumor induction, the site of tumor implantation and the histopathological characteristics [178].

The first experiments with spontaneous tumor animal models involved the use of a chemical viral induction, or the application of experimental genetic techniques in rats [179] and hamsters [180]. More recent attention has focused on the introduction of oncogenes (especially mutant KRAS genes) into mouse embryonic or somatic cells using transgenic, gene knock-in and gene knock-out techniques to transfer specific genes into mice via retrovirus. Exploiting this technique, Hingorani and co-workers created the first prenatal GEMM (called KC) that developed the full spectrum of PanIN lesions, which progressed towards PDAC with age [181], and observed that some of these mice developed metastatic tumors after a long latency. Since this model developed PanINs shortly after birth and therefore showed a different PDAC etiology from human patients, a second generation of GEMMs was established by Guerra and colleagues [182]. These postnatal models allowed temporal control of Kras activation in the pancreas, but they proved that mature acinar cells were resistant to transformation by oncogenic Kras. Nevertheless, in the presence of pancreatitis-induced inflammation, the progression in PanINs and PDACs with high penetrance was observed. Later on, tissue damage and proliferation of acinar cells were proved to be an effect of inflammation [183,184] and the mechanism of inhibition of oncogene-mediated senescence [185] in high-grade PanIN-2/3s and in low-grade ones in the presence of acute or chronic pancreatitis was suggested among other inflammatory pathway activations (such as STAT3/Socs3) as a possible cause for PDAC development [186]. Based on these results, many other mouse models combining Kras mutations with other common genetic alterations such as CDKN2A (INK4A/ARF), TP53 and SMAD4, were implemented to induce PDAC [187].

A notable example derived from the KC strain is the KPC mouse model, developed by Hingorani's team, which expresses a mutated form of TP53 and better mimicked the PDAC TME from a pathological and immunological point of view [188]. In fact, this mouse model (I) retraced the progression, metastasis and stromal complexities of the tumors; (II) offered a very fast PDAC progression (20-24 weeks); (III) exhibited high penetrance and gemcitabine resistance [156,189]; (IV) developed a dense desmoplasia and poor vasculature, closely mimicking the dynamics of TME; (V) provided samples of tissues, serum and tumor cell lines exploitable in further researches; (VI) was used to develop gene specific knockout (KO) models, suitable to study the effect of certain genes on the pathogenesis; (VII) produced an intact immune system, hence allowing the study of immune response in PDAC; (VIII) offered autochthonous tumors. Therefore, the application of KPC mouse models considerably boosted the understanding of biomarker development [188,190–192], the role of tumor stroma [132,189,193,194] and signaling pathways [195–202,156] concerning PDAC. Moreover, they were exploited for preclinical applications of chemotherapy [189], targeted therapies [132,193] and immunotherapy [203–207]. Experimental murine models have also been thoroughly used to study the impact of risk factors for PDAC, such as family history [208], pancreatitis [209], smoking [56,210,211], alcohol [212] and diabetes [213], and the evolution of precursor lesions [190–192]. The exploitation of these and many other GEMMs, which have been thoroughly described in dedicated reviews [187,214,215], is however accompanied by several limitations, such as (I) variability in tumor initiation, progression and metastasis incidence; (II) labor intensive and time-consuming breeding of mice colonies; (III) fewer mutations and less genetic complexity with respect to humans; (IV) the need of crossing three or more lines of mice.

Xenografts derived from human pancreatic cancer cell lines, implanted subcutaneously or orthotopically in athymic and therefore immunodeficient mice, have been extensively used to evaluate and optimize therapeutic approaches, especially targeted therapies. For this purpose, cell lines have been the preferred choice for a long time due to their defined growth kinetics, their easy maintenance at specific culture conditions, their reproducible behaviour and a solid literature background. Common drawbacks to cell derived xenografts (CDXs) are the absence of the immune system influence, the lack of genetic and phenotypic heterogeneity offered by immortalized cell lines, the absence of tumor stroma, the risk of alterations during in vitro passages, the infrequent metastasis formation. Part of these limitations have been addressed by co-implantation models using CAFs, and more recently by patient-derived xenografts (PDXs), namely fragments of primary tumors derived from surgical resection [216] and implanted subcutaneously (SC),

orthotopically (OT) or under the renal capsule (SRC) [187,178] in mice. The main advantages of this model are the retention of the morphological characteristics of the parental tumor, the preserved metastatic potential and the genomic/architectural stability of the obtained xenografts, which make them able to respond to therapy as the original tumor [193]. Conversely, critical issues are mainly related to the long growing time, the infiltration of murine stroma after implantation [217], the absence of host immune system influence and the propagation of aggressive phenotypes in mouse models [218].

Many alternative approaches have been suggested and carried out, like (I) the co-implementation of stromal cells derived from patients, (II) the use of syngeneic/allograft mouse models, consisting of tumor tissues derived from the same genetic strain of mice which do not elicit an immune reaction and therefore allow the use of immunocompetent animals [219], (III) the production of humanized mice able to develop human immune system; their application was hence mainly focused on immunotherapy studies [220,221].

Overall, the absence of a golden standard able to perfectly mimic PDAC, its microenvironment and the immune system has led to some discrepancies between therapeutical results obtained in mouse models and the actual response in clinical trials [222,202]. Nevertheless, all these mouse models are still an essential step in preclinical studies and have contributed to considerable advance in the understanding of PDAC progression, metastasis, stromal heterogeneity and response to therapies, continuously evolving thanks to emerging knowledge.

1.11 Current treatments and guidelines

Currently, the standard therapeutical approach to PDAC is surgery followed by adjuvant multi-agent chemotherapy in case of resectable tumors [223,21], with a recorded median survival of up to 26 months. On the other hand, borderline resectable tumors are generally pre-treated with a neoadjuvant therapy before surgery, to allow tumor shrinkage and a better resection outcome [15]. Surgical resection is the only hope for long term survival, however most of the times diagnosis is given when the disease is already unresectable or metastatic. Nevertheless, advances in surgical techniques and systemic chemotherapy have enabled, after the application of neoadjuvant protocols, the extension of resection to locally advanced tumors [12] (not so long ago generally excluded from surgical options [224]) along with borderline resectable ones. As far as metastatic tumors are concerned, systemic palliative chemotherapy is usually offered as first-line treatment and combinational therapies are nowadays producing promising results

in prolonging the median survival of patients. Most pancreatic cancers progress after first-line palliative chemotherapy, leading to the need of a second-line one [225]. This second-cycle chemotherapy must be carefully chosen depending on the first administered therapy, but promising results are today evidence-based. In 2015, ESMO (European Society for Medical Oncology) Clinical Practice Guidelines collected an overview of therapy recommendations, including the application of clinical trials to borderline resectable tumors [226].

A 2018 extensive review concerning therapeutical developments in pancreatic cancer reported that targeted therapies and antiangiogenic drugs generally failed due to the hypovascular nature of the stroma surrounding cancer cells. In addition to that, the authors did not highlight any breakthrough in immunotherapy applied to PDAC, but concluded that the application of recent understanding regarding its complex molecular mechanisms and the TME could be the key to future clinical improvements and success [15]. NCCN (National Comprehensive Cancer Network) Clinical Practice Guidelines in Oncology, published in 2021, reported an update of recommendations for diagnosis, evaluation, treatment and follow-up for patients with pancreatic cancer [227]. **Figure 2** presents a summarizing and simplified scheme based on the main points highlighted by this guideline, merged with information extracted from other aforementioned sources [226,15].

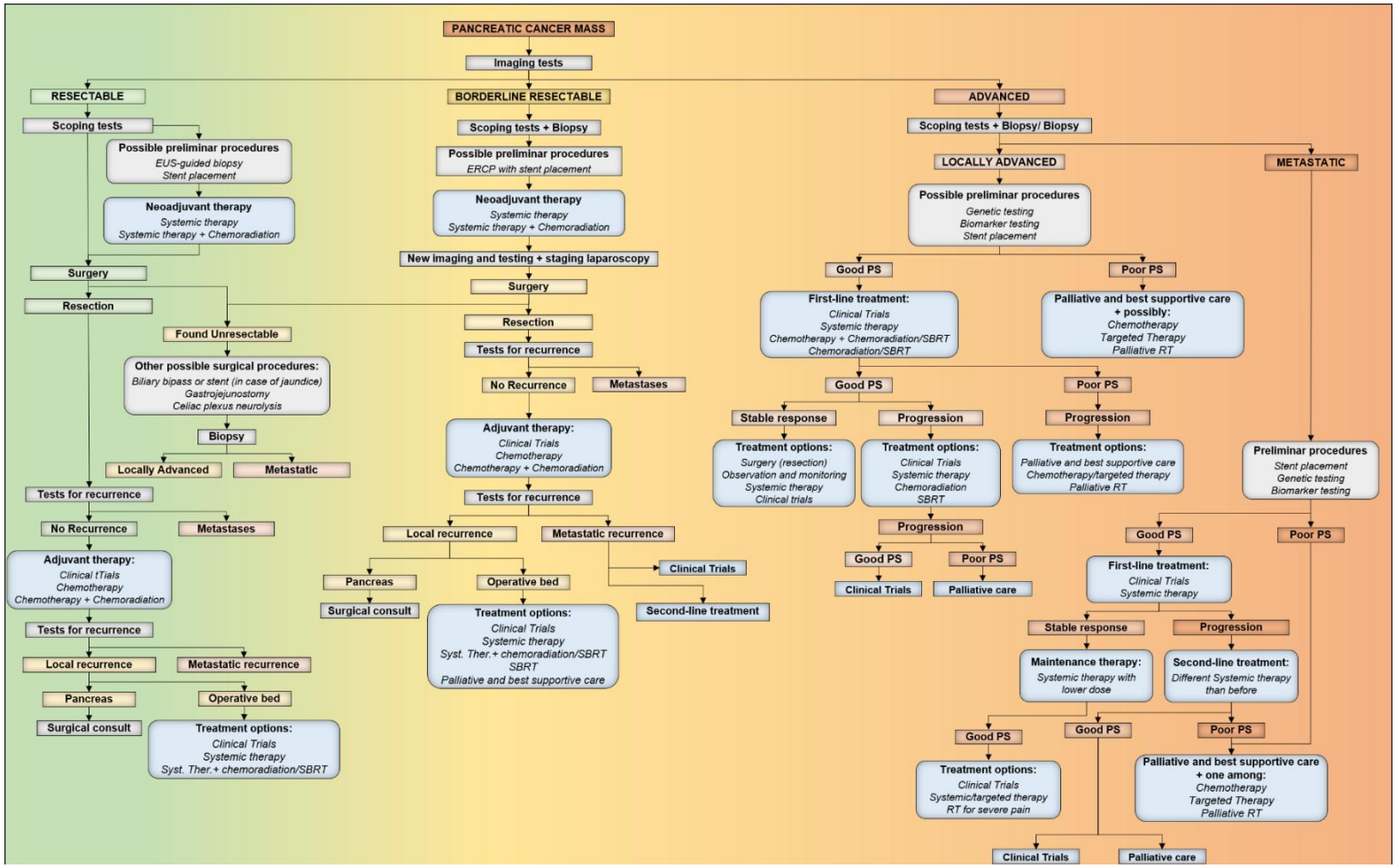

Figure 2. Schematic representation of current recommendations for diagnosis, treatment and follow up of patients affected by PDAC, depending on the stage of the tumor

1.11.1 Surgery

PDAC usually takes more than a decade to metastasize, however early stages and precancerous lesions are largely asymptomatic. Consequently, they are difficult to be diagnosed in time for surgery to represent the main route to avoid further spreading of the disease into nearby organs. The tumour stages are generally referred according to the American Joint Committee on Cancer (AJCC) "TNM" classification, namely tumour size (T), spread to nearby lymph nodes (N) and metastasis to distant sites (M). The standard stage classification includes resectable, borderline resectable (BR) and/or locally advanced (LA) unresectable and metastatic tumour, while the Eastern cooperative oncology group (ECOG) defined a score indicating performance status (PS), which varies from 0 to 5 [228]. Other important prognostic factors are tumour grade (G), which describes the tumour likeliness to normal tissue under a microscope, and extent of resection (R), that indicates whether or not all the tumour is removed after surgery and ranges from R0 (the desirable outcome of any surgical resection) to R2 (visible tumour not removed) [229].

For patients eligible for surgery, some options are available depending on their overall status, extension of the tumour and venous involvement: pancreaticoduodenectomy, distal pancreatectomy, total pancreatectomy or palliative surgery [12,230]. Complete resection (R0) followed by adjuvant therapy still represents the course of action with best results over time. In this regard, some recent systematic reviews and meta-analyses argued that the achievement of a radical resection could effectively change the outcome in patients with clinical N0 disease (no lymph nodes involved) by prolonging their overall survival (OS) [231,232]. Moreover, these studies linked some specific initial recurrence patterns and clinicopathological factors or surgery outcomes such as R1 resection to recurrence locations, proposing strict post-surgery follow-ups to monitor patients and promptly start systemic chemotherapy [233]. Altogether, it has conclusively been shown that, although undisputed progress in terms of surgical techniques has been made over the last 20 years [12], systemic recurrence within 2 years from surgery is nonetheless as prominent today [234,235] as it had been previously reported [236,237].

1.11.2 Chemotherapy evolution over time

Over the years, only few but pivotal improvements have been made in terms of new clinically approved chemotherapeutic drugs for PDAC, and here a brief summary of their history is reported. The first anticancer drug used for PDAC treatment was 5-fluorouracil (5-FU), which had been first introduced in 1957 and

already applied to tumours such as breast and colorectal cancers [238]. It is an S-phase specific uracil analogue whose accumulation in cells results in increased cytotoxicity, eventually leading to cell death. In fact, once inside the cell, it is converted to several active metabolites which disrupt RNA synthesis and the action of the nucleotide synthetic enzyme thymidylate synthase (TS). Its main drawback is the low stability due to the presence of an enzyme called dihydropyrimidine dehydrogenase (DPD), abundantly expressed in the liver, and therefore in the last 20 years important modulation strategies have been developed in order to increase its anticancer activity and decrease its degradation [239]. Another critical aspect that has been increasingly considered is 5-FU emerging resistance in PC [240]; a recent systematic literature review thoroughly discussed its mechanisms and proposed some novel approaches to overcome chemoresistance such as combination of 5-FU with other therapeutics, DNA repair pathways targeting, nano-formulated drug delivery, novel MDR modulators [241].

Gemcitabine (Gem) is a prodrug which undergoes phospho-activation after cell uptake via nucleoside transporters; the derived active drug metabolites inhibit DNA synthesis [242]. Since 1997 it has been proposed as first-line therapy over 5-FU against pancreatic cancer, due to the undeniable improvements in terms of median overall survival rate and one-year survival rate [243]. Unfortunately, despite the initial sensitivity of PDAC to gemcitabine, drug resistance occurs within several weeks of treatment [244] and metabolic clearance of gemcitabine was observed in vitro in the PDA cell line Panc-1 [245], due to the macrophage induced cytidine deaminase (CDA) upregulation, whose effect is gemcitabine inactivation and excretion out of the cells.

Whilst multiple different agents have been proposed over the years in combination with gemcitabine, none of them has ever shown signs of significant survival advantages, although some studies suggested some potential benefits on patients with good performance status (PS).

CO-101, a lipid-drug conjugate of gemcitabine, was developed to overcome cancer Gem resistance by entering cells independently of human equilibrative nucleoside transporter-1 (hHENT1), but the results of a randomized study carried out in 2013 showed that CO-101 was not superior to gemcitabine in patients with metastatic PDAC [246].

Gemcitabine was hence combined with capecitabine, another nucleoside analogue with which a synergistic antitumour activity had been previously demonstrated without any overlapping toxicity. On this matter, a phase III trial was carried out almost 20 years ago to compare the efficacy of the GEMCAP combination with respect to Gem alone. The results showed that GEMCAP could

be considered as a valuable alternative to Gem if applied to patients with a good PS [247].

In a study conducted by Heinemann et al. in the same period, the addition of cisplatin (CDDP) to gemcitabine every 2 weeks did not show any statistically significant increase in progression-free survival (PFS) and OS of patients with advanced PDAC [248]. GEMOX, a combination of gemcitabine and oxaliplatin, was tested in a phase III study which confirmed its safety and efficacy but failed to prove statistically significant improvements of metastatic overall survival (mOS) [249], and a following randomized phase III confirmed the lack of an improvement in PFS as well [250]. The same lack of improvements was pointed out in a phase III study concerning gemcitabine plus irinotecan (IRINOGEM) versus gemcitabine monotherapy [251].

In 2011, a multidrug combination called FOLFIRINOX (irinotecan, oxaliplatin, fluorouracil, leucovorin) was proposed in the PRODIGE 4/ACCORD 11 trial in patients with metastatic pancreatic cancer, and it showed a median overall survival of 11.1 months with respect to the 6.8 months previously achieved with gemcitabine [252]. PFS, one-year survival and the time to definite deterioration of the quality of life were significantly improved as compared to gemcitabine, but the safety profile of the treatment raised major issues concerning its toxicity [253]. For this reason, FOLFIRINOX was suggested since then as a first-line option specifically for patients younger than 76 years, with a good PS and without limiting comorbidities. In a following study, FOLFIRINOX regimen was proved biologically active in borderline resectable and locally unresectable PDAC, with a 33% R0 resection rate achieved [254], and its role in downstaging the tumour and improving resection rates was further confirmed in a recent review on the topic [231].

Erlotinib, a tyrosine kinase inhibitor, was added to gemcitabine in a phase III trial on patients with advanced pancreatic cancer, which often overexpress human epidermal growth factor receptor type 1 (HER1/EGFR), but the OS was prolonged by only 2 weeks. However, this result was statistically significant and therefore considered clinically meaningful with respect to previous failures [195].

To enhance the effect of Paclitaxel (PTX), an anti-microtubule agent which is insoluble in aqueous medium and whose efficacy in patients with PDAC had previously been disappointing, it was conjugated with human serum albumin to form negatively charged spherical nanoparticles (nab-paclitaxel, Abraxane). Stromal SPARC was suggested as a potential target, although its role was debated and resized over time, but evidences confirmed stroma disruption as an exclusive effect of Abraxane, which could be related to SPARC mediation [255]. Moreover,

micropinocytosis was suggested to enhance nab-paclitaxel uptake thanks to the presence of albumin [256].

Nab-paclitaxel was administered in combination with gemcitabine, and their synergistic activity resulted in prevention of tumour growth in genetically engineered mice and sometimes even in a regression of the tumour size [189].

Overall, these multidrug regimens were accompanied by diverse and severe side effects and showed higher toxicity with respect to single-agent gemcitabine, without contributing in an effective way to the improvement of OS in patients unless these showed a good PS in the first place. All the above-mentioned studies support the hypothesis that a better drug intratumoral delivery was often the main explanation behind some of the few improvements observed in the course of the last decade. Consequently, improving the targeting of drug administration seems the best way toward new therapeutical approaches.

1.11.3 Palliative and second-line therapies

For patients with locally unresectable PDAC or distant metastases, most of the current available therapies are palliative and hence their aim is to relieve symptoms and to prolong survival as long as possible, preserving an acceptable quality of life [227]. Before the debut of FOLFIRINOX regimen against pancreatic cancer in 2011 [252], gemcitabine had been the only standard care since the trial that assessed its superiority over 5-FU [243]. In 2013, the introduction of the combination therapy including nab-paclitaxel and gemcitabine offered a new treatment option with a survival benefit over gemcitabine monotherapy [257]. However, a careful patient selection is a crucial point to consider, especially for combination therapies, since their administration is accompanied by many toxicity issues [226].

Moreover, since tumour progression within few months is very common after first-line palliative care, many patients find themselves in need of second line chemotherapy, whose option are nowadays very limited [17]. Usually, only patients with good PS despite progression of disease on frontline treatment are included in second-line regimens. In this regard, the role of first-line FOLFIRINOX and Gem/nab-paclitaxel in following lines of therapies must be elucidated in view of the conflicting results obtained so far [19]. Nanoliposomal irinotecan (nan-IRI) and/or 5-FU-folinic acid (FA) is by now considered the best second-line option for patients previously treated with Gem therapy [258], while studies analyzing second-line therapies after the failure of FOLFIRINOX regimens are currently under investigation to confirm the suitability of Gem-based treatments [17].

1.11.4 Drug resistance

As stated above, PDAC multidrug resistance (MDR) is currently one of the major obstacles to treatment. In the last decade, the mechanisms underlying its behaviour have been thoroughly analyzed in order to better understand this phenomenon and eventually overcome it [7,120,240,244]. As recent findings pointed out, MDR is driven by many molecular mechanisms such as overexpression of signals responsible for cell survival, DNA damage repair mechanisms, redistribution of the drug from the cell nucleus to cytoplasm, downregulation of apoptotic activity and the presence of drug efflux pump which alter the drug concentration inside the cancer cells [8,259,260]. Furthermore, another pointed out effect of EMT in addition to invasiveness appears to be the loss of sensibility towards drugs (to gemcitabine in particular), and the resulting release of mediators such as cytokines and transcriptional factors might as well be related to this acquired mechanism [261].

Moreover, drug resistance is believed to be associated with metabolic aberrations that lead to altered angiogenesis and apoptosis, and it is supported and promoted by the TME [120]. Tumour stroma seems to be one of the main actors involved in gemcitabine resistance [260], because it prevents chemotherapeutic drugs from reaching the tumour microenvironment and at the same time it promotes metastasis and PDAC cells penetration of the surrounding tissues [262].

Finally, drug resistance is undoubtedly a result of the interaction of the above-mentioned factors, since all the main cells of PDAC and the innate immune cell population are responsible for the instigation of a highly hostile environment, and their continuous crosstalk with tumour stroma induces and enhances chemoresistance [263].

However, further extensive study of the molecular mechanisms of survival and MDR is surely necessary to design new therapies, which are nowadays focusing on addressing TME and stromal components with the aim of improving PDAC response to chemotherapy [4].

1.11.5 Targeted therapies

In order to enhance drug delivery into the tumour microenvironment and to improve the toxicity profile of drug treatments, new strategies have been implemented over the years and resulted in targeted therapies. Their aim is interfering with some of the many dysregulated signaling pathways in PDAC, which result from the considerable variety of accumulating mutations taking place during carcinogenesis [29,264]. In fact, due to its pivotal role in tumour development, TME has been considered as a target for cancer treatment. The main advantage of

TME targeting is the higher genetical stability of non-tumoral cells, which results in their reduced predisposition toward the development of drug resistance [265], but a major related challenge is minimizing toxicity to normal and healthy cells. Moreover, the complexity of pancreatic cancer TME and its stromal interactions have caused the failure of most of the targeted therapies widely used with other types of tumours, since they showed good results in preclinical settings but disappointing ones when it came to phase II/III clinical trial translation.

Among others, targeting the growth factor receptors has been a typically implemented strategy over time. EGFR, over-activated in PDAC patients, was addressed by both antibodies, blocking its activation (cetuximab plus capecitabine [222]), and inhibitors of tyrosine kinase domain of the receptor (gefitinib plus gemcitabine [266]), which however failed to show improvements over standard therapies. Human epidermal growth factor receptor 2 (HER-2) is correlated with poor patient survival, and its targeting by means of capecitabine and trastuzumab [267] was unsuccessful in phase II clinical trials; lapatinib in combination with capecitabine [268] was tested as second-line therapy but the low number of enrolled patients impaired the interpretation of its clinical benefit. Likewise, the targeting of insulin-like growth factor 1 receptor (IGF1R) by monoclonal antibodies (ganitumab and cixutumumab [269]) and by a combination of ganitumab and gemcitabine [270] was proved to be unsuccessful.

Inhibition of KRAS pathways by direct targeting was proved ineffective as well, hence upstream effectors of RAS or KRAS downstream signaling molecules such as MAPK pathway were targeted with a combination of tipifarnib and gemcitabine [271] and with selumetinib [272], respectively. Although these approaches were unsuccessful, ERK inhibition is currently explored as a potential PDAC treatment because of preclinical promising results, with combinations of gemcitabine/nab-paclitaxel and Ulixertinib BVD-523 [273].

PI3K signaling is considered a crucial pathway to be addressed for PDAC therapy, and it was the target of studies involving gemcitabine and rigosertib, that however did not show huge improvements in patients' response [274].

Everolimus, which suggested preliminary promising results in terms of progression-free survival time [275], was combined with capecitabine, prolonging capecitabine monotherapy's OS to 8.9 months [276]. Nevertheless, due to differences in the studies' design and populations, this last comparative result could be arguable. Notably, a combination of PI3K and MEK inhibitors was suggested to possess a potential synergic activity [277], as well as that of Notch and JAK-STAT pathways. The inhibition of the former by anti-DLL4 antibodies showed a therapeutic potential in possibly reversing chemoresistance [278], but this outcome

was not echoed by following beneficial results; however, new studies have uncovered the use of γ-secretase inhibitors, such as RO4929097 [279]. JAK-STAT pathways inhibition in patients resistant to gemcitabine was achieved with ruxolitinib and capecitabine and showed improved PS and pain management in those with evidence of systemic inflammation [280]. Finally, poly ADP-Ribose pathway (PARP) [281] and tumour suppressor TP53 [282] are currently being studied in clinical trials.

Much of the available literature on targeted therapies deals with the huge heterogeneity and complexity of PDAC, whose crosstalk between molecular and signaling pathways has usually led to the failure of these treatments. Moreover, other typically highlighted issues are the presence of surrounding stromal and inflammatory components and the unselected patient populations. In fact, none of them actually improved patient survival, apart from a combination of gemcitabine and erlotinib that conferred a statistically significant mean survival benefit of 2 weeks over gemcitabine alone [195]. This effect was however marginal and raised many questions concerning its underlying molecular mechanisms [45].

Undoubtedly, combinations of chemotherapy and multiple targeted molecules have generally reported better results than targeting individual molecules, reducing upregulations and compensations implemented by adjacent pathways, and should be further explored. Nonetheless, future studies should focus on combined therapies involving Abraxane and FOLFIRINOX as chemotherapeutic drugs rather than just gemcitabine [15], and the eventual determination of predictive biomarkers could definitely help determining in advance possible responding patients [45].

1.11.6 Anti-angiogenic therapy

Anti-angiogenic approaches to PDAC focus on targeting specific angiogenic pathways, such as VEGF and its receptors, these being the most studied among many others. Such approaches aim at blocking tumour blood vessels increase by reducing proliferation of endothelial cells, oxygen and nutrient supplies and thus inhibiting cancer growth [167]. Nevertheless, despite promising preclinical results, targeting the tumour vasculature was proved unsuccessful in different clinical studies, eventually leading to more invasive tumour phenotypes and metastases spreading [283]. Some abortive attempts in the last decades included the use of bevacizumab combined with gemcitabine [284], axitinib plus gemcitabine [285], sorafenib alone or in combination with gemcitabine [286] and aflibercept plus gemcitabine [287].

Multiple factors supporting the failure of vascular targeting studies have hence been proposed: (I) long term anti-angiogenic therapies sometimes lead to tumour

hypoxia, triggering VEGF production and genetic instability in tumour endothelial cells [288]; (II) as previously reported, other mechanisms such as vessel co-option [168] and vasculogenic mimicry [169] are implemented by the tumour microenvironment to compensate the anti-angiogenic treatments; (III) hypoxia in turn negatively affects drug delivery and contributes to the creation of a hostile TME, increasing chemoresistance; (IV) these treatments determine a compensatory upregulation of pro-angiogenic and pro-metastatic cytokines, some of which recruit immune cells to create new metastatic niches [170].

Taken together, these results suggested that vasculature normalization should be preferred over anti-angiogenic strategies aimed at starving tumour cells [289]: the benefits provided by such approach include a subsequent more effective drug administration, a potential attenuation of tumour hypoxia-associated EMT and a promotion of PDAC immune response through the infiltration of immune effector cells [290].

This emerging therapeutic strategy appears very promising and should therefore be validated by further studies, to carefully identify the key regulators of angiogenesis and to eventually propose personalized therapies based on the use of molecular biomarkers to select appropriate patient populations prone to responding to vascular normalization. Finally, the emerged critical role of tumour stroma in blood vessel compression suggests that a stromal normalization should be taken into account as well, by targeting its components [170].

1.11.7 Stroma targeting

One of the hallmark pathological features of PDAC is the disproportion between stromal elements, which constitute the majority of the tumour volume, and malignant cells.

This dense stroma was proved to promote tumour progression and metastasis and to impair drug delivery, hence it has been addressed over the years by multiple targeted therapies with the aim of depleting it [39,290]. However, despite the effort made by researchers into studying and understanding the complex tumour-stroma crosstalk, many antistromal therapies resulted in failure during recent clinical trials because they somehow favored tumour aggressiveness [291].

The above-mentioned phase I/II clinical trial involving nab-paclitaxel plus gemcitabine for the treatment of metastatic pancreatic cancer pointed out a significant OS increase in patients with high stromal SPARC expression [255]. Due to this promising result, the randomized phase III MPACT trial was performed with the hope of finding an existing correlation between stromal SPARC levels and

overall survival in patients [292], but no evidence of it was pointed out. Furthermore, another recent study using patient derived PC xenografts (PDX) suggested that SPARC expression and nab-paclitaxel tumour delivery might not be correlated, and that the main responsible for the drug accumulation might be SPARC expressed by the stroma rather than that one expressed by tumour cells. Finally, the authors did not observe a depletion of tumour stroma or a change in tumour microvascular perfusion due to nab-paclitaxel, concluding that the key to previously reported nab-paclitaxel encouraging results could be mainly due to its improved delivery in PDAC thanks to the albumin carrier [293].

Another crucial pathway of PDAC, Hh, was proved to regulate stroma through the signaling between cancer cells and CAFs, but its inhibition showed contradictory results [294]. IPI-926, an inhibitor of the sonic hedgehog (SHH) pathway, caused a reduction of tumour stroma, increased mean vessel density and perfusion, and therefore provoked a higher gemcitabine delivery and a subsequent enhanced therapeutic response in mouse models [156]. This result led scientists to postulate that the therapeutic resistance in PDAC could be caused by the biophysical rigidity of the ECM and its compressing action on blood vessels [40,295]. When translated to clinical trials, however, the combination of IPI-926 and gemcitabine failed to show improved survival over gemcitabine monotherapy.

Another SHH inhibitor, vismodegib, was not able to improve overall outcomes in phase I/II studies when added to chemotherapy [296,297].

Further preclinical studies focused on relieving vessel compression by addressing some crucial non-cellular stroma compartments, with the aim of reducing IFP and enabling the delivery of chemotherapeutic agents. The abundance of hyaluronic acid in PDAC stroma, associated with elevated IFP, was addressed by hyauronidase encapsulated by polyethylene glycol (PEGPH20), combined with gemcitabine. Their effect was a depletion of HA, a decreased intratumoral IFP and an increase in vessel diameter in mouse models, which in turn provoked a decreased incidence in metastases and an increased survival [84]. A similar experiment was performed by the group of Jacobetz, in which PEGPH20 enhanced intratumoral gemcitabine delivery leading to a doubling of mice survival [132]. Despite promising preclinical results, clinical translations of this treatment were proved unsuccessful: a phase Ib/II trial applying PEGPH20 plus mFOLFIRINOX (modified FOLFIRINOX) in patients unselected for tumour hyaluronic acid (HA) status observed an increased toxicity which resulted in decreased treatment duration [298]; likewise, the combination of PEGPH20 and gemcitabine plus nab-paclitaxel, administered to patients whose eligibility criteria included high levels of HA, did not prolong OS and PFS with respect to chemotherapy alone [299].

These negative findings suggested the inadequacy of targeting desmoplasia alone, therefore current studies are now including the addition of immune checkpoint inhibitors to PEGPH20 [300,301], after promising results obtained in murine models [302,303].

Connective tissue growth factor (CTGF), whose overexpression in PDAC results in pancreatic stem cells proliferation, migration and fibrogenesis mediated by chemokines activation [304], was addressed by Pamrevlumab, a monoclonal antibody, in mouse models as a single agent or with gemcitabine [206]. In clinical trials, its combination with gemcitabine and erlotinib in a phase I study did not show further toxicity [305], while a phase I/II combining it with gemcitabine/nab-paclitaxel showed higher percentage of surgical resection and improved median survival rate than chemotherapy alone [306]. A phase III trial on locally advanced, unresectable PC treated with Pamrevlumab plus gemcitabine/nab-paclitaxel is currently ongoing [307].

Rho-associated protein kinases (ROCKs), whose expression in PDAC correlates with decreased survival [308], were addressed in KPC models by small-molecule inhibitor Fasudil. A pre-treatment (called priming) of the animals with Fasudil before the administration of gemcitabine or nab-paclitaxel resulted in enhanced disease control, due to increased microvessel density and consequent improved drug delivery. This priming strategy was also proved effective when applied before the administration of a combination of gemcitabine and nab-paclitaxel, which in turn resulted in increased animal survival [309].

Focal adhesion kinases (FAKs), whose activation is correlated with the formation of an immunosuppressive TME, were targeted in KPC mouse models by another inhibitor, defacitinib, resulting in reduced tumour metastasis and infiltrated immunosuppressive myeloid populations, and eventually leading to improved survival [310].

The contradictory results obtained so far have brought the ambivalent effect of stroma depletion into focus: on the one hand the subsequent relief from interstitial pressure led to undeniable enhancement of therapeutic delivery in many studies, on the other hand it might support the release of cancer cells and thus metastasis formation [38]. Therefore, strong evidence reinforced the emerging approach of tumour stroma reprogramming and normalization as a new and more effective therapy against PDAC [39].

The effectiveness of the reprogramming technique was illustrated in a 2014 study by Sherman and co-workers, in which the regulation of PSCs via vitamin D receptor (VDR) activation was successfully achieved. Indeed, activated stellate cells were reversed into a quiescent phenotype, leading to reduced fibrosis. TME

was hence reprogrammed to a non-inflammatory and physiological state; consequently, tumour delivery of gemcitabine was enhanced and resulted in improved antitumour response in GEMMs [311].

Nevertheless, it is imperative to take stroma duplicity into careful consideration from now on while designing new combinational targeted therapies addressing PDAC TME [312]. **Figure 3** resumes some of the afore mentioned studies regarding targeted and stromal therapies.

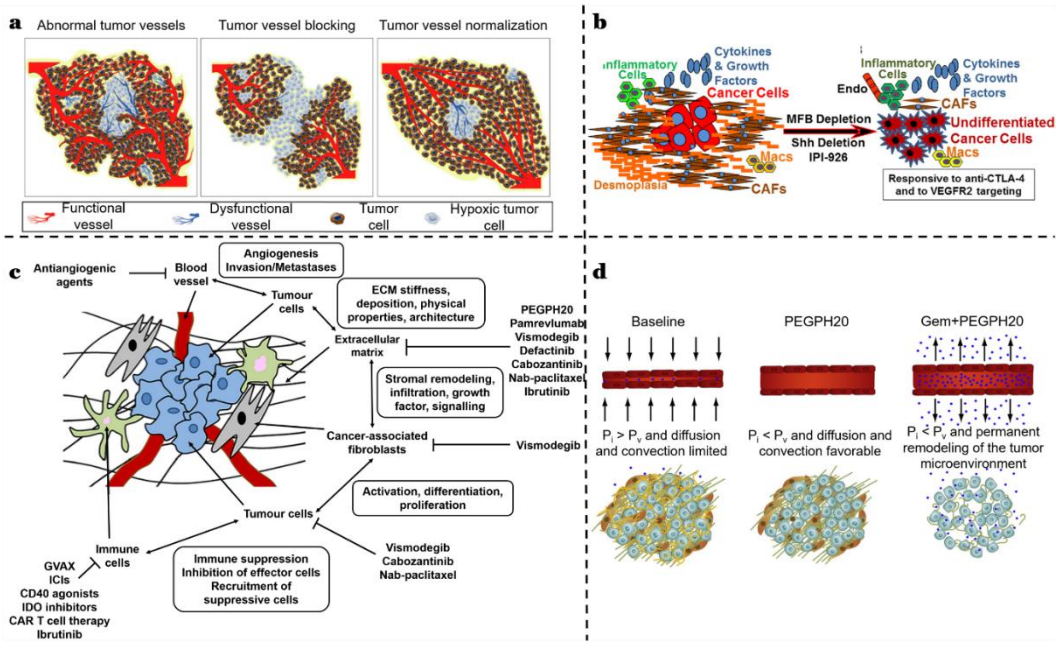

Figure 3. A) Schematic representation of tumour vessel normalization. Reproduced with permission [289]. Copyright 2015, The Authors, Published by FEBS. B) Unexpected effects of stroma targeting in PDAC, such as enhanced EMT, increased PC cell differentiation, altered immune cell infiltrate profiles. Reproduced with permission from [5]. Copyright 2014, The Authors, Published by Elsevier Inc.. C) Scheme of some strategies implemented to address PDAC stroma. Reproduced under terms of the CC-BY license [312]. Copyright 2021, Edwards, Kang and Chau. D) Stroma remodeling by means of enzymatic degradation or combined enzymatic and cytotoxic therapy. Reproduced under terms of the CC-BY license [84]. Copyright 2012, Published by Elsevier Inc.

1.11.8 Immunotherapy

Activating T cells against cancer is the cardinal principle of checkpoint inhibitors, a class of recently approved immunotherapy drugs that aim at disrupting the signals sent by cancer cells to evade patrolling T cells [313]. T cells are a type of lymphocyte that play a crucial role in the adaptive immune response: through cytokines as messenger molecules, they send chemical instruction to the immune system in order to elicit its response.

In brief, when a foreign antigen in a peripheral lymphoid organ is displayed on the surface of antigen-presenting cells (APCs, like dendritic cells, macrophages, B cells) by class II major histocompatibility complex (MHC) molecules, naïve helper T cells recognize it and hence activate. As a consequence, they secrete the cytokine interleukin-2 (IL-2) and make high affinity IL-2 receptors, whose mutual binding causes their proliferation and differentiation into effector T_H1 and T_H2 cells, depending on the cytokines produced by APCs at the site of infection. T_H1 cells secrete interferon-gamma (IFN-γ) and TNF-α, display the costimulatory protein CD40 ligand, migrate to the site of infection and activate macrophages. On the other hand, effector T_H2 cells remain in the lymphoid organ, secrete interleukins IL-4, IL-5, IL-10, IL-13 and help the activation of B cells to produce antibodies [314]. T_H1 cells can also help activate cytotoxic T cells, which provide protection against intracellular pathogens by making infected target cells kill themselves by apoptosis. Cytotoxic T cells are activated into effector cells by APC, but in this case through class I MHC proteins. This distinction is crucial, since each class of T cells expresses a co-receptor able to recognize an invariant part of the appropriate class of MHC protein, in order not to misdirect the cytotoxic and helper functions. Cytotoxic T cells express CD8 co-receptor, which binds to class I MCH proteins, while helper T cells express CD4, which recognizes class II MHC proteins [315]. Finally, T cell activation is controlled by negative feedback. A cell surface protein called CTLA-4 (Cytotoxic T-Lymphocyte Associated Protein 4), expressed during T cells activation, binds to B7 proteins on the APCs. This way, it acts as a CD28 antagonist and suppresses one of the two signals necessary to activate the differentiation of helper T cells, thus inhibiting their action [314].

The major breakthrough of immune checkpoints inhibition (ICI) immunotherapy consists in addressing the immune cells that inhibit cytotoxic T cell activity rather than cancer cells, by blocking immune checkpoints like CTLA-4, PD-1 (Programmed cell death protein 1) or its ligand PD-L1 (Programmed death-ligand 1) [316].

This therapeutic approach has so far offered many advantages in terms of treatment reproducibility and stability, since immune checkpoints represent a stationary target while cancer cells possess a mutational status that varies over time and within the single lesion [317]. Furthermore, it has led to a complete view of cancer by highlighting the role of the immune environment or the tumour mutational burden (TMB) [318], whose crucial contribution to immunotherapy was from that point taken into account. ICI immunotherapy was proved to induce delayed tumour responses at the cost of an initial increase in size, therefore new guidelines for evaluation criteria in the immune RECIST (Response Evaluation

Criteria in Solid Tumours [319]) evaluation system had to be incorporated [320]; it introduced a whole new spectrum of related adverse events [316] and caused long term remissions in spite of therapy interruptions in some patients with melanoma [321].

Despite representing a major step forward in the context of cancer treatment, ICI is still far from being adaptable to all kind of tumours: in fact, PDAC does not respond as well as other cancer types to this therapeutic option. The most plausible hypotheses to this atypical behaviour are to be found in cancer cell-intrinsic mechanisms and in the immunosuppressive role of TME [322]. Another highlighted immunological avoidance mechanism carried out by PDAC is autophagy: selective lysosomal degradation leads to a reduced expression of class I MHC, which finally results in immune evasion [323].

Indeed in a study by Clark and colleagues, since early stages of preinvasive lesions, immunosuppressive cells such as TAMs, MDSCs and regulatory T cells (T_{reg} cells) were found to persist in the TME, while no sign of effector T cells activation was detected in GEM models. The authors suggested that this premature invasion could undermine tumour immunity from the very beginning of carcinogenesis [324].

Moreover PD-1, usually overexpressed in other tumours and whose binding to its ligand PD-L1 prevents autoimmunity, is nearly absent from PCs due to the lack of T cell infiltration [325]. For this reason, current PD1/PD-L1 treatments were proved rather ineffective in preclinical studies and were not translated into clinical trials [27].

CTLA-4, a coinhibitory molecule expressed by T_{reg} cells, was targeted by antibody monotherapy but the treatment proved to be ineffective in pancreatic cancer, probably due to another immune checkpoint called VISTA (V-domain immunoglobulin-containing suppressor of T cell activation) [326]. In fact, its expression on TAMs allows them to bypass single-agent anti CTLA-4 therapy. In view of this, novel anti-VISTA antibodies, now under a terminated clinical trial [327], might be able to disrupt the established but so far unsuccessful immune checkpoint therapies applied to pancreatic cancer.

Alternatively, pancreatic cancer antigens such as CEA, MUC-1 and MUC-4, shared by the majority of pancreatic cancers, could be used as vaccines to activate APC and the consequent immune response [28,328]. In addition to that, whole cancer cell-based, peptide-based (like those including mutated KRAS peptide products) [329] and multipeptide vaccines administered after surgical resection [330] have shown very encouraging results too and must be further studied in view of combinatory therapies [26].

GVAX, a whole-cell vaccine aimed at inducing the expression of proinflammatory cytokine granulocyte monocyte-colony stimulating factor (GM-CSF) in pancreatic cancer cells, was combined with anti PD-1 therapy and showed a promising synergistic effect in preclinical models of PC [331]. A clinical trial including GVAX and other immunotherapy combinations is currently ongoing on patients with surgically resectable PDAC [332].

Indeed, due to the therapeutic impermeability provided by pancreatic cancer TME, traditional immunotherapies have been progressively dismissed in favour of combination approaches [322]. Their strategy consists in reprogramming TME first, in order to eventually allow immunotherapy to fulfil its potential [27].

As a matter of fact, different clinical trials are now exploring these innovative approaches: genetic or pharmacological inhibition of autophagy synergized with anti-PD1 and anti-CTLA-4 antibodies [323]; colony-stimulating factor 1 receptor (CSF1R) blockade on TAMs and MDSCs to improve antitumor immunity, in combination with ICI [333,334]; CXCL12/CXCR4 targeting with antagonist Plerixafor to investigate the tumour-stromal crosstalk, combined with ICI to reverse immunosuppression [335]; CD40 agonist monoclonal antibodies (mAbs) treatment in conjunction with chemotherapy to reduce T_{reg} and increase infiltrated $CD8^+$ T cells [336].

Notably, agonist CD40 mAbs were proved to enhance the efficacy of cancer vaccines [337] and to be well-suited to combination therapies involving anti-CTLA-4 and anti-PD-1 mAbs [338] in KPC models. For these reasons, they were then proposed in combination with chemotherapy [339]. The sequence and timing of treatment were shown to play a crucial role in determining the outcome of the therapy, as well as the choice of the most appropriate drug; other major issues that emerged throughout preclinical studies were macrophage activation and re-education rather than depletion [340]. The best combination therapy so far involves gemcitabine, nab-paclitaxel, CD40 mAb, PD-1/PD-L1 mAb and CTLA-4 mAb and was proposed in a 2015 study [207], which proved that this combo was able to successfully overcome PDAC resistance to PD-1 and CTLA-4 blockade, improving survival in GEM mice. Being mostly composed by FDA-approved reagents, the study was easily translated into clinical trials and offered initial promising results on metastatic PC patients [341]. According to a recent review on the topic, the efficacy of therapies which involve agonist CD40 mAbs is manifest and supported by evidence of immune activation [342,343] and should be further explored, almost exclusively in combination with chemotherapy, radiotherapy and immunotherapy due to the exceptional synergistic potential emerged throughout the years [344]. Therefore, PDAC represents a particularly promising niche for future CD40

applications and its TME is the ideal testing ground for combined therapies aimed at eliciting a robust immune response, otherwise alarmingly absent.

1.11.9 Exosomes in PDAC

Extracellular vesicles, namely lipid bilayer particles naturally released by cells and unable to replicate [345], are classified into three main groups [346] among which nanosized exosomes have recently emerged for their roles in cancers. In fact, they act as intermediaries of tumour progression and metastasis formation [347] and as mediators of immune regulation of lymphoid and myeloid cells in cancer [348]. Moreover, they are innate biological carriers which can be exploited as delivery nanosystems, since they are able to cross the main biological barriers while avoiding lysosomal degradation [349] and they possess unique intrinsic targeting activity towards the tumour site [350].

Their non-toxic and non-immunogenic nature makes them preferable to synthetic liposome formulations as vehicles for chemotherapy and immunotherapy drugs, which result well protected and shielded from degradation. Another major advantage is that they can be produced using cells derived from the patients, so as to avoid any immune reaction [351]. A recent review highlighted the existing controversy on the most suitable cell types to be used as exosome donors, since those deriving from cancer cells have generally provoked undesired effects and showed inability to stimulate the immune system. Conversely, immune cell-derived exosomes (and specifically DC-derived ones) have been successfully applied in cancer vaccines and therefore considered as a particular form of immunotherapy [352]. Besides, they were proved to overcome DC-based immunotherapy issues and to possess immunostimulatory abilities which have been extensively explored in different preclinical and clinical studies on exosome-based cancer vaccines. The most common strategy consists in stimulating DCs with cancer peptides, in order to produce exosomes carrying specific antigens able to induce an immune response [353].

Interesting applications cited in the above-mentioned review include (I) immune checkpoint blockade therapy combined with exosomes, and more broadly EVs, carrying silencing immunosuppressive genes via siRNA; (II) cell-free cancer vaccines based on tumour-derived exosomes, containing or functionalized with antigens able to induce a T cell-dependent antitumour response [354] ; (III) cancer vaccines based on exosome-pulsed DCs [355]; (IV) EVs vaccines derived from modified cancer cells [356].

This last approach was echoed in a study in which mesenchymal stromal donor cells were engineered to produce EVs already loaded with paclitaxel, then used as

drug delivery systems to treat a human pancreatic adenocarcinoma cell line [357]. Another similar experiment involved a melanoma cell line, engineered to produce EVs loaded with survivin T34A and gemcitabine, whose synergy produced a strong cytotoxic effect when administered to PDAC cells [358]. DCs were loaded with TEX (tumour-exosome) and injected in pancreatic cancer-bearing mice in another study by Xiao and colleagues. The aim of this work was to prove the improvement made by drugs affecting MDSCs (specifically ATRA, sunitinib or gemcitabine) to DC-TEX vaccination. This goal was actually achieved and evinced by a higher activation of T cells in the tumour and a longer survival time [359].

Exosomes play a crucial role in the PDAC tumour environment (**Figure 4**), participating in tumorigenesis and tumour progression [360], travelling from the primary tumour location and inducing premetastatic niche formation in distant organs [361], and favouring cell-to-cell communication mediated by exosomal miRNAs (microRNA being a small single-stranded non-coding RNA molecule able to silence or degrade RNA at a post-transcriptional level). Indeed, several studies reported their impact on the TME: (I) exosomes derived from pancreatic cancer cells were proved to induce M2 macrophage polarization to promote metastases [362]; (II) on the contrary, NK cells were observed to produce exosomes whose miRNA cargo was able to reduce cancer progression in vitro and in vivo by targeting IL-26 [363]; (III) CAFs derived exosomal miRNA was shown to contribute to gemcitabine resistance and to be transferred to cancer cells via exosomes, and therefore preventing this transfer and addressing the involved target gene (TP53INP1) was suggested to reverse chemoresistance [364]; (IV) exosomes derived from PSCs and cultured with Gem-sensitive BxPC-3 and PANC-1 cells could impart them Gem resistance by means of miRNA transfection [365]; (V) furthermore, PSC-derived exosomal miRNA was proved to promote EMT in pancreatic cancer cells through the enhancement of different signaling pathways [366].

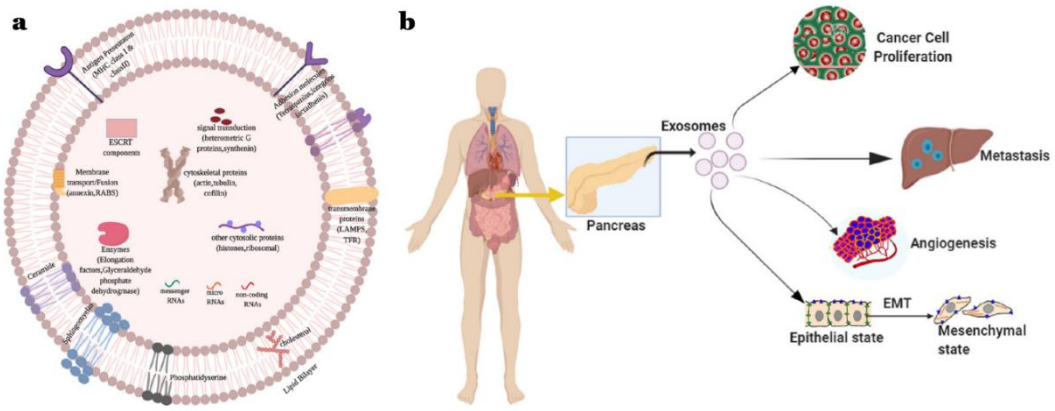

Figure 4. A) Schematic representation of the components of exosomes. B) Roles of exosomes in PDAC progression: cancer cell proliferation, metastasis, angiogenesis, EMT. Reproduced under terms of the CC-BY license [367]. 2020, The Authors, Published by Springer Nature.

In addition to that, exosomes have been considered as potential biomarkers of PDAC [368]. In fact, they can be isolated from different body fluids and their membrane is able to protect diagnostic molecules at their core, thus overcoming the limitations of traditional serum tumour markers [369,370].

Their employment as drug carriers has also been extensively studied [371], due to the low toxicity, high biocompatibility and ability to penetrate the blood-tissue barrier to efficiently deliver cargoes [372]. For these reasons, miRNA and siRNA (a class of double-stranded RNA able to interfere with the expression of specific genes) capable of blocking some of the abnormal signaling pathways in PDAC cells were loaded in engineered exosomes: a 2017 study successfully delivered MSCs-derived exosomes loaded with siRNA molecules to immunocompetent mice models, targeting oncogenic KRAS better than previously achieved with liposomes carriers and increasing OS by cancer suppression [373]. This promising outcome paved the way for a phase-I clinical trial in patients with $Kras^{G12D}$ mutations (NCT03608631) [374].

Finally, the application of exosomes to disrupt cell-to-cell communication could be the key to provoking an angiogenic regulation in PDAC, thus overcoming the failures of prior anti-angiogenesis therapies [375]. Although encouraging results have been achieved with other types of tumours, the role of exosome-mediated interactions between endothelial cells and other components of pancreatic cancer must be further investigated under hypoxia, and future developments should include strategies to impart more specific targeting abilities to exosomes, in order to better direct them to PDAC tumour cells [376].

As shown by the reported studies, once exosomes are delivered to the target cells, the carried immunomodulatory agents can either stimulate anti tumour responses or block immunosuppression; this latter outcome could be achieved through the inhibition of PDAC T_{reg} cells via exosomes-based therapy [43].

Evidence suggests that the most promising strategy to exploit exosomes' potential in PDAC might be once more a combination therapy involving the use of chemotherapy, to effectively eliminate cancer cells while minimizing side effects, with the final aim of facilitating a subsequent surgical removal. Nowadays, the main drawbacks to the clinical use of exosomes are related to technological issues rather than safety ones: a thorough study and a following standardization of purification processes is urgently needed to eventually achieve large-scale productions, which however would be still very expensive and subjected to strict controls in order to receive pharmaceutical approval. Nevertheless, the development of re-engineered exosomes able to mimic the pivotal features of the natural ones might represent a challenging alternative route to follow, which could lead to new useful critical insights about these promising tools and their application on PDAC [345].

1.11.10 Neoadjuvant therapy

Since recurrence rates after surgery are very high [377], it is now well established from a variety of studies that there is an urgent need of preoperative and postoperative therapies to improve long-term survival [378] in patients affected by PDAC.

Preoperative or neoadjuvant therapy, mainly consisting in the aforementioned combination regimens, is a strategy meant to (I) improve the likelihood of complete macroscopic and microscopic resection of localized PDAC, (II) while treating potential micro-metastases not yet visible at the time of diagnosis [379,380], (III) penetrate neoplastic tissues not altered by the inflammation and fibrosis typically induced by surgery [381], (IV) cause tumour shrinking, (V) reduce nodal involvement [382] and (VI) result in increased radical resection rates and superior OS in borderline resectable tumours [383,384].

Examples of post-operative therapies mainly consist of chemoradiation [385] and second-line drug administrations [223,386], among which the combination gemcitabine-capecitabine emerged as a new possible benchmark therapy over gemcitabine alone [387], and was recommended by the American Society of Clinical Oncology (ASCO) in the Clinical Practice Guideline for potentially curable PC [388] updated in 2017.

Although it has been shown that neoadjuvant treatments can be safely used preoperatively in PC patients without negative effects on their recovery [11], several related limitations have been raised. In particular, retrospective studies published on the subject have remarked the need to further address the topic with additional randomized controlled trials, some of which are currently ongoing [389–392]. New evidences suggest that the main role of neoadjuvant therapies has shifted over time from tumour shrinkage to micrometastases control [393], but fundamental questions in this regard remain unanswered. These limits thus preclude at present the establishment of a gold-standard for neoadjuvant treatments.

The present lack of a standardized approach is the underlying issue in a retrospective review of the National Cancer Database (NCDB), at present the most up-to-date piece of literature regarding total neoadjuvant therapy (TNT) for PDAC [394]. Barrak and colleagues started defining TNT as the administration of both chemotherapy and chemoradiation before definitive resection. They observed the rates of pathologic complete response (pCR), namely tumour downstaging to a pathological stage 0, in the patients involved in the study.

Drawing on an extensive range of sources through the latest studies on neoadjuvant therapy, the authors sorted the advantages of identifying aggressive tumours, to avoid inappropriate surgery [16], and of completing multimodal treatments before resection [395]. Furthermore, they reported the improved OS of patients treated with TNT approaches based on FOLFIRINOX and chemoradiation [396,397] and those involving multimodal chemotherapy followed by chemoradiation [398]. Finally, they concluded that total neoadjuvant therapy could be associated with improved pCR and thus selected as the treatment of choice for patients with stage II pancreatic cancer. Nevertheless, they suggested more detailed investigations on vascular grade and toxicity data in future guidelines [394].

In view of what has been mentioned so far, the implementation of a personalized treatment to better direct neoadjuvant therapy might represent the keystone to effectively fight PC. This can be achieved by exploiting precision medicine and molecular prognostic biomarkers [399] to create subsets of selected patients who could benefit from tailored therapy and thus improve their survival outcomes [400].

1.11.11 Radiation therapy

Radiotherapy (RT) failed in proving its superiority over chemotherapy in terms of survival, so the two approaches were combined together and as a matter of fact they showed more encouraging results when proposed as a neoadjuvant therapy before surgery [401,402]. In particular, gemcitabine proved to be the drug whose

combination with radiation led to the best results with respect to other chemotherapeutics [403]. This trend was further confirmed by means of a more recent study concerning resectable or borderline resectable PDAC tumours, which claimed that preoperative chemoradiotherapy effect on secondary end points such as disease-free survival (DFS), distant metastasis-free interval and resection rate was superior to postoperative adjuvant chemotherapy, despite an absence of OS benefits [404]. A 2017 study was the first to investigate the outcome of chemotherapy and radiotherapy (RT) treatments (in brief PORT, postoperative radiotherapy) administered after microscopically-positive margin (R1) resection surgery. Park and colleagues noted that PORT was associated with a favourable survival outcome, confirming previously reported literature evidences, and that adjuvant chemotherapy was a prognostic factor for OS and DFS [385], thus confirming the efficacy of the synergistic effect of the postoperative therapy.

In spite of previous discouraging results in terms of survival benefit, neoadjuvant radiation in addition to multiagent chemotherapy also suggested increased rates of tumour downstaging and R0 resection rates [405,406]. This combination was hence explored in a recent study by Vidri et al., who hypothesized a positive effect of preoperative radiotherapy on OS and pathological response in the context of a multimodal treatment. Nevertheless, although increased rate of R0 resection and improved outcomes like downstaging were achieved, no effect on OS was pointed out [407].

Given the conflicting results concerning radiotherapy, a 2019 review by Hall and Goodman concluded that, in view of the continuous transformations and advances of radiation therapy like real-time MR guidance [408], this technology is likely to offer enormous advantages to PDAC treatment, especially in the context of neoadjuvant therapy in borderline resectable tumours, provided it is robustly evaluated and proven by future clinical trials [409].

1.11.12 Local ablative therapies

The most frequently applied local therapies for unresectable pancreatic tumours are radiofrequency ablation (RFA), irreversible electroporation (IRE), stereotactic body radiation therapy (SBRT) and high intensity focused ultrasound (HIFU). However, these local ablative therapies suffer from the lack of randomized controlled trials and the absence of univocally established procedures. Indeed, many studies have been published on the subject throughout the years with heavily biased and overall sparse results [25].

RFA and IRE belong to the thermal and non-thermal ablation techniques, respectively. The former is based on the generation of high local temperatures through the application of high-frequency alternating current conducted by one or more needle electrode. The needle is introduced inside the tumour under US or CT guidance with laparotomy, percutaneously or using an endoscopic approach. Its effect is to provoke coagulative necrosis, protein denaturation and irreversible damage to the cells of the neoplastic tissue [23].

IRE has been more recently applied to locally advanced pancreatic cancer and is ought to preserve surrounding structures, since it does not produce significant thermal energy [410]. It achieves cell membrane disruption by applying around the tumour tissue at least two needles pulsing short high-voltage direct current. Such current, whose rate is synchronized to the heart rate for safety reasons, causes the irreversible permeabilization of the lipid bilayer with consequent disruption of intracellular homeostasis and eventual activation of apoptotic pathways [411,23]. The whole procedure takes place under general anesthesia and paralytic induction.

The two techniques have generally been applied to stage-III patients not responding to standard systemic treatments (more rarely to stage-IV ones) in combination with systemic chemotherapy with the aim of achieving local tumour control [412,413].

The most frequently reported drawbacks after RFA are the risk of thermal injuries to adjacent structures (such as vessels and nerves), pancreatic fistulae, gastrointestinal hemorrhages, acute pancreatitis and duodenum injury [414,415,25]. Notably, after IRE some common complications such as pancreatitis, pneumothorax, abdominal pain, duodenal leakage and deep vein thrombosis have been described as well [23,416].

Another major concern is the type of imaging technique to use for follow-ups and recovery assessments of these ablative therapies. Actually CT, which is the first choice in the case of PC, has sometimes failed in correctly detecting or staging this specific tumour. In addition to that, factual evidence appears to confirm the reduction of CT diagnostic performance after therapy, and especially after these ablative treatments [417].

RFA and IRE have shown some undeniable advantages like low morbidity, possible percutaneous application and consequent involvement of patients at high-risk for surgery, limited damage to surrounding tissues and low cost [23]. However, the absence of solid clinical studies leaves some important questions open, such as the optimal sequential combination with chemotherapy and chemoradiotherapy within the context of multimodal treatments, the choice of patients, the best technique to access the organ [411]. Moreover, the causes underlying their several

adverse consequences give rise to many concerns even nowadays, and they are reported and extensively argued in recent reviews on the topic [224,416,418].

SBRT consists in delivering high-dose radiation to the pancreas with submillimeter precision, in single or multiple sessions. The main challenges related to this application are the respiratory movement of the target and the nearby presence of sensitive organs at risk. Typically, one week after the implantation of three or four gold seeds (fiducial markers) into or near the pancreatic tumour using endoscopic ultrasound guidance, a four-dimensional CT simulation is performed during free breathing, then the scans are examined and the motion ranges are considered by applying respiratory tracking or gating schemes. After assessing the planned target volume, the prescribed radiation dose is administered considering the maximal point dose of the surrounding organs [419].

Over the course of the last decade, SBRT has been considered as a safe local treatment for unresectable PDAC. A 2012 study by Goyal et al. observed an increase in OS in patients involved in the treatment. It pointed out the low adverse events and excellent local control rates from radiotherapy or fiducial marker placement and suggested the use of SBRT as a palliative option for unresectable tumours to prevent or delay local recurrence. Furthermore, the application of this technique was proposed in the context of a multimodal treatment including chemotherapy [420].

In addition to safety and feasibility encouraging results concerning SBRT, a 2015 systematic review on ablation therapies by Rombouts and colleagues reported promising quality-of-life outcomes for this technique [25].

A recent research article confirmed the beneficial effects of SBRT in terms of freedom from local disease progression (FFLP) and OS in patients with local advanced pancreatic cancer, with minimal toxicity related to the treatment. The authors however argued that, since distant metastases represent the major pattern of failure, local control of the tumour by SBRT alone is not sufficient to avoid progression. Therefore, SBRT should be further studied in combination with chemotherapy in order to establish an optimal scheme of treatment [419].

Overall, as reported by Ruarus and colleagues, the literature on SBRT is heterogeneous with respect to the delivered radiation doses and fraction, making any kind of comparison to other ablative techniques hard to draw. Some major disadvantages such as the risk of complications after more than 3 months from the treatment and the maximum tolerable dose of nearby organs at risk (with consequent reduction of radiation at the borders of the tumour) must be carefully addressed in future studies [24].

HIFU is an ultrasound-based system which causes thermal tissue destruction and is currently used against a variety of solid malignant tumours [421]. Applied to pancreatic cancer, it increases the local temperature up to 65 °C, killing tumour cells and disrupting the PC stromal barrier, potentially allowing chemotherapy delivery to the tumour [422]. Therefore, in the last 20 years, it has been successfully employed alone or in combination with chemotherapy [25,411], generally showing promising results in terms of tumour reduction and survival rates. HIFU is now recommended for the treatment of unresectable PDAC [423]. As far as side effects are concerned, they range from absence of complications to pain, transient pancreatitis, skin burn and subcutaneous and fat necrosis [424].

Once again, the lack of randomization and potential selective bias of the studies on the topic represent an issue that must be overcome to elucidate the mutual influence between HIFU and chemotherapeutic drugs [425], with the final aim of formulating new treatment schemes for future applications.

A 2020 systematic review on endoscopy ultrasound-guided thermal ablation therapy for pancreatic cancer drew the attention on the postnecrotic infiltration or the marginal tumour zone by neutrophils, macrophages, dendritic cells, T and B lymphocytes and natural killer cells, with consequent enhancement of the anti-tumour systemic immune response. The suggested reason behind this recruitment was thermal-mediated tissue damage, but the authors cautiously concluded to wait for further studies to validate this high-potential induced secondary effect [426]. Indeed, the balance between apoptosis and necrosis following thermal ablation therapies is a crucial issue influencing the acquired immune system activation [427]. In fact, the apoptotic bodies are not capable of triggering dendritic cells, thus preventing the cascade of events that results in T cell activation [428]. On the other hand, cells that undergo necrosis produce necrotic fragments and activate damage-associated molecular patterns (DAMP) that cause an immune response [429].

Nevertheless, the immune implications of ablation techniques of locally advanced PC had already been proposed in previous publications.

With respect to RFA, it was demonstrated that the accumulation of immune infiltrates mainly takes place in the peripheral or transitional zone of the tumour, namely those cells that surround the central coagulative necrosis zone and that are subjected to a steep negative temperature-gradient; they receive oxygen from the increased blood flow, which in turn enhances the formation of ROS and favours drug accumulation [430]. Immune cells subsets were also observed in distant and untreated tumours, once again suggesting an overall immune activation provoked by RFA, and the combination of ablative techniques and topic immunotherapy was hence proposed to elicit an antitumour reaction aiming to a systemic immune

response [23]. Later, Giardino and colleagues observed a general activation of the adaptive response and a reduction on immunosuppression in 10 patients with locally advanced pancreatic cancer treated with RFA; despite being limited by the small sample and the open approach adopted (laparotomy), this study reported the presence of immunogenic molecules after ablation, that improved dendritic cells activation and maturation and cross-priming of T lymphocytes. A systemic reaction to RFA in terms of immunomodulation was witnessed by a marked difference between typical patterns of surgical stress or inflammation and the general detected trend towards a decrease in immunosuppressive chemokines and immune cells (which normally contribute to tumour progression). The authors concluded with the hypothesis of a prolonged immune activity even weeks after the procedure, which however should be further confirmed by studies with larger numbers of patients [431].

RFA was also proved to reduce the levels of T_{reg} cells [432], and higher levels of tumour-specific T cells were detected after this ablation therapy, with related improved survival in hepatocellular carcinoma patients [433]. On the other hand, an often-encountered adverse effect of RFA in liver models was distant tumour growth and development of metastases [434], whose immunologic interpretation is nowadays being elucidated [428].

Moreover, the first performed clinical trials proved the superior overall response rate of patients treated with IRE and NK cells [435], the longer PFS and OS in those who received IRE and allogenic Vγ9Vδ2 T cell infusion [436] and the higher median OS in patients treated with cryoablation and immunotherapy [437]. A clinical trial in course, named PANFIRE-III, is currently testing a combination of IRE, systemic anti-PD1 and intra-tumoral TLR-9 agonist in metastasized PDAC patients [438].

The discovery of immune activation following local ablative therapies has opened new horizons for PDAC treatment possibilities, paving the way for new combination therapies which could take advantage of the immunomodulation witnessed after the application of such procedures.

1.11.13 Light/ultrasound -triggered minimally invasive therapies

Among other ablative therapies based on external stimulation with an energetic source, photodynamic therapy (PDT) and sonodynamic therapy (SDT) are emerging in the context of minimally invasive treatments for cancer applications. For the application on PC, both techniques are still nowadays poorly documented, and for this reason here reported in detail.

a. **Photodynamic therapy**

An extensive recent review highlighted the salient points of photodynamic therapy reported in literature, with respect to PDAC current and future applications [35].

PDT is a technique which selectively destroys target tissues by means of a photosensitizer (PS), previously injected to allow its accumulation in malignant tissues by passive or active targeting, exposed to a light at a certain wavelength. The effect of light absorption by the molecular PSs is an excitement from their ground state, which can rapidly drop back by emitting fluorescence or undergo intersystem crossing to an excited triplet state, whose lifetime is very long and cannot return to a ground state. As a result, PS molecules can transfer electrons to form reactive oxygen species (ROS) or give rise to singlet oxygen molecules ($^1O_2$) through collisional quenching [439].

ROS effects in biological environments have been thoroughly investigated over time: they possess high reactivity and are thus responsible for redox modifications of biomolecules [440,441]. They act as intracellular signaling molecules but can also provoke cell death if overly produced. Therefore, a delicate redox homeostasis takes place in healthy cells to balance ROS production and elimination. However, many endogenous factors such as hypoxia can trigger an exaggerated generation of these radical species: their effects are an increased disease incidence, pathological dysfunctions, ageing, tumorigenesis and eventually cell death [442–444]. When generated in the tumour proximity through PDT, ROS can exert their cytotoxic action on cancerous tissues [445].

The advantages of PDT technique are the preservation of connective tissues, mechanical integrity of critical structures [24] and the absence of accumulating toxicity derived by ionizing radiation. A main drawback is the limited penetration in tissues of most light wavelengths used, such as red and near-infrared ones, together with possible toxicity of the PS over time. Early preclinical developments of PDT for pancreatic cancer highlighted the importance of PS and light delivery strategy selection. The first clinical trials assessed the use of verteporfin as PS, thanks of its absorption at 690 nm and rapid excretion with respect to the previously used mesotetrahydroxyphenylchlorin (mTHPC) [446].

After the assessment of endoscopic ultrasound (EUS)-guided PDT, disclosed in previous studies, a 2019 phase I clinical study reported on the use of porfimer sodium-mediated EUS-PDT followed by nab-paclitaxel and gemcitabine chemotherapy in patients with locally advanced PC. The treatment proved to be safe and effective in prolonging progression-free survival rate [447] and was followed

shortly after by another trial, in which porfimer sodium was replaced by verteporfin, a short half-life and FDA approved PS [448].
Due to the deeply hypoxic tumour microenvironment, PDAC response to PDT is typically poor and should be enhanced by means of new strategies meant to deliver or produce oxygen in situ, like the use of microbubbles [449] or the exploitation of the excessive amount of H_2O_2 produced by cancer cells.
Collectively, much of the current literature on the subject agrees on the considerable potential of PDT [450] and of its combination with chemotherapy as a pre-treatment to enhance drug transport [34,451]. Other light-based approaches such as photothermal therapy (PTT) [452,453] and an ultrasound based one, sonodynamic therapy (SDT) [454], have also been encouraged so far together with PDT by promising results.

b. **Sonodynamic therapy**

Sonodynamic therapy is a US-based technique which consists in the simultaneous combination of low-intensity US, molecular oxygen and a sonosensitizer, able to produce ROS.bThe main advantage with respect to PDT is the greater penetration of ultrasound, which enables deep tumour treatment while avoiding tissue sensitization and skin phototoxicity [422,455]. Moreover, US is also a widely-accepted safe technology in the context of clinical imaging due to its low cost, high sensitivity and absence of ionizing radiation [456].

When a biological medium is exposed to US, it undergoes thermal and mechanical effects. Thermal effects are those exploited with HIFU, as reported above, while the main mechanical ones are sonoporation and cavitation. Sonoporation is namely the formation of pores in cell membranes which are usually exploited to enhance drugs' penetration, gene delivery or NPs uptake [457] inside cells. Cavitation consists in the nucleation and growth of gaseous bubbles from gases dissolved in liquid media when exposed to ultrasound pressure waves. Typically, such gas bubbles can either rapidly collapse (inertial cavitation) or maintain their oscillatory motion (stable cavitation). The violent collapse due to inertial cavitation can produce acoustic emissions, microstreaming, jetting and shockwaves, all leading to mechanical damages. Alternatively, it can mark the beginning of chemical reactions like ROS production from water molecules, including singlet oxygen ($^1O_2$), hydroxyl radicals ($\cdot O_2$) and superoxide anions ($O_2^{\bullet -}$) [456,458]. Since their generation rate is limited and their spatial distribution is highly heterogeneous, the amount of produced ROS is typically not therapeutically effective. Therefore, the presence of sonosensitizers is needed and by now generally approved in combination with ultrasound to achieve an effective SDT [459].

The currently available and applied sonosensitizers are either organic or inorganic. Examples of the most commonly used organic sonosensitizers are porphyrins and protoporphyrins (such as PpIX) [460,461], hematoporphyrins, hematoporphyrin monomethyl ether (HMMA), rose Bengal (RB) [462], indocyanine green (ICG), drugs such as doxorubicin [463], IR-780 iodide [464]. They possess excellent catalytic performances and broad-ranging optoelectronic features [465]. However, they show poor water solubility and are subjected to enzymatic degradation, therefore they are rapidly eliminated from the blood circulation with the result of not providing an adequate concentration in the tumour site [458,466].

On the other hand, titania (TiO_2) nanoparticles (NPs) are the most employed inorganic sonosensitizers [467]. They possess chemical stability and reduced phototoxicity, which however are counterbalanced by a low ROS quantum yield and a fast recombination of electrons on their surface. Since hypoxia is one of the hallmarks of pancreatic cancer, particular attention has been given to efficient O_2 tumour delivery with the aim of enhancing the efficacy of chemotherapy, PDT and SDT, by direct oxygen delivery in the TME or by triggering the transformation of the overly expressed H_2O_2 in O_2 in situ. In 2016, a combination of ultrasound, microbubble and chemotherapy was proposed by Dimcevski et al. in a clinical trial. The treatment consisted in gemcitabine infusion followed by an ultrasound treatment during the injection of SonoVue (a contrast agent made of microbubbles stabilized by phospholipids and containing sulphur hexafluoride). The consequences of this combination therapy were an enhancement of the tolerated gemcitabine cycles, an increase of the median survival and a decrease of the maximum tumour diameter in some of the patients involved [468]. In the last decade, data from several studies suggest that a multimodal approach involving a combination of SDT with different techniques such as chemotherapy, starvation therapy, PTT, PDT or immunotherapy is the most promising strategy to pursue, in the light of the documented synergistic cancer effects achieved so far. Although many applications of SDT-based combination therapies on cancers have generally provided promising results [422,34,465,466,469–471], literature concerning pancreatic cancer is still poor and mostly limited to in vitro studies [472,473].

1.12 Nanoparticle-based medicine and theranostic approaches

1.12.1 Nanomedicine and nanoparticles in cancer treatment

As repeatedly highlighted above, the major drawbacks and limitations of currently applied treatments prevent them from being the ultimate PDAC solution, or from being applicable indistinctly to all patients. Nevertheless, promising findings in the field of nanomedicine are allowing scientists to develop more personalized therapies, with the final challenging aim of being able to meet the specific needs of each tumour in question. Nanomedicine has been described as the application of nanotechnology for medical purposes, exploiting nanomaterials for diagnosis, monitoring and treatment of diseases [474].

Nanomaterials, typically defined as engineered materials with at least one dimension in the nanoscale range (1-100 nm) [475], possess physiochemical characteristics which differ from those of their bulk counterparts and confer them remarkable properties [476–479]. Among the plethora of currently available nanomaterials, nanoparticles have emerged thanks to their countless therapeutic uses in cancer therapy, mainly reported for imaging and diagnostic purposes and for drug delivery applications [31,480–482].

In this last case, their use offers various advantages: (I) they are able to protect the eventual cargo from biodegradation, prolonging the circulation time and thus maximizing the chances of reaching the tumour without being cleared from the body; (II) they improve the therapeutic window by providing a sustained release over time [483]; (III) they can accumulate in the tumour site by both passive or active targeting; (IV) they can be internalized by cancer cells to release their payload without interference of drug efflux pumps, thus reducing toxicity to other cells; (V) they can simultaneously transport more than a single drug, enabling combination and multimodal therapies; (V) their surface can be modified with coatings in order to avoid immune surveillance, or with ligands to actively target the tumour in question [484–487]. Finally, their ability to combine diagnosis and therapy in a single construct, referred to as theranostic, is nowadays the most promising investigated application of nanomedicine in the context of cancer treatment [49,123].

The most commonly used and approved formulations of NPs are lipid-based, polymeric and inorganic nanoparticles [488–490], chosen depending on the nature of the cargoes to be delivered and to the therapeutical application they are destined to [491]. Size, shape and surface properties of NPs are all factors hugely influencing

their behaviour in biological media and the subsequent reaction of the body to their presence [492,493], and therefore must be carefully tuned and optimized [494–496].

Different camouflage strategies, such as PEG grafting on the NP surface (which has however recently raised some concerns with respect to its immunogenicity [497]), the addition of self-markers like CD47 peptides and the coating with phospholipidic or cell-derived membranes to inhibit their phagocytosis [498–500] have hence been proposed to avoid the capture of NPs by macrophages and other phagocytes.

Once in the bloodstream, the key point of an efficient delivery is the localization into the tumour site [485]. Although most of the existing literature concerning nanoparticles considers passive targeting, and hence the EPR effect [501], as the main responsible for their accumulation in tumours, a series of experiments depicted in a 2020 study by Sindhwanin et al. were carried out in order to prove the real extent of EPR in solid tumours and proved that an active transport through endothelial cells via trans-endothelial pathways was the main tumour accumulation mechanism shown by NPs in mouse and human models [484].

In addition to that, passive targeting is strongly dependent on the leaky tumour vasculature adjacent to the tumour, which is limited in some types of cancers. In regards, a review by Liu et al. raised an important issue connected to drug delivery in PDAC, in which the presence of thick tumour stroma has the effect of hindering the access to the tumour site. The authors hence suggested transcytosis as the major mechanism for PDAC drug delivery [502,503]. Moreover, as previously reported by the same authors, the presence of iRGD peptides was proved to further promote the penetration of irinotecan-loaded silicasome-based carriers in patient-derived xenograft [504]. Taken together, these findings pointed out the role of specific ligands and tumor-penetrating peptides in NPs selective accumulation, and the evidence-based importance of relying on their use by means of NPs surface functionalization for efficient active targeting [505,506], especially in stroma-rich tumours like PDAC [507].

1.12.2 Pancreatic cancer nanomedicine applications

In the last decades, nanotechnology has been profusely applied to both pancreatic cancer diagnosis and therapy [508]. Thanks to the use of nanoparticle-based medicine, some of the major drawbacks of conventional therapies have been addressed, especially in the context of drug delivery. Nevertheless, chemotherapy is not the only field that could definitely benefit from nanotechnology applications. **Table 1** reports some selected nanomedicine approaches, discussed hereinafter in detail, which have already been applied to PDAC in the last decade to overcome certain limitations and drawbacks shown by conventional treatments.

Table 1. Selected alternative nanomedicine approaches recently applied to PDAC.

Conventional treatment	Major limitations and drawbacks	Possible nanomedicine solutions
Surgery	• Surgeon and hospital dependent [509] • Late diagnosis, mostly when PDAC is unresectable [9]	• Modern combination therapies and neoadjuvant therapy to downstage tumours and extend surgery [12,510] • NP-based contrast agents to reduce positive resection margins [511–516] • Novel biomarkers to identify at risk populations [399,517,518]
Chemotherapy	• Limited tumour accumulation, high toxicity, significant side effects [4] • Poor selectivity toward cancer cells [519]	• Nanoparticle-based drug delivery [486] • Nanoformulations of hydrophobic [189,256] and hydrophilic [258,520] chemotherapeutic drugs • Stimuli-responsive NPs to trigger drug release [521,522] • Targeted theranostic NPs [523] • Gemcitabine combination nanotherapies [524]
Radiation Therapy	• Radioresistance and damages to nearby normal tissues [525]	• NPs to radiosensitize PC cells or to protect healthy ones [526–529]
Targeted/Stromal Therapies	• Difficulties in successfully penetrating the stromal barrier with drugs [291] • Conflicting preclinical/clinical results [5] • Stroma depletion can also enhance the tumour [38]	• NPs to improve siRNA and miRNA distribution [530–533] • Stimuli-responsive nanoconstructs [534,535] • Active targeted drug delivery with modified specific ligands [534,535]
EVs and exosomes	• Scaling and technological issues [536] • PDAC applications limited to cells or animal models in normoxic conditions [376]	• Biomimetic nano-engineered EVs [345] • Exosomes' engineering strategies [537] • Nanotechnologies exploiting exosomes as diagnostic biomarkers [525,538] • Exosome-based nanovehicles [539,540]
Immunotherapy	• Immunosuppressive TME [541] • Poor response to ICI [322] • Early immune infiltration [542]	• NP to deliver innate immune agonists [543] or to induce immunogenic cell death [544,545] • NPs to disrupt tumour-pancreatic stem cells interplay [546,547] • NPs to target macrophages [548]

		• NPs to target MDSCs and T_{reg} cells [549]
Local ablative therapies	• No standard procedures [25] • Injuries to nearby systems [24] • Inadequate imaging for follow up [417]	• Intracellular hyperthermia through NPs [550–552] • Dynamic monitoring of PC through MRI nanoprobes [553]
PDT	• Poor penetration of photosensitizers [450]	• Nanovehicles to better deliver photosensitizers [554–557] • Nanovehicles delivering oxygen to alleviate hypoxia [558,559]
SDT	• Limits of organic and inorganic sonosensitizers [455,466,560]	• NPs to protect organic sonosensitizers [455] • Surface functionalizations of inorganic sonosensitizers [561] • Gas-generating nanosystems [562]

The next paragraph will discuss the application of nanotechnological tools to different conventional therapeutic treatments.

a. Surgery

As far as PDAC surgery is concerned, for example, it has extensively been proved that clean resection margins are correlated with better outcomes in patients which undergo surgery, whereas late diagnoses are usually made when the tumour is not localized anymore and thus not easily resectable [9]. Thus, improvements in terms of correct staging, tumour visualization and recurrence detection could be the key to enhance tumour response to surgery. Neoadjuvant therapy, and more generally systemic therapies administered before resection could benefit from the use of nanotechnology: (I) a more efficient delivery of drugs could help tumour shrinking and favor downstaging, enabling the extension of surgery indications to a larger slice of PDAC stages [12,510]; (II) moreover, NP-based contrast agents could help defining tumour margins with higher precision via medical imaging, improving the chances of achieving clean resection margins [511–516,563]; (III) finally, the discovery of novel biomarkers targetable by means of nanoconstructs could help identifying at risk population for mass screening purposes, patients' stratification and more personalized therapeutic approaches [399,517].

b. Chemotherapy

Limited accumulation of chemotherapeutic drugs in PDAC TME, their high systemic toxicity and their poor selectivity towards cancer cells have been

overcome by nanoparticle-based drug delivery [486] and the implementation of nanocarriers able to incorporate hydrophilic [258,520] and hydrophobic [189,256] drugs, improving their circulation in the bloodstream. Moreover, their surface functionalization with targeting peptides can confer them tumour homing abilities [523], while the use of stimuli-responsive NPs can trigger drug release once the nanocarrier is located inside the tumour [521,522], thus providing a selective and precise delivering to cancer cells.

Inspired by Abraxane coadministration with gemcitabine, Meng and colleagues designed a lipid-coated mesoporous silica NP co-delivering both paclitaxel and gemcitabine via intravenous (IV) injection in mice carrying subcutaneous PANC-1 xenografts. The obtained nanocarriers achieved an effective inhibition of primary tumour growth and eliminated metastatic foci outperforming the free drug counterparts, while allowing a precise ratiometric drug loading and cargo protection thanks to the uniform surface coating provided by the lipid bilayer [564]. Liu and co-workers designed a mesoporous silica NP platform loaded with high-dose irinotecan and coated by a lipid bilayer (LB-MSNP), whose administration to an orthotopic Kras-derived PDAC model in immunocompetent mice resulted in enhanced primary tumour killing and metastases reduction, along with controlled release and toxicity decrease with respect to liposomes [565]. Multifunctionalized iron oxide NPs including anti-CD47 antibody and gemcitabine were successfully tested on various primary cell cultures and PC cell lines, showing a selective drug release and an efficient induction of apoptosis with respect to the free antibody in another recent study [566].

To overcome gemcitabine rapid clearance and resistance, various nanotechnologies have been applied to shield it from metabolic inactivation; one of these strategies, as previously mentioned, involved the combination of gemcitabine with the paclitaxel nanoformulation Abraxane [189]. Previous works regarding the design and construction of gemcitabine prodrug nanoparticles have provided superior antitumour activity against PDAC, such as stereocomplex prodrugs of Oligo(lactic acid)n-Gemcitabine in Poly(ethylene glycol)-block-poly(D,L-lactic acid) micelles [567], whose improved physical stability resulted in enhanced antitumour efficacy on PANC-1 pancreatic cancer cells, and self-assembled gemcitabine prodrug nanoparticles coated with PEG and decorated with a target peptide [568], whose administration in xenograft models of human PDAC inhibited tumour progression. In other studies, gemcitabine or its derivatives were directly entrapped in nanoparticles, achieving both high and prolonged accumulation in the tumour tissue compared with the free drug. Various gemcitabine combination nanotherapies applied to PDAC exploiting micelles, liposomes, metal-based

nanoparticles and hydrogels have already been reported in detail in a 2019 review [524]; hereinafter some additional applications, focused on multimodal approaches, are briefly described. Das et al. used lipid coated calcium phosphate NPs to entrap gemcitabine monophosphate and triggered a strong antitumor response by delivering them to a treatment refractory PDAC model, bypassing the typical hallmarks of gemcitabine chemoresistance [569]; Chen and co-workers coloaded phosphorylated gemcitabine with paclitaxel in a micelle (CDM) coated with PEG and decorated with a stroma targeting peptide (AE105), which could take advantage of the distinctive low pH of PDAC TME by means of a pH-triggered disintegration and the resulting dual drug release [570] (**Figure 5a**). A study by Zhao reported the employment of biocompatible lipid-polymer hybrid NPs for the co-delivery of hypoxia-inducible factor 1α (HIFα)siRNA and gemcitabine, further coated by a lipid bilayer to avoid aggregation as well as gem leakage, tested on subcutaneous and orthotopic tumour models; results showed a suppression of HIFα expression and the inhibition of tumour metastases, proving the efficacy of the combination therapy strategy [530] (**Figure 5b**). Han and colleagues developed gemcitabine nanovectors based on CdSe/ZnS quantum dots conjugated with MMP-9 detachable PEG and a targeting ligand (cycloRGD), hence able to achieve prolonged blood circulation and enhanced tumour internalization [571] (**Figure 5c**). Uz and colleagues designed temperature and pH responsive polymeric nanoscale devices to co-deliver microRNA (miR-345) and gemcitabine to PC cells and to mice carrying xenograft tumours; their documented effect was a downregulation of SHH signaling, which in turn enhanced gem perfusion, and a significant decrease in metastasis [572]. Meng et al. reported a multi-functional superparamagnetic iron oxide nanoparticle (SPION) formulation of curcumin combined with gemcitabine administration, applied to HPAF-II and Panc-1 cells and to an orthotopic mouse model. They actively targeted the TME and facilitated gemcitabine uptake by inhibiting the activation of SHH signaling, reducing tumour growth and metastasis and inducing changes in cell stiffness [573]. Gemcitabine loaded, PEGylated gold nanoparticles were employed by Elechalawar et al. as delivery systems to specifically inhibit PC cells and PSCs proliferation in vitro, with the use of the anti-EGFR antibody cetuximab (C225/C) as a targeting agent [574].

c. Radiation therapy

In order to avoid the huge side effects related to RT, radiation protectants for normal tissues and radiation sensitizers to enhance the damage induced in cancer cells have been developed [575]. Cerium oxide nanoparticles (CONPs) have typically been employed as adjuvants in RT due to their antioxidant properties, but their pro-

oxidant behaviour has recently been highlighted as well. In this regard, a study by Wason et al. reported the effect of CONP treatment prior to RT in potentiating pancreatic cancer cell apoptosis, while protecting normal tissues depending on the environmental acidity [526]. Other types of NPs have successively been employed for the same purpose: titanium peroxide nanoparticles (TiOxNPs) were shown to be promising agents for ROS production upon X-Ray irradiation in a mouse model using engrafted human PC cells [528], while gold nanoparticles (Au NPs) were incorporated into microgels to create stealth constructs acting as radiosensitizers in a mouse model of PC, as described in a 2019 study [527].

d. Targeted/stromal therapies

As previously mentioned, the abnormal vascular structure of this kind of tumours is characterized by tortuous, saccular chaotically organized vessels, which lead to heterogeneous blood perfusion, high IFP, vascular compression and hypoxia. Taken together, these conditions hinder an effective drug penetration into PDAC, even in the presence of stromal and targeted therapies [291]. Stroma targeting via nanoconstructs relies on different delivery mechanisms than those used by conventional non-encapsulated drugs, and hence has been proposed to improve PDAC penetration and treatment [38]. For this purpose, strategies as specific ligands to enhance active targeting and smart nanoparticles designed to respond to environmental or external stimuli have been implemented [534,535]. Another novel approach consists of the simultaneous targeting of stromal and tumour compartments, by means of multifunctional nanoconstructs [576], in order to alleviate TME stiffness and favor the local delivery of chemotherapeutic drugs. Acting on tumour vasculature was also proved effective in a study by Meng et al., which exploited a mesoporous silica nanoparticle (MSNP) targeting a molecular pathway involved in pericyte recruitment as the first step of an engineered approach meant to enhance the penetrance of a nanoformulation of gemcitabine [577].

As recently pointed out by an up-to-date review on the topic, CAFs still represent an under-explored target for PDAC treatment, although their central role in the multistep processes of tumour initiation, progression, invasion and metastases has repeatedly been pointed out [578]. Nevertheless, in the context of stromal modulation approaches, some nanomedicine applications targeting CAFs have emerged over the last decade and their resulting tumour tissue normalization has led to promising improvements in PDAC, especially in terms of tumour progression [579], growth [580] and immune response [576,581]. These studies had the double effect of improving PDAC therapy by enhancing drug delivery into the tumour site whilst elucidating the complex and dual role of CAFs in desmoplasia [582]. They involved,

among many other mechanisms [507], the use of polymeric micelle-based nanoformulations to inhibit SHH pathway [581], nab-paclitaxel to target SPARC glycoprotein [583], miRNA inhibitors to reprogram CAFs [584] and anti-microRNA as part of peptide-based nanocomplexes aimed at inhibiting PSCs differentiation into CAFs [585].

PSCs, as stated above, are the main responsible for the increased ECM production which ultimately provokes reduced intratumoral perfusion and nanotherapeutic delivery [586]. To overcome the physical barrier of desmoplastic tissue, nanocarriers targeting the stroma have been proposed to enhance drug penetration [587]. As an example, a two-step sequential delivery strategy employing at first liposomes loaded with a nitric oxide donor (aimed at inhibiting the production of dense stroma) and then gemcitabine-loaded liposomes resulted in enhanced gem delivery and tumour growth inhibition [588]. Another recent study applied to orthotopic xenograft mouse models of PDAC involved an anti-stromal pre-treatment with chloroquine-loaded poly lactic-co-glycolic acid (PLGA) NPs targeting PSCs prior to gemcitabine administration, whose effect was the restraint of tumour progression and a reduction of PSCs activation [589].

These works strongly support the idea of an efficient stroma modulation as a necessary first step to perform in order to normalize the TME and therefore allow a better intratumoral therapy administration.

e. Exosomes

Exosomes' nano-engineering has been recently proposed as a promising way to obtain biomimetic as well as highly tunable vehicles for cancer therapies, and some attempts have already been applied to pancreatic cancer therapy in the context of diagnosis, drug delivery and immunotherapy.

A 2021 study by Choi and colleagues [538] proposed a technology exploiting lectin-conjugated Janus nanoparticles (JNPs), able to detect pancreatic cancer cell-derived exosomes with high affinity in a microfluidic device thanks to the lectin-glycan interaction; Pu and co-workers [525] used a tethered cation lipoplex nanoparticle biochip to examine the level of exosomal microRNA-21 as a biomarker for PC. Both these approaches were non-invasive ones, based on blood and plasma samples and meant for diagnostic purposes. The incorporation of galectin-9 siRNA by means of electroporation and the surface modification with oxaliplatin of bone marrow mesenchymal stem cell (BM-MSC) exosomes was proposed by Zhou et al. [537] to target PC and to elicit anti-tumour immunity through immunosuppressive reversal of M2-like tumour associated macrophages (**Figure 5d**). Exosomes' engineering by membrane fusion with liposomes using the freeze-

thaw method was reported in a study by Sato to obtain hybrid tunable nanocarriers for drug delivery [590]. Finally, an immunotherapy nanoparticle-based approach was proposed to deliver plasmid DNA to pancreatic cancer cells via hyaluronic acid-poly(ethylene imine)/hyaluronic acid-poly(ethylene glycol) (HA-PEI/HA-PEG) self-assembling nanoparticle-based non-viral vectors, in order to modulate their exosomal cargo to achieve a macrophage reprogramming [591]. Exosomes are usually the object rather than the active subject of the afore-mentioned pancreatic cancer nanomedicine approaches, which instead are mainly focused on influencing their composition by engineering the cells of origin or on targeting them with nanoparticles to improve diagnosis. A 2016 study on murine hepatoma reported dual-functional exosome-based superparamagnetic nanoparticle cluster used as drug delivery systems [539]. Some years later, Liu and co-workers designed a functionalized smart nanosonosensitizer by loading a porphyrin sensitizer, with therapeutic and imaging functions, on both the surface and in the core of homotypic tumour cell-derived exosomes, for US-responsive controlled release and enhanced SDT tested on various tumour models [540]; nevertheless, literature regarding pancreatic cancer applications is currently missing. A promising multimodal therapy could involve exosomes as biomimetic coatings of inorganic nanoparticles, to enhance their biostability while imparting them specific tumour homing capabilities, thanks to the surface proteins exposed by their membranes [592].

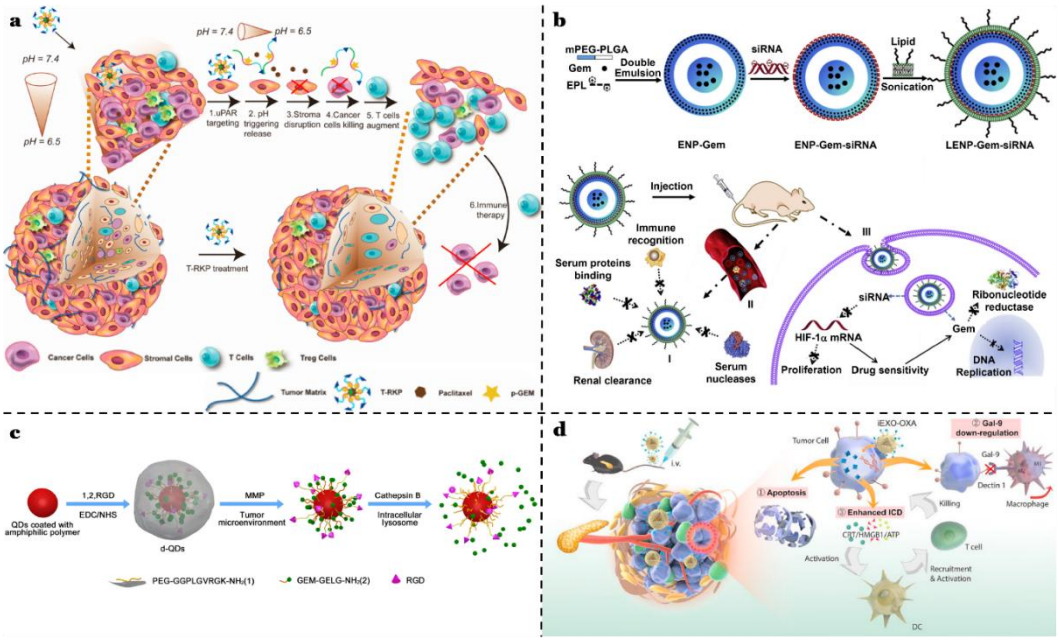

Figure 5. A) Mechanism of TME targeting strategy and pH-triggered micelles disintegration, with consequent dual drug release. Reproduced with permission from [570].

Copyright 2019, The Authors, Published by American Chemical Society. B) Schematic illustration of the fabrication and the tumour cell uptake of lipid-polymer hybrid NPs co-delivering (HIFα)siRNA and gemcitabine. Reproduced with permission from [530]. Copyright 2014, The Authors, Published by Elsevier Ltd. C) Scheme of the preparation of dual enzymatic reaction-assisted gem nanovectors, able to achieve multistage tumour targeting and drug release. Reproduced with permission from [571]. Copyright 2017, The Authors, Published by American Chemical Society. D) Mechanism of immunotherapy enhancement by PC-targeting exosomes, resulting in reversal of immunosuppressive M2-TAMs. Reproduced with permission from [537]. Copyright 2020, The Authors, Published by Elsevier Ltd.

f. Photodynamic therapy

The use of nanoparticles has been proposed to overcome some limitations of photodynamic and sonodynamic therapies when applied to pancreatic cancer. The delivery of photosensitizers to the TME could be facilitated by encapsulating them into nanocarriers [554,555]. Even more simplified, semiconductor nanoparticles able to be photoexcited by light to produce ROS can be used to carry PDT, taking care to coat such inorganic particles with a biomimetic lipid bilayer to promote stability in biological media and rapid cell internalization [593]. Furthermore, nanoparticles or nanorods could be exploited to produce oxygen in situ, thus alleviating hypoxia [558,559].

A recent review reported current clinical studies concerning PDT against PC, highlighting the main advantages of its use: better tumour targeting, improved quantum yield and hypoxia relief [556]. Herein, those involving the use of photosensitizer nanoparticles in the context of multimodal treatments are briefly described. In a 2016 study, the use of nanophotoactivable liposomes co-delivering the photocytotoxic chromophore benzoporphyrin derivative monoacid A (BDP) and the anti-VEGF monoclonal antibody bevacizumab was proved successful when applied to ASPC-1 cells and to a subcutaneous mouse model of PDAC, since their combination enhanced cytotoxicity and tumour reduction thanks to the simultaneous spatiotemporal delivery of both agents [594]. A multi-inhibitor nanoliposome (PMIL) was then proposed by Spring et al. to impart light-induced phototoxicity combined with a spatiotemporal-synchronized release of a multimolecular inhibitor with anti-angiogenic activity, in order to avoid treatment escape signaling pathways while suppressing tumour regrowth in two mouse models of PDAC [595]. A year later, a gold nanocluster-based platform for PTT/PDT composed by a PTT-carrier gold nanocluster, a targeting peptide, a PDT therapy prodrug and an imaging agent was proposed as an innovative strategy to enhance PDAC treatment (**Figure 6a**), showing high tumour uptake and accumulation [453].

A chemo-photodynamic combination therapy was applied in a study by Zhang and colleagues to alleviate PDAC hypoxia by using Fe(III)-complexed porous coordination network (PNC) encapsulating PTX NPs. The obtained nanoconstruct, tested on both cell lines and animal models of PC, was able to release drug in response to laser irradiation and pH changes and to convert H_2O_2 in the tumour site to O_2, regulating hypoxia; moreover, it was suitable as MRI contrast agent [596]. Another recent multimodal strategy included oxygen-delivering polyfluorocarbon nanovehicles loaded with photodynamic $DiIC_{18}(5)$-DS (DiD) and chemo-immunomodulatory gemcitabine prodrug (**Figure 6b**), which exhibited preferential tumour accumulation and ROS production upon laser irradiation, with consequent antitumor immune responses in a PANC02-induced pancreatic cancer model [597].

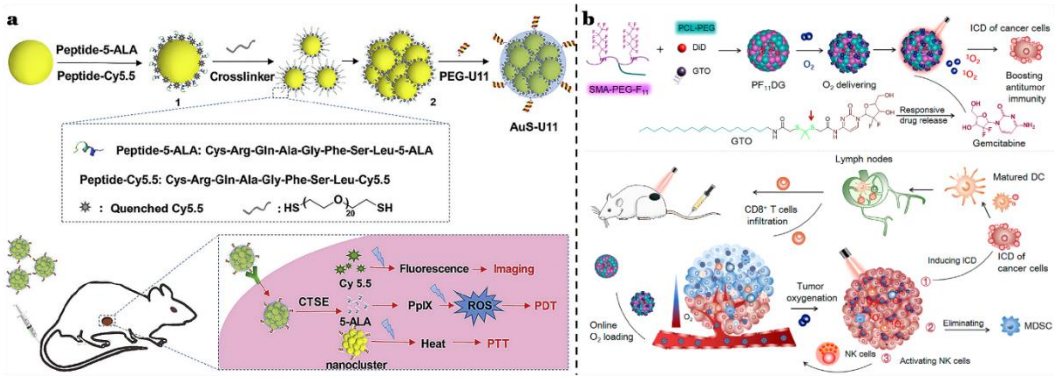

Figure 6. A) Preparation and mechanism of action of gold nanocluster-based platforms for synergistic PTT/PDT. Reproduced with permission from [453]. Copyright 2017, The Authors, Published by Elsevier Ltd.; B) Schematization of oxygen-delivering polyfluorocarbon nanovehicles preparation and their ROS production and gem release upon laser irradiation. Reproduced with permission from [597]. Copyright 2021, The Authors, Published by American Chemical Society.

g. Sonodynamic therapy

Due to the nature of its TME, PDAC poses many obstacles to the effective delivery of sonosensitizers and to a successful application of sonodynamic therapies. The limitations of organic sonosensitizers can be mitigated by their conjugation with nanosized particles able to deliver them to the target regions, thus improving their accumulation and efficacy [455] ; on the other hand, the drawbacks of inorganic sonosensitizers have been addressed in the course of the years with different surface modification strategies [561] such as electrostatic adsorption using grafted copolymers exploiting exposed -OH groups [598], creation of oxygen-deficient layers on the surface of the NPs [599] or noble metal coupling [560]. Other

inorganic sonosensitizers are silicon (Si) NPs [600,601], polyhydroxy fullerene (PHF) [602], composite nano-sensitizers consisting in graphene oxide nanosheets coated by mesoporous silica and decorated with RB-PEG-conjugated iron oxide NPs [603], Au NPs conjugated with PpIX [604] and other nanocomposites made up of metal coordinated porphyrins [465,605].

A novel technique that is currently capturing increasing attention is the so-called Sonosensitizer-Free SDT: its aim is the generation of ROS species to kill cancer cells by means of an indirect US trigger to boost the initial reaction and enhance inertial cavitation, without using any traditional sonosensitizers [606–609]. To achieve this goal, solid state semiconductor nanoparticles like titania or zinc oxide were proposed, combined with ultrasonic shock waves, achieving relevant cell damage and a so-called nanoscalpel effect, leading to cell death [610,611]. Most recently, gas-generating nanosystems have emerged as theranostic nanoplatforms that can be activated by either exogenous or endogenous triggers, enhancing the presence of specific gases in the TME with consequent cytotoxic or therapeutic effects [562].

An example of CO_2 delivery to pancreatic tumour was proposed in a study by Zhang and colleagues, in which a carrier consisting in hollow mesoporous silica nanoparticles (HMSNs) and L-arginine (LA) was triggered by low intensity US, generating and releasing a large amount of CO_2 bubbles **(Figure 7)**. According to the authors, necrosis in Panc-1 cells in vitro and in vivo was due to a combination of the acidic environment (endogenous trigger) and the US stimulus (exogenous trigger) [612].

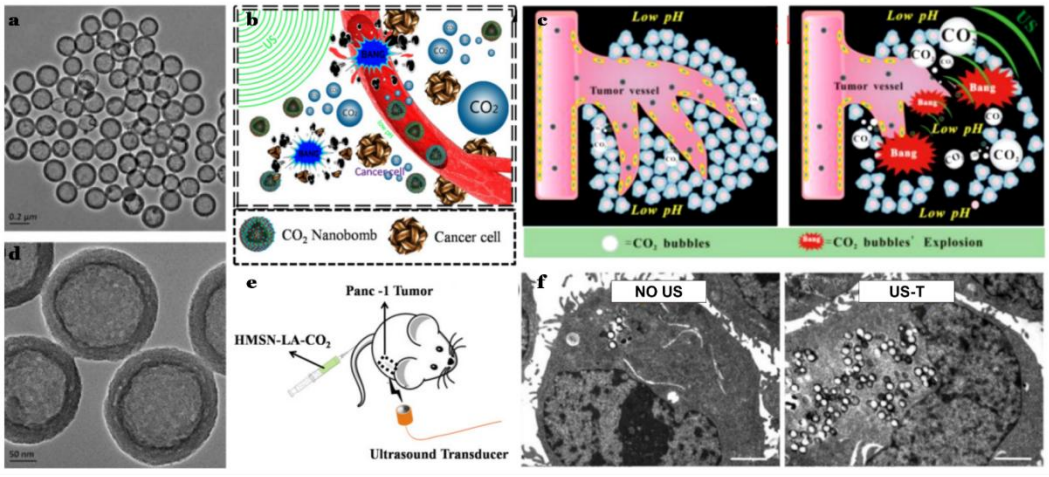

Figure 7. A,D) TEM images of HMSN-LA-CO_2. B) Schematization of CO_2 nanobombs' therapeutic mechanism. C) CO_2 bubbles' explosion (inertial cavitation) triggered by US radiation (right), compared to suppressed inertial cavitation taking place

in absence of US stimulation (left). E) therapeutic procedure of HMSN-LA-CO_2. F) Bio-TEM images of panc-1 cells treated with HMSN-LA-CO_2, showing internalization with (right) and without (left) US. Reproduced under terms of the CC-BY-NC license. [612] Copyright 2015, The Authors, Published by Ivyspring International Publisher.

A 2015 study applied oxygen-carrying lipid-stabilized microbubbles (MB) decorated with a Rose Bengal sensitizer (MB-RB) on pancreatic cancer models (BxPC-3) in vitro and in vivo. Their effects were a higher cytotoxicity in cells cultured under hypoxic conditions and treated with US and a reduction of the tumour volume in mice. Overall, this result confirmed the efficacy of oxygen delivery in hypoxic tumours and its valuable contribution to SDT enhancement [449], and echoed similar studies proposed by the same author, which exploited polymeric microbubbles as delivery vehicles for sensitizers [613] and a novel combination of chemotherapy and sonodynamic therapy using gemcitabine loaded/oxygen carrying microbubbles [614].

Another example of multimodal therapy involving SDT was proposed in 2017 by Sheng et al.: their study designed magnetically responsive microbubbles consisting of an oxygen core and a phospholipid coating functionalized with RB and/or 5-FU, for the combination of antimetabolite and sonodynamic therapy on PC, which produced promising results [615]. A similar study by Nesbitt proposed the use of gemcitabine loaded microbubbles for a targeted chemo-sonodynamic combination therapy of PC [616]. Although the size of these lastly mentioned particles was at the microscale, excluding them from the category of purely nanomedicine approaches, these studies are of pivotal importance to understand the role of multimodal strategies to better address PDAC treatment and hence have been here briefly reported (**Figure 8b**).

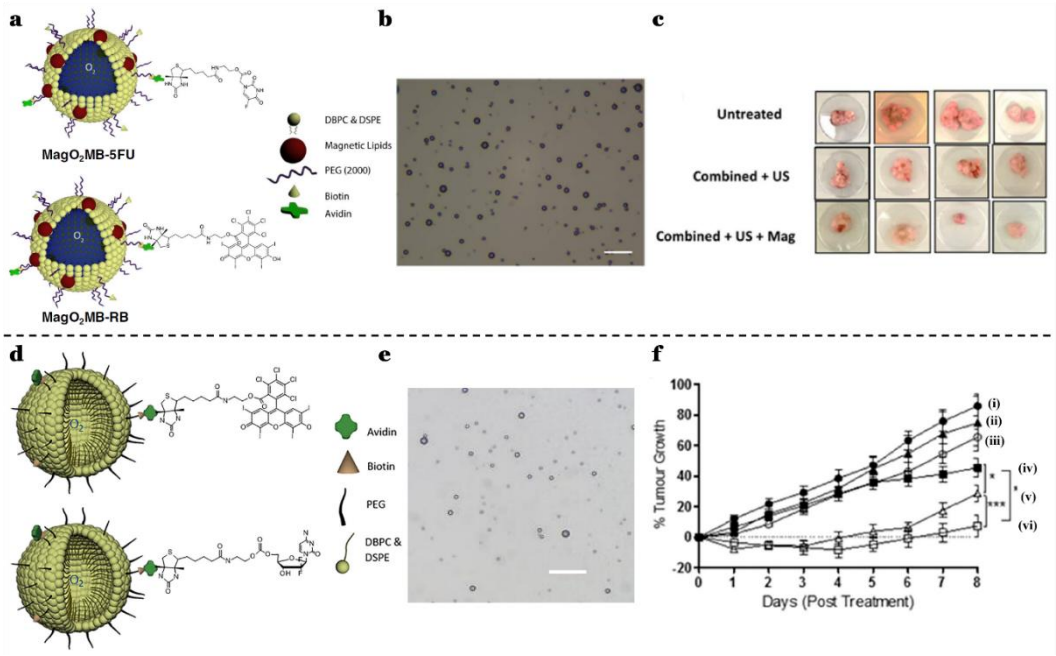

Figure 8. A) Scheme of the MagO$_2$MB-RB and MagO$_2$MB-5FU conjugates. B) Optical microscopic images, scale bar 20 μm. C) photos of removed orthotopic BxPC-3 Luc tumours untreated (top), treated with the two combined conjugates MagO$_2$MB-RB and MagO$_2$MB-5FU + US (center), treated with the two combined conjugates + US and magnet (bottom) Reproduced under terms of the CC-BY license. [615] Copyright 2017, The Authors, Published by Elsevier B.V. D) Scheme of the O$_2$MB-RB and O$_2$MB-Gem conjugates. E) brightfield images of a suspension of the two conjugates, scale bar 20 μm; (f) tumour growth in mice models with (i) no treatment, (ii) O$_2$MBGem/O$_2$MB-RB on Day 0 and Day 3 - ultrasound, (iii) ultrasound only, (iv) Gem IP at 120 mg/kg, (v) O$_2$MB-Gem/O$_2$MB-RB on Day 0 + ultrasound, (vi) O$_2$MB-Gem/O$_2$MB-RB on Day 0 and Day 3 + ultrasound. Reproduced with permission from [616]. Copyright 2018, The Authors, Published by Elsevier B.V.

A nanoplatform able to self-produce oxygen in hypoxic PANC-1 pancreatic cancer was proposed by Chen and colleagues **(Figure 9)** and consisted in hollow mesoporous organosilica NP carriers loaded with IR-780 iodide sonosensitizer and coated in modified fluorocarbon (FC) chains that provided binding sites for oxygen (the final nanoplatform was called FHMONs). In vitro applications of FHMONs proved that US could enhance their intracellular uptake via sonoporation; once internalized, they reduced hypoxia providing oxygen supply, which in turn helped the production of ROS and enhanced the efficacy of SDT. In vivo studies showed that US application fulfilled a triple function: (I) it provoked the breaching of tumour barriers, allowing the accumulation of the nanoconstructs into the solid

tumour; (II) it generated O_2 bubbles and their release broke stroma barriers and reduced hypoxia; (III) it reinforced SDT effect by diminishing hypoxia-induced resistance to SDT [617].

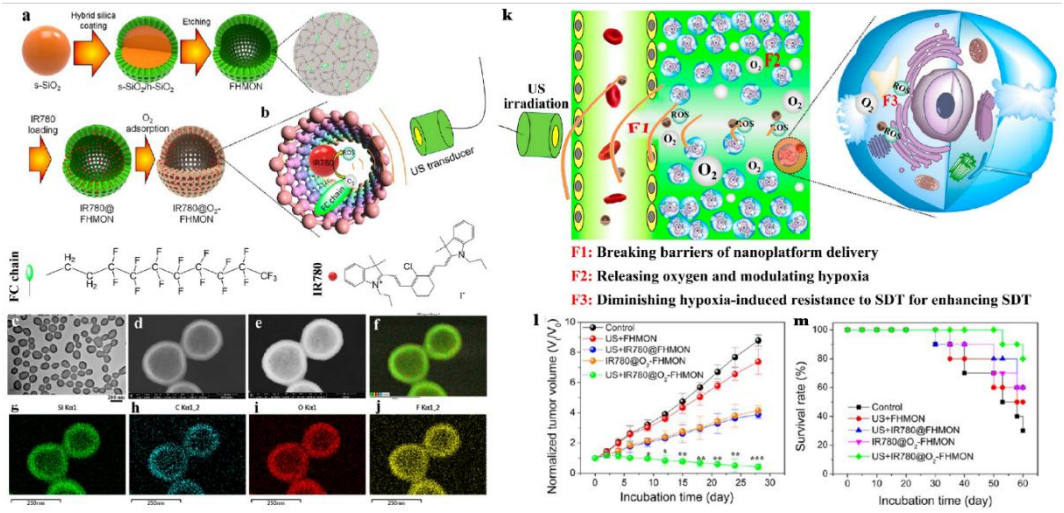

Figure 9. A-J) Scheme of the synthesis process, mechanism of action and characterizations of IR780@O_2-FHMONs. K) in vivo triple effect of IR780@O_2-FHMON nanoplatforms. L) tumour volume variation of PANC-1 solid tumours after the reported treatments. M) Survival rate of solid tumour-bearing mice after treatments. Reproduced with permission from [617]. Copyright 2017, The Authors, Published by American Chemical Society.

Finally, a recent study proposed a pioneering pancreatic cancer therapeutical approach based on SDT: a US trigger of a cascade process **(Figure 10)**. Thanks to this, polymer-peptide conjugates self-assembled into nanoparticles once inside a pancreatic cancer orthotopic model. In brief, the complete nanoconstructs (called PTPK) comprised a sonosensitizer (purpurin 18, P18) decorated by a cytotoxic peptide (KLAK), linked via thioketal bond to a mPEG; being hydrophilic, the PTPK could dissolve as a single chain in blood circulation and penetrate the tumour, where a following focused US led to the formation of $^1O_2$. The effects of this radical were the thioketal bond cleavage and the consequent acquisition of hydrophobicity. This in turn resulted in a self-assembly in the tumour site, where the nanoparticles proved to induce enhanced tumour inhibition through apoptosis by mitochondrial disruption [618].

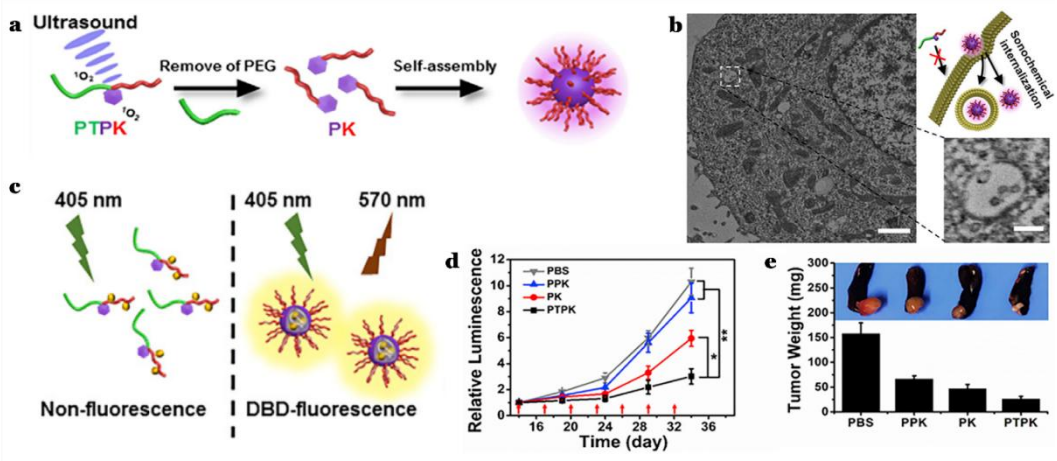

Figure 10. A) Scheme of the proposed cascade effect triggered by US to self-assemble polymer-peptide conjugates into nanoparticles once inside a pancreatic cancer orthotopic model. B) Bio-TEM images of Panc-1 cells incubated with PTPK after US treatment, scale bar 1 μm (left), 400 nm (right). C) Fluorescence detection to verify the self-assembly under US irradiation. D) Tumour volume changes in mice after different reported treatments and US irradiation. E) Average tumour weight and photos. Reproduced with permission from [618]. Copyright 2020, The Authors, Published by Elsevier.

The studies presented so far provide evidence that micro/nanocarriers play a crucial role in reinforcing the effect of organic sonosensitizers or gas molecules, by protecting them in biological media and by ensuring their correct delivery and accumulation in the tumour sites. Moreover, they offer the possibility of incorporating multiple agents as payloads, thus obtaining highly tunable nanoconstructs whose US activation can be exploited not only for the for the SDT enhancement due to the presence of the sonosensitizers, but also for the release of chemotherapy drugs or other cargoes with different and complementary therapeutic activities.

However, important issues concerning nanocarriers have been raised with respect to their biostability and biodegradability, which must be ensured to avoid cytotoxic effects. Furthermore, their ability to potentially introduce chemical modifications to their cargoes has to be carefully evaluated, since the cargo pharmacodynamics, pharmacokinetics and therefore potency could consequently be compromised. Biosafety becomes particularly relevant when the previously reported inorganic materials such as TiO_2 [598], silicon NPs [560] and HMONs [617] are used as sonosensitizers or in addition to them to enhance SDT. On the contrary, liposomes are mainly employed as organic sonosensitizers carriers and are supported by an extensive literature about their use as drug delivery systems [312].

They are typically composed by FDA approved chemical species and consequently they arouse less biocompatibility concerns.

h. Immunotherapy

Due to promising results reported with other tumour types [619,620], the employment of NPs has been proposed to potentiate anti-tumor immune response in PDAC too, given the typically limited success achieved by means of conventional immunotherapy.

Xie and colleagues proposed intraperitoneal (IP) administration of cholesterol-modified polymeric CXCR4 antagonist (PCX) NPs for the co-delivering of anti-miR-210 and siKRAS^{G12D} to an orthotopic syngeneic pancreatic tumour (**Figure 11a**). The nanoconstruct in question possessed a triple therapeutic effect, namely blocking cancer-stroma interaction, inactivating PSCs and killing PC cancer cells. This combined therapy resulted in stroma depletion, reduction of immunosuppression, inhibition of metastases and prolonged mice survival [547].

Lu et al. reported the design of an IV injectable nanocarrier composed by a lipid bilayer (LB) coated MSNP platform incorporating oxaliplatin in the porous interior and IND-PL (an IDO inhibitor) contained in the LB. The novelty of the study was the generation of a synergistic immune response by co-delivering an immunogenic cell death stimulus through OX, while interfering in immune suppression thanks to the IDO inhibitor [545] (**Figure 11b**).

Paclitaxel-loaded 3-aminophenylboronic acid-modified low molecular weight heparin–D-α-tocopheryl succinate micellar nanoparticles (PLT/PTX NPs) were designed and injected by tail vein in orthotopic PAN02 pancreatic mouse models to investigate their effect on both primary tumour and metastases, and showed an inhibition of tumour growth as well as a reduction of distant metastases, due to the improvement of the immune microenvironment of PDAC [549] (**Figure 11c**).

Lorkowski's team developed an immune-stimulatory nanoparticle (immuno-NP) co-delivering two immune agonists (cyclic diguanylate monophosphate, cdGMP, and monophosphoryl lipid A, MPLA) aimed at inducing the production of Type I interferons (IFNs), which in turn are known to promote the recruitment of antigen-presenting cells (APCs) and activate T cell priming. Results showed that the systemic administration of immuno-NPs in an orthotopic murine Panc02 model of PDAC and their subsequent accumulation in the perivascular region resulted in an effective uptake by APCs, that eventually lead to an innate immunity boosting [543]. Finally, Li and co-workers developed M2 TAM targeting nanomicelles decorated with a targeting peptide (M2pep) to co-deliver PI3K-γ inhibitor NVP-BEZ 235 and CSF-1R-siRNA both in vitro and in vivo. This co-administration

resulted in the activation of antitumor immune response and in the remodeling of the tumour immune microenvironment [548].Considering the proven immunomodulatory capacities of ablation techniques such as RFA, IRE, microwave ablation (MWA) and cryotherapy, their combination with local immunotherapy was recently proposed for the treatment of locally advanced pancreatic cancer. This multimodal approach showed a marked synergistic effect with respect to the single monotherapies [621]. The most promising results were achieved with SBRT combined with IL-12 microsphere injection in immunocompetent mice [220], IRE and systemic anti PD1 treatment [622] and IRE combined with systemic anti PD1 and intra-tumoral TLR-7 agonist [623] in mouse models.

Likewise, stimuli-responsive treatments such as PDT were shown to enhance antitumour immune response by releasing antigens and immunogenic factors such as DAMPs from dying cells [624–626], and these findings paved the way for their combination with immunotherapy. As an example, a pancreatic cancer mouse model study included the use of a nanoplatform codelivering a bromodomain-containing protein 4 (BRD4) inhibitor aimed at blocking PD-1/PD-L1 pathway and a photosensitizer to enhance PDT; their synergy increased immunogenicity and promoted intratumoral activation and infiltration of cytotoxic T cells [627] **(Figure 11d).**

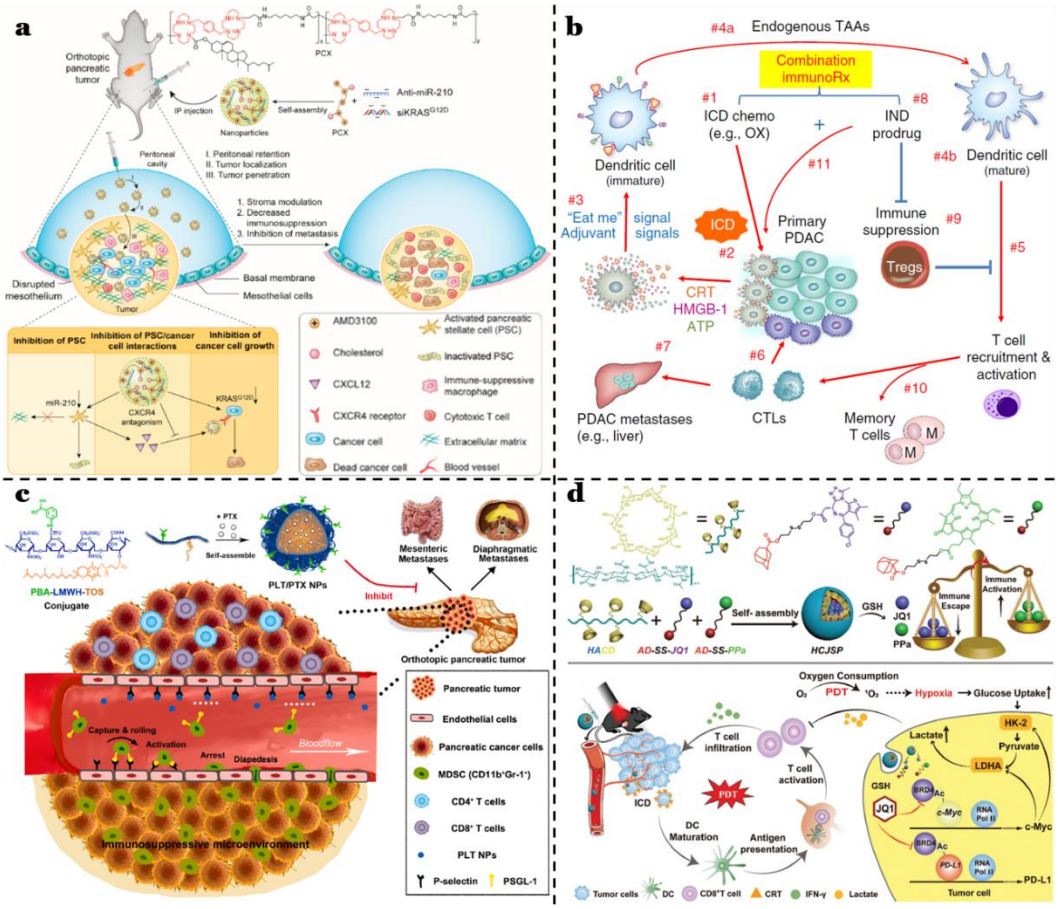

Figure 11. A) Mechanism of EPR-independent delivery of intraperitoneal injected triple miRNA/siRNA nanotherapy and consequent stromal modulation, decrease of immunosuppression and metastases inhibition. Reproduced with permission from [547]. Copyright 2020, The Authors, Published by American Chemical Society. B) Proposed mechanism of PDAC immune response to the synergistic administration of a chemotherapeutic agent (OX) and an IDO inhibitor (IND), resulting in enhanced induced cell death (ICD) and T cell recruitment. Reproduced under terms of the CC-BY license. [545] Copyright 2017, The Authors, Published by Springer Nature. C) Mechanism of micellar NPs' self-delivery to both an orthotopic PC and to its spontaneous metastases, with consequent remodulation of the immune microenvironment. Reproduced with permission from [549]. Copyright 2021, The Authors, Published by Elsevier B.V. D) Prodrug NP preparation via self-assembly and proposed mechanism of combinatory immunotherapy, promoting T cell activation and infiltration and overcoming adaptive immune resistance. Reproduced under terms of the CC-BY license. [627]. Copyright 2021, The Authors, Published by Wiley-VCH GmbH.

Since SDT was proved to induce apoptosis and necrosis as well, and to elicit inflammatory immune response as a consequence of tumour cell debris release and necrosis [628], a mechanism of immunomodulation similar to that triggered by PDT was suggested. In particular, a 2017 study demonstrated that high levels of IL-2 and low levels of IL-10 were observed in mice treated with sonosensitizer-assisted SDT up to 10 days after treatment, denoting an activation of immune response, inflammation and a switch from T_H2 to T_H1 cells in hepatocellular subcutaneous and artificially engineered metastatic tumour models [469]. Although not applied to pancreatic cancer, this result was very encouraging since it suggested that a similar strategy could be employed in combination with immune adjuvant therapy to provide a systemic treatment modality, as later effectively demonstrated on murine hepatoma cells and subcutaneous heap1-6 tumour models [629] and to deep-seated tumours such as PDAC thanks to US penetration.

In fact, a very recent study applied SDT during systemic administration of MB-RB, combined with PD-L1 ICI treatment in a mouse model of pancreatic cancer. The mechanism proposed by the authors was a production of DAMPs due to SDT, which in turn provoked DCs maturation and migration to lymph nodes. Once there, they could present antigens to $CD4^+$ and $CD8^+$ T cells, that therefore were activated and returned to the circulation to infiltrate the tumour. Finally, PD-1/PD-L1 blockade by means of antibodies avoided the inhibition of T cell activation and enhanced the therapeutic effect, indicating a strong systemic immunogenic response [630].

Finally, chimeric antigen receptor T (CAR-T) cell therapy is rapidly emerging as a promising new cancer treatment [631]. It consists of the modification of autologous T cells, engineered to expose specific receptors (CARs) which then can specifically direct them towards tumour-associated antigens in an MHC-independent manner, eventually leading to the elimination of the tumour in question. Although being currently studied in view of pancreatic cancer applications [632,633], its effective application is typically hindered by the TME strong antagonism to T cells exhibited by PDAC [263,322].

A recent review reported in detail all the currently ongoing clinical trials regarding PDAC application of CAR-T cell therapy, and highlighted the importance of a multidisciplinary approach, involving immunotherapy or chemotherapy administrations, aimed at preconditioning and sensitizing the TME to achieve better therapeutic outcomes [634]. Therefore, the use of nanoconstructs and nanocarriers able to specifically target the tumour zone could be exploited to enhance these cell therapies in various ways. In this regard, a study by Zhang and colleagues proved that the administration of lipidic nanoparticles decorated with an iRGD peptide and

loaded with a PI3K inhibitor and an α-GalCer agonist could create a therapeutic window of TME immune stimulation, exploitable for T cell therapy, in different solid tumour mouse models [635]. A mild hyperthermia elicited by photothermal therapy was observed to promote solid tumour infiltration and antitumor activity of CAR-T cells [636], and the use of nanoparticles could potentially further increase this effect: indeed, a recent work by Yu et al. reported the enhancement of ICI-based immunotherapy against metastatic pancreatic cancer when photothermal therapy was applied in the presence of dual responsive lipid-albumin NPs [637] (**Figure 12**). Another study reported the administration of polymeric nanoparticles, loaded with a DNA payload coding for CAR (specifically leukemia CAR genes), to circulating T cells to impart them with long-lasting tumour-recognizing capabilities in mouse models [638]. Current research in the context of PDAC immunotherapy is also focusing on the search of further cancer-associated antigens as possible targets for CAR-T therapy, and promising data have emerged with respect to the use of anti-CD40 antibody for immune modulation; therefore, the use of antibody-decorated nanoparticles could help enhancing the efficacy of these two applications [3].

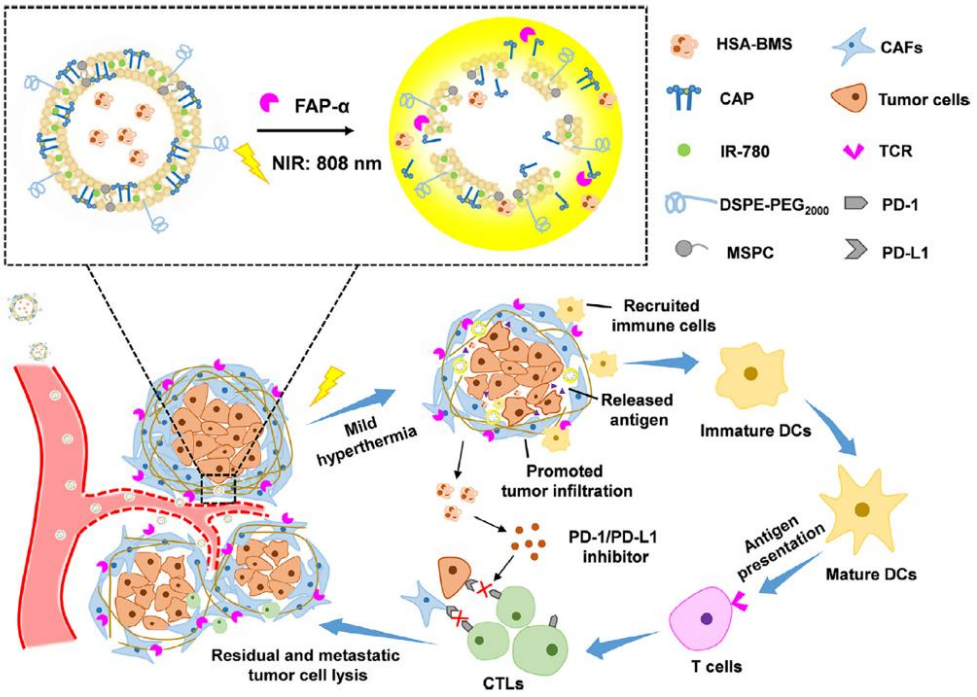

Figure 12**.** Effect of mild-hyperthermia induced by PTT and combined with ICI therapy in pancreatic cancer, enhanced by the presence of size-adjustable and thermosensitive lipid-albumin NPs: reduced tumour hypoxia, enhanced blood perfusion, promotion of tumour infiltration by immune cells. Reproduced with permission from [637]. Copyright 2021, Acta Materialia Inc. Published by Elsevier Ltd.

i. Multimodal treatments

Taken together, these findings suggest that the most promising therapeutic options in order to undermine the intricate panorama of dysregulated signaling pathways, chemoresistance, intrinsic and TME-regulated impaired immunogenicity characterizing PDAC should include a multimodal therapy. **Table 2** summarizes the salient multimodal nanomedicine-based PDAC treatments reported so far. In particular, combining local treatments with immunotherapy was proven a promising strategy in the above-reported studies [220,622,623].

Although many combinations have already been established and tested on different tumours in the course of the last decades, little improvements have been achieved with respect to PDAC. Nevertheless, a thorough characterization and understanding of the specific tumours in question could certainly lead to more personalized combined therapies [639], with the final aim of reducing and controlling metastases currently evading the immune response in all those cases in which complete regression of the primary tumour is not achievable.

Table 2. Innovative multimodal therapies against PDAC reported in this work.

Multimodal treatment	Mechanism of action	Preclinical model	Results	Ref
• Lipid-coated mesoporous silica nanoparticle platform codelivering gemcitabine and paclitaxel	• Combination therapy inspired by Abraxane's enhancement of gemcitabine activity • PEG-containing lipid-film-coating procedure to seal the pores and entrap drugs	• Mice carrying subcutaneous PANC-1 xenografts	• Effective tumour shrinkage with respect to free Abraxane • Inhibition of cancer growth • Elimination of metastatic foci	[564]
• Multifunctionalized iron oxide magnetic NPs for selective targeting of PC cells	• Anti-CD47 antibody and gemcitabine included in a single formulation	• Primary cell cultures and PC cell lines, (Panc-1, BxPC-3)	• Drug release occurring under reducing intracellular conditions	[566]

			• Efficient induction of apoptosis compared to the free antibody	
• Stimuli-responsive micelle platforms codelivering paclitaxel and phosphorylated gemcitabine	• PEG coating to enhance biocompatibility • Stroma targeting peptide (AE105) • pH-triggered micelle disintegration for drug release	• MiaPaCa-2 and PANC-02 cells • Balb/c orthotopic PC tumour model (PANC02)	• Disruption of the central stroma • Maintenance of external stroma to prevent metastases • Increase in the number of cytotoxic T cells	[570]
• Dual-enzyme-sensitive gemcitabine nanovectors	• CdSe/ZnS quantum dots • Conjugation with MMP-9 detachable PEG • Targeting ligand (cycloRGD)	• BxPC-3 cells • BxPC-3 xenografts	• Prolonged blood circulation • Enhanced tumour internalization • Effective and specific drug release • Reduced gemcitabine deactivation in blood	[571]
• Co-delivery of HIFαsiRNA and gemcitabine via lipid-polymer NPs	• Lipid coating to prevent aggregation and gemcitabine leakage • Combination therapy strategy with siRNA and chemotherapy	• Panc-1 cells • Subcutaneous and orthotopic Balb/c nude mouse models	• Prolonged life in bloodstream • Synergistic antitumour effects • Inhibition of tumour metastasis in mice	[530]
• Polymeric dual delivery nanosystem for miR-345 and gemcitabine delivery	• Temperature and pH-responsive copolymer	• Capan-1 and CD18/HPAF PC cells	• Sonic hedgehog signaling downregulation	[572]

	• Tunable miR-345 and gemcitabine release • Sustained co-release	• Mice carrying xenograft tumours	• Improved gemcitabine perfusion • Reduced tumour growth • Downregulation of desmoplastic reaction	
• Superparamagnetic iron oxide NPs of curcumin (SP-CUR) enhancing gemcitabine efficacy	• Suppression of aberrant SHH expression in PC • Targeted and sustained curcumin delivery into tumour • Possible application in MRI	• HPAF-II and Panc-1 cells • HPAF-II cells orthotopically injected Into mice	• Effective delivery of curcumin in pancreatic cancer • Combination effect of gemcitabine and SP-CUR • Reduced tumour growth and metastasis • Improved survival	[573]
• Polymeric micelle formulation co-delivering Cyclopamine and paclitaxel	• Extravasation due to small size • Cargo protection in bloodstream • Combination therapy of Hedgehog inhibitor and cytotoxic chemotherapy drug	• Orthotopic PDX mouse models • KPC-Luc transgenic mouse models	• Synergistic attack on both tumour and stromal components • ECM remodeling • Increase of microvessel density • Hypoxia attenuation • Disruption of tumour cells-CAF communication	[576]
• Two-step engineered approach to enhance gemcitabine penetrance	• First-wave nanocarrier based on copolymer-coated mesoporous silica carrying a TGF-β inhibitor • Second-wave PEGylated	• BxPC-3 cells • BxPC-3 tumour xenograft model	• Decreased pericyte coverage of the vasculature • Facilitated systemic biodistribution and retention at the tumour site • Rapid tumour entry of liposomes	[577]

	gemcitabine-carrying liposome		• Shrinkage of tumour xenografts	
• Nanophotoactivatable liposomes co-delivering cytotoxic (BPD) and biologic (bevacizumab) therapeutics (nanoPAL)	• nanoPAL-PDT treatment • Simultaneous spatiotemporal delivery of bevacizumab • Neutralization of VEGF burst following PDT	• AsPC-1 cells • Subcutaneous mouse model of PDAC using AsPC-1 cells	• Photocytotoxicity enhancement • Enhanced cytotoxicity in vitro • Tumour reduction in vivo	[594]
• Photoactivable multi-inhibitor nanoliposome (PMIL) to suppress tumour regrowth and treatment escape pathways	• XL184-loaded NPs encapsulated in nanoliposomes carrying a photoactivable chromophore BPD in the lipid bilayer • PMIL intravenous administration • Near-infrared tumour irradiation	• AsPC-1 cells • Xenograft tumours from AsPC-1 cells (implantation in mice) • Metastatic mouse model by PDAC cells (implantation in the pancreas)	• Photodynamic damage of tumour cells and microvessel • XL184 intratumoral delivery • Prolonged tumour reduction • Suppression of metastatic escape	[595]
• NPs for MRI guided chemo-photodynamic therapy alleviating tumour hypoxia	• Paclitaxel encapsulation in Fe(III)-complexed porous coordination network • Combination of PDT and chemotherapy	• PANC-1 cells • Nude mice implanted with PANC-1 cells	• Drug release in response to laser irradiation • Drug release in response to pH changes • Hypoxia regulation ROS generation in vivo	[596]

	• Fenton-like reaction to convert H_2O_2 to O_2 • MRI imaging for therapy monitoring			
• Oxygen-delivering polyfluorocarbon nanovehicles	• Photodynamic DiD and chemo-immunomodulatory gemcitabine prodrug loading • Laser irradiation	• PANC02 pancreatic cancer model	• Hypoxia-relieving capacity (10-fold enhancement of tumour oxygenation) • ROS production • Responsive drug release • Delay of tumour growth • Boost in antitumour immunity	[597]
• Oxygen-self-produced sonodynamic therapy nanoplatforms (IR780@O_2-FHMONs)	• Mesoporous organosilica nanoparticle carriers • Fluorocarbon (FC) chains offer binding sites for oxygen and IR780 storage • Ultrasound radiation (SDT)	• Hypoxic PANC-1 cells • Nude mice bearing hypoxic PANC-1 solid tumour	• In vitro oxygen supply from IR780@O_2-FHMONs • In vitro ROS generation • Accumulation in hypoxic tumour • In vivo permanent hypoxia relief • Reduction of SDT resistance	[617]
• US-activated self-assembled polymer-peptide nanoparticles (PTPK)	• Deep tissue penetrating polymer-peptide conjugate • Self-assembly due to US irradiation • Departure of hydrophilic PEG	• Panc-1 cells • Panc-1 subcutaneous xenograft mouse models	• Remarkable solid tumour penetrability and spatial precision • US-assisted membrane permealization and	[618]

	from PTPK, resulting hydrophobic interaction		enhanced cellular internalization • Effective inhibition of tumour growth	
• Local administration of triple miRNA/siRNA nanotherapy for stromal modulation	• Cholesterol-modified polymeric CXCR4 antagonist nanoparticles (blocking of cancer-stroma interactions) • Codelivery of anti-miR-210 (PSCs inactivation) and siKRAS^{G12D} (PC cells killing)	• Primary tumour cell line KPC8060 • Orthotopic KPC-derived PC model	• Modulation of desmoplastic TME • Inactivation of PSCs • Promotion of T cells' infiltration • Delayed tumour growth • Stroma depletion • Inhibition of metastasis	[547]
• Supramolecular prodrug nanoplatform for combinatory photoimmunotherapy of PC	• Co-delivery of a photosensitizer and a prodrug of BRD4i • HA-based nanosystem addressing CD44 receptor	• Panc02 cells • Subcutaneous Panc02 model	• Prolonged retention and deep tumour penetration • Promotion of T lymphocyte intratumoral infiltration • Inhibition of tumour growth	[627]
• Combination of sonodynamic therapy and PD-L1 immune checkpoint inhibitor	• Microbubble (MB)-mediated SDT • Lipid-stabilized MBs loaded with Rose Bengal (MB-RB) • IV injection of O_2MB-RB, anti-PD-L1 treatment, SDT	• Bilateral tumour model of PC generated using T110299 cell line	• Decrease in tumour volume • DAMPs production due to SDT and resulting T cell recruitment • Infiltration of $CD4^+$ and $CD8^+$ T lymphocytes	[630]

			• Elicited immune response, potentiated by anti-PD-L1 ICI	
• Exosome-based dual delivery biosystem (iEXO-OXA) to enhance PC immunotherapy and reprogram tumour microenvironment	• Galectin-9 siRNA loaded by electroporation • Surface modification with oxaliplatin (OXA) prodrug as an ICD trigger • Reversal of immunosuppression of M2-like tumour associated macrophages (M2-TAMs)	• PANC-02 cells • Orthotopic PANC-02 PC tumour model	• Exosome-mediated enhancement of tumour targeting • Induction of ICD stimulus • Interference in immunosuppression • Improved DC maturation • Increase of T lymphocyte infiltration	[537]
• PTX-loaded self-delivery micellar nanoparticles able to target PC and its spontaneous metastases	• Immune microenvironment regulation mechanism • Synergistic PTX cytotoxicity • Phenylboronic acid modification improves tumour targeting thanks to sialic acid residues in PC cells	• PAN02 cells • Orthotopic PAN02 pancreatic tumour-bearing mouse models	• Inhibition of MSDC recruitment to PC tissues • Inhibition of spontaneous metastases • Increase in the activity and infiltration of effector T cells ($CD4^+$ and $CD8^+$)	[549]
• Dual immune agonist-loaded immunostimulatory NPs to induce a pro-inflammatory	• Precise ratio control of the immune modulators • Systemic administration	• Orthotopic murine Panc02 model of PDAC	• Deposition in the perivascular regions of the tumour	[543]

immune microenvironment	• Synergistic effect of STING and TLR4 agonists to expand APCs and increase local IFNβ secretion		• Significant uptake by dendritic cells and expansion of APCs • Increase of T lymphocyte tumour infiltration	
• Dual delivery nanocarrier for immunogenic cell death (ICD) induction and immunosuppression interference	• Lipid-bilayer coated mesoporous silica NPs incorporating an immunosuppressive IDO pathway inhibitor (IDN) and an ICD-inducing agent (Oxiplatin) • IV administration	• Orthotopic KPC model	• Induction of effective innate and adaptive anti-PDAC immunity • Recruitment of cytotoxic T lymphocytes in the tumour • Significant tumour reduction • Increase in animal survival	[545]

j. Current nanomedicine-based clinical trials

As stated above, only a small percentage of nanomedicine-based preclinical trials are effectively translated to clinical ones. In fact, there are still several obstacles to nanomedicine systematic application, and failures in clinical trials dramatically increase when it comes to phase II and III. Huge heterogeneity of tumour biology, incomplete understanding of nanoparticles' interactions with biological components, safety issues, difficulties in scaling and production, poor pharmacokinetics, low tumour accumulation and the lack of fully adequate animal models are just some of the reasons behind delays in clinical translation, which in turn has to face issues concerning patient selection and the choice of the best combination therapy to maximize its therapeutic efficacy [640]. **Table 3** reports some selected pancreatic cancer nanomedicines which are currently undergoing phase II and III clinical trials.

Table 3. Nanomedicine-based selected pancreatic cancer clinical trials.

Product	Nanocarrier	Payload	Current Application	Trial Phase	Status
SGT-53	Cationic liposome nanoconstruct	Human wild-type p53 DNA	Combination with gemcitabine/nab-PTX	Phase II study	Ongoing [282] (NCT02340117)
Genexol-PM	Polymeric micelle	Paclitaxel	Combination with gemcitabine	Phase II study	Ongoing [641] (NCT02739633)
NC-6004 (Nanoplatin)	Micellar formulation	Cisplatin	Combination with gemcitabine	Phase III study	Completed [642] (NCT02043288)
Atu027	Cationic liposomal formulation	AtuRNAi	Combination with gemcitabine	Phase I/II study	Completed [643] (NCT01808638)
Nano-SMART	Gadolinium-based NPs	/	Activation and Guidance of Irradiation X (AGuIX) combined with MR-guided SBRT	Phase I/II study	Recruiting [644] (NCT04789486)
NBTXR3	Hafnium Oxide-containing NPs	/	Activation by radiation therapy	Phase I study	Recruiting [645] (NCT04484909)

As far as clinically approved nanomedicines are concerned, two products recognized by both FDA and EMA for PDAC treatment after completing phase III studies are the previously mentioned Abraxane ® (nab-PTX, Abraxis BioScience, CA, USA), and Onivyde ® (Merrimack Pharmaceuticals, Inc., MA, USA, also known as MM-398 or PEP02).

Abraxane was approved by FDA for the treatment of patients with metastatic PDAC in combination with gemcitabine as a first-line treatment in 2013 [257], while Onivyde, namely nanoliposomal irinotecan, was found to be effective in extending the survival of patients with metastatic PDAC previously treated with gemcitabine and was combined with 5-FU and FF in a phase III study (NAPOLI-1) [258,520].

k. Novel preclinical models

Although the contribution of mouse models to major advancements in the understanding of PDAC is undeniable, many current limitations hinder a proper reproduction of its actual microenvironment. Recent advances such as 3D organoids, 3D bio-printing and organs-on-chip aim at better mimicking the intricate tumour/stroma interactions, the influence of the immune system and all the morphological features that contribute to the complexity characterizing PDAC but not provided by other current preclinical platforms [646].

3D Organoids

Tissue-derived embryonic or adult stem cells embedded into a 3D matrix are able to grow and self-organize in structures called organoids [647]. They reproduce more closely the morphology of the in vivo original tissues and are mainly used in cancer research for xenotransplantation, drug screening and discovery, stromal cells co-cultures, immuno-oncology and analyses of mutational signatures, gene expression patterns or proteomics [648]. With the aim of better identifying genes and pathways involved in pancreatic tumorigenesis, a 2015 study [649] modified some existing approaches already applied to other tumours to generate organoids from normal and neoplastic murine and human pancreas tissues. These pancreatic organoids were then used to investigate PDAC pathogenesis since, after orthotopically transplantation into immune-deficient mice, they generated lesions similar to PanIN that were able to progress to locally invasive and metastatic carcinomas. Meanwhile, Huang and colleagues established a procedure to generate pancreatic progenitor organoids from human pluripotent stem cells and from freshly resected PDAC. In contrast with the formerly mentioned study, their culture conditions promoted histostasis, namely the preservation of the differentiation status observed in the original primary tumour. Moreover, they pointed out the short time required by their protocol to establish organoid cultures from the time of surgery (21-45 days), which could minimize genetic drifts. Therefore, they suggested that the resulting organoids, better representing the primary tumour than cell lines and whose realization was relatively fast, could be used to personalize cancer treatments [650].

As previously mentioned, it is now well established that distinct populations of CAFs with different phenotypes exist in mouse and human PDAC tissues. This finding emerged in a 2017 study, in which a co-culture of murine pancreatic stellate cells and PDAC organoids revealed the presence of a subpopulation of CAFs

located distantly from neoplastic cells, later named iCAFs, and activated by paracrine factors secreted from cancer cells. The authors highlighted the importance of this study in partly accounting for the conflicting results emerged in the context of stroma targeting therapies, which had not taken into account the heterogeneity of CAFs populations and behaviors until then [103].

A co-culture protocol of organoids composed by PDAC cells and CAFs derived from the same patient was proposed by Seino and co-workers to investigate the role of stem cell niche factors dependency during tumour progression. In fact, after establishing a library of 39 PDAC organoid lines, they noticed that various Wnt-niche dependencies existed (Wnt being a molecular pathway involved in initiation and progression of PDAC [651]). They concluded that CAFs could transmit a pro-tumorigenic niche signal to PDAC through the production of stromal Wnt ligands, and proposed Wnt-targeting therapeutic strategies as a possible future application, exploiting organoid-centered screenings [652].

The importance of patient-derived organoids (PDOs) resides in their ability to recapitulate the disease of the original tumour and to allow personalized drug screenings: Driehuis et al. compared the molecular characteristics of 30 tumour organoids and then exposed them to therapeutic agents to reveal their drug sensitivity. Therapy responses differed among the PDOs, suggesting that a personalized approach could be the key for future effective treatments and that organoids might be used to guide therapeutic decisions, as previously reported [653], after further validations [654].

Some limitations of organoids, like the lack of some important components of the in vivo TME such as blood vessels and immune cells, must nevertheless be addressed [655]. A recent study by Tsai et al. was the first to report a co-culture of pancreatic cancer organoids, CAFs and T cells, and observed promising results such as activation of myofibroblast-like CAFs and tumour-dependent lymphocyte infiltration, which however require further mechanistic studies to be validated [656].

Emerging innovative techniques therefore aim at improving the poor representation of the TME by simulating its architecture and vascularization [657].

To improve the formation of PDAC cells spheroids realized with the assessed hanging drop technique, Ware and colleagues modified this method by adding methylcellulose polymer. This study was an early attempt of incorporating biopolymers into 3D cell cultures, and the authors observed uniform spheroid formation of 5 different cancer cell lines, namely Panc-1, BxPC-3, AsPC-1, MiaPaCa-2 and Capan-1, with distinct hallmarks of solid tumours such as the presence of a necrotic core, hypoxia and apoptotic regions. Their robustness and

mechanical properties, enhanced by the use of methylcellulose, made them resistant to manipulations and thus applicable as study platforms [658].

3D bioprinting

3D bioprinting consists in the precise deposition of multiple layers of various cell types and biomaterials to generate 3D bioengineered tissues. The main 3D bioprinting techniques are laser-assisted bioprinting, micro-extrusion and inkjet. Cells are suspended in a biocompatible gel-like material (bioink) able to retain their viability and functionality in terms of growth, proliferation and signaling [659]. Cancer applications of 3D bioprinting involve the realization of tumour models based on a computer-assisted design, which eventually contain patient-derived cancer and stromal cells, bioink, ECM proteins, growth factors and genetic material and thus accurately reflect the heterogeneity of real tumours. By mimicking the cell-to-cell and cell-matrix interactions of the TME and the 3D heterogeneity of real tumours, they provide an excellent in vitro support for the study of cancer behaviour in drug screenings and personalized therapies [660,661].

This technique has already been applied to PDAC in some pioneering studies. 3D organoids, produced in flat-bottom well plates with a cell-repellent surface employing a bioprinting technology incorporating a magnetic force, were applied for high throughput screening (HST) purposes. Briefly, two pancreatic cancer cell lines, hT1 and hM1, and two types of cancer-associated fibroblasts (CAFs), hT1-CAFs and hM1-CAFs, were employed to create these organoids, which were tested with more than 3000 approved drugs in a large-scale screening and better reflected the in vivo tumour architecture and drug resistance by comparison to 2D models [662].

In another study, the authors incorporated multiple cell types into bioprinted pancreatic tumour tissues and observed self-organization capabilities, secretion of ECM factors and abilities to respond to extrinsic signals (in the present case GFs). The first part of the study involved the use of a pancreatic cell line, HPAF-II, bioprinted in stromal bioink of pancreatic stellate cells and HUVECs (Human umbilical vein endothelial cells). The resulting tissue was then treated with gemcitabine, showing dose-dependent response. Then, a trial with primary patient-derived tissue, enzymatically disassociated and bioprinted in stromal bioink to compensate the lack of stromal tissue typical of PDXs, was performed. Notably, similar morphology to the PDX model but also to the primary tumour was observed, and the spatial organization was replicated thanks to 3D organization of cells. Finally, the bioprinted tissue derived from PDX tissue showed resistance to

gemcitabine and therefore was suggested to be used as a test platform for therapeutic sensitivity [663].

Finally, a 2020 study executed laser assisted bioprinting (LAB) of spheroid arrays from exocrine acinar and ductal pancreatic cells on a gelatin methacrylate (GelMA) substrate to study the initial stages of PDAC development. The evolution of the bioprinted spheroids was explored over time, and cell-to-cell communication by heterotypic signaling between acinar and ductal cells was proved to be implicated in the proliferation/survival of these last [664].

3D-printing technologies offer great control over geometry, cell deposition and composition; moreover, cells can be manipulated prior to printing and cell composition in bioinks is highly customizable. Therefore, stromal cells can be incorporated to better mimic the TME, and they can be tuned in order to match with the composition observed in patients, thus allowing personalized therapies. Future improvements should include the addition of other main components of the TME, such as well-established vascular networks and cellular secretions to study paracrine signaling intrinsic of each studied tumour. Nevertheless, the lack of standardized protocols is the main obstacle in terms of clinical translation of these bioprinted tissue models [661].

A preliminary study concerning 3D scaffold [665] applications to pancreatic cancer was reported in 2015. Ricci and colleagues analyzed the interaction between PDAC cells and three polymeric scaffolds, which offered different pore topographies and architectures. Their results suggested that a sponge-like scaffold was able to support the generation of aggressive pancreatic tumour models [666].

A work by Totti et al. was the first to fabricate 3D highly porous polyurethane (PU) scaffolds coated in fibronectin to support the proliferation of pancreatic tumour cells; the resulting system was close to in vivo models in terms of cells proliferation, collagen production, formation of hypoxic regions and heterogeneity of biomarker spatial distribution [667].

Recently, Gupta and co-workers improved the previously mentioned work by developing a multicellular model involving cancer cells, endothelial cells and stellate cells cultured on a PU scaffold. Moreover, specific ECM protein-coated zones were implemented to mimic in vivo different cell distributions and induce selective cell adhesion. With respect to prior works, this hybrid model of the PDAC niche successfully supported proliferation and migration for longer time [668].

Scaffold-based cultures are undoubtedly showing very promising results, but they must be further improved to incorporate crucial PDAC elements such as blood vessels and immune cells. Future applications should also involve the

implementation of perfusion systems to provide these models with more physiological culture conditions.

Organs-on-chip

Organs on chip (OOC) are microfluidic devices made of plastic, glass or polymers (mostly Polydimethylsiloxane, PDMS) with hollow micro-channels containing viable cells, which are nourished with controlled flowing culture medium and thus provided with nutrient and oxygen supplies. Cancer applications include (I) the incorporation of multiple cell types, like those typically present in the TME, to allow the study of the interactions between cancer cells and surrounding tissues, (II) the modelling of microvascular networks to assess anti-angiogenic drugs and study tumour vascular perfusion; (III) the study of cancer cells' extravasation and migration to induce metastasis formation [669].

Due to their ability in recapitulating the microenvironments of in vivo tissues, OOC models have been applied to pancreatic cancer with the final aim of providing a complex multicellular model of human PDAC on a chip, designed for drugs and therapeutics testing. One of the first applications included an in vitro model consisting of pancreatic stellate cells co-cultured with PDAC cells in an accessible 3D construct with a spatially controlled architecture, which was proposed as an alternative platform for drug evaluation [670].

Later on, Beer and colleagues cultured PDAC cells into a cyclic olefin polymer microfluidic chamber enriched in collagen, which offered an optimal surface for cell attachment and proliferation. In fact, cells showed morphological appearance and growth characteristics resembling grown 3D spheroid models and responded to cisplatin treatment, perfused through the chip, bearing higher doses than classical in vitro 2D and 3D cultures [671].

A 2019 study reported an OOC that emulated tumour-blood vessel interactions and vascular invasion in PDAC. A biomimetic ductal channel containing PDAC cells was juxtaposed to a rudimentary blood vessel consisting of a perfusable endothelial lumen. Endothelial ablation and PDAC cells invasion into the vessel lumen were observed, and these behaviors were consistent with poorly vascularized tumour tissues noticed in histological studies and the high rate of circulating tumour cells and metastases formation in PDAC [672].

A recent work focused on the study of EMT and local invasion using a microfluidic platform called ductal tumour-microenvironment-on-chip (dT-MOC), in which murine pancreatic cancer cells isolated from GEMMs were embedded in a perfused collagen matrix and co-cultured, forming a biomimetic duct. The integration of cancer cells whose genetics and molecular characteristics were

carefully engineered ensured a close imitation of the intratumoral heterogeneity; nevertheless, future developments could involve the culture of stromal cells derived by patients [673]. Finally, a 2020 study combined patient organoids and an OOC platform mimicking a perfusable vascularized vessel to accurately recapitulate a dynamic TME. Fibroblasts and endothelial cells (HUVECs) were included in the culture, and the crosstalk between the organoid and stromal fibroblasts resulted in their activation into myofibroblasts and in an increased proliferation of the resulting co-culture. Moreover, collagen secretion by fibroblasts contributed to gemcitabine resistance when the drug was perfused through the vasculature [674]. The high degree of control and flexibility is certainly one of the main advantages of bioengineered 3D approaches, and their enormous potential in implementing PDAC biomimetic platforms will certainly be the key to future patient-specific therapies.

1.13 Conclusions and future outlooks

Despite major scientific and medical progress, pancreatic cancer is one of the most lethal malignancies nowadays, and its diagnosis and treatment are hindered by the bewildering complexity and resistance displayed by its microenvironment. In fact, the plethora of interlinked molecular and signaling pathways, the highly hypoxic TME, the innate and acquired drug resistance and the impaired immune response are all factors that must be taken into careful consideration while designing new PDAC treatments. Moreover, the options which go beyond conventional therapies are still very limited and must face many difficulties related to their application to clinic. A thorough understanding of PDAC pathology, carcinogenesis, altered molecular pathways, tumour biology and current therapeutic limitations is an imperative requirement in order to successfully design and implement new strategies to ultimately overcome this malignancy. The purpose of this review was therefore to provide an in-depth and updated dissertation on the topic first, before reporting major advances in current treatments and focusing on their possible future evolution.

The studies presented thus far provide evidence that multimodal approaches might be the most promising way forward ultimate PDAC treatment, and that nanomedicine advances will continue to boost the efficacy of emerging treatment options. Nanoparticles nowadays constitute an impressive arsenal of highly customizable weapons against tumours, however enormous challenges need to be faced to treat advanced and metastatic PDAC, and current research on personalized therapies is still under intensive investigation. In fact, cell cultures and animal models are not able to recapitulate the EPR effect in humans and are therefore

inadequate to accurately mimic drug distribution and more broadly PDAC heterogeneity and response. Therefore, exploiting new bionanotechnological insights to establish new preclinical models, presently at their infancy, is urgently required to guarantee a more robust reproducibility of PDAC TME; furthermore, these engineered models might provide more effective and precise testing platforms for novel promising nanomedicine-based approaches.

A multimodal and highly interdisciplinary approach, combining conventional and novel therapies and applying nanomedicine and nanotechnological advances to our continuously evolving PDAC knowledge, is expected to eventually lead to robust patient and tumour specific treatments. Finally, the necessary convergence of local and systemic therapies and their consequent coadministrations, according to precise and evidence-based ratios and time intervals, has the potential to maximize the effectiveness of both approaches. The final aim will be developing high precision and personalized treatments, eventually able to dramatically improve PDAC patients' survival rates in the foreseeable future.

Chapter 2

Lipidic formulations inspired by Covid vaccines as smart coating to enhance nanoparticle-based cancer therapy

The first step towards the preparation of a complex nanoparticle-based multimodal therapy against PDAC as those introduced in the first chapter of this PhD dissertation must therefore include a strong core material and a biomimetic coating. The rationale for selecting zinc oxide nanoparticles as the preferred material will be discussed in detail in the third Chapter. The present Chapter will focus on the implementation of lipidic formulations inspired by COVID-19 vaccines, with the dual purpose of both shielding the zinc oxide nanoparticles and providing a customizable platform for additional functionalization.

2.1 Introduction

Liposomes have been an object of research since the 1960s, when they were first introduced as innovative and efficient drug delivery systems (DDSs), able to overcome the low therapeutic indexes of traditional chemotherapy [675,676]. Since that time, the use of liposomes and more in general lipid molecules has interested different branches of nanomedicine, with the aim of addressing the numerous challenges raised by the need for an efficient delivery of both therapeutics and genetic material to specific target sites, with applications ranging from cancer therapy to gene therapy and vaccination [677].

In this latter case, the notorious Covid-19 pandemic certainly boosted worldwide the search for a robust solution to provide a rapid and unprecedented mass production of vaccines. When it came to deciding the way to convey the immunization to hundreds of millions of people, different alternatives were taken into account and finally mRNA vaccines were selected [678]. In order to guarantee a

prolonged blood circulation and the precious cargo protection, the scientific community agreed on the use of already well-known ionizable lipid-based nanoparticles (LNPs) [679], which were implemented by different pharmaceutical companies in parallel to guarantee a shortening of the conventionally long validation process by the competent regulatory agencies [680].

In particular, two main vaccines debuted to the market almost simultaneously after receiving the first historical authorization by FDA (Food and Drug Administration) and EMA (European Medicines Agency) for emergency use [681]: those produced by BioNTech/Pfizer (BNT162b2) and those realized by Moderna (mRNA-1273). Leaving aside the differences among the two in terms of antigen choice and mRNA design and modification, the focus was placed on the implementation of the delivery system employed in these two case studies. Briefly, both were formulated through microfluidic mixing in a scalable production system, exploiting the ability of their proprietary and innovative ionizable lipids, included in the formulation, to acquire a positive charge in some specific pH condition, thus enabling an electrostatic complexation of the negatively charged mRNA. A further part of the process, carried out at neutral pH, allowed the formation of uncharged solid-core lipid nanoparticles, densely packaging mRNA and able to release their cargo via endosomal escape once internalized by cells, according to mechanisms still not fully understood [682].

The compositions of these LNPs, initially hypothesized according to previous works of the developers which had employed the same type of lipid nanoparticles in Phase I/II studies [683–685], were later disclosed or confirmed in official patents published by Moderna [686,687] and Pfizer [688], respectively. In details, they consisted of a combination of a new class of ionizable cationic lipids, a neutral phospholipid, cholesterol and a polyethylene-glycol(PEG)-lipid [689], whose molar ratios, composition and choice were the result of years of trials carried out in the context of delivery systems for mRNA vaccines [690], reporting the use of cationic nanoemulsions [691], nanostructured lipid nanoparticles [692], cationic polymers [693], LNPs encoding antibodies [694] as strategies to efficiently delivery mRNA strands in vaccines.

The underlying common principle of all these studies was the interaction between the negatively-charged nucleic acid and the positively charged lipids composing the carrier in question, to guarantee a dense packaging and an enhanced protection of the cargo. This notion was our starting point to develop covid vaccine-inspired permanently charged lipidic formulations, aimed at being used as smart coatings of nanoparticles or even drug carriers of charged moieties for cancer application [695] . At first, the use of ionizable lipids was put aside in favor of a less

complex system, replacing them with permanently charged positive or negative lipids, to have a first idea of their behavior when electrostatically interacting with the cargoes. Acuitas patent and the above-mentioned first speculations on the composition of the LNPs were thoroughly studied to establish the molar ratios of the various components of the shell, namely charged lipids, neutral lipids, cholesterol and PEGylated lipids, finally set at 50:10:38,5:1,5.

Different techniques and solvents were employed to realize the liposomes and characterize them, and afterwards a precise protocol was established to achieve a reproducible and successful coating of metal oxide nanoparticles (NPs). Firstly, a mini extruder was used to obtain monodisperse and highly stable uncharged and charged liposomes, employable as drug carriers for charged moieties and applicable to cancer treatments as well as gene therapy [696]. Then, in order to successfully use the lipidic formulations as coating of charged solid inorganic nanoparticles, another methodology was implemented and optimized, namely the solvent exchange technique. As diffusely discussed in previous reviews on the topic [676], the decoration and coating of metal oxide and, more in general, solid-state inorganic nanoparticles with artificially or naturally-derived phospholipidic bilayers to confer them a higher biostability and biocompatibility is the main path taken to guarantee a better interaction of the nanomaterials in object with the organism, by drastically reducing their toxicity and immunogenic response [697,698].

With respect to the existing body of research already published on this specific topic (namely lipid-coated zinc oxide nanoparticles for cancer applications) by either this group [593,699] or other research teams [700], the importance and originality of this study consist in the use of an innovative and highly customizable lipidic shell, whose interaction with the cargo is inspired by the most recent and worldwide spread – and therefore broadly tried-and-tested – lipid nanoparticles' formulations. As a proof of concept, these lipid-coated NPs were tested against a pancreatic cancer cell line (BxPC-3) to show their increased biostability and biocompatibility with respect to uncoated nanoparticles. To fully exploit the potential of the lipidic shell, designed to be further functionalized with targeting peptides or fragmented antibodies for theranostic or immunotherapeutic purposes, a pancreatic cancer targeting peptide, CKAAKN, was conjugated to the lipidic shell, showing an increased cell uptake with respect to lipid-coated NPs when administered to BxPC-3 cells. A scheme of the procedures described in this work is reported in **Figure 13.**

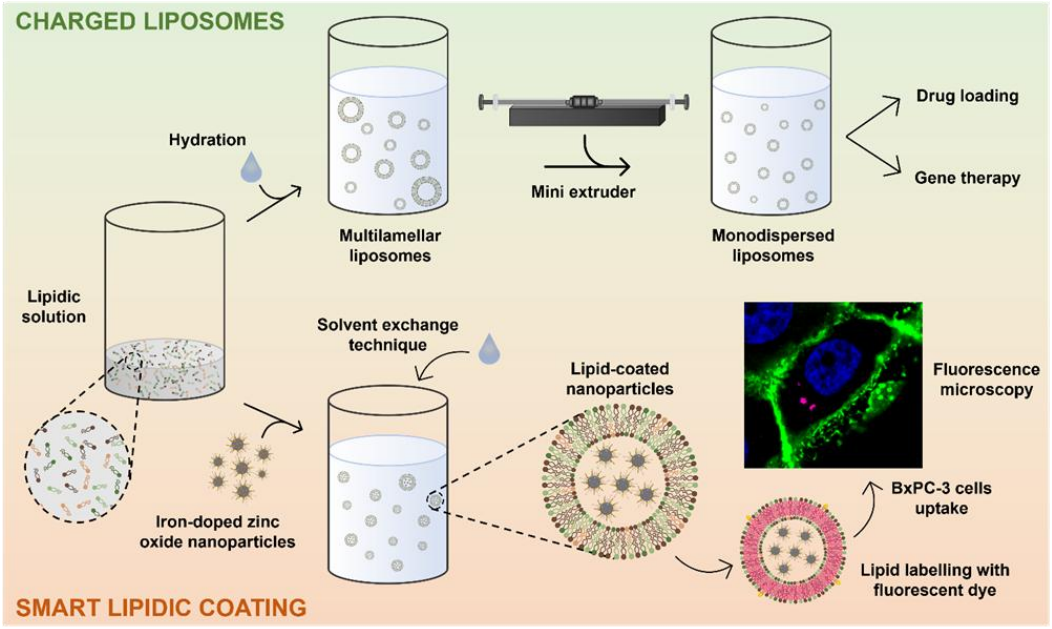

Figure 13. Scheme reporting the formation of the extruded liposomes and the solvent exchange technique employed to coat metal oxide nanoparticles.

2.1 Materials and Methods

2.1.1 Lipidic formulations

All the employed lipids were purchased by Avanti Polar Lipids Inc.: DOPA (18:1 PA, 1,2-dioleoyl-sn-glycero-3-phosphate (sodium salt), chloroform solution), DOPC (18:1 (Δ9-Cis) PC (DOPC), 1,2-dioleoyl-sn-glycero-3-phosphocholine, chloroform solution), DSPE-PEG(2000) Amine (1,2-distearoyl-sn-glycero-3-phosphoethanolamine-N-[amino(polyethylene glycol)-2000] (ammonium salt)) and DSPE-PEG(2000) Maleimide (1,2-distearoyl-sn-glycero-3-phosphoethanolamine-N-[maleimide(polyethylene glycol)-2000] (ammonium salt)); the cholesterol solution in chloroform was purchased by Sigma-Aldrich. Three different lipidic formulations were realized: a neutral one, hereinafter called Formulation 1C (Form1C for brevity), a positive one, called Formulation 2C (Form2C) and a negative one, Formulation 3C (Form3C). **Table 4** reports the types of lipids and the molar ratios employed to realize them.

Table 4. Lipids and molar ratios of the three realized formulations.

	Formulation 1C		Formulation 2C		Formulation 3C	
	Lipids	**Molar ratio**	**Lipids**	**Molar ratio**	**Lipids**	**Molar ratio**
Charged lipids	/	/	DOTAP	50 %	DOPA	50 %
Neutral lipids	DOPC	60%	DOPC	10 %	DOPC	10 %
Cholesterol	Cholesterol	38.5 %	Cholesterol	38.5 %	Cholesterol	38.5%
PEGylated lipids	DSPE-PEG(2000)-Amine	1.5 %	DSPE-PEG(2000)-Amine	1.5 %	DSPE-PEG(2000)-Amine	1.5 %

According to these proportions, the lipidic solutions (either in chloroform as provided by the manufacturers or in methanol for the PEGylated lipids, supplied in powder and later dispersed in this solvent) were put in a glass vial to let the solvent evaporate overnight under vacuum. From this common starting point, different strands of research have been drawn, in order to develop various methodologies and to identify the best protocol for future experiments. The main differences consisted in the solvent employed for the redispersion of lipids and in the technique carried out to obtain the liposomes.

2.2.2 Mini extruder technique

The first experiment involved the use of a mini-extruder, purchased by Avanti Polar Lipids. The dried lipids were rehydrated in a solution made up of bidistilled water (obtained from a Direct Q3 system, Millipore, Burlington, MA, USA) and physiological solution (Galenica Senese S.r.l, Italy), to allow the formation of liposomes. The obtained multilamellar liposomes were characterized in terms of hydrodynamic size (Dynamic Light Scattering, DLS) and zeta potential using a Zetasizer Nano ZS90 (Malvern Panalytical, Malvern, UK) by diluting a volume corresponding to 100 µg of liposomes in 1 ml of bidistilled water. Afterwards, they were subjected to a total of 11 passages through the membrane of the mini-extruder (whose pores had a diameter of 100 nm) at a temperature of 60 °C. The aim of the extrusion was to obtain well dispersed liposomes, reducing their size range and improving their stability over time. After the extrusion process, the previously mentioned characterizations were carried out again. Moreover, a Nanoparticle Tracking Analysis (NTA), using the NanoSight NS300 from Malvern Panalytical, was performed on the extruded samples. Once assessed the success of the extrusion technique, the obtained liposomes were stored at +4 °C and analyzed in terms of

hydrodynamic size and zeta potential in water after 10 days, to prove their stability over time and their ability to maintain their charge unaltered, comparing their behavior before and after the extrusion. The established protocol was easily adaptable for the future incorporation of drugs, which could be dissolved in either organic solvents (therefore dried with the lipids) or in the aqueous phase and therefore added during the rehydration step, right before the extrusion. However, such approach was not suitable for the incorporation of nanoparticles into the liposomes due to the small dimension of the pores of the extruder, since the NPs would remain stuck into the filter. For this reason, another route was chosen to incorporate them into the lipidic shell, namely an adaptation of the previously reported solvent exchange technique [698,701]. The choice of the best formulation to be used as a coating for our positively-charged iron-doped zinc oxide NPs (whose fabrication and physio-chemical characterizations have been thoroughly described in a previous work [702] by Carofiglio et al.) naturally fell on the Form3C, to exploit the electrostatic interaction between cargo and shell. Moreover, the formulation was consistently referred to as Form3C throughout the manuscript since its name refers to both the number of lipidic components employed (i.e., 3 different phospholipids) and the presence of the cholesterol (C) in the shell.

2.2.3 Solvent exchange method

Briefly, after the lipids were left dry overnight under vacuum, they were hydrated with a solution consisting of ethanol (99%, Sigma Aldrich) and bidistilled water in a volume proportion of 40%-60% (**Figure 14**). This ratio was carefully studied so as to avoid any unwanted self-assembly of the lipids, and for this purpose ethanol was added as first solvent. The resulting lipid dispersion, whose color would turn to whitish after the addition of water, was stable and kept at 4 °C for the following steps.

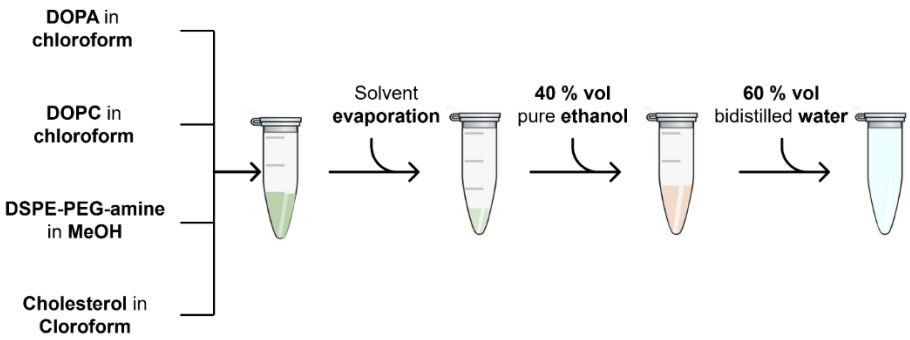

Figure 14. Process scheme of the preparation of the lipidic formulations.

The coating process consisted in pelleting a certain amount (defined later on for the optimized NPs coating protocol) of nanoparticles from the ethanolic stock by centrifuging them at 14000 g for 10 minutes and removing the supernatant. Then, a volume of lipid solution was added to the pellet and a first step of sonication (3 minutes) employing an ultrasound bath (59 kHz, Branson 3800 CPXH, Branson Ultrasonics Corporation) was performed, to allow a good dispersion of the nanoparticles and the lipids. Afterwards, bidistilled water was suddenly added to the mixture, and a second cycle of sonication (5 minutes) was performed. From the resulting solution, the volume corresponding to 100 μg of NPs was withdrawn, added to 900 μL of bidistilled water and analyzed by means of DLS and zeta potential. **Figure 15** reports the process scheme just described.

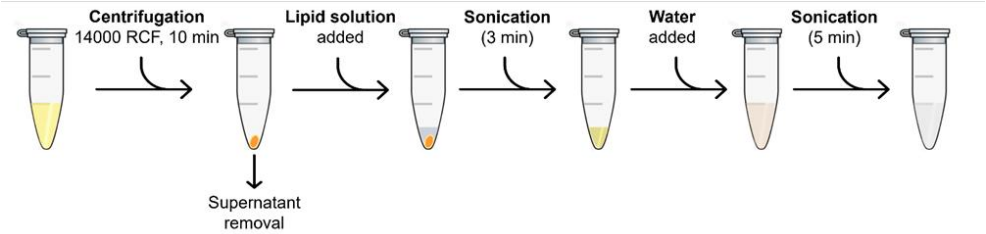

Figure 15. Process scheme of the NPs coating with the lipidic formulations.

After several trials, described in the Result and in the Supporting Information (S.I.) sections, an optimal ratio between the weight of the NPs and the weight of the lipids employed for the lipidic coating was established, and used for all the following performed experiments.

2.2.4 Cytotoxicity study on BxPC-3 cells

As a proof of concept, the lipid-coated nanoparticles were tested against a human pancreatic cancer cell line, BxPC-3 (ATCC CRL-1687). The cell line was cultivated with RPMI 1640 medium (ATCC) supplemented with 10% heat-inactivated FBS (ATCC), 100 μg/mL streptomycin and 100 units/mL penicillin (Sigma Aldrich) and grown at 37 °C with 5% CO_2 atmosphere. Briefly, 2500 cells were seeded in each well of a 96-well culture plate (TC-Treated, Corning, Corning, NY, USA) and incubated for 24 h at 37 °C in 5% CO_2 atmosphere. Then, the cell culture medium was replaced with fresh medium containing different doses of either naked (10, 15, 20 and 30 μg/mL) or lipid-coated (10, 15, 20, 30, 40, 50, 75, 100 and 150 μg/mL) NPs. To prepare naked NPs dispersions, the NPs were first sonicated in their ethanolic stock solution for 10 minutes, and then the volume corresponding to the correct amount for each sample was withdrawn from the stock

solution and put in cell culture medium. For coated NPs dispersions, the NPs were simply withdrawn from freshly-prepared aqueous stock solution prepared as in section 2.3 and directly dispersed in the correct amount in RPMI. Background wells containing just NPs dispersed in RPMI were also prepared. After 24, 48 and 72 hours of incubation with the NPs, the WST-1 proliferation assay (Roche) was performed to assess cell viability. Briefly, 10 μL of WST-1 reagent was added to the wells 2 hours prior to each time step, and incubated at 37 °C in 5% CO_2 atmosphere. Then, the absorbance was measured with a Multiskan GO microplate spectrophotometer (Thermo Fisher Scientific) at 450 nm using 620 nm as reference wavelength. All the background values were subtracted from the absorbance value of each sample, and the measurements were referred to the control cells, named those incubated in simple RPMI and set as 100% viability. All the measurements carried out throughout the work were taken at least in triplicates, and the statistical one-way or two-way ANOVA analysis of variance was performed with Origin software.

2.2.5 Functionalizations and targeting peptide

One of the key features of the lipidic formulation here implemented is its customizable value, thanks to the presence of the DSPE-PEG(2000) Maleimide lipid in the shell. In fact, by means of simple chemical reactions it is possible to attach species such as peptides and fragments of antibodies, exploiting the cysteine residue of the maleimide compound. To assess the ability of the nanoconstructs to target pancreatic cancer cells, a custom-made targeting peptide, namely CKAAKN, was purchased by Bio-Fab Research and linked to the DSPE-PEG(2000) Maleimide lipid as reported hereinafter.

a. DSPE-PEG(2000) Maleimide coupling to peptide

Briefly, the DSPE-PEG(2000) Maleimide lipid and the CKAAKN peptide (molar ratio 3:1) were dissolved in N, N-Dimethylformamide (DMF, Sigma Aldrich) at a concentration of 37.5 mM and 50 mM, respectively. Then, the peptide solution was diluted in 0.1 M sodium phosphate buffer (PBS, pH 7.4) and the DSPE-PEG(2000) Maleimide solution was then added, obtaining a final reaction mixture of 1:1 DMF/PBS and therefore a 5 mM peptide and a 15 mM lipid concentration. The reaction was allowed to proceed at room temperature for 1 hour, then the resulting mixture (DSPE-PEG(2000)-CKAAKN, hereinafter called functional lipid for brevity) was stored at -20 °C and kept as a stock, diluting it in ethanol (1:10 dilution) before using it in the lipidic formulation in the molar ratio

of 0.1 % (**Figure 16**). To assess the correct coating of the nanoparticles, a custom-made CKAAKN peptide already linked to fluorescein isothiocyanate (FITC) was purchased by Bio-Fab Research and linked to the DSPE-PEG(2000) Maleimide lipid for imaging purposes, following the same procedure reported above (this other compound, DSPE-PEG(2000)-CKAAKN-FITC, will be referred to as fluorescent functional lipid).

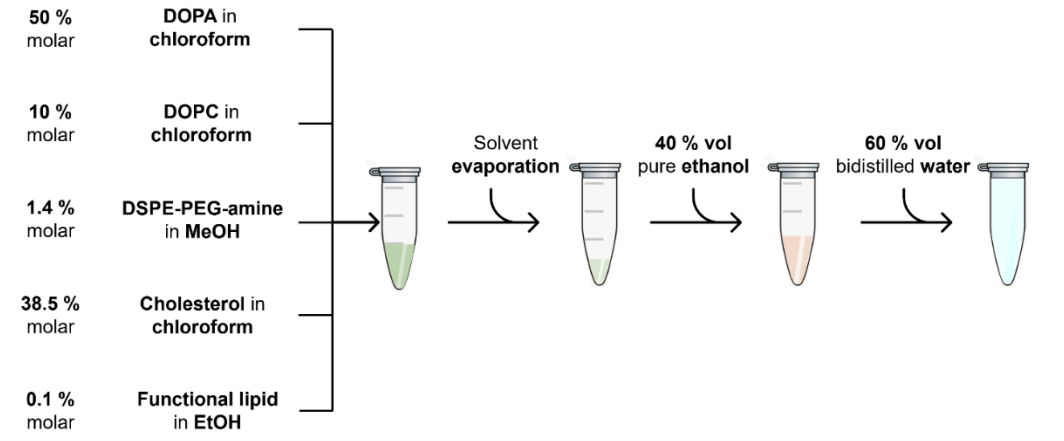

Figure 16. Process scheme of the preparation of the Form3C lipidic formulation with the incorporation of the functional lipid, in this case either DSPE-PEG(2000)-CKAAKN or the fluorescent DSPE-PEG(2000)-CKAAKN-FITC.

b. Colocalization with fluorescence microscopy

In order to perform the qualitative colocalization studies by means of fluorescence microscopy, the process of lipid coating was carried out on previously labelled NPs. Briefly, NPs were withdrawn from the ethanolic stock and Atto647 NHS ester (ThermoFisher) was added (2 µg/mg of NPs) in the dark and stirred overnight. Then, the NPs were washed 3 times by means of centrifugation at 14000 g for 10 min and redispersions in ethanol. Then, the protocol for lipid drying and coating was followed taking care to add the previously prepared fluorescent functional lipid to the formulation, in the molar ratio of 0.1 % (Figure S3, S.I.). For the fluorescence microscopy assay, the obtained nanoconstructs were further diluted in water and 2 µL of sample was spotted on a microscope slide, coated with a cover slide and let dry in the dark. The samples were imaged with a wide-field inverted fluorescence microscope (Eclipse TiE from Nikon) equipped with a 100× objective (NA =1.30). Then, employing the colocalization tool of the NIS software (Nikon) and adapting some optimized settings reported in a previous work [703], the percentage of colocalization was evaluated.

2.2.6 Internalization studies

To show the internalization of the NPs inside BxPC-3 cells, two distinct experiments were carried out once the optimal safe concentration of NPs was established (as described in the Result section, 50 μg/mL). First, an uptake study employing a flow cytometer and then a qualitative fluorescence microscopy analysis.

a. Flow cytometry

For the flow cytometry study, BxPC-3 cells (3×10^5 cells in 500 μL of cell culture media) were seeded in 24-well culture plates (TC treated, Thermo Fisher) and incubated for 24 hours at 37 °C with 5% CO_2 atmosphere. NPs were previously labelled with Atto647 NHS ester as described above and then coated with three different coatings, namely Form3C, Form3C containing the CKAAKN peptide and finally Form3C with the CKAAKN-FITC peptide, to compare the effect of the targeting peptide in terms of internalization. After the standard coating process, the nanoconstructs were incubated with DiD' dye (DiIC18(5) solid (1,1'-Dioctadecyl-3,3,3',3'-Tetramethylindodicarbocyanine, 4-Chlorobenzenesulfonate Salt), Invitrogen) previously dissolved in dimethyl sulfoxide (DMSO, Sigma Aldrich) at 37 °C for 30 minutes under continuous shaking and then dispersed in cell culture medium and administered to cells. After further 24 hours of incubation, cells were washed twice with PBS to remove the non-internalized NPs and then detached by trypsinization, collected and centrifuged at 130 g for 5 min. Finally, they were dispersed in PBS and analysed with a Guava Easycyte 6-2L flow cytometer (Merck Millipore, Burlington, MA, USA). The number of events corresponding to the analysed cells was acquired and analysed as described in previous works [610]. The analyses were performed with Incyte Software (Merck Millipore), while graphs were obtained through FCS Express Software (DeNovo Software) and Origin software (OriginLab). Tests were performed in triplicates and ANOVA analysis of variance was performed with Origin software.

b. Fluorescence microscopy

To provide a qualitative proof of NPs internalization into cells and to locate their position, fluorescence microscopy analyses were performed on BxPC-3 cells 24 hours after NPs administration employing a spinning-disk confocal fluorescence microscopy (Ti2 Nikon equipped with a crest large FOV laser and a 60×PlanAPO objective, NA = 1.40). Briefly, 1×10^4 cells were seeded into eight-well chamber

slides (Nunc Lab-Tek II CC2 Chamber Slide system, Thermo Fisher Scientific) with 250 µL of complete cell culture medium. After 24 hours of incubation Form3C-CKAAKN NPs, previously labeled with DiD as described above, were administered to cells at the concentration of 50 µg/mL. After further 24 h, cells were fixed by replacing cell culture medium with 150 µL of Image-IT fixative solution (Thermo Fisher). After 10 min at room temperature, they were washed twice with PBS and the membranes were stained with 250 µL PBS containing wheat germ agglutinin conjugated with an Alexa Fluor 488 dye (WGA-488, Thermo Fisher) at a concentration of 2.5 µg/mL for 10 min at 37 °C in 5% CO_2 atmosphere. Again, cells were washed twice with PBS and Hoechst (Thermo Fisher), at a concentration of 0.3 µg/mL in PBS, was administered for nuclei staining. After further 5 min in normal cell culture conditions, they were washed twice with PBS and live cell imaging (LCI, Molecular Probes) solution was added. The obtained samples were analyzed right after the staining.

2.2.9 Hemocompatibility test

To assess the effect of the lipidic shell in improving the NPs hemocompatibility, a plasma recalcification test was conducted following an established protocol [704–706]. The lipidic coating process was carried out as described in Section 2.3, but the whole procedure took place under sterile hood. Naked and the so-obtained Form3C NPs were both resuspended in 0.1 µm filtered physiological solution (0.9 % NaCl w/w water solution), at a final concentration of 50 and 100 µg/mL, while pure physiological solution was used as control sample. Six wells per sample of a 96-well plate were filled with 75 µL of human citrated plasma (Human Recovered Plasma Pooled-frozen - NaCitrate from ZenBio) pre-heated at 37°C, and 75 µL of sample (either control or zinc oxide NPs naked or coated and at the two different concentrations) was added in each well. After 5 minutes of incubation at 37°C, 150 µL of 25 mM calcium chloride ($CaCl_2$) was quickly added in 3 wells for each sample to induce the coagulation of plasma. Right afterwards, the absorbance at 405 nm was periodically measured by inserting the plate in a 37°C pre-heated UV-Vis spectrophotometer. In details, every 30 seconds a measurement was carried out for a total of 45 minutes, at an incubation temperature of 37 °C. Three independent experiments were conducted and the resulting coagulation times, determined as reported in details in a previous work [707], were averaged.

2.3 Results and discussion

2.3.1 Mini extruder technique

The results displayed in **Table 5** and **Figure 17** show all three lipidic formulations before and after the extrusion. As reported, the extrusion process positively affected the PDI and the size of the liposomes, which were heavily reduced in all cases. In fact, the passages through the membrane of the mini-extruder had the effect of creating unilamellar vesicles by means of the application of shear stress combined with the heating of the whole system over the phase transition temperature of the involved lipids [708]. Moreover, in accordance with what was expected, the values of the zeta potential reflected the employment of neutral, positive and negative lipids in each formulation. The effect of the extrusion on the charge of the liposomes was not as marked as for the size and the PDI, but the standard deviation of the measurements was reduced for all the samples. To confirm the results obtained by means of the DLS, a NTA measurement was carried out for all the extruded samples, showing monodisperse liposomes whose sizes were comparable to those obtained with the DLS measures.

Table 5. DLS Size, zeta potential and NTA measurements of the three lipidic formulations before and after the extrusion**.**

	Formulation 1C		**Formulation 2C**		**Formulation 3C**	
	DLS Size		**DLS Size**		**DLS Size**	
	Zeta Average	PDI	Zeta Average	PDI	Zeta Average	PDI
Before extrusion	407.7 nm	0.731	216.5 nm	0.437	371.4 nm	0.527
After extrusion	138.7 nm	0.144	151.2 nm	0.106	150.7 nm	0.148
	Zeta Potential		**Zeta Potential**		**Zeta Potential**	
	Zeta Potential	SD	Zeta Potential	SD	Zeta Potential	SD
Before extrusion	1.6 mV	1.4 mV	57.5 mV	2.7 mV	-58.5 mV	4.3 mV
After extrusion	2.0 mV	0.4 mV	47.9 mV	1.3 mV	-51.9 mV	0.4 mV
	NTA		**NTA**		**NTA**	
	Mean	SD	Mean	SD	Mean	SD
After extrusion	122.4 nm	24.8 nm	152.5 nm	42.6 nm	121.0 nm	29.5 nm

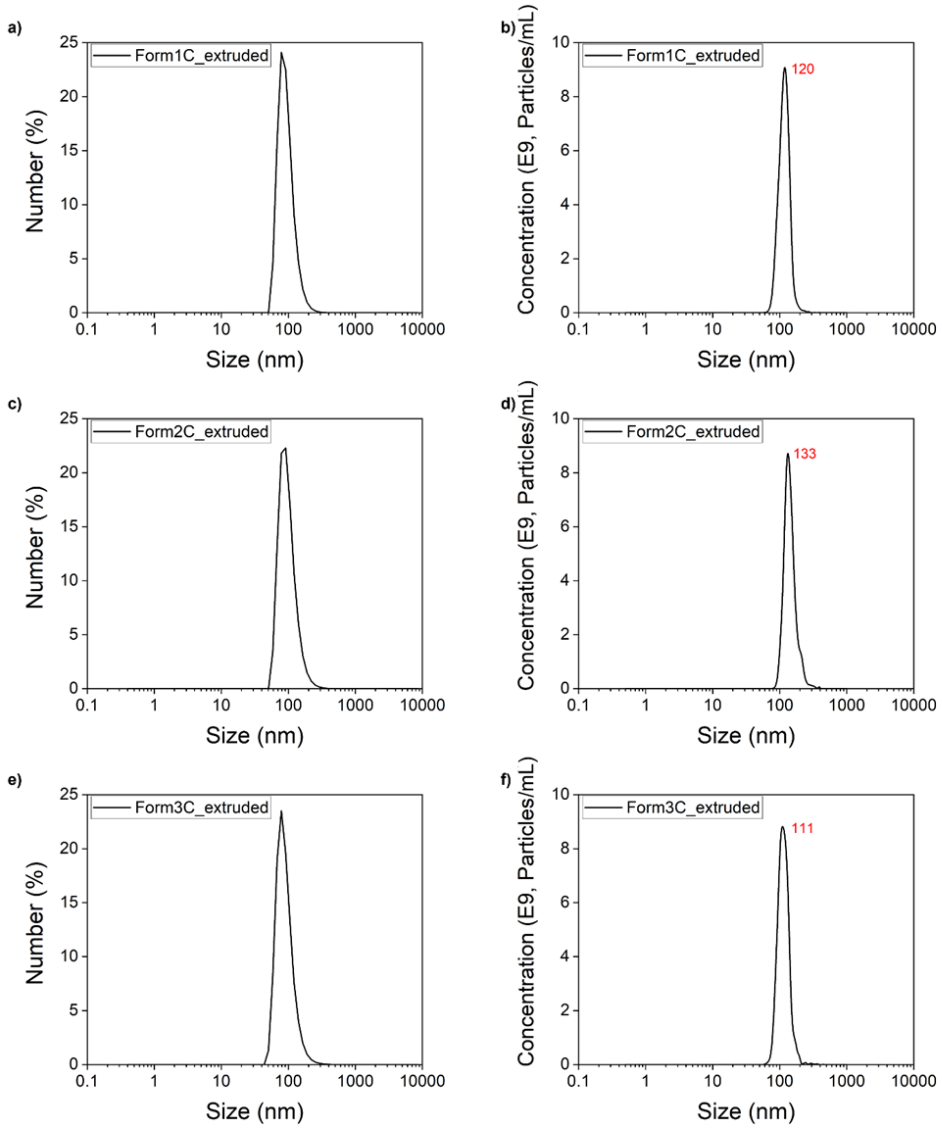

Figure 17. DLS size (A,C,E) and NTA (B,D,F) measurements of the three liposomal formulations after the extrusion process.

Overall, these results confirmed that the mini extruder technique could successfully be used to realize monodispersed liposomes regardless of the charge of the lipids, with robust and predictable results suitable for further functionalizations or cargo loadings.

a. Stability assay

After the previously reported characterizations, the samples were stored at +4 °C and analyzed after 10 days to assess their stability by means of DLS and zeta

potential measurements. As shown by **Figure 18** and **Table 6**, all the extruded samples were extremely stable even after 10 days of storage, since PDI, size and zeta potential remained almost unchanged over time.

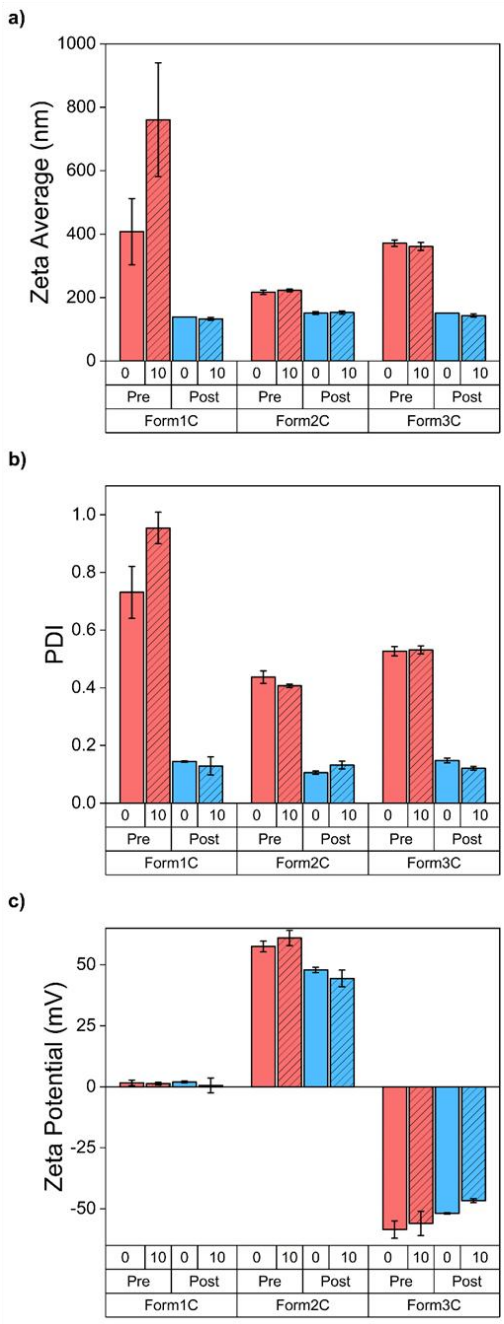

Figure 18. Comparison between A) zeta average, B) PDI and C) zeta potential measurements of the three liposomal formulations pre and post extrusion, and stability assay after 10 days of storage at +4 °C.

Table 6. Schematic content of Figure 17, comparing zeta average, PDI and Zeta Potential of the liposomes before and after the extrusion, and after 10 days of storage.

Zeta Average				
	Before extrusion		**After extrusion**	
	Day 0	**Day 10**	**Day 0**	**Day 10**
Form1C	407.7 nm	760.6 nm	138.7 nm	133.1 nm
Form2C	216.5 nm	222.6 nm	151.2 nm	152.9 nm
Form3C	371.4 nm	361.3 nm	150.7 nm	143.2 nm
PDI				
	Before extrusion		**After extrusion**	
	Day 0	**Day 10**	**Day 0**	**Day 10**
Form1C	0.731	0.954	0.144	0.129
Form2C	0.437	0.407	0.106	0.132
Form3C	0.527	0.531	0.148	0.121
Zeta Potential				
	Before extrusion		**After extrusion**	
	Day 0	**Day 10**	**Day 0**	**Day 10**
Form1C	1.6 mV	1.3 mV	2.0 mV	0.6 mV
Form2C	57.5 mV	61.0 mV	47.9 mV	44.4 mV
Form3C	-58.5 mV	-56.0 mV	-51.9 mV	-46.7 mV

These stability results were of outmost importance, since they proved that the lipidic formulations could be potentially prepared in stocks and kept in controlled conditions after the liposomal formation and the extrusion, without compromising their size and charge but rather offering the opportunity for future scale-up of the whole process in view of massive dosage needed for *in vitro* or *in vivo* applications.

2.3.2 Solvent exchange technique for iron-doped zinc oxide nanoparticles coating

As previously outlined, the negatively charged Form3C was chosen to coat our positively charged zinc oxide nanoparticles, and the whole procedure was finely tuned over time to find the best conditions to obtain a stable shell on the surface of the NPs.

As diffusely reported in various works on the subject [709–711], the main underlying mechanism of the lipidic shell formation on the surface of the NPs is the

minimization of the Gibbs free energy of the lipids, previously dispersed as disassembled monomers or conventional micelles in the organic solvent mixture. When the aqueous buffer, in this case bidistilled water, is suddenly added to the lipidic mixture, the lipids reorganize themselves and spontaneously self-assemble into various structures, among which lipid bilayers on the available substrates (in the present case the hydrophilic surface offered by zinc oxide NPs) are the most energetically favorable [712]. To achieve this goal, the amount of water added to the lipidic mixture was finely tuned to be equal to at least 10 times the volume of the organic solvent. Finally, the first sonication step performed during the procedure was introduced to guarantee a good and homogeneous dispersion of the organic phase around the NPs before the addition of water, and the second one was meant to reduce the size of the so-formed Form3C-NPs. The lipid coating process using the Form3C was repeated employing different lipids/NPs weight ratios, and DLS and zeta potential measurements were carried out on the obtained nanoconstructs to check their stability in aqueous media and assess their surface charge. As shown by the results of **Figure 19a**, depending on the weight ratio between lipids and nanoparticles, different values of size and zeta potential were obtained. In particular, with increasing amount of lipids, the zeta potential of the coated nanoparticles shifted towards lower values, and a higher degree of aggregation was evidenced by an increase of both the PDI and the size values (**Table 3**). A plot displaying the trend of the zeta potential values at these different lipids/NPs ratio was then produced (**Figure 19b**), and the values were shown to have a linear relation, further proven by means of a simple linear regression trendline (visible in red in **Figure 6b**, while the green horizontal one highlights the 0 mV value). This way, by imposing a desired markedly negative zeta potential value (around -25 mV as optimum ideal value), useful to avoid aggregation in biological media [713,714], the most appropriate lipids/NPs weight ratio was easily determined. For the following experiments, in fact, the weight of lipids added to the nanoparticles was always half of the NPs weight (so a lipids/NPs ratio of 50 %wt).

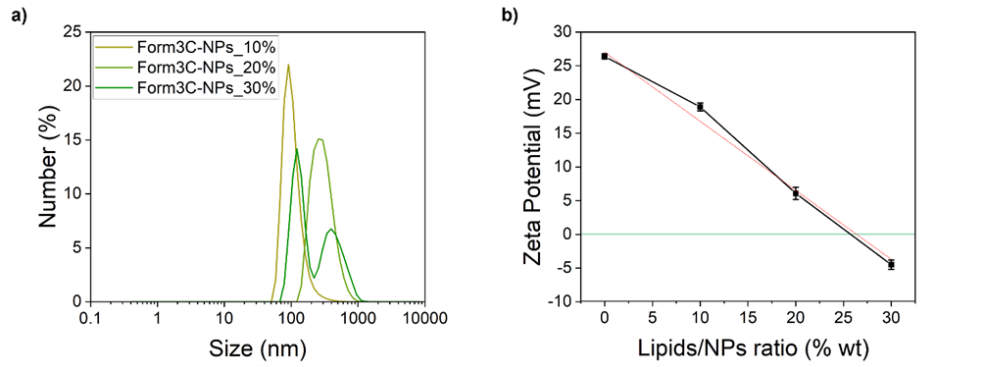

Figure 19. A) DLS size measurements and B) trend of the zeta potential values of the Form3C-NPs depending on the employed lipids/NPs ratio.

Table 7. DLS size and zeta potential values of the Form3C-NPs obtained employing different lipids/NPs weight ratios in the solvent exchange process.

	Form3C-NPs			
	DLS Size		**Zeta Potential**	
Lipids/NPs ratio	**Zeta Average**	**PDI**	**Zeta Potential**	**SD**
10 %wt	197.2 nm	0.212	18.9 mV	0.6 mV
20 %wt	368.0 nm	0.164	6.0 mV	0.9 mV
30 %wt	572.5 nm	0.292	-4.5 mV	0.7 mV

The whole coating procedure was then repeated as previously described, and DLS and zeta potential were measured again in water. The obtained results are displayed in **Figure 20a** and in **Table 8**. An extremely low value of PDI was reported, in accordance with the pronounced negative value of zeta potential, which prevented aggregation due to the electrostatic interactions caused by the presence of the charged lipids in the shell. Moreover, the shift of the zeta potential towards negative values was a first tangible proof of the successful coating of the nanoparticles with the lipidic shell, which was further assessed by means of other techniques, described in the following sections. To confirm the DLS analysis, a NTA measurement was performed as well and the result, shown in **Figure 20b** and reported in **Table 8**, was consistent with those obtained with the DLS. The NTA measure of Form3C-NPs can be directly compared to that of the naked NPs, displayed in **Figure 21**, to appreciate the enhancement of the NPs dispersion in water due to the presence of the lipidic shell.

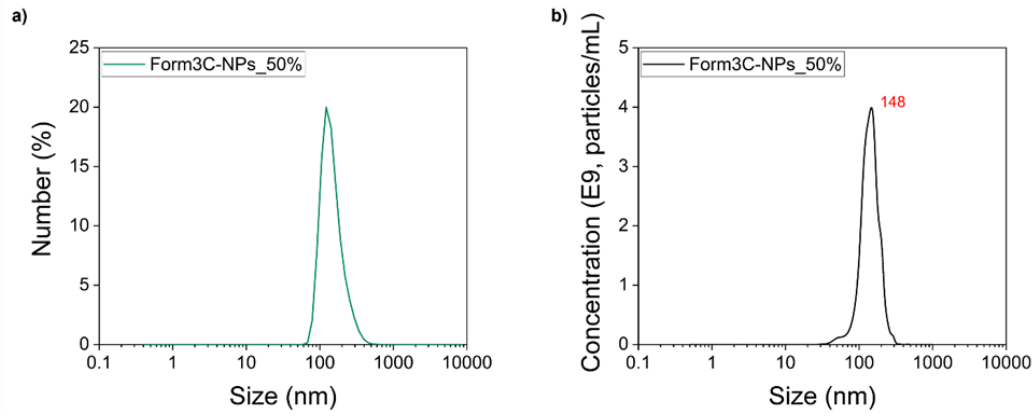

Figure 20. A) DLS and B) NTA measurements of the Form3C-NPs obtained employing the optimized lipid/NPs ratio of 50 %wt.

Table 8. DLS size, zeta potential and NTA measurements of the Form3C-NPs obtained employing the optimized lipid ratio. Based on these results, the definitive coating protocol was finally established, and this lipids/NPs ratio was kept unaltered throughout the rest of the study for all the following experiments.

	DLS Size			Zeta Potential		NTA	
	Z-Avg	**PDI**	**Derived Count Rate**	**Z-Pot**	**SD**	**Mean**	**SD**
Form3C-NPs 50% wt	203.2 nm	0.125	2624.7 kcps	-20.4 mV	0.4 mV	156.0 nm	42.8 nm

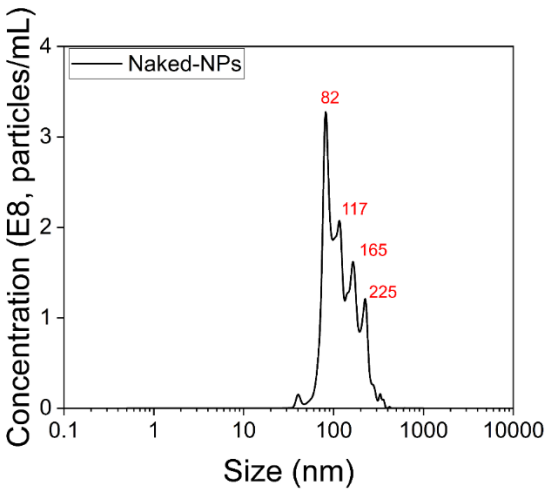

Figure 21. NTA measurement of Naked NPs in bidistilled water

Since one of the issues related to the use of inorganic nanoparticles is their tendency to aggregate in biological media, an experiment was carried out to prove the ability of the lipid coating to improve the NPs dispersion in RPMI 1640 medium supplemented with 10% heat-inactivated FBS. First, 1 mL of simple RPMI was analysed with the DLS as baseline. Then, 100 µg of naked NPs were dispersed in 1 mL of RPMI and analysed. Finally, 100 µg of lipid-coated NPs were dispersed in the same volume and analysed. As shown by **Figure 22a** and **Table 9**, the signal related to simple RPMI was very low in terms of both size and derived count rate, reflecting the presence of just the FBS content (namely proteins, lipids, growth factors, and anyway filtered with a 0.1 µm pore filter as stated by the manufacturer). When naked NPs were dispersed in RPMI, however, an important degree of aggregation was evidenced by both the PDI and the derived count rate values. In the presence of the lipid coating, instead, the PDI was markedly reduced and the aggregation rate was far lower, as witnessed by the increased value of the derived count rate. These results were stable even up to 1 week, as shown in **Figure 22b**, which reports the size, PDI and derived count rate values of the Form3C-NPs measured in RPMI over time.

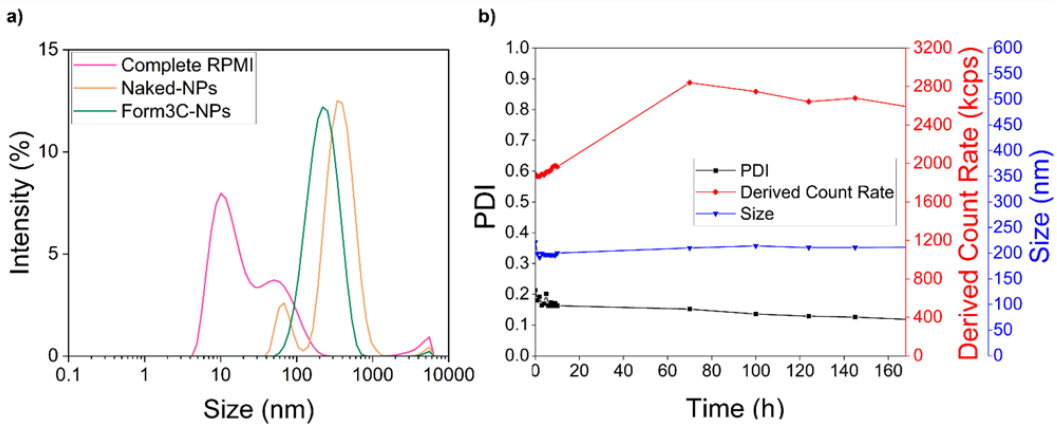

Figure 22. A) DLS size measurements of complete RPMI, naked NPs and Form3C-NPs analysed in RPMI. B) Size, PDI and derived count rate values of Form3C-NPs measured in RPMI over time.

Table 9. Zeta Average, PDI and derived count rate of complete RPMI, naked NPs in RPMI and Form3C-NPs in RPMI.

	Zeta Average	PDI	Derived Count Rate
Complete RPMI	16.15 nm	0.440	49.6 kcps
Naked NPs	275.0 nm	0.306	1713.2 kcps
Form3C-NPs	199.4 nm	0.181	2620.6 kcps

These results proved that the presence of the lipidic coating on the NPs could markedly reduce their aggregation in biological media, increasing their biocompatibility and their stability over time. Moreover, switching to a strong negative surface charge could enhance the NPs hemocompatibility in view of in vivo applications, since blood is known to coagulate on positively charged surfaces and biomaterials [715]. It is now well established from a variety of studies that the surface charge of NPs can strongly influence their biodistribution, clearance and induced immunological response, together with the formation of the protein corona [493,716–718]. In addition to that, an electrostatic interaction between positive NPs and the well known negatively charged cell membranes can enhance their non-specific uptake, increasing their toxicity to healthy tissues as well as the target ones [719]. By coating them with our Form3C lipidic shell, these risks can be significantly reduced in favour of a more controlled administration to target cells, achievable by means of functionalizations with targeting peptides or fragments of antibodies incorporated in the lipidic shell, or even pH-responsive lipids such as acid liable-PEG, to promote tumor accumulation and smart release of theranostics or immunotherapeutic agents [720].

2.3.3 Cytotoxicity study on BxPC-3 cells

As shown by **Figure 23**, when administered to BxPC-3 cells, naked NPs caused a marked toxicity at 20 µg/mL at all time steps (data were not produced from 40 µg/mL since all cells were dead at this concentration), while lipid-coated NPs were proven to be safe up to 100 µg/mL, and started to show signs of toxicity only at 150 µg/mL. Therefore, the presence of the lipidic shell improved astonishingly the cell viability. The possible explanation to this phenomenon is the shielding effect of the lipidic coating, which prevents zinc dissolution in toxic Zn^{2+} ions and increases the biostability of the NPs. Indeed, several lines of evidence suggest that the main mechanism of zinc oxide toxicity is the release of Zn^{2+} ions, whose uncontrolled

increase above the physiological threshold cause the disruption of zinc homeostasis and important damages to mitochondria and other cellular compartments [721,722]. The main ways of regulating zinc oxide cytotoxicity therefore consist in a fine tuning of its dissolution rate by means of surface functionalization or coatings and the introduction of crystal defects achieved by doping [723,724]. To produce Form3C-NPs, both strategies were implemented: iron doping and functionalization with amino-propyl groups [702], followed by the coating with the lipidic shell. The reported increase in cell viability serves as strong evidence of the mitigation of zinc oxide toxicity.

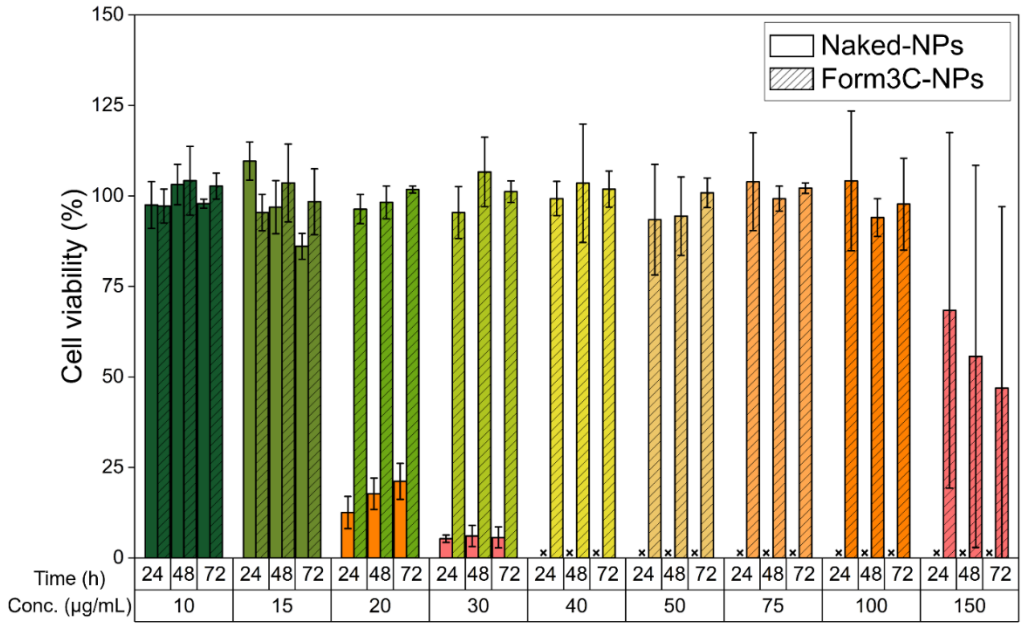

Figure 23. Viability of BxPC-3 cells treated with increasing amounts of both naked and Form3C-coated NPs. x=data not produced due to complete cell death from 40 µg/mL of administered naked NPs.

2.3.4 Colocalization with fluorescence microscopy

Another technique employed to assess the successful lipid coating of the nanoparticles was the qualitative colocalization study by means of fluorescence microscopy, exploiting the incorporation of the fluorescent functional lipid into the lipidic shell.

As shown by **Figure 24**, the signal of the far-red channel, showing the NPs previously labelled with Atto647, and that of the green channel, showing the FITC dye attached to the CKAAKN peptide and conjugated to the lipidic shells were almost fully colocalized (colocalization percentage of 94%), as visible in the merged channel.

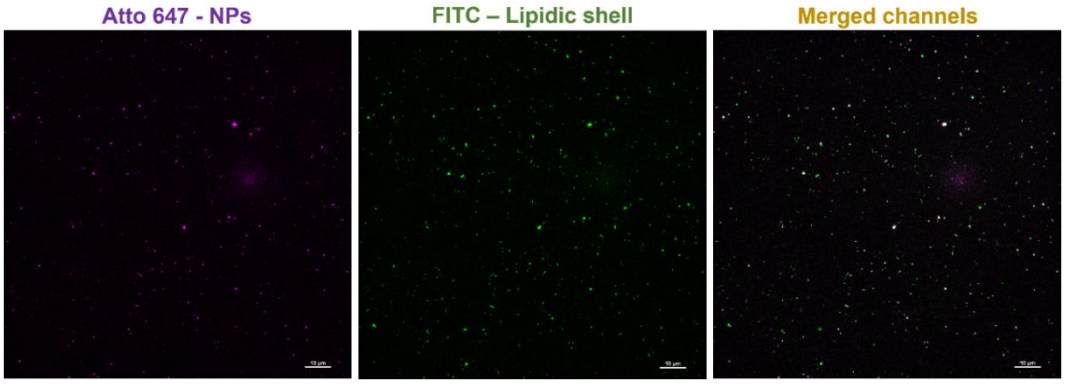

Figure 24. Fluorescence microscopy images showing the colocalization of the signal corresponding to the NPs (Atto647, far red channel) with the signal corresponding to the lipidic shell (FITC, green channel) in the merged channels on the right. Scale bars are set to 10 μm.

Together with the zeta potential shift to negative values, the decreased hydrodynamic size and PDI values, the enhanced stability in biological media and the acquired stability over time of the Form3C-NPs with respect to naked NPs, this colocalization study confirmed the undeniable presence of the lipidic shell on the NPs surface.

2.3.5 Cytotoxicity study with targeting peptide

A second cytotoxicity study meant to compare the naked and the Form3C-coated NPs in the presence of the targeting peptide was then carried out employing the same protocol previously reported. As shown in **Figure 25**, naked nanoparticles killed almost all cells at a concentration of 30 μg/ml, while when coated with the lipidic shell, even in the presence of the targeting peptide, cell viability was almost 100% with respect to the control up to 75 μg/mL. At 100 μg/mL cell viability was still more than 50% for all time steps but started to show a decrease. Therefore, it can be concluded that the presence of the targeting peptide, incorporated via the functional lipid in the lipidic shell, did not affect the toxicity of the NPs towards BxPC-3 cells.

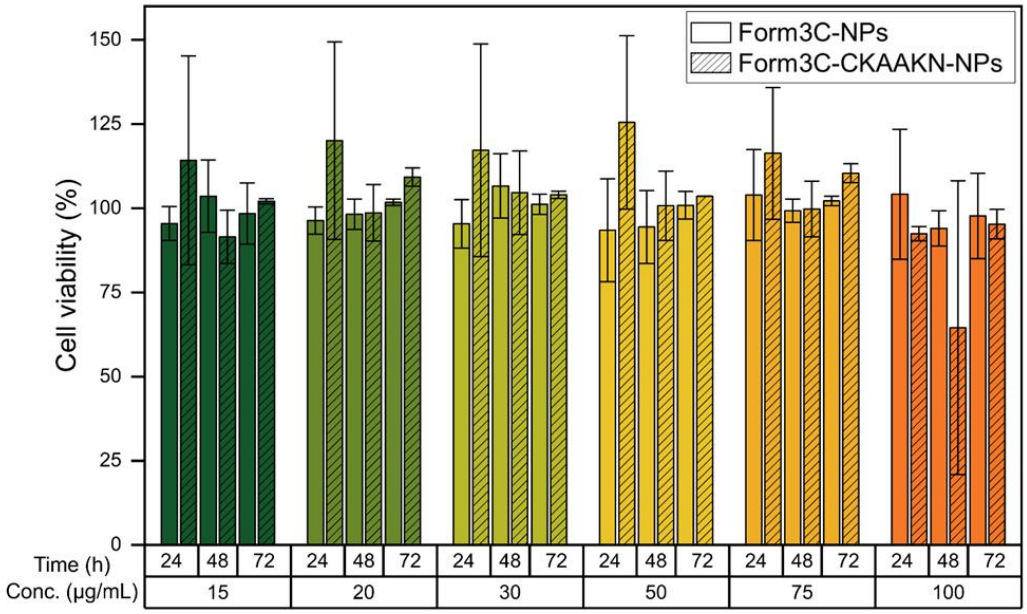

Figure 25. Viability of BxPC-3 cells treated with increasing doses of Form3C-NPs in the presence of the targeting peptide CKAAKN, compared to the same NPs without targeting peptide incorporated in the lipidic shell.

2.3.6 Flow cytometry and internalization in BxPC-3 cells

The Form3C-NPs concentration selected to perform the uptake experiment was 50 µg/mL, to minimize the risk of any cell death while administering a conspicuous amount of NPs to be detectable via flow cytometry. It should be noted that, compared to naked NPs, this dose was already more than 3 times the previous tolerated threshold and therefore a remarkable improvement with respect to past experiments [702].

As reported in **Figure 26**, Form3C-coated NPs already showed a slightly enhanced internalization, here expressed in terms of % of positive events with respect to control cells (untreated), meaning cells that were able to internalize or immobilize Form3C-NPs at the outer cell membrane. In the presence of the targeting peptide, however, the internalization rate was astonishingly higher. It is worth to mention that there was a slight difference in terms of fluorescence intensity retrieved by cells treated with the CKAAKN peptide and the CKAAKN-FITC one, suggesting a higher uptake for the system without the dye. A possible explanation

for that might be that some of the sites of the peptides are occupied by the FITC dye attached to it, reducing its targeting ability and therefore causing a slightly lower cell internalization.

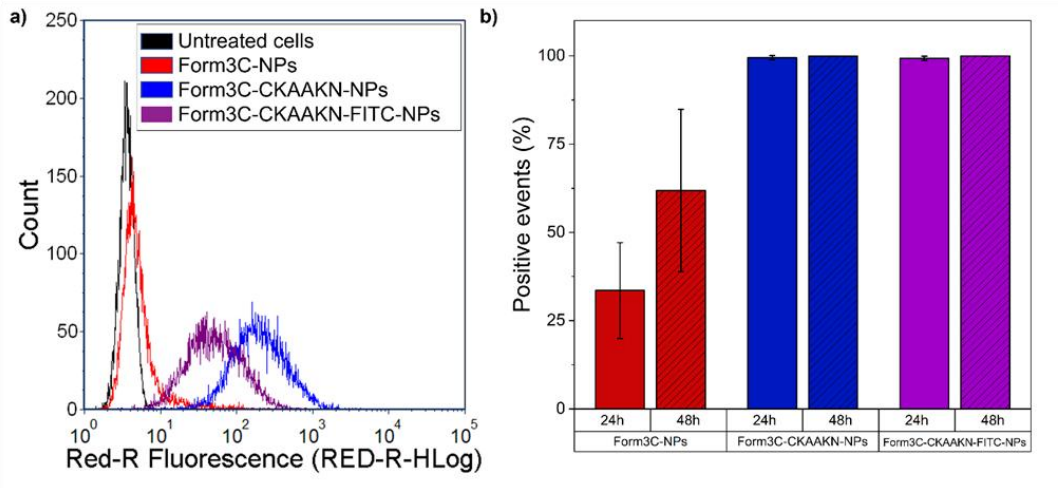

Figure 26. A) Representative histogram of the fluorescence intensity of cells measured through the cytofluorimetric assays performed to assess Form3C-NPs internalization and B) BxPC-3 cells measured as positive events due to the internalization or immobilization at the outer cell membrane of Form3C-NPs.

2.3.7 Fluorescence microscopy

To further assess the presence of the NPs inside the cells and not just on the cell membrane, z-stack images through the Z axis of the samples were collected (data not shown, while the 3D reconstructions of such images are reported in **Figure 27**).

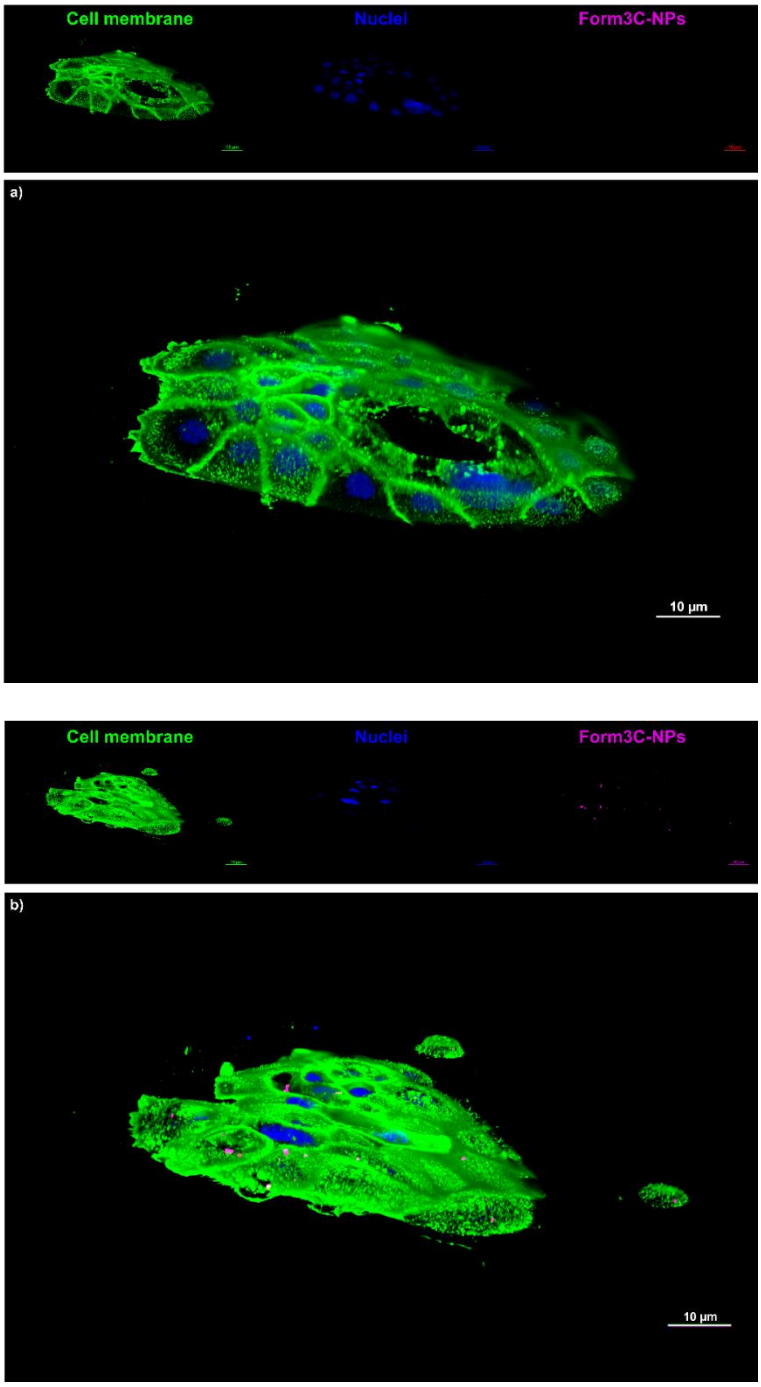

Figure 27. A) 3D reconstructions of BxPC-3 spinning disk confocal fluorescence microscopy images at different focuses of the control cells (namely incubated in complete medium without NPs) and of B) cells incubated in complete medium containing 50 µg/mL Form3C-NPs. Scale bars are set to 10 µm.

As shown in **Figure 28b**, extracted from an intermediate slice of the previously mentioned z-stack collection of images, the presence of the nanoparticles inside the cell membranes can be appreciated in the picture reporting all the 3 merged channels (blue for nuclei, green for cell membranes, far red for Form3C-coated NP). As expected the control cells (**Figure 28a**), not treated with Form3C-NPs, did not show any fluorescent signals in the far red channel. It must be noted that the selected dose of Form3C-NPs (50 µg/mL) was perfectly tolerated by cells, which did not show any morphological change or sign of cell death after the administration and the incubation.

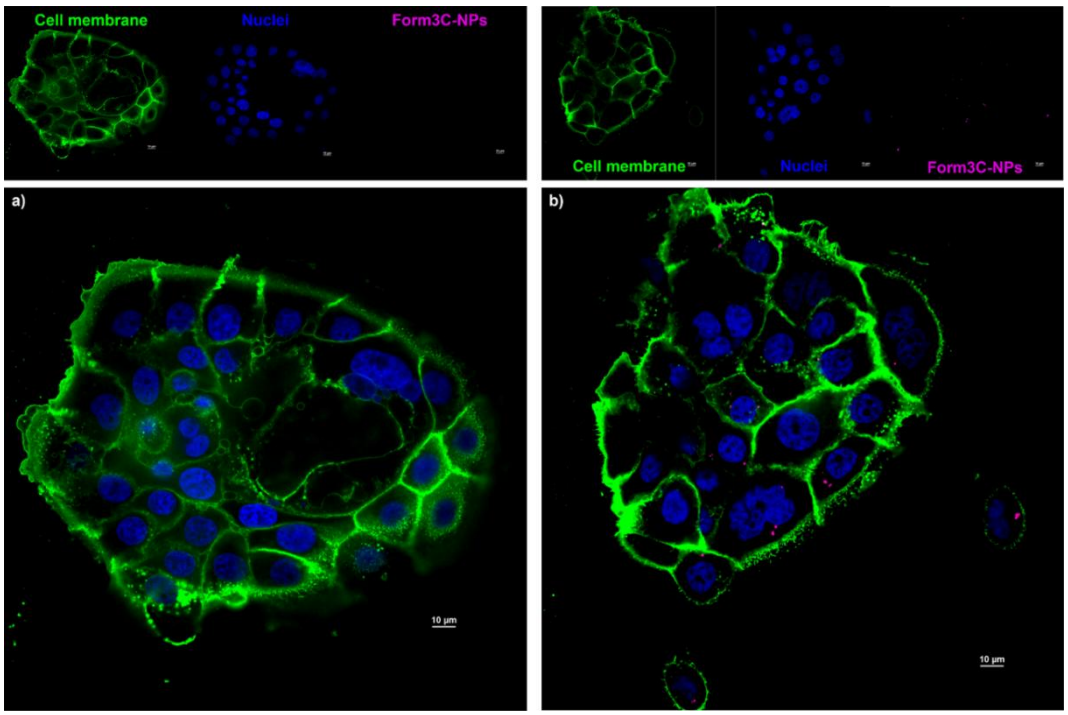

Figure 28. A) Fluorescence microscopy images of the control cells (namely incubated in complete medium without NPs) and of B) cells incubated in complete medium containing 50 µg/mL Form3C-NPs. Scale bars are set to 10 µm.

2.3.8 Hemocompatibility test

The results of the hemocompatibility test which was performed to evaluate the time necessary for plasma to clot in the presence of NPs are reported in **Figure 14**. Plasma citrate was used to simulate the use of anticoagulants to prevent blood clotting, and calcium chloride ($CaCl_2$) was added to induce a rapid calcification, manifested by an increase of turbidity in the course of approximately 15 minutes. Both the safe doses of Form3C-NPs (50 µg/mL) and a concentration equal to twice

the safe one (i.e. 100 µg/mL) were employed and compared. In this way a general idea can be obtained for planning future *in vivo* tests, which will include higher doses of NPs than those administered to cells *in vitro* to achieve their therapeutical goal in much complex systems. Compared to naked NPs (orange bars in **Figure 29**), the presence of the lipidic shell (green bars) had the effect of inducing coagulation at nearly the same time of the pure citrate plasma treated with physiological solution (Control sample in **Figure 29**) after the addition of $CaCl_2$. Therefore, it can be concluded that the lipidic shell essentially counteracts the tendency of blood to clot when in contact with positively-charged naked NPs. These results are consistent with the points made in Section 3.1.2 about the importance of a negatively charged lipid coating on the surface of the NPs, and can constitute an optimal starting point for future *in vivo* validations of our nanoconstructs, suggesting that their employment in intravenous injection would not constitute a hazard even in presence of high doses of NPs.

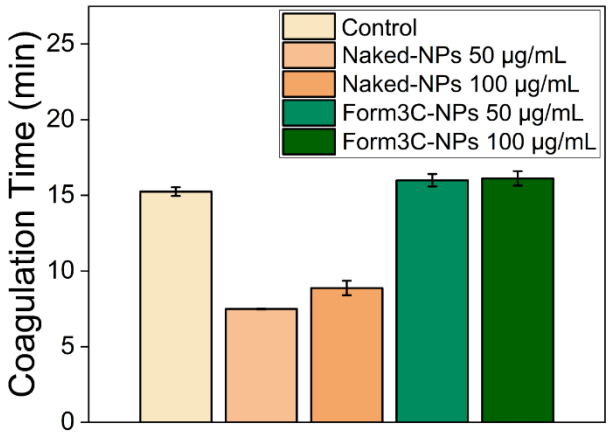

Figure 29. Coagulation times (min) of plasma in the presence of physiological solution (control), naked NPs and Form3C NPs, after the addition of calcium chloride.

2.4 Conclusions and future outlooks

The aim of this work was to develop a customizable lipidic shell meant to be applied as a carrier for liquid moieties and drugs or as a coating for inorganic nanoparticles. Based on the same principle of electrostatic interaction of the solid lipid nanoparticles employed to carry mRNA in the newly diffused Covid vaccines, our lipidic formulations are designed to interact with their charged cargo. When employed as smart coating for charged metal oxide nanoparticles, in the present case iron-doped zinc oxide nanoparticles, they provide them with a better dispersion

in biological media and a high stability over time. The administration of Form3C-coated NPs to BxPC-3 cells in the proof-of-concept study resulted in a massive increase of their biocompatibility with respect to pristine NPs, which enabled an escalation of the safe dose that could potentially be administered to cells in view of future theranostic treatments. Moreover, the high degree of customization of the lipidic formulation, achievable through the incorporation of a functional lipid linked to peptides or even antibody fragments, makes it suitable for a plethora of different applications that range from tumor targeting to immunotherapy. Finally, increasing the safe NPs dose can improve the outcome of many therapies based on the stimulation of previously administered nanoconstructs by means of ultrasound or light irradiation. Overall, the results of the chemical characterizations and the preliminary cell culture experiments here presented support the use of these lipidic formulations as a solid starting point of much more complex systems, thanks to their high versatility and enormous potential in future multimodal cancer therapy applications.

Chapter 3

Ultrasound-stimulated Zinc Oxide Nanoconstructs as a Pancreatic Cancer Treatment

The third Chapter of this PhD dissertation focuses on developing and testing hybrid nanoconstructs consisting of lipid-coated zinc oxide nanoparticles, activated with an ultrasound stimulation to maximize their antitumor potential against PDAC. Their fabrication largely follows the methods outlined in the second Chapter, with the addition of a sonosensitizer, the IR780 organic molecule, to the lipidic formulation to further enhance the effect of the ultrasounds. This Chapter further outlines the rationale for selecting zinc oxide as the core of the nanoconstructs and demonstrates the application of this nanomedicine-based multimodal therapy as a proof of concept in an in vivo setting.

3.1 Introduction

Pancreatic ductal adenocarcinoma (PDAC) remains one of the most difficult cancers to treat. Its "cold" tumor immune microenvironment, dense desmoplastic stroma and poorly organized vasculature causing hypoxia impede immune cells recruitment [725,726]. Innovative strategies are urgently needed to overcome this challenge. Current research focuses on multimodal approaches for cancer treatment, where different therapies synergistically lead to more successful tumor elimination than single treatments [727]. However, deep-seated organs like the pancreas are difficult to reach, making locally applied therapies like photodynamic therapy (PDT), photothermal therapy (PTT), radiotherapy and radiodynamic therapy (RDT) less effective [728,729] and often associated with severe side effects [730,731]. Conversely, sonodynamic therapy (SDT) offers a promising balance between low side effects, deep tissue penetration, and exceptional spatiotemporal selectivity [732,733]. SDT's cytotoxic mechanism is based on inertial cavitation, where gas bubbles violently collapse generating reactive oxygen species (ROS) that induce

cancer cell apoptosis [734,735]. Ultrasound treatments applied as cancer therapy have been proven to elicit an inflammatory immune activation, not only at the application site but also systemically [733].

The release of tumor cell debris and apoptotic bodies/necrosis fragments has the potential to elicit the so-called immunogenic cell death (ICD) [736], a mechanism that activates damage-associated molecular patterns (DAMPs) [429], leading to dendritic cell maturation and migration to lymph nodes. Here they present tumor antigens to $CD4^+$ and $CD8^+$ T cells, which in turn are activated and redirected to systemic circulation to finally infiltrate the tumor mass [630].

PDAC therapies do not rely on the tumor's enhanced permeability and retention effect; transcytosis rather than passive accumulation is the main route for drug or nanoconstruct infiltration in the tumor [503]. Ultrasounds may enhance tumor permeability and vessel fenestration, improving tumor accumulation in both intratumoral and intravenous administrations [737,738]. However, SDT alone can be impaired by PDAC's hypoxic nature, since the lack of available oxygen severely reduces the cavitation effect and consequently ROS generation, requiring smart nanomedicine-based strategies [732,738–741].

This study proposes a multimodal therapy using lipid-coated iron-doped zinc oxide (ZnO) nanoparticles (NPs) stimulated by a clinically approved ultrasound transducer. ZnO NPs have inherent anticancer properties, with a dose-dependent toxicity relying on various mechanisms [721]. To enhance the biocompatibility of ZnO NPs and ensure they remain intrinsically safe unless activated via ultrasound, iron is incorporated as a doping agent. This incorporation leads to significant improvements in their physico-chemical properties, including a slower dissolution rate and a more favorable toxicity profile. These enhancements, extensively documented in the literature [723,742], were also thoroughly detailed in a previous study from our research group [609], establishing iron-doped ZnO NPs as an ideal starting biocompatible material for further optimization. Functionalizing ZnO with amino-propyl groups allows gas nanobubbles absorption, enhancing inertial cavitation even in hypoxic conditions [607]. A tailored lipidic shell inspired by COVID-19 vaccines boosts tolerability and prevents aggregation [743], while incorporating the lipophilic sonosensitizer IR780 maximizes ultrasound stimulation effects and offers imaging potential, due to its strong optical absorption in the near infrared spectrum [464,744–746].

To date, only a few research groups have explored similar treatment combinations using nanoparticles-assisted ultrasound [465,540,595,747]. This prompted a focus on a proof-of-concept study of the multimodal therapy, starting with intratumoral administration of the NPs. This approach was chosen due to the poor

blood perfusion considered a hallmark of PDAC [727,748]. Intratumoral drug administration would help concentrate the nanoconstructs in the tumor area and further deeply distribute them under the effect of US stimulation. Additionally, local administrations has been shown to mitigate side effects compared to systemic administration [749]. In vitro tests further suggested that the tumor cell cytotoxicity is dose-dependent [750–752], leading to the search for approaches that improve their retention in the tumor area within the first 48 hours post-administration, without contending with barriers like the dense extracellular matrix and high interstitial fluid pressure, often seen in PDACs.

Here, the aim was to demonstrate that intratumoral injection of these lipid-coated ZnO NPs followed by ultrasound (US) stimulation could reduce tumor burdens and elicit both local and systemic responses. The nanoconstructs were tested in vitro for cytotoxicity, internalization, and mechanisms of action, and then validated in vivo for biodistribution, side effects, and efficacy in the presence or absence of the US treatment. In vivo studies confirmed that both the nanoconstructs and ultrasound application, when administered individually, were well-tolerated with no observed toxicity issues. Combined, they caused a synergistic cytotoxic response, resulting in tumor shrinkage with tumor cell apoptosis and immune cells recruitment. Mice treated with the lipid-coated NPs or lipid-coated-IR780 NPs in combination with US showed significantly prolonged survival compared to controls, demonstrating the efficacy of the combined treatment.

3.2 Materials and Methods

3.2.1 Nanoconstructs fabrication and characterizations

Oleic acid capped and iron doped zinc oxide NPs were synthetized following a protocol developed by Carofiglio et al. [609] and characterized by Dynamic Light Scattering (DLS), Zeta Potential, Nanoparticle Tracking Analysis (NTA), Scanning Electron Microscopy (SEM), Energy-dispersive X-Ray (EDX) and X-Ray Diffraction (XRD) analyses. The lipidic shell formulation used to coat the NPs consisted of DOPA (18:1 PA, 1,2-dioleoyl-sn-glycero-3-phosphate (sodium salt), chloroform solution), DOPC (18:1 (Δ9-Cis) PC (DOPC), 1,2-dioleoyl-sn-glycero-3-phosphocholine, chloroform solution), DSPE-PEG(2000) Amine (1,2-distearoyl-sn-glycero-3-phosphoethanolamine-N-[amino(polyethylene glycol)-2000] (ammonium salt)) and cholesterol solution in chloroform, purchased by Avanti Polar Lipids Inc. (Birmingham, AL, USA). The coating was achieved using a simple solvent exchange method, as recently described [743]. To assess the efficacy

of the lipidic coating, DLS, Zeta Potential, NTA and Cryo-EM analyses were carried out.

For CryoEM imaging, naked and lipid-coated NPs were vitrified and imaged at the Baylor College of Medicine Cryo-Electron Microscopy Core Facility (Texas Medical Center, Houston). A Pelco EasiGlow machine (Ted Pella, Inc) was used to glow discharge Quantifoil R1.2/1.3 300Cu (Quantifoil Micro Tools GmbH, Jena, Germany). Each grid was transferred to a Vitrobot Mark IV (FEI Company, Hillsboro, OR) where 3 µL of sample was applied to the grid. The samples were blotted and vitrified, then the grids were transferred to a Thermo Fisher Glacios Electron Microscope (Thermo Fischer Scientific Inc) operating at 200 kV. Images were captured using a the built-in EPU and Velox programs.

A lipophilic sonosensitizer, IR780 (Sigma-Aldrich), was incorporated in the lipidic shell and dried together with the lipids. A calibration curve of IR780 in water was employed to calculate IR780 retention in the lipidic shell, which was analyzed with UV-Vis spectroscopy after centrifugation of lipid-coated-IR780 NPs. To concentrate the NPs in saline solution in view of in vivo applications, the following protocol was developed: NPs were centrifuged, redispersed in a small volume of water, and then combined with 10x concentrated saline solution to achieve a final 0.9% w/v saline solution without impairing the lipid coating.

NPs were labeled with either AlexaFluor647 or AlexaFluor700 for in vitro flow cytometry and fluorescence microscopy studies, as well as for in vivo IVIS imaging studies.

3.2.2 ROS production in water

To evaluate ROS production under US stimulation, EPR coupled with the spin trapping technique was performed. A water solution containing a hydroxyl radical chemical trap 5,5-dimethyl-L-pyrroline-N-oxide (DMPO, Sigma-Aldrich) and the nanoconstructs was prepared. The solution was stimulated with US radiation at different power densities (0.2 - 2.0 W/cm^2), at 1 MHz for 1 minute, with a 2 cm^2 US transducer (Chattanooga Intelect Transport Ultrasound, DJO LLC and coupled with an acoustic water-based gel (Stosswellen Gel, ELvation Medical GmbH). The hydroxyl radical concentration was immediately measured using an EMXNano X-band spectrometer (Bruker, center field 3426 G, 10 scans, 60 s sweep timeand data were processed using the Bruker Xenon software (Bruker).

3.2.3 ICP-OES

An Agilent 5800 ICP-OES machine was used to assess the dissolution of zinc in either saline solution or cell culture medium, using Yttrium (Sigma Aldrich, St. Louis, MO, USA, Cat#01357) as an internal standard. Calibration curves were obtained using a Zinc standard for ICP (TraceCERT®, 1 g/L Zn in nitric acid), opportunely diluted. Wavelengths of 202.548 nm and 213.857 nm were used to measure zinc emission. The zinc concentration was obtained using the ICP-OES software ICP Expert (v7.6), and averaged between the two wavelengths. Briefly, 200 µg of naked or lipid-coated NPs was dispersed in 200 µL of saline or cell culture medium in Eppendorf tubes, and they stirred at 37 °C for up to one week. At different time points (1h, 5h, 24h, 72h, 168h), the samples were centrifuged, and both the pellet and the supernatant were digested in 1.8 mL of aqua regia (a mixture of nitric acid and hydrochloric acid, in a molar ratio of 1:3). All samples were diluted with 2 mL of a solution composed of 10% hydrochloric acid and 1% nitric acid (diluting solution) and analyzed. All experiments were conducted in triplicate, and the sum of the amount of zinc detected in the pellet and supernatant was set as 100% for each sample.

3.2.4 Cytotoxicity

The cytotoxicity of the nanoconstructs was preliminarily tested on KPC cells (gifted by Dr. Sankar Mitra, Houston Methodist Research Institute). Different concentrations of naked NPs, lipid-coated NPs, and lipid-coated NPs containing the IR780 sonosensitizer were added directly into the culture media (Gibco medium DMEM/F12 supplemented with 10% of Fetal Bovine Serum, ATTC, 1% of 100 µg/mL of streptomycin, and 100 units/mL of penicillin, Sigma-Aldrich) and administered to cells, and their viability was determined using WST-1 (Roche) assay after 24, 48 and 72 hours of incubation.

3.2.5 Ultrasound efficacy study

The efficacy of US treatment on KPC cells seeded in 24-well plates was evaluated with an ultrasound transducer (Chattanooga Intelect Transport Ultrasound, DJO LLC). Cells were treated with US 24 hours after NP administration. Cells were treated for 1 minute, with a power density of 0.8 and 1 W/cm^2, at a frequency of 1 MHz and a continuous operation mode (DC 100%) with the 2 cm^2 applicator, coupled with a water-based gel; then, they were detached and

seeded in 96 well plates to perform the viability assay after further 24 and 48 hours at standard cell culture conditions.

3.2.6 Internalization study

To assess NPs internalization, a protocol by Giordano et al.[753] was carried out as follows: cells were seeded in 24-well plates (µ-Plate 24 Well ibiTreat, ibidi) and treated with lipid-coated-IR780 NPs, where ZnO was previously labeled with AlexaFluor647 NHS ester. After 24 hours, the ultrasound treatment was carried out with a power density of 0.8 W/cm^2. Then, cells were incubated with ROS probe, 2',7'-Dichlorofluorescein Diacetate (DCF-DA) (Invitrogen), at standard cell culture conditions for 30 minutes in PBS, following a protocol by Liu et al.[754]. DCF-DA is a cell permeable non-fluorescent probe that becomes fluorescent in the presence of intracellular ROS, by oxidation to dichlorofluorescein (DCF).

After that, cells were washed with PBS, fixed with Paraformaldehyde, 2% in PBS for 10 minutes at room temperature, washed twice and incubated with 5 µg/mL wheat germ agglutinin (WGA) S-10 Alexa Fluor™ 550 Conjugate (Invitrogen) for 10 minutes in standard cell culture conditions, then washed twice again with PBS and incubated with 1 µg/mL DAPI (Abcam) for 3 minutes at room temperature. After a last wash, walls were removed, a drop of ProLong Diamond Antifade Mountant media (Invitrogen) was placed on the slide and a cover slip was placed on top. Images were acquired with a confocal fluorescence microscope (Olympus FV3000).

3.2.7 Flow Cytometry study

Cells were seeded in 24-well plates, treated with a safe dose of all treatment groups of NPs (previously labeled with AlexaFluor 647 NHS ester, Invitrogen) and received ultrasound stimulation (1 min, 0.8 W/cm^2). Right after the stimulation, cells were trypsinized and centrifuged, media was replaced with PBS and DCF-DA was added and incubated at standard cell culture conditions for 30 minutes. DAPI was then added for nuclei staining and the obtained cell suspension was analyzed with a BD FACSymphony A5 SE Cell Analyzer (BD Biosciences). Events were acquired employing the R660 channel to detect AlexaFluor647-labeled NPs, the R780 channel to detect the signal of IR780, the B510 channel to detect the ROS probe and the UV446 channel to gate viable cells.

3.2.8 Animals

6-week-old C57BL/6 mice were purchased from Taconic Biosciences (Rensselaer, New York). Mice were kept in the comparative medicine facility at Houston Methodist Research Institute (HMRI, Houston, TX). They underwent a 72-hour acclimation period to their new environment and received unrestricted access to food and water on a 12-hour day/night cycle. All experiments adhered to protocols reviewed by an independent Institutional Animal Care and Use Committee (IACUC) and following the guidelines of the National Institutes of Health Guide for the Care and Use of Laboratory Animals and Animal Welfare Act and the ARRIVE guideline.

3.2.9 Tumor model

To establish the PDAC tumor model, $1x10^6$ KPC cells were suspended in 100 µL of a 3:1 mixture of PBS and Matrigel (Corning™, CB40234) and inoculated subcutaneously in the right flank. Mouse KPC cell line was chosen since it models the disease accurately, retaining key genetic mutations and providing a well-established tumor model for PDAC.[755–757] Tumor volume, mice weight and basal temperature were monitored every other day with a digital caliper and a scale. Tumor volume was determined using the formula (Length x $Width^2$)/2, where length represents the longest dimension and width is its perpendicular counterpart.

3.2.11 Biodistribution study

When tumors reached 100-150 mm^3 in volume, mice were randomized into designated groups (n=5/group) and treated with naked and lipid-coated NPs (previously labelled with AlexaFluor 700 NHS ester (Invitrogen), dispersed in saline solution, and injected intratumorally at a dose of 30 mg/kg of weight. Control mice received saline solution only. Mice were monitored for 14 days after the injection and imaged with an in vivo bioluminescence/fluorescence imaging system (IVIS Spectrum, Perkin Elmer). The right flank was shaved before acquiring the baseline image, and mice anesthetized with isoflurane were fluorescently imaged to detect the signal of NPs at specific timepoints, (excitation of 675 nm and emission of 720 nm). Two small cohorts of n=4 animals per group were also treated with NPs and sacrificed after 1 day and 3 days from NPs injection. At the established endpoints, all animals were euthanized by CO_2 asphyxiation and organs were harvested for ex vivo imaging. The images were processed by Living Image Software (Perkin Elmer) by drawing a region of interest (ROI) around the tumor

area in vivo and the extracted organs, measuring the fluorescent signal in radiance ([p/s] / [µW/cm²]). Blood was collected in BD Microtainer collection tubes, centrifuged at 5000 x g for 12 min and the obtained plasma was frozen at -80 °C for further analyses, together with the harvested tumors, previously weighted.

3.2.12 ICP-OES of Tumors and Plasma

Tumors and plasma were dissolved in aqua regia by adapting an established digestion protocol [758,759]. Briefly, tumors were thawed, immersed in 4 mL of fresh aqua regia overnight under in a chemical fume hood on a heating plate (T = 60 °C). After complete digestion, 8 mL of diluting solution was added, and the final volume was filtered with a 0.45 µm pore size Nylon syringe strainers (Whatman™ Puradisc™). Plasma was thawed and 200 µL from each sample was digested in 2 mL of aqua regia overnight under a chemical fume hood. Afterwards, 4 mL of diluting solution was added to the digested samples and a filtration step was performed before the analysis. All measurements were performed in triplicate.

3.2.13 Ultrasound efficacy study in vivo

After reaching a tumor volume of 100-150 mm^3, n=6 mice per group were treated with naked, lipid-coated, and lipid-coated-IR780 NPs, as described above. Control mice received saline solution. Mice were anesthetized, shaved in the tumor area and a baseline image was acquired with IVIS Spectrum. To detect the signal of IR780, the excitation wavelength was set at 745 nm and the emission at 820 nm. Right after the injection, another IVIS image was acquired and the US stimulation (2 W cm2, 1MHz, DC 100%, 2 minutes) was applied with the 2 cm^2 applicator. Water-based gel was employed to avoid any unwanted overheating.. Mice were imaged once again with the IVIS Spectrum. The US treatment was repeated for the two following days, and IVIS pictures were collected at established timepoints. After 7 days from the first NP administration, the treatment was repeated with a second injection of NPs at the same dose and an US treatment for three consecutive days. After 14 days from the first injection, mice were sacrificed. Tumors and organs were collected, imaged with IVIS and formalin fixed.

3.2.14 Histopathology analysis of tumors

Tumors were harvested, imaged with IVIS and then formalin-fixed, paraffin-embedded (FFPE) and stained (n=5/group) with an apoptosis kit (ApopTag Peroxidase in Situ Apoptosis Detection Kit, Sigma-Aldrich) and Masson’s

Trichrome. Ten ROI from each section and the full tumor area were acquired with an inverted fluorescence microscope (Keyence BZ-X810) and analysed with Keyence BZ-X800 Analysis Software. ImageJ software was employed to apply a color deconvolution and calculate the percentage of the apoptotic area with respect to the total tumor area in n=5 /group samples stained with ApopTag.

3.2.15 Flow Cytometry study

Saline solution, lipid-coated NPs or lipid-coated-IR780 NPs were intratumorally injected, and US stimulation was applied for three consecutive days of all groups (n=6/group), as previously described. Mice receiving only saline solution and no US treatment were set as control. After 5 days from the NPs administration, all mice were sacrificed and tumors, TdLNs and spleens were collected and processed for flow cytometry. Briefly, spleens were dissociated into single-cell suspensions by mechanical filtration through 40 μm cell strainers (Fisherbrand, 22-363-547) and red blood cells were lysed with two cycles of ACK lysis buffer (Quality biological, 118-156-101). TdLNs were digested in RPMI-1640 with 1x collagenase/hyaluronidase (STEMCELL Technologies, NC2031808) and mechanically dissociated through 40 μm cell strainers. Tumors were cut into 1 mm sections and then incubated for 1 h at 37 °C on an orbital shaker in RPMI-1640 with 1x collagenase/hyaluronidase and 20U mL^{-1} of DNase I (Sigma-Aldrich, 11284932001), then mechanically dissociated through 40 μm cell strainers into single cell suspension. Tumor-infiltrating leukocytes were then separated using Lymphoprep (StemCell Technologies, NC0665098). Cells from all the organs were finally resuspended in FACS buffer (Corning Dulbecco's Phosphate-Buffered Saline, 1X without calcium and magnesium, 21-031-CV + 2% of Corning Fetal Bovine Serum, 35-011-CV) and plated in 96-well V-bottom plates. Cells were washed and stained with Rat Anti-mouse CD16/CD32 (BD Biosciences, 553141) for 30 minutes, then stained with either the myeloid or lymphoid antibody panel. Events were acquired employing the A5 SE FACSymphony Cell Analyzer (BD Biosciences) and analysed using FlowJo v10.9 software.

3.2.16 Survival study

A survival study was conducted on a separate mouse cohort (n=8/group), following the same treatment plan described in the US Treatment section. Additionally, the US irradiation was repeated every week for 3 consecutive days until the mice reached the humane endpoint; the tumor mass was measured, along with the body weight and rectal temperature, every other day. Kaplan-Meier

survival curves were generated, and log-rank tests were used to compare survival between groups.

3.2.17 Statistical Analysis

Statistical analyses were conducted using GraphPad Prism 9.1.6. An analysis of variance (ANOVA) was employed for multiple group comparisons. Significance was analyzed by either unpaired one-way or two-way ANOVA. Multiple comparisons were carried out with Tukey‘s correction. $P<0.05$ was considered statistically significant: *$p < 0.05$; **$p < 0.005$; ***$p < 0.0005$; **** $p < 0.0001$.

3.3 Results and discussion

3.3.1 Fabrication and Characterization of Lipid-coated ZnO NPs Enhanced with IR780

The iron-doped ZnO NPs were obtained following an established wet-chemical synthesis protocol [609]. They had a diameter of about 8-10 nm, as confirmed by the Scanning Electron Microscopy (SEM) images (**Figure 30a**), and tended to form irregular aggregates in aqueous media, as observed in Cryo Electron Microscopy (CryoEM) image (**Figure 30b**). Energy-dispersive X-Ray (EDX) analysis confirmed a distinct peak for zinc and the presence of iron doping, with a final atomic ratio of 3.55 at% (**Figure 30c**). The X-Ray Diffraction (XRD) pattern displayed diffraction peaks typical of the wurtzitic structure of ZnO (JCPDS-ICDD, card No. 89-1397), with no additional peaks indicating other oxide phases from unwanted iron nucleation (**Figure 30d**).

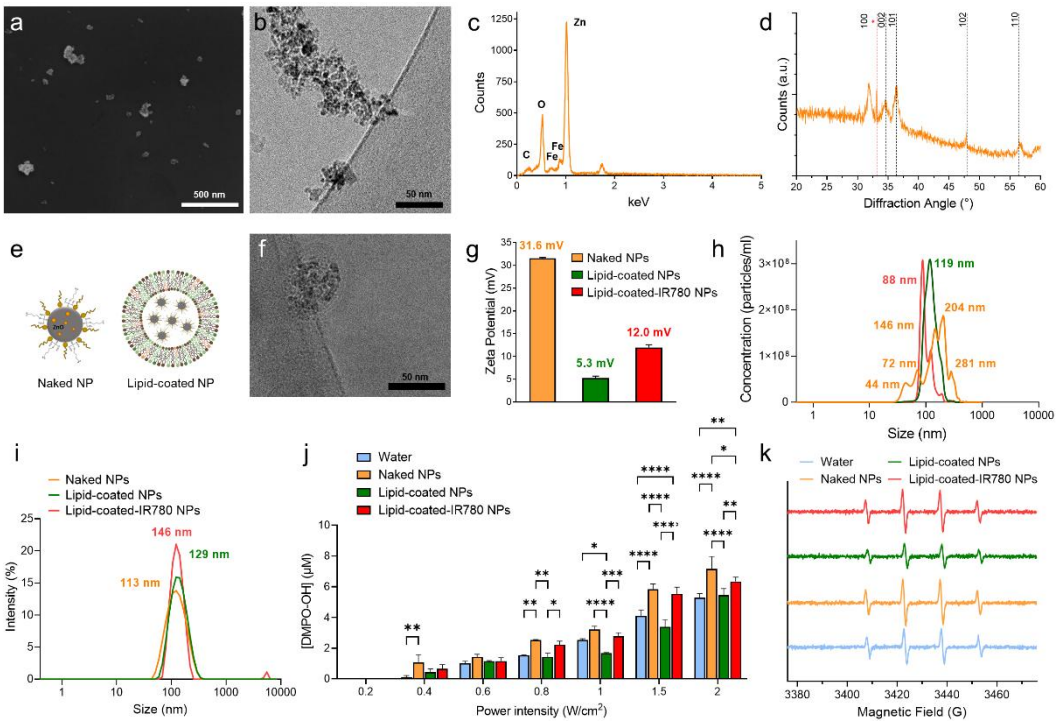

Figure 30 A) SEM picture, B) CryoEM image, C) EDX and D) XRD of the naked NPs. E) Schematic representation of naked and lipid-coated NPs. F) CryoEM image of lipid-coated NPs. G) Zeta potential and H) NTA of naked (orange), lipid-coated (green) and lipid-coated-IR780 (red) NPs. I) DLS of the naked (orange), lipid-coated (green) and lipid-coated-IR780 (red) NPs. J) EPR measurements of ROS production of the various nanoconstructs in water upon ultrasound stimulation. K) Representative image of the spin-adduct of the DMPO-OH complex obtained after US stimulation at 1.5 W/cm^2. Data are expressed as mean ± standard deviation. Significance was analyzed by two-way ANOVA. *p < 0.05; **p < 0.005; ***p < 0.0005; **** p < 0.0001. Tukey's correction was applied for multiple comparison.

When coated with a lipidic shell (**Figure 30e**), the final nanoconstructs had a size of approximately 50 nm as confirmed by CryoEM imaging, depicting the lipid bilayer incorporating multiple NPs (**Figure 30f**).

Zinc release from naked or lipid-coated NPs in saline or cell culture media over time were measured using Inductively Coupled Plasma-Optical Emission Spectrometry (ICP-OES, **Figure 31a and Figure 31b**). Less than 20% of total zinc was released into the supernatant after a week for all groups. Naked NPs tended to dissolve more easily in cell culture medium than in saline, likely due to phosphate groups forming complexes with zinc and increasing its solubility. In contrast, lipid-coated NPs showed similar degradation in both water and medium, indicating higher stability in different aqueous environments (**Figure 31c**).

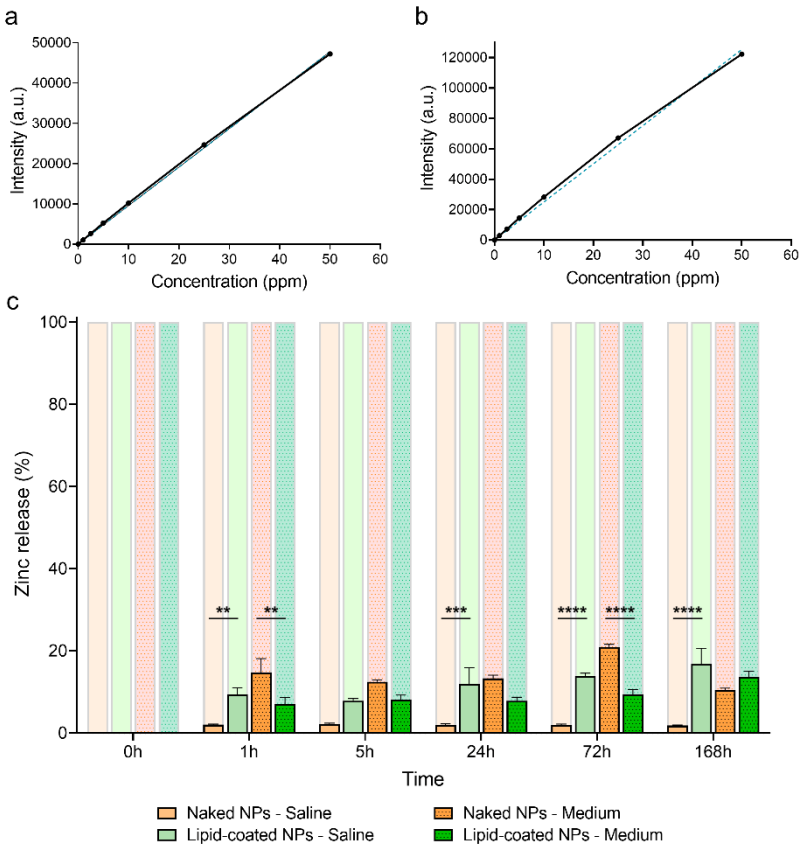

Figure 31. A) Zinc standard calibration curves obtained at 202.548 nm and B) 213.857 nm. C) Histograms reporting zinc release in saline and cell culture medium (patterned columns) of naked (orange) and lipid-coated (green) NPs over one week of incubation at 37 °C. Data are expressed as mean ± standard deviation. Significance was analyzed by two-way ANOVA. *$p < 0.05$; **$p < 0.005$; ***$p < 0.0005$; **** $p < 0.0001$. Tukey's correction was applied for multiple comparison.

To potentiate the effects of US stimulation, IR780 sonosensitizer was added to the lipidic coating of NPs exploiting its lipophilic nature and ensuring adequate retention of the dye in the shell (**Figure 32a-Figure 32d**).

Compared to pristine NPs, lipid-coated NPs exhibited a marked shift in zeta potential, likely due to the interaction between the positively charged ZnO NPs and negatively charged lipidic shell. In the presence of IR780, a cationic lipophilic dye, the zeta potential consequently increased slightly (**Figure 30g**) [743]. Nanoparticle Tracking Analysis (NTA) showed naked NPs forming clusters of various sizes (orange line), while lipid-coated NPs displayed a monodisperse size distribution (single green peak). Therefore, coating of the NPs improved their dispersion in aqueous media, overcoming the tendency of pristine inorganic NPs such as ZnO to

aggregate [492,494] in view of in vivo applications. The incorporation of IR780 did not affect much the monodispersity of the nanoconstructs in aqueous medium (**Figure 30h** and **Figure 30i**).

Electron Paramagnetic Resonance (EPR) spectroscopy indicated that the NPs enhanced ROS production in water upon US stimulation. While pure water could generate ROS through inertial cavitation induced by US, ZnO NPs reduced the cavitation threshold and enhanced ROS concentration [606]. Iron-doped ZnO NPs showed increased ROS production at US power densities of 0.4, 0.8, 1.5 and 2 W/cm^2, compared to water. In contrast, lipid-coated NPs produced less ROS suggesting lipids may scavenge the hydroxyl radicals' production. Despite this, lipidic coating was necessary to safely administer the ZnO NPs due to their inherent cytotoxicity at high dosages and to reduce their aggregation. Thus, inclusion of the sonosensitizer IR780 played a pivotal role in the nanoconstructs' effectiveness by restoring ROS production. Indeed, lipid-coated-IR780 NPs produced comparable ROS to naked NPs at powers densities up to 1.5 W/cm^2 (**Figure 30j-k**). These results indicated promising potential for subsequent in vitro and in vivo efficacy studies, as the lipidic shell ensures high biocompatibility and colloidal stability, while ZnO NPs and IR780 enhance the response to US stimulation.

Lipid-coated NPs were dispersed in water at 1 mg/mL, which is suitable for in vitro applications [743]. For in vivo applications, lipid-coated NPs were concentrated in 0.9% w/v saline (**Figure 32e**). The zeta potential and DLS showed comparable surface charge (+4.0 mV) and dispersibility in saline solution to those in water (**Figure 32f**). Concentrations of up to 40 mg/mL were thus achieved for in vivo intratumoral injections. The incorporation of fluorescent dyes, necessary to visualize NPs in subsequent in vitro and in vivo experiments, did not affect the dispersibility or the lipidic coating of the NPs (**Figure 32h-32i**).

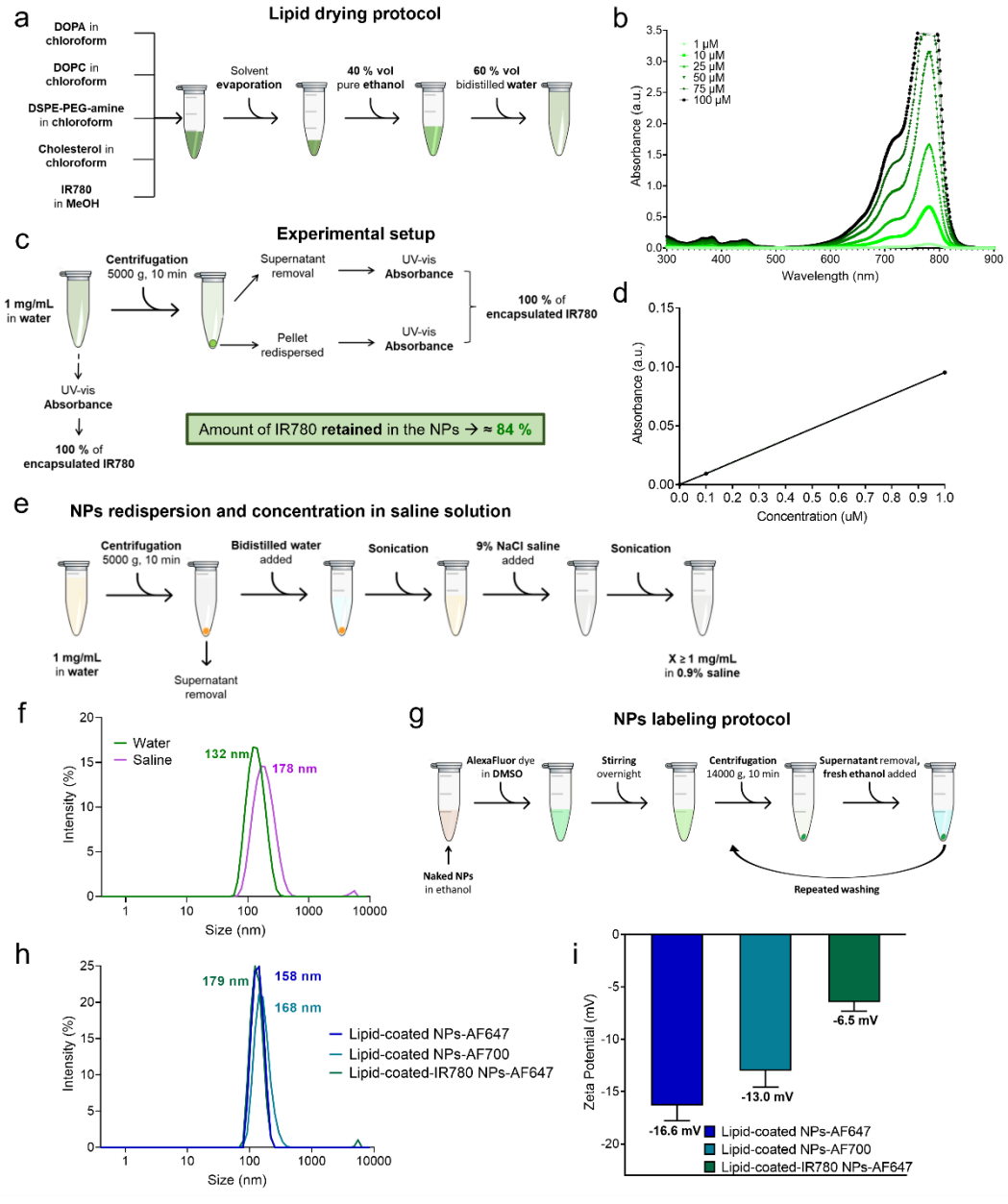

Figure 32. A) Scheme of the lipid-drying protocol incorporating the IR780 sonosensitizer. B) IR780 absorbance spectrum in methanol at different concentrations. C) Experimental setup to assess IR780 retention in the lipidic shell. D) Calibration curve of IR780 in water employed to evaluate IR780 retention E) Protocol to resuspend NPs in saline solution at higher concentrations than in water (up to 40 mg/mL), consisting in a first redispersion in a small volume of water and the successive addition of 10x concentrated saline solution, to get to a 0.9 %v/w saline solution suitable for injection. F) DLS of lipid-coated NPs in water (green) and saline solution (purple). G) NPs labeling

protocol with fluorescent dyes for imaging, flow cytometry and in vivo applications. H) DLS and I) zeta potential of lipid-coated-AlexaFluor647 (blue), lipid-coated-AlexaFluor700 (cyan) and lipid-coated-IR780-AlexaFluor647 NPs (dark green). The observed shift in zeta potential towards negative values is due to the dye coupling, covalently bound to amino-propyl groups on the NP surface. Data are expressed as mean ± standard deviation.

3.3.2 In vitro validation of the combined NPs/US treatment

Naked, lipid-coated and lipid-coated-IR780 NPs were tested on KPC cells at increasing concentrations to assess their cytotoxicity after 24, 48- and 72-hour exposure (**Figure 33a**, **Figure 34a** and **Figure 34b**, respectively). At a concentration of 20 μg/mL, naked NPs markedly affected cell viability after 24 hours of exposure (**Figure 33a**). Following a threshold of 70% [760], lipid-coated NPs were non-cytotoxic up to 50 μg/mL owing to the presence of the lipidic shell, as also previously reported [743]. When IR780 was incorporated in the lipidic shell, there was a decrease in cell viability, while the free IR780 counterpart exhibited no significant toxicity up to 50 μg/mL.

To compare all treatment groups, NPs concentration of 15 μg/mL was chosen to perform the following in vitro experiments. The viability of KPC cells was assessed after 24 hours post US treatment at 0.8 and 1 W/cm^2 following NPs administration (**Figure 33b)**. Control KPC cells (without NPs treatment) were unaffected by US stimulation, and US stimulation at both doses did not significantly affect KPC cells also treated with the naked NPs. Strikingly, US stimulation significantly decreased cell viability with lipid-coated NPs, in a power density-dependent manner, with a p-value of < 0.0001 at 1W/cm^2 compared to control US stimulation alone. Comparatively, the incorporation of IR780 further enhanced the impact of lipid-coated NPs on cell viability. In particular, upon US exposure at 1 W/cm^2, the recorded cell viability with lipid-coated-IR780 was significantly lower ($p < 0.0001$) than with control US administration, and markedly lower than the cytotoxicity produced by lipid-coated NPs and US. (**Figure 33c**).

Confocal microscopy imaging showed KPC cell internalization of lipid-coated IR780 NPs after US stimulation at 0.8 W/cm^2 (**Figure 33d**). Specifically, the NPs (labeled with AlexaFluor 647) and IR780 dye were visible in the cytoplasm. Further, ROS production was detected via 2',7'-Dichlorofluorescin (DCF) signal, which showed cytosolic presence.

Flow cytometry was employed to assess the fluorescence intensity associated with internalized NPs (NPs-R660) and ROS generation (DCF-B510) among various treatment groups (**Figure 33e).** Quantitative assessment of the percentage of cells expressing the DCF signal showed that ROS production was increased in all NPs-treated groups, with and without US stimulation (0.8 W/cm^2), compared to control cells. Remarkably, the group treated with lipid-coated NPs alone did not cause excess of ROS generation or enhanced cell death. However, when stimulated with US, an increase in ROS production was observed (**Figure 33f**). These results strongly suggest that the lipidic shell minimized zinc oxide NPs toxicity and reduced oxidative stress, as further confirmed by the low percentage of dead cells in this treatment group, comparable to untreated controls (**Figure 33g**). Indeed, only the combination with US restored ROS production and cell death to the levels observed in other treatment groups. The percentage of cells internalizing NPs and IR780 was over 95% for all treated groups, proving that the production of ROS is effectively intracellular. (**Figure 33h** and **Figure 33i**, respectively).

Thus, in conclusion to the in vitro experiments, it can be assumed that the lipid-coated-IR780 NPs are more cytotoxic across all concentrations compared to lipid-coated NPs. Furthermore, US increases the cytotoxicity of lipid-coated IR780 NPs, although the production of ROS in KPC cells remains comparable. Although preliminary data (**Figure 30I**) showed a significant improvement of ROS production, it is important to note that these experiments were conducted in a solution volume of NPs (see the Experimental Section below). In contrast, the flat cell monolayer considered in 2D experiments may not be ideal for fully unraveling the mechanisms of the NP+US combination. Ultrasounds consists of acoustic pressure waves propagating in a volume (of liquid or tissue) and likely has minimal effect on a single cell surface, such as the in vitro monolayer. Therefore, in vivo experiments are needed to better understand the phenomenon in a three-dimensional tumor model and to demonstrate therapeutic efficacy.

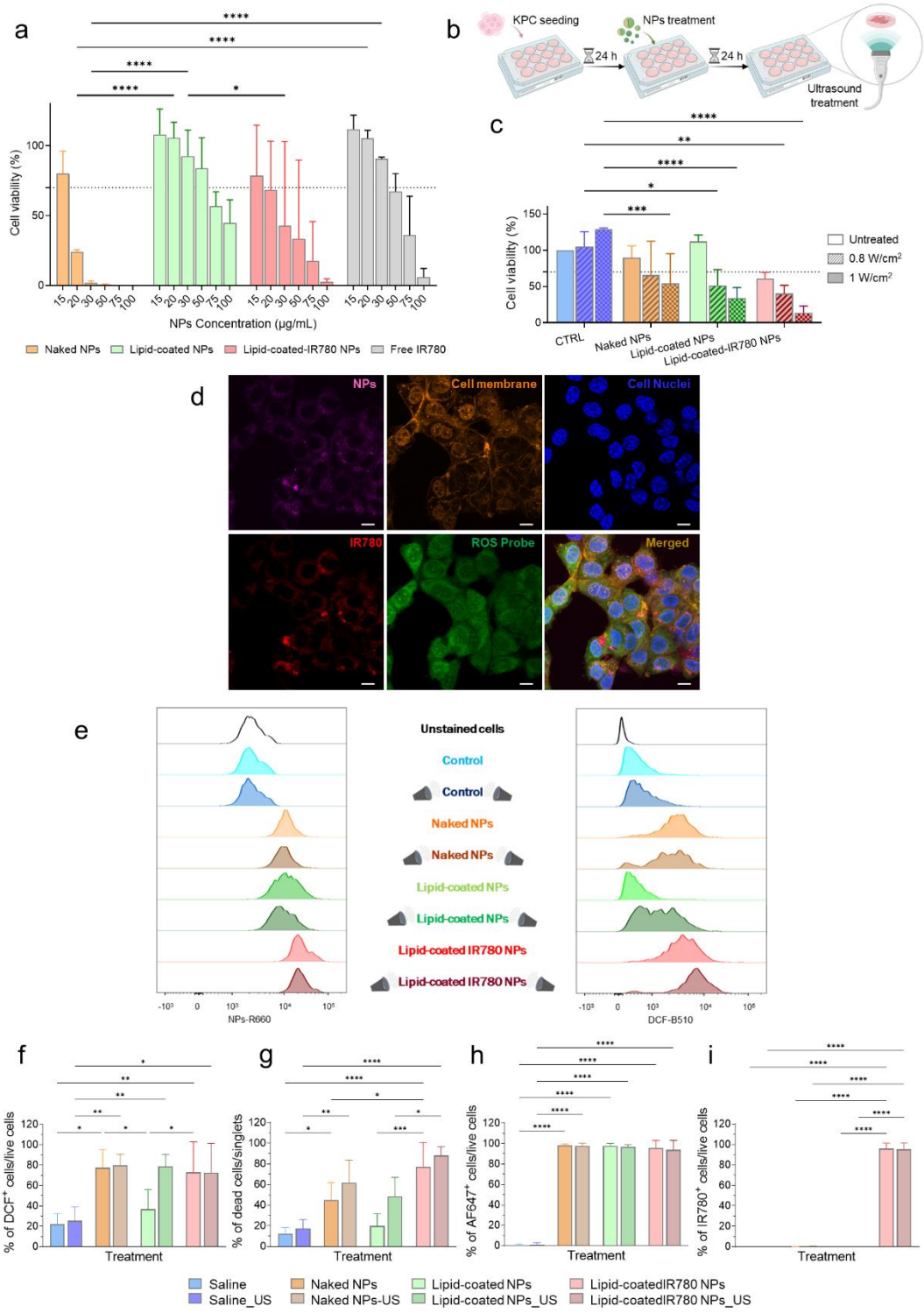

Figure 33. A) Cytotoxicity of naked, lipid-coated, lipid-coated-IR780 and free IR780 on KPC cells after 24-hour exposure. B) Schematic protocol of in vitro tests. C) Cell

viability of KPC cells after NPs administration, with and without US stimulation, measured 24 hours after US. D) Fluorescent confocal microscopy of KPC cells internalizing lipid-coated-IR780 NPs after US stimulation at 0.8 W/cm^2 for 1 minute. The NPs, labelled with AlexaFluor 647, are shown in the pink channel, IR780 is imaged in the red channel, nuclei are stained with DAPI (blue channel), membranes with WGA 550 (orange channel) and the green channel shows DCF signal due to the generation of ROS. E) One-dimensional histograms of the fluorescence intensity associated with NPs internalization (NPs-R660) and DCF production (DCF-B510) for all treatment groups. F) Histograms reporting the percentage of DCF producing cells, G) dead cells, H) cells internalizing NPs and I) cells internalizing IR780 (US treatment 0.8 W/cm^2, 1 min, 100% DC). Data are expressed as mean ± standard deviation. Significance was analyzed by two-way ANOVA. *p < 0.05; **p < 0.005; ***p < 0.0005; **** p < 0.0001. Tukey's correction was applied for multiple comparison.

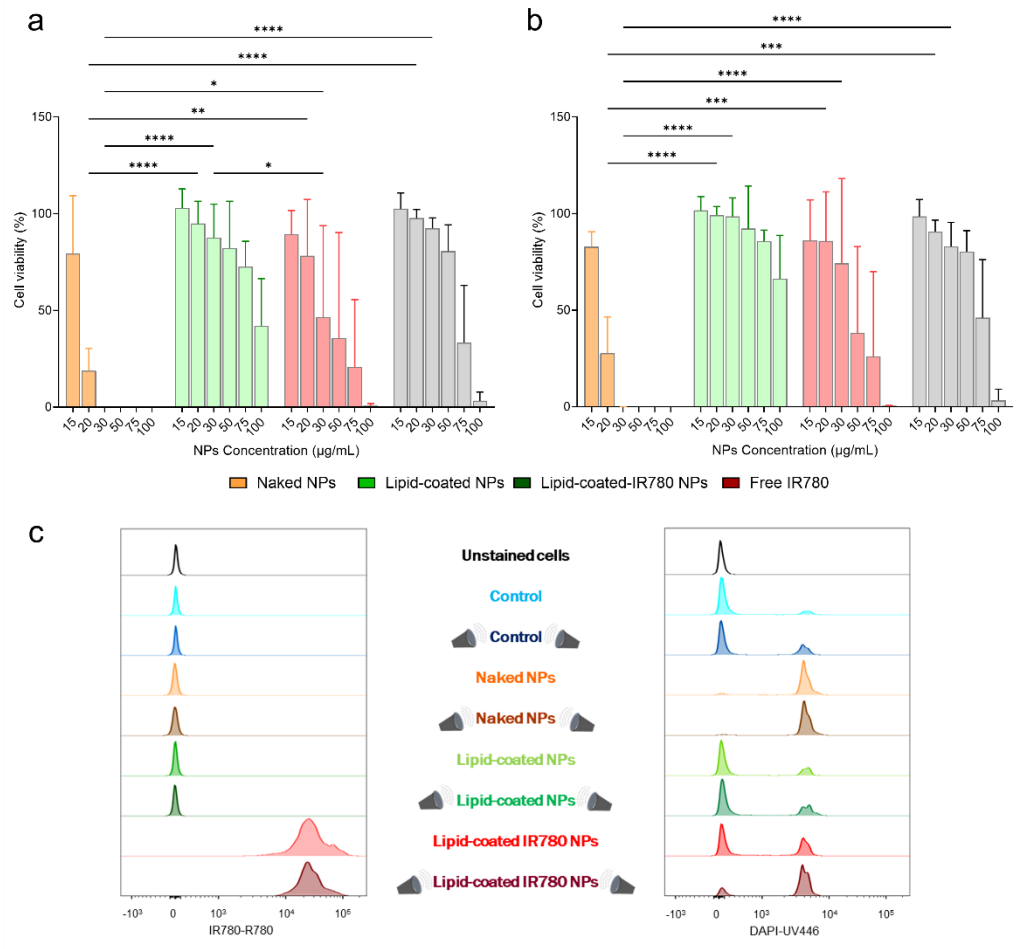

Figure 34. Cytotoxicity on KPC cells after A) 48h and B) 72h from NPs administration. Data are expressed as mean ± standard deviation. Significance was

analyzed by two-way ANOVA. *p < 0.05; **p < 0.005; ***p < 0.0005; **** p < 0.0001. Tukey's correction was applied for multiple comparison. C) One-dimensional histograms reporting the fluorescent intensity associated with cells internalizing IR780 (IR780-R780) and dead cells positive to DAPI (DAPI-UV446).

3.3.3 Biodistribution study

A biodistribution study was performed by injecting the naked NPs and lipid-coated NPs intratumorally in KPC subcutaneous murine model of PDAC. Mice receiving saline only were used as controls. Mice were imaged with IVIS pre- and post-NPs administration (day 0) and at pre-determined timepoints. Ex vivo IVIS was performed on days 1 (n=11), 3 (n=11) and 14 (n=15) (**Figure 35a**). Tumor weights measured ex vivo were comparable across treatment groups, indicating no significant effects of NPs of tumor shrinkage (**Figure 35b**). This finding was corroborated by the in vivo progression of tumor volumes (**Figure 36a**) and visual comparisons of extracted tumors, which showed no differences among experimental groups (**Figure 36b**).

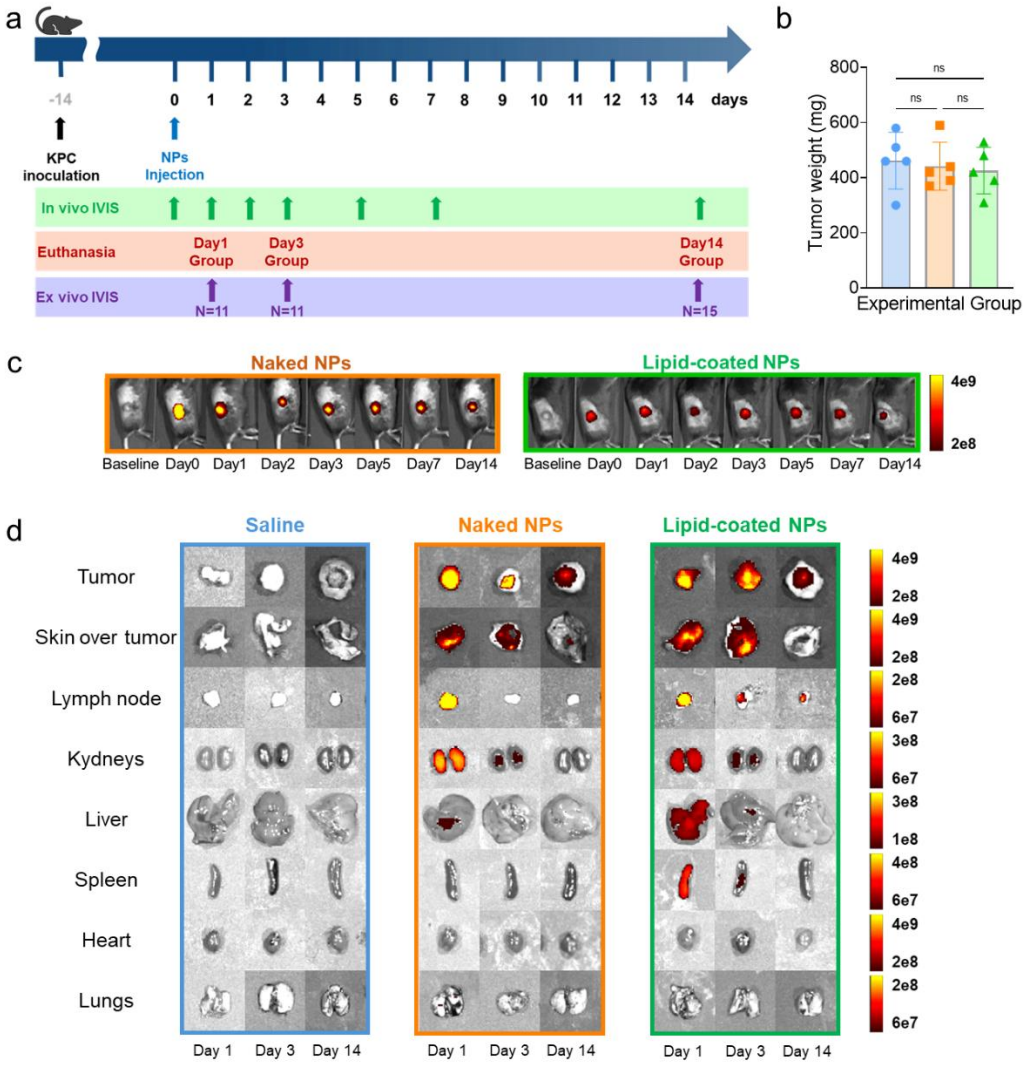

Figure 35. A) Scheme of the treatment plan. B) Tumor weights on day 14. C) In vivo IVIS imaging over time of naked and lipid-coated NPs dyed with AlexaFluor700 (excitation 675 nm, emission 720 nm). D) IVIS pictures of organs explanted at various timepoints (excitation 675 nm, emission 720 nm). Data are expressed as mean ± standard deviation. Significance was analyzed by either one-way or two-way ANOVA. *$p < 0.05$; **$p < 0.005$; ***$p < 0.0005$; **** $p < 0.0001$. Tukey's correction was applied for multiple comparison.

Throughout the study, the fluorescent signal of both naked and lipid-coated NPs (labeled with AlexaFluor700 covalently conjugated to ZnO NPs) remained clearly detectable (**Figure 35c**). The fluorescence intensity of lipid-coated NPs was consistently lower than that of the naked NPs. This could be due either to the lipidic

coating's shielding and quenching effect or the improved dispersibility of NPs when surrounded by the lipid bilayer [761]. Initial systemic accumulation in filtration organs (lymph nodes, kidneys, and spleen) was observed in ex vivo IVIS images on day 1 and to a lesser extent on day 3. Both naked and lipid-coated NPs were rapidly expelled, with no detectable traces in organs other than tumors and surrounding skin by the endpoint day 14 (**Figure 35d**). Tumors extracted on day 1, 3 and 14 were analyzed with the ICP-OES to detect residual zinc, expressed as a percentage of the initially injected dose (% ID).

Mice exhibited no signs of toxicity, as evidenced by stable body weight and basal temperature, further confirming the safety of NPs injection (**Figure 36c and Figure 36d)**.

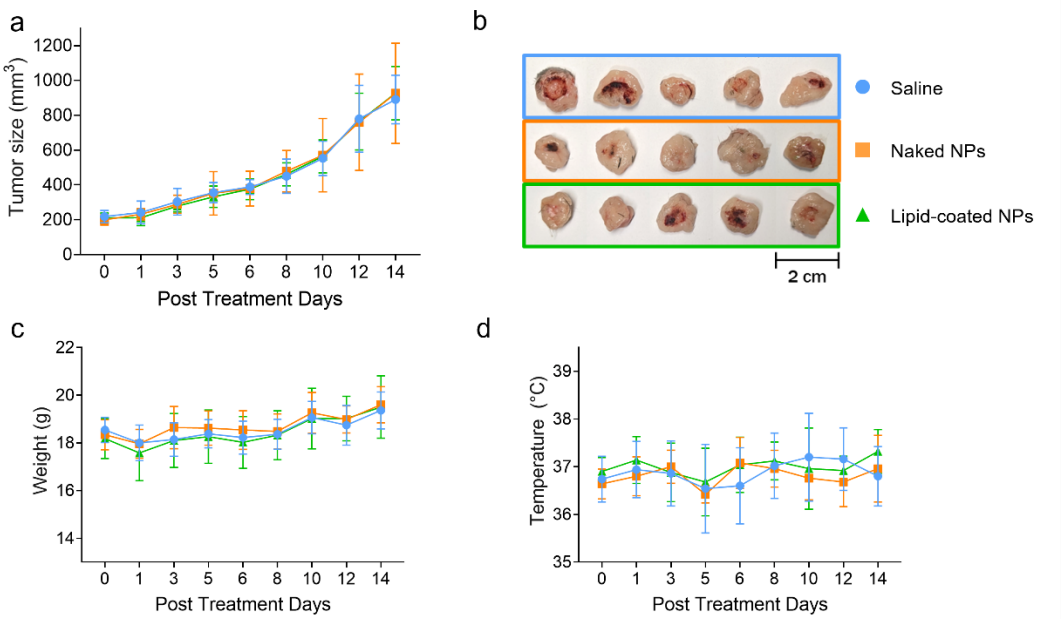

Figure 36. A) Tumor volume progression in vivo. B) Digital photos of tumors explanted on day 14. C) Mouse weight progression over time. D) Animal temperature progression over time. Data are expressed as mean ± standard deviation.

A declining trend in zinc retention was observed, with up to 80% of naked NPs retained in the tumors on day 1, decreasing to 20% of the injected dose by day 14 (**Figure 37a**). Tumors injected with lipid-coated NPs exhibited a lower initial zinc accumulation, following a similar descending trend over time, which however was not statistically significant. On the other hand, all plasma samples showed zinc levels around 1% of the injected dose, similar to saline controls, suggesting the absence of systemic zinc diffusion (**Figure 37b**).

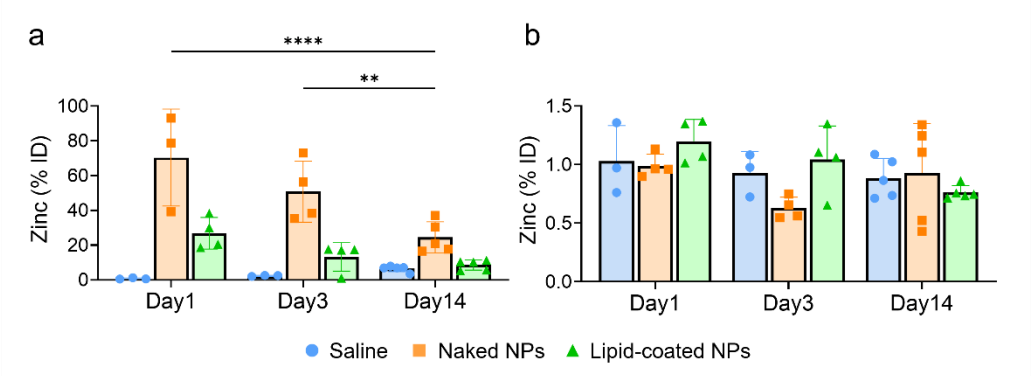

Figure 37. A) Zinc concentration expressed as a percentage of the injected dose in tumors and B) plasma. Data are expressed as mean ± standard deviation. Significance was analyzed by two-way ANOVA. *p < 0.05; **p < 0.005; ***p < 0.0005; **** p < 0.0001. Tukey's correction was applied for multiple comparison.

3.3.4 Efficacy Study of the combined treatment

The biodistribution study results showed that the intratumoral injection of the nanoconstructs was safe per se and did not elicit any adverse reactions. Therefore, an efficacy study was carried out by combining intratumoral injection of the NPs and US stimulation, including a treatment group with the sonosensitizer. IVIS imaging data revealed a robust fluorescent signal persisting up to 48 hours post-injection. This finding supported the strategy of applying US stimulation after NPs administration daily over three consecutive days, to ensure their tumor retention during the treatment. Additionally, a second NPs injection followed by three additional US stimulations over consecutive days was included to enhance the combined treatment's efficacy (**Figure 38a**). The most promising results were observed in the group treated with lipid-coated-IR780 NPs and US, as reflected by the significantly lower tumor weights compared to groups not receiving US ($p<0.007$) (**Figure 38b**) and noticeable tumor shrinkage (**Figure 38c**). Tumor sizes, measured in vivo over 14 days, were consistent with ex vivo measurements and showed significantly slower tumor growth in the group treated with lipid-coated-IR780 NPs and US (**Figure 38d**). IVIS imaging confirmed that all treatment groups retained NPs in the tumors until study endpoint (**Figure 38e**). In particular, the fluorescence intensity of the nanoconstructs over time decreased until day 7 followed by restoration after the second NP administration (**Figure 38f**). Interestingly, the first US stimulation resulted in a slight increase of the total radiant efficiency across all US-treated groups (**Figure 38g**).

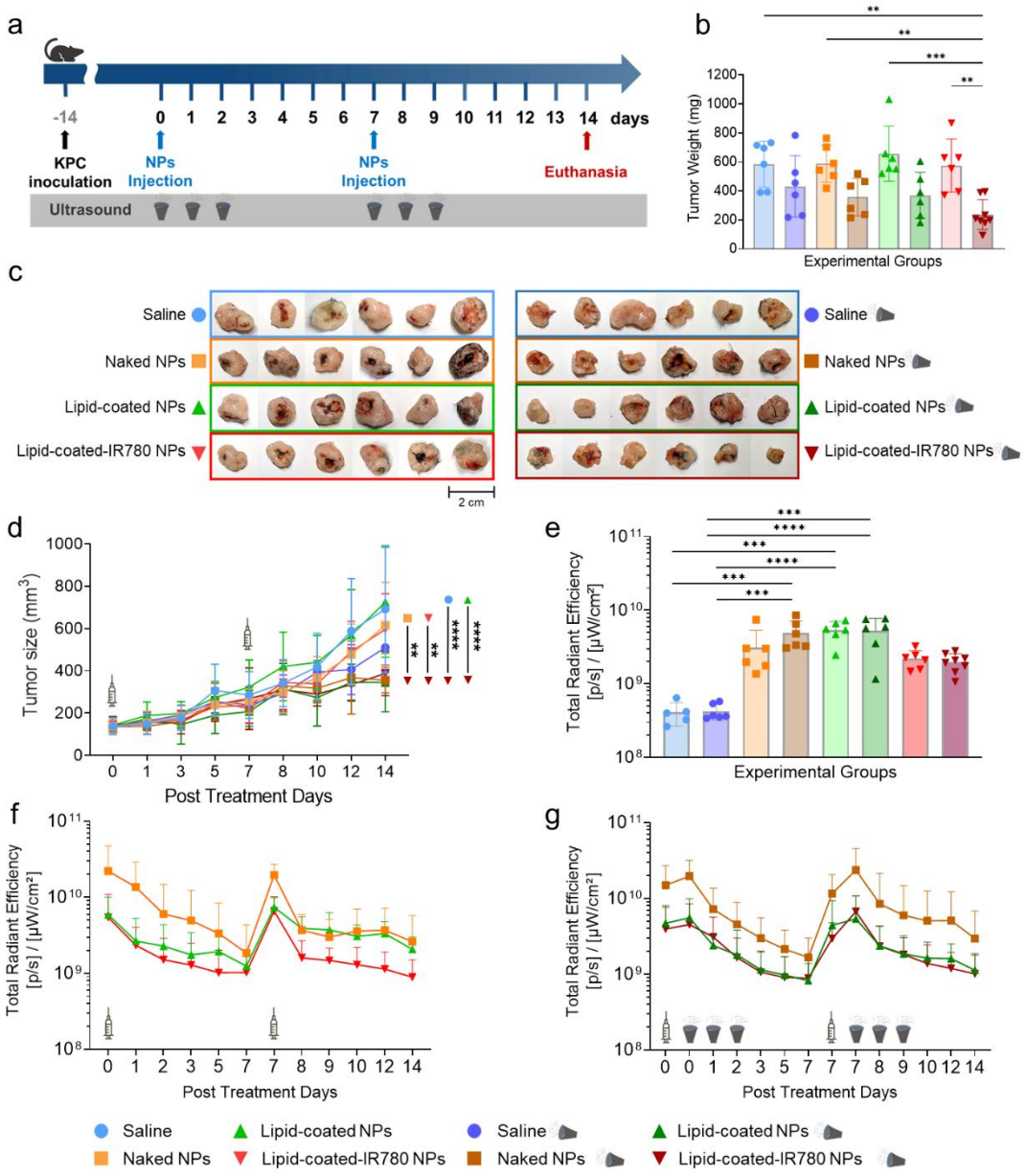

Figure 38. A) Scheme of the treatment plan. B) Tumor weights on day 14. C) Digital photos of tumors explanted on day 14. D) Tumor volume progression in vivo over time. E) Total radiant efficiency (excitation 675 nm, emission 720 nm) of the explanted tumors. F) In vivo total radiant efficiency progression within tumor regions of interest (ROIs) of the groups treated with NPs only and G) those treated with NPs and ultrasound (excitation 675 nm, emission 720 nm). Data are expressed as mean ± standard deviation. Significance was analyzed by either one-way or two-way ANOVA. *$p < 0.05$; **$p < 0.005$; ***$p < 0.0005$; **** $p < 0.0001$. Tukey's correction was applied for multiple comparison.

No significant fluorescence intensity with respect to control groups was detected in other organs (kidneys, lymph nodes, spleen, liver, lungs, and scabs) despite the second NP administration, except for a slight increase in groups treated with lipid-coated-IR780 NPs (**Figures 39a-39f**). Finally, no spectral overlap with the signal of AlexaFluor 700-dyed NPs was detected at the excitation and emission wavelenghts of the IR780, excluding any kind of fluorescence cross-talk (**Figure 39g** and **Figure 39h**).

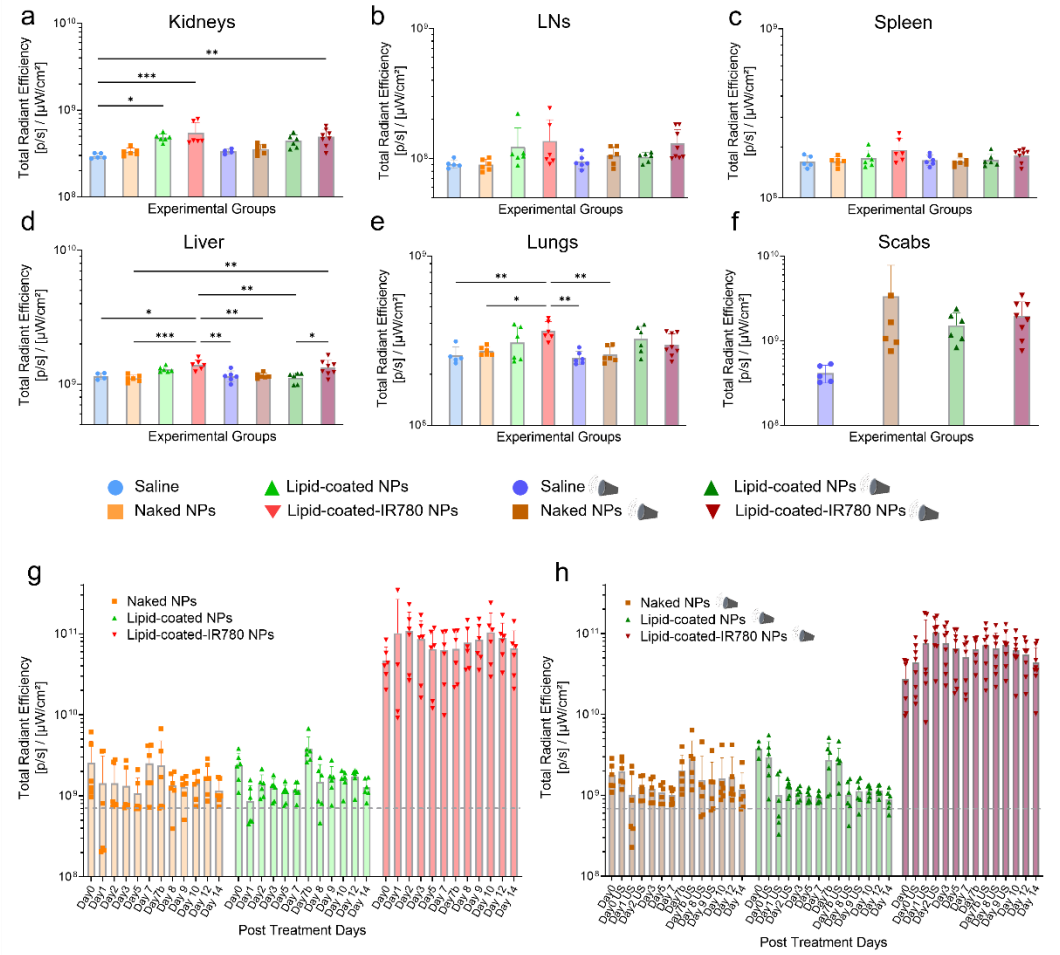

Figure 39. A-F) Histograms reporting the total radiant efficiency (excitation 675 nm, emission 720 nm) of kidneys, LNs, spleen, liver, lungs and scabs explanted on day 14. G) Histograms reporting the total radiant efficiency progression in vivo in groups treated with NPs only and H) groups treated with NPs and ultrasound stimulation (excitation 745 nm, emission 820 nm) to prove the absence of spectral overlap of AlexaFluor700 on the IR780 signal.

Tumor slides subjected to TUNEL staining revealed an increase in apoptotic cells in samples treated with both NPs and US, especially when the sonosensitizer was present in the lipidic shell (**Figure 40a**). These results underscored that the combination treatment induced significant apoptosis in pancreatic cancer cells, suggesting it as a potential route of cell death due to treatment. Quantification of the apoptotic area relative to the total tumor section area confirmed that the treatment consisting in lipid-coated-IR780 NPs and US led to statistically larger apoptotic regions (**Figure 40b)**. Tumors treated with the combination of lipid-coated-IR780 NPs and US and stained with Masson's Trichrome showed a reduction in fibrosis, resulting in a morphology more closely resembling healthy tissue [762–764]. On the contrary, untreated tumors and tumors receiving US only revealed a predominance of collagen fibers, associated with the dense stroma characteristic of PDAC (**Figure 40c**).

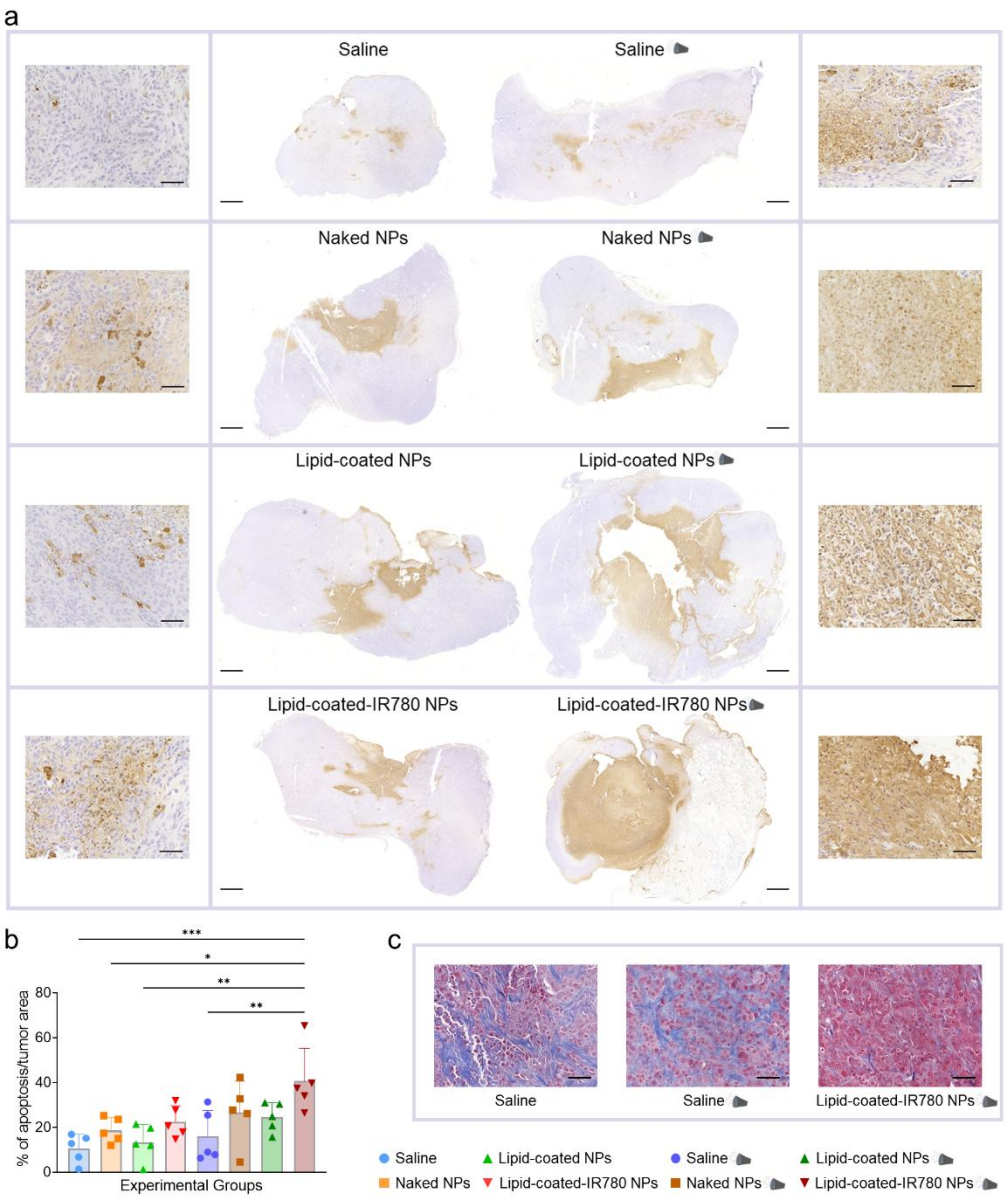

Figure 40. A) Representative tumor sections, stained with the apoptosis assay, showing increasingly bigger apoptotic regions (brown) with respect to the total tumor slice area in groups receiving the combined treatment (scalebar 1 mm) and corresponding magnifications (scalebar 50 µm). B) Percentage of apoptotic areas with respect to total tumor area for all treatment group (n=5/group). Data are expressed as mean ± standard deviation. Significance was analyzed by one-way ANOVA. *$p < 0.05$; **$p < 0.005$; ***$p < 0.0005$; **** $p < 0.0001$. C) Representative Masson's Trichrome staining of tumor slides where collagen fibers, stained in blue, decrease in the sample receiving the combined treatment (scalebar 50 µm).

3.3.5 Flow Cytometry study

Flow cytometry was used to assess immune infiltration in response to the combined therapy on a subset of the treatment groups. Tumors were explanted on Day 5, to prevent excessive shrinkage of those treated with lipid-coated-IR780 NPs, ensuring consistent comparisons among groups (**Figure 41a)**. Although almost no significant difference in tumor volumes was detected in vivo over time (**Figure 41b)**, tumor weights ex vivo indicated significant reduction in treated groups compared to the saline control (**Figure 41c**), as further evidenced by their visible shrinkage (**Figure 41d**). To investigate the immune response due to the combined treatment, myeloid and lymphoid cell panels were tested on spleens, tumors and tumor draining lymph nodes (TdLNs). No major systemic response was observed in the spleens, however interesting findings were noted in the TdLNs and tumors.

In the lymph nodes, an increase in proliferating helper T cells ($CD4^+Ki67^+$) suggested enhanced T cell activation, primarily supporting cytotoxic $CD8^+$ T cells against tumor cells (**Figure 41e**). A statistically significant increase in effector Tregs (here defined as $CD4^+CD25^+Foxp3^+CTLA\text{-}4^+$ T cells) was observed in the experimental group treated with lipid-coated-IR780 NPs and US. Although Tregs are usually associated with poor prognosis, effector Tregs exhibit a more effector-like response and can help maintain immune balance [765]. Their increase, indicating inflammation, could be due to the presence of ROS.

Tumors treated with lipid-coated-IR780 NPs and US showed an increase of infiltrating T cells ($CD3^+$), associated with tumor cell detection and elimination. Specifically, there was a marked increase in $CD4^+CD3^+$ T cells, which can activate cytotoxic $CD8^+$ T cells, and whose presence is linked to improved survival and outcomes. Additionally, a marked increase of $CD8^+$ T cells producing interferon-γ (IFN-γ^+CD8^+), a cytokine involved in the activation and proliferation of anti-tumor $CD8^+$ T cells, was observed, with important implications for tumor cell apoptosis and elimination (**Figure 41f**).

Strikingly, this experimental group did not show an increased polarization towards M1-like macrophages, contrary to previous expectations based on the in vivo efficacy study, where tumor reduction was observed. On the other hand, the group treated with US but lacking the sonosensitizers in the lipidic shell showed an increase in M1-like macrophages ($CD80^+F4/80^+CD11b^+$), a decrease in M2 like macrophages ($CD206^+F4/80^+CD11b^+$), and an increased M1/M2 ratio, demonstrating an anti-tumoral response due to the treatment. A possible

explanation for these observations could be a complex interplay between treatment-dependent ROS generation and immune cell response. Excessive ROS production might disrupt the balance between M1 and M2 macrophage polarization and impair antigen presentation [766,767]. Preliminary data (**Figure 30i**) indicated that ROS production was significantly higher with the lipid-coated-IR780 NPs than without the sonosensitizer, supporting this hypothesis.

Additionally, a potential limitation related to the flow analysis experimental design must be acknowledged. By restricting the immune cell phenotypes characterization to a single time point, time-dependent events and dynamic changes occurring before or after day 5 were potentially missed. Despite this potential limitation, there were measurable differences on lymphoid and myeloid cells, with marked statistical significances between groups treated with lipid-coated NPs (either with and without IR780) and US vs saline only. Notably, US stimulation alone did not affect M1 polarization nor enhance cytotoxic T cell infiltration in the tumor area, suggesting that the presence of NPs is required to initiate this whole chain of events leading to local immune response.

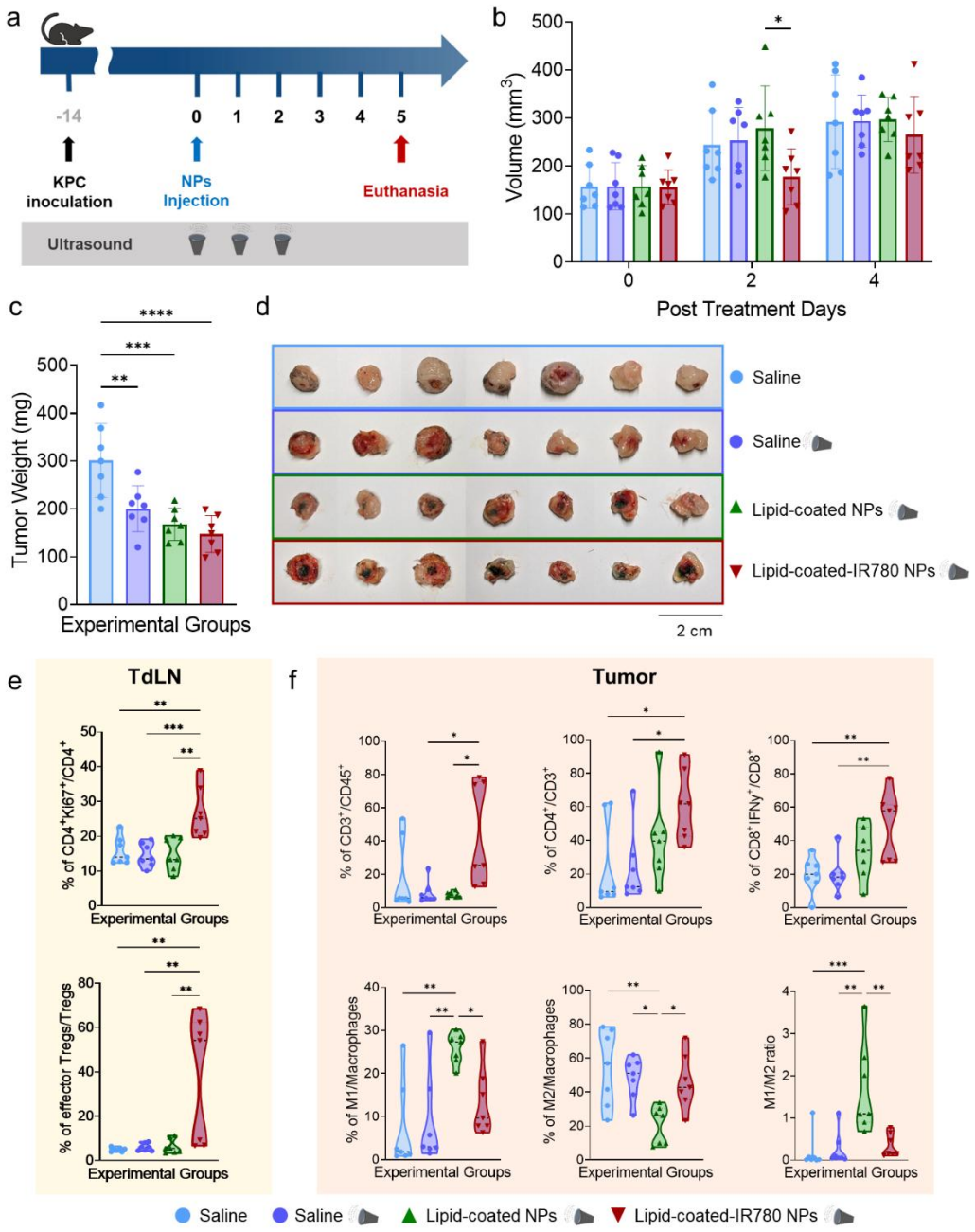

Figure 41. A) Scheme of the treatment plan. B) Tumor volume progression in vivo. C) Tumor weights of the explanted tumors. D) Digital photos of the explanted tumors. E) Percentage of $CD4^+Ki67^+$ cells (top) and effector Tregs ($CD4^+$ $CD25^+Foxp3^+CTLA\text{-}4^+$, bottom) in TdLN. F) Percentage of $CD3^+$, $CD4^+$ and $CD8^+ki67^+$ cells (top) and M1, M2 and M1/M2 ratio (bottom) in tumors. Data are expressed as mean ± standard deviation. Significance was analyzed by either one-way or two-way ANOVA. *$p < 0.05$; **$p < 0.005$; ***$p < 0.0005$; **** $p < 0.0001$. Tukey's correction was applied for multiple comparison.

3.3.6 Survival Study

To evaluate the long-term efficacy of the treatment, mice were treated for two successive weeks with an injection of NPs followed by three daily consecutive US irradiations and then treated weekly with US only, until the humane endpoints were reached (**Figure 42a**). Tumor volume progression in vivo showed a clear and consistent response to the treatment, dependent on the presence of US stimulation in the treatment groups (**Figure 42b** and **42d)**.

Mice receiving only NPs quickly reached the tumor volume endpoint, with a median survival of 21 days. In contrast, mice undergoing the combined treatment exhibited significantly prolonged survival with median survival of 28 and 22.5 days, lasting up to 48 days after the first injection. Mice receiving only US stimulation died within 28 days from the first treatment, due to tumor cavitation and ulceration (**Figure 42c**).

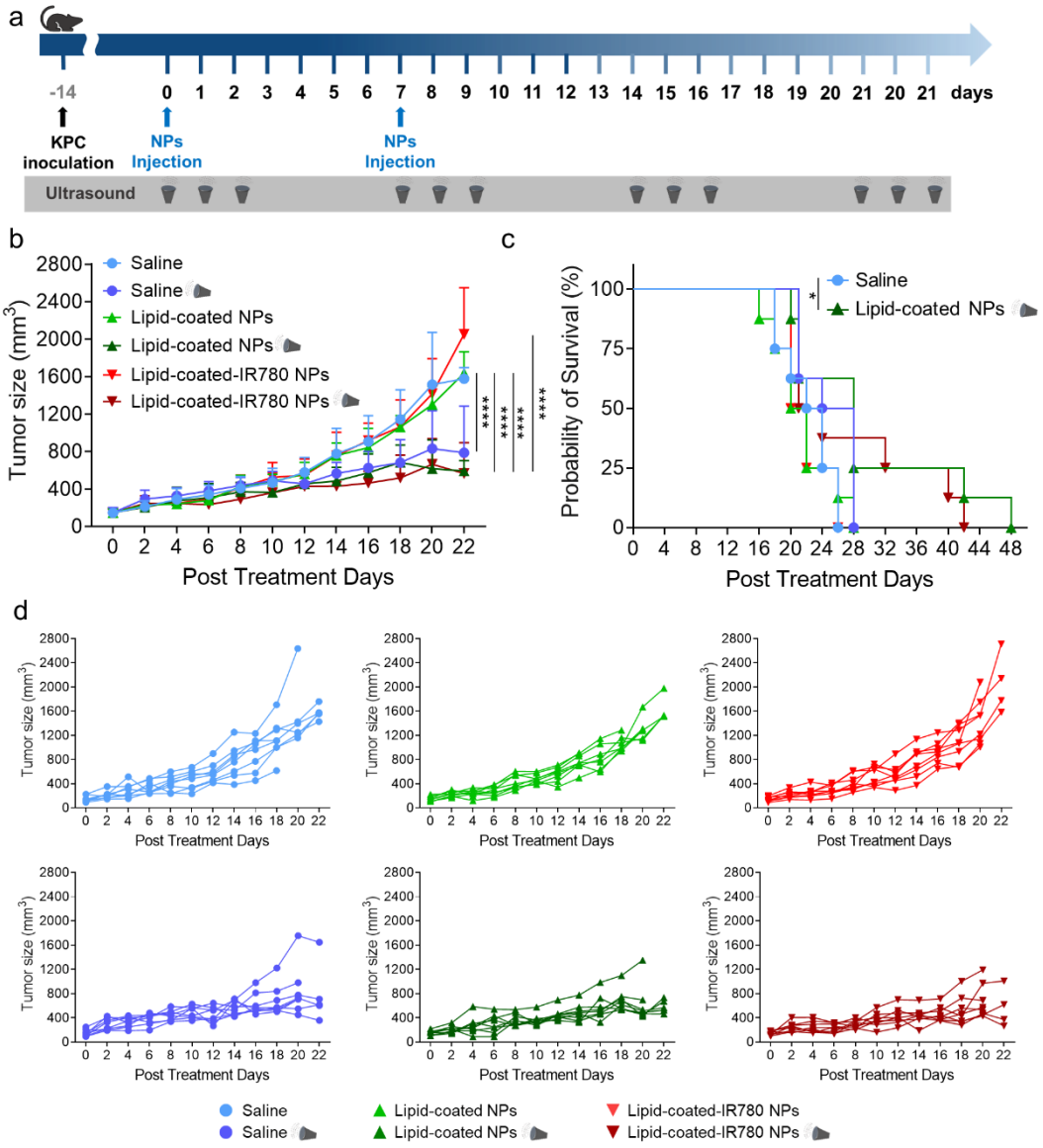

Figure 42. A) Scheme of the treatment plan. B) Tumor volume progression in vivo. Data are expressed as mean ± standard deviation. Significance was analyzed by two-way ANOVA. *$p < 0.05$; **$p < 0.005$; ***$p < 0.0005$; **** $p < 0.0001$. Tukey's correction was applied for multiple comparison. C) Kaplan-Meier survival curves. Significance was analyzed by log-rank test; n = 8/group; **$p < 0.001$; ***$p < 0.0005$). D) tumor growth curve in vivo, each plot referred to a single experimental group.

3.4 Conclusions

This study demonstrates the potential of US-stimulated zinc oxide NPs as an alternative therapeutic approach for pancreatic cancer. Our nanoconstructs are consistently reproducible and are thoroughly characterized, exhibiting safety and biocompatibility due to the protective lipidic shell. In vitro data show that ROS generation is triggered by US application on the NPs, leading to tumor cell death. In vivo, the combined therapy results in tumor shrinkage, likely due to cancer cell apoptosis, significant immune cell infiltration with macrophages polarization, and prolonged mouse survival. Although a degree of anti-tumor effect in KPC mice is observed with US treatment alone, flow cytometry data indicate that only the combination of lipid-coated(-IR780) NPs and US could be advantageous for generating an anti-tumor immune response. While the combined therapy did not achieve complete tumor clearance in vivo, an essential consideration is the inherent safety of the individual treatment components. The injected NPs were far below any subtoxic threshold, and the US were administered through an FDA-approved transducer, allowing for numerous future potential combinations by simply tuning NPs dosages and treatment durations.

The versatile lipidic shell inspired by COVID-19 vaccines formulations allows for the potential inclusion of various functional lipids, covalently bound to targeting peptides [743], antibodies [752], or proteins. Thus, combining this treatment with immunotherapy, such as incorporating an agonistic anti-CD40 monoclonal antibody covalently bound to the lipidic shell, could further enhance the systemic immune response, leveraging the multimodal therapy potential of the nanoconstructs. Therefore, minor adjustments in the nanoconstruct design and dosage, along with intravenous injection could be implemented in future experiments towards a more realistic clinical setting.

Based on the results, it can be postulated that stronger efficacy in the reduction of tumor growth may be attained with higher NP concentrations. Furthermore, it is possible that other cancer models may be more responsive than the highly fibrotic and desmoplastic KPC model. Additionally, the results suggest that the effect of NPs on tumor reduction may be more visible at a later stage, necessitating further investigations. Overall, the study confirms that the combination of NPs and US could effectively treat aggressive tumors like pancreatic cancer. These findings provide a strong foundation for future research into innovative multimodal therapies against pancreatic cancer.

Chapter 4

Conclusions

This dissertation provides a comprehensive exploration of innovative and multimodal approaches to address the significant challenge posed by pancreatic ductal adenocarcinoma (PDAC). Despite significant advancements in cancer treatment, PDAC remains one of the most lethal and challenging tumors to manage. The first chapter of this dissertation provides an essential foundation by exploring the complexities of PDAC physiology, its tumor microenvironment and its resistance mechanisms, marking a crucial step towards a deeper understanding of this malignancy.

The reviewed literature demonstrates that addressing PDAC must require not only a thorough comprehension of its biology and therapeutic constraints, but also the development of innovative approaches to overcome the current therapeutic limitations. Nanomedicine-based treatments emerge as a key player in enhancing treatment efficacy, with current research acknowledging the potential of multimodal therapies.

The subsequent two chapters propose a therapeutic strategy based on the use of zinc oxide nanoparticles, chosen as the core component of advanced nanoconstructs. The development of tailored lipidic formulations inspired by COVID-19 vaccines and the use of external stimulation to leverage their therapeutic potential is explored and rigorously tested up to an in-vivo setting. The findings demonstrate the potential of these ultrasound-stimulated nanoconstructs in PDAC treatment. Additionally, the importance of this study lies in the use of inherently safe single treatments, since the nanoconstructs are proved biocompatible and the ultrasound stimulation is performed using a clinically approved transducer. Finally, both the nanoconstructs and the ultrasound stimulation are highly tunable, revealing significant opportunities for further improvements.

This work emphasizes the need for highly customizable and targeted approaches, tailored to the characteristics of both the tumor and the patient, thus paving the way for personalized treatments. Nevertheless, additional experiments should be conducted by finely tuning the treatment dosages and the administration routes towards a more realistic clinical setting. Future research should focus on refining these therapies and exploring their applicability to a broader range of cancer types, incorporating immunotherapeutic strategies in view of clinical applications.

References

[1] P. Rawla, T. Sunkara, V. Gaduputi, *World J Oncol* **2019**, *10*, 10.

[2] L. Rahib, B. D. Smith, R. Aizenberg, A. B. Rosenzweig, J. M. Fleshman, L. M. Matrisian, *Cancer Res* **2014**, *74*, 2913.

[3] P. Sarantis, E. Koustas, A. Papadimitropoulou, A. G. Papavassiliou, M. V. Karamouzis, *WJGO* **2020**, *12*, 173.

[4] Zeng, Pöttler, Lan, Grützmann, Pilarsky, Yang, *IJMS* **2019**, *20*, 4504.

[5] J. Gore, M. Korc, *Cancer Cell* **2014**, *25*, 711.

[6] F. Di Maggio, P. Arumugam, F. R. Delvecchio, S. Batista, T. Lechertier, K. Hodivala-Dilke, H. M. Kocher, *Pancreatology* **2016**, *16*, 995.

[7] A. Belalcazar, G. P. Nagaraju, in *Theranostic Approach for Pancreatic Cancer*, Elsevier, **2019**, pp. 69–80.

[8] B. Dariya, G. Srivani, B. Farran, R. Vadde, A. Alam, G. P. Nagaraju, in *Theranostic Approach for Pancreatic Cancer*, **2019**.

[9] R. H. Hruban, M. M. Gaida, E. Thompson, S.-M. Hong, M. Noë, L. A. Brosens, M. Jongepier, G. J. A. Offerhaus, L. D. Wood, *The Journal of Pathology* **2019**, *248*, 131.

[10] E. Versteijne, M. Suker, K. Groothuis, J. M. Akkermans-Vogelaar, M. G. Besselink, B. A. Bonsing, J. Buijsen, O. R. Busch, G.-J. M. Creemers, R. M. van Dam, F. A. L. M. Eskens, S. Festen, J. W. B. de Groot, B. Groot Koerkamp, I. H. de Hingh, M. Y. V. Homs, J. E. van Hooft, E. D. Kerver, S. A. C. Luelmo, K. J. Neelis, J. Nuyttens, G. M. R. M. Paardekooper, G. A. Patijn, M. J. C. van der Sangen, J. de Vos-Geelen, J. W. Wilmink, A. H. Zwinderman, C. J. Punt, C. H. van Eijck, G. van Tienhoven, *J Clin Oncol* **2020**, *38*, 1763.

[11] N. Pecorelli, M. Pagnanelli, L. Cinelli, F. Di Salvo, S. Partelli, S. Crippa, D. Tamburrino, R. Castoldi, G. Belfiori, M. Reni, M. Falconi, G. Balzano, *Frontiers in Oncology* **2019**, *9*.

[12] O. Strobel, J. Neoptolemos, D. Jäger, M. W. Büchler, *Nat Rev Clin Oncol* **2019**, *16*, 11.

[13] R. L. Siegel, K. D. Miller, A. Jemal, *CA A Cancer J Clin* **2020**, *70*, 7.

[14] E. M. O'Reilly, C. Ferrone, *Journal of Clinical Oncology* **2020**, DOI 10.1200/JCO.19.03318.

[15] J. P. Neoptolemos, J. Kleeff, P. Michl, E. Costello, W. Greenhalf, D. H. Palmer, *Nat Rev Gastroenterol Hepatol* **2018**, *15*, 333.

[16] C. L. Roland, M. H. G. Katz, C.-W. D. Tzeng, H. Lin, G. R. Varadhachary, R. Shroff, M. Javle, D. Fogelman, R. A. Wolff, J. N. Vauthey, C. H. Crane, J. E. Lee, J. B. Fleming, *Ann Surg Oncol* **2015**, *22*, 1221.

[17] R. K. Paluri, A. Kasi, C. Young, J. A. Posey, *Clin Adv Hematol Oncol* **2020**, *18*, 106.

[18] A. M. Nagrial, V. T. Chin, K. M. Sjoquist, M. Pajic, L. G. Horvath, A. V. Biankin, D. Yip, *Critical Reviews in Oncology/Hematology* **2015**, *96*, 483.

[19] J. M. Riedl, F. Posch, L. Horvath, A. Gantschnigg, F. Renneberg, E. Schwarzenbacher, F. Moik, D. A. Barth, C. H. Rossmann, M. Stotz, R. Schaberl-Moser, M. Pichler, H. Stöger, R. Greil, A. Djanani, K. Schlick, A. Gerger, *European Journal of Cancer* **2021**, *151*, 3.

[20] V. Chin, A. Nagrial, K. Sjoquist, C. A. O'Connor, L. Chantrill, A. V. Biankin, R. J. Scholten, D. Yip, *Cochrane Database of Systematic Reviews* **2018**, DOI 10.1002/14651858.CD011044.pub2.

[21] J. P. Neoptolemos, D. D. Stocken, H. Friess, C. Bassi, J. A. Dunn, H. Hickey, H. Beger, L. Fernandez-Cruz, C. Dervenis, F. Lacaine, M. Falconi, P. Pederzoli, A. Pap, D. Spooner, D. J. Kerr, M. W. Büchler, *New England Journal of Medicine* **2004**, *350*, 1200.

[22] A. G. Morganti, F. Cellini, M. Buwenge, A. Arcelli, S. Alfieri, F. A. Calvo, R. Casadei, S. Cilla, F. Deodato, G. Di Gioia, M. Di Marco, L. Fuccio, F. Bertini, A. Guido, J. M. Herman, G. Macchia, B. W. Maidment, R. C. Miller, F. Minni, P. Passoni, C. Valentini, A. Re, W. F. Regine, M. Reni, M. Falconi, V. Valentini, G. C. Mattiucci, *BMC Cancer* **2019**, *19*, 569.

[23] S. Paiella, R. Salvia, M. Ramera, R. Girelli, I. Frigerio, A. Giardino, V. Allegrini, C. Bassi, *Gastroenterol Res Pract* **2016**, *2016*, 4508376.

[24] A. Ruarus, L. Vroomen, R. Puijk, H. Scheffer, M. Meijerink, *Cancers (Basel)* **2018**, *10*, 16.

[25] S. J. E. Rombouts, J. A. Vogel, H. C. van Santvoort, K. P. van Lienden, R. van Hillegersberg, O. R. C. Busch, M. G. H. Besselink, I. Q. Molenaar, *British Journal of Surgery* **2015**, *102*, 182.

[26] D. Schizas, N. Charalampakis, C. Kole, P. Economopoulou, E. Koustas, E. Gkotsis, D. Ziogas, A. Psyrri, M. V. Karamouzis, *Cancer Treat Rev* **2020**, *86*, 102016.

[27] R. J. Torphy, Y. Zhu, R. D. Schulick, *Ann Gastroenterol Surg* **2018**, *2*, 274.

[28] K. C. Soares, L. Zheng, B. Edil, E. M. Jaffee, *Cancer J* **2012**, *18*, 642.

[29] D. Singh, G. Upadhyay, R. K. Srivastava, S. Shankar, *Biochimica et Biophysica Acta (BBA) - Reviews on Cancer* **2015**, *1856*, 13.

[30] A. McGuigan, P. Kelly, R. C. Turkington, C. Jones, H. G. Coleman, R. S. McCain, *WJG* **2018**, *24*, 4846.

[31] J. Shi, P. W. Kantoff, R. Wooster, O. C. Farokhzad, *Nat Rev Cancer* **2017**, *17*, 20.

[32] M. Norouzi, M. Amerian, M. Amerian, F. Atyabi, *Drug Discovery Today* **2020**, *25*, 107.

[33] M. K. Greene, M. C. Johnston, C. J. Scott, *Cancers* **2021**, *13*, 6175.

[34] J. An, Y.-G. Hu, K. Cheng, C. Li, X.-L. Hou, G.-L. Wang, X.-S. Zhang, B. Liu, Y.-D. Zhao, M.-Z. Zhang, *Biomaterials* **2020**, *234*, 119761.

[35] V. Karimnia, F. J. Slack, J. P. Celli, *Cancers (Basel)* **2021**, *13*, 4354.

[36] R. Ortíz, F. Quiñonero, B. García-Pinel, M. Fuel, C. Mesas, L. Cabeza, C. Melguizo, J. Prados, *Cancers* **2021**, *13*, 2058.

[37] J. A. Roacho-Pérez, E. N. Garza-Treviño, P. Delgado-Gonzalez, Z. G-Buentello, J. L. Delgado-Gallegos, C. Chapa-Gonzalez, M. Sánchez-Domínguez, C. N. Sánchez-Domínguez, J. F. Islas, *Life* **2021**, *11*, 1187.

[38] B. Jiang, L. Zhou, J. Lu, Y. Wang, C. Liu, L. You, J. Guo, *Frontiers in Oncology* **2020**, *10*.

[39] A. Neesse, H. Algül, D. A. Tuveson, T. M. Gress, *Gut* **2015**, *64*, 1476.

[40] I. M. Stromnes, K. E. DelGiorno, P. D. Greenberg, S. R. Hingorani, *Carcinogenesis* **2014**, *35*, 1451.

[41] A. Neesse, S. Krug, T. M. Gress, D. A. Tuveson, P. Michl, *OTT* **2013**, *7*, 33.

[42] L. Srinivas, D. S, D. Kgk, R. R. Malla, *Crit Rev Oncog* **2019**, *24*, 179.

[43] I. A. Batista, S. A. Melo, *International Journal of Molecular Sciences* **2019**, *20*, 567.

[44] K. Chen, Q. Wang, M. Kornmann, X. Tian, Y. Yang, *Frontiers in Oncology* **2021**, *11*.

[45] A. Adamska, A. Domenichini, M. Falasca, *IJMS* **2017**, *18*, 1338.

[46] Y. Huang, Y. Li, *Acta Pharmacol Sin* **2017**, *38*, 735.

[47] J. Li, M. Yao, Y. Shao, D. Yao, *Nanotechnology Reviews* **2018**, *7*, 257.

[48] L. R. Jaidev, L. S. Chede, H. K. Kandikattu, *Endocr Metab Immune Disord Drug Targets* **2021**, *21*, 203.

[49] A. Nedelcu, T. Mocan, C. Grapa, L. Mocan, *Int J Mol Sci* **2021**, *22*, 8060.

[50] B. Zhou, J.-W. Xu, Y.-G. Cheng, J.-Y. Gao, S.-Y. Hu, L. Wang, H.-X. Zhan, *International Journal of Cancer* **2017**, *141*, 231.

[51] L. Zhang, S. Sanagapalli, A. Stoita, *World J Gastroenterol* **2018**, *24*, 2047.

[52] R. Clay, S. A. Siddiqi, in *Theranostic Approach for Pancreatic Cancer*, Elsevier, **2019**, pp. 325–367.

[53] S. Midha, S. Chawla, P. K. Garg, *Cancer Letters* **2016**, *381*, 269.

[54] "Cancer today," can be found under http://gco.iarc.fr/today/home, **n.d.**

[55] R. Huxley, A. Ansary-Moghaddam, A. Berrington de González, F. Barzi, M. Woodward, *Br J Cancer* **2005**, *92*, 2076.

[56] C. Bosetti, E. Lucenteforte, D. T. Silverman, G. Petersen, P. M. Bracci, B. T. Ji, E. Negri, D. Li, H. A. Risch, S. H. Olson, S. Gallinger, A. B. Miller, H. B. Bueno-de-Mesquita, R. Talamini, J. Polesel, P. Ghadirian, P. A. Baghurst, W. Zatonski, E. Fontham, W. R. Bamlet, E. A. Holly, P. Bertuccio, Y. T. Gao, M. Hassan, H. Yu, R. C. Kurtz, M. Cotterchio, J. Su, P. Maisonneuve, E. J. Duell, P. Boffetta, C. La Vecchia, *Ann Oncol* **2012**, *23*, 1880.

[57] **2012**, 43.

[58] S. Raimondi, A. B. Lowenfels, A. M. Morselli-Labate, P. Maisonneuve, R. Pezzilli, *Best Practice & Research Clinical Gastroenterology* **2010**, *24*, 349.

[59] F. Chen, N. J. Roberts, A. P. Klein, *Chinese Clinical Oncology* **2018**, *6*, 2.

[60] P. Bailey, D. K. Chang, K. Nones, A. L. Johns, A.-M. Patch, M.-C. Gingras, D. K. Miller, A. N. Christ, T. J. C. Bruxner, M. C. Quinn, C. Nourse, L. C. Murtaugh, I. Harliwong, S. Idrisoglu, S. Manning, E. Nourbakhsh, S. Wani, L. Fink, O. Holmes, V. Chin, M. J. Anderson, S. Kazakoff, C. Leonard, F. Newell, N. Waddell, S. Wood, Q. Xu, P. J. Wilson, N. Cloonan, K. S. Kassahn, D. Taylor, K. Quek, A. Robertson, L. Pantano, L. Mincarelli, L. N. Sanchez, L. Evers, J. Wu, M. Pinese, M. J. Cowley, M. D. Jones, E. K. Colvin, A. M. Nagrial, E. S. Humphrey, L. A. Chantrill, A. Mawson, J. Humphris, A. Chou, M. Pajic, C. J. Scarlett, A. V. Pinho, M. Giry-Laterriere, I. Rooman, J. S. Samra, J. G. Kench, J. A. Lovell, N. D. Merrett, C. W. Toon, K. Epari, N. Q. Nguyen, A. Barbour, N. Zeps, K. Moran-Jones, N. B. Jamieson, J. S. Graham, F. Duthie, K. Oien, J. Hair, R. Grützmann, A. Maitra, C. A. Iacobuzio-Donahue, C. L. Wolfgang, R. A. Morgan, R. T. Lawlor, V. Corbo, C. Bassi, B. Rusev, P. Capelli, R. Salvia, G. Tortora, D. Mukhopadhyay, G. M. Petersen, D. M. Munzy, W. E. Fisher, S. A. Karim, J. R. Eshleman, R. H. Hruban, C. Pilarsky, J. P. Morton, O. J. Sansom, A. Scarpa, E. A. Musgrove, U.-M. H. Bailey, O. Hofmann, R. L. Sutherland, D. A. Wheeler, A. J. Gill, R. A. Gibbs, J. V. Pearson, N. Waddell, A. V. Biankin, S. M. Grimmond, *Nature* **2016**, *531*, 47.

[61] A. Vincent, J. Herman, R. Schulick, R. H. Hruban, M. Goggins, *The Lancet* **2011**, *378*, 607.

[62] S. Eser, A. Schnieke, G. Schneider, D. Saur, *Br J Cancer* **2014**, *111*, 817.

[63] R. R. McWilliams, E. D. Wieben, K. G. Rabe, K. S. Pedersen, Y. Wu, H. Sicotte, G. M. Petersen, *Eur J Hum Genet* **2011**, *19*, 472.

[64] S. Weissmueller, E. Manchado, M. Saborowski, J. P. Morris, E. Wagenblast, C. A. Davis, S.-H. Moon, N. T. Pfister, D. F. Tschaharganeh, T. Kitzing, D. Aust, E. K. Markert, J. Wu, S. M. Grimmond, C. Pilarsky, C. Prives, A. V. Biankin, S. W. Lowe, *Cell* **2014**, *157*, 382.

[65] X. Shugang, Y. Hongfa, L. Jianpeng, Z. Xu, F. Jingqi, L. Xiangxiang, L. Wei, *Translational Oncology* **2016**, *9*, 1.

[66] R. Pilarski, *American Society of Clinical Oncology Educational Book* **2019**, 79.

[67] N. T. van Heek, A. K. Meeker, S. E. Kern, C. J. Yeo, K. D. Lillemoe, J. L. Cameron, G. J. A. Offerhaus, J. L. Hicks, R. E. Wilentz, M. G. Goggins, A. M. De Marzo, R. H. Hruban, A. Maitra, *The American Journal of Pathology* **2002**, *161*, 1541.

[68] N. Omura, M. Goggins, *Int J Clin Exp Pathol* **2008**, *2*, 310.

[69] C. Roldo, E. Missiaglia, J. P. Hagan, M. Falconi, P. Capelli, S. Bersani, G. A. Calin, S. Volinia, C.-G. Liu, A. Scarpa, C. M. Croce, *JCO* **2006**, *24*, 4677.

[70] A. Li, J. Yu, H. Kim, C. L. Wolfgang, M. I. Canto, R. H. Hruban, M. Goggins, *Clin Cancer Res* **2013**, *19*, 3600.

[71] B. Dariya, A. Alam, G. P. Nagaraju, in *Theranostic Approach for Pancreatic Cancer*, Elsevier, **2019**, pp. 1–50.

[72] R. H. Hruban, A. Maitra, M. Goggins, **2008**, 11.

[73] C. Shi, R. H. Hruban, *Human Pathology* **2012**, *43*, 1.

[74] N. U. Din, M. Zubair, J. Abdul-Ghafar, Z. Ahmad, *Surg Exp Pathol* **2020**, *3*, 6.

[75] M. Distler, D. Aust, J. Weitz, C. Pilarsky, R. Grützmann, *BioMed Research International* **2014**, *2014*, e474905.

[76] S. Pandol, M. Edderkaoui, I. Gukovsky, A. Lugea, A. Gukovskaya, *Clinical Gastroenterology and Hepatology* **2009**, *7*, S44.

[77] A. Cannon, C. Thompson, B. R. Hall, M. Jain, S. Kumar, S. K. Batra, *Genes Cancer* **2018**, *9*, 78.

[78] C. Guerra, M. Barbacid, *Molecular Oncology* **2013**, *7*, 232.

[79] C. J. Whatcott, C. H. Diep, P. Jiang, A. Watanabe, J. LoBello, C. Sima, G. Hostetter, H. M. Shepard, D. D. Von Hoff, H. Han, *Clin Cancer Res* **2015**, *21*, 3561.

[80] P. Lu, V. M. Weaver, Z. Werb, *Journal of Cell Biology* **2012**, *196*, 395.

[81] V. Veenstra, A. Garcia-Garijo, H. van Laarhoven, M. Bijlsma, *Cancers* **2018**, *10*, 34.

[82] D. Thomas, P. Radhakrishnan, *Mol Cancer* **2019**, *18*, 14.

[83] B. P. Toole, M. G. Slomiany, *Seminars in Cancer Biology* **2008**, *18*, 244.

[84] P. P. Provenzano, C. Cuevas, A. E. Chang, V. K. Goel, D. D. Von Hoff, S. R. Hingorani, *Cancer Cell* **2012**, *21*, 418.

[85] M. D. Nieskoski, K. Marra, J. R. Gunn, P. J. Hoopes, M. M. Doyley, T. Hasan, B. S. Trembly, B. W. Pogue, *Sci Rep* **2017**, *7*, 10093.

[86] S. Berchtold, B. Grünwald, A. Krüger, A. Reithmeier, T. Hähl, T. Cheng, A. Feuchtinger, D. Born, M. Erkan, J. Kleeff, I. Esposito, *Cancer Letters* **2015**, *356*, 721.

[87] Y. Matsuo, M. Raimondo, T. A. Woodward, M. B. Wallace, K. R. Gill, Z. Tong, M. D. Burdick, Z. Yang, R. M. Strieter, R. M. Hoffman, S. Guha, *International Journal of Cancer* **2009**, *125*, 1027.

[88] Y. Matsuo, N. Ochi, H. Sawai, A. Yasuda, H. Takahashi, H. Funahashi, H. Takeyama, Z. Tong, S. Guha, *International Journal of Cancer* **2009**, *124*, 853.

[89] A. Masamune, T. Watanabe, K. Kikuta, T. Shimosegawa, *Clinical Gastroenterology and Hepatology* **2009**, *7*, S48.

[90] M. V. Apte, S. Park, P. A. Phillips, N. Santucci, D. Goldstein, R. K. Kumar, G. A. Ramm, M. Buchler, H. Friess, J. A. McCarroll, G. Keogh, N. Merrett, R. Pirola, J. S. Wilson, *Pancreas* **2004**, *29*, 179.

[91] A. Vonlaufen, S. Joshi, C. Qu, P. A. Phillips, Z. Xu, N. R. Parker, C. S. Toi, R. C. Pirola, J. S. Wilson, D. Goldstein, M. V. Apte, *Cancer Res* **2008**, *68*, 2085.

[92] K. Kikuta, A. Masamune, T. Watanabe, H. Ariga, H. Itoh, S. Hamada, K. Satoh, S. Egawa, M. Unno, T. Shimosegawa, *Biochemical and Biophysical Research Communications* **2010**, *403*, 380.

[93] M. Zeisberg, E. G. Neilson, *J. Clin. Invest.* **2009**, *119*, 1429.

[94] Z. Wang, Y. Li, D. Kong, S. Banerjee, A. Ahmad, A. S. Azmi, S. Ali, J. L. Abbruzzese, G. E. Gallick, F. H. Sarkar, *Cancer Res* **2009**, *69*, 2400.

[95] Z. Xu, A. Vonlaufen, P. A. Phillips, E. Fiala-Beer, X. Zhang, L. Yang, A. V. Biankin, D. Goldstein, R. C. Pirola, J. S. Wilson, M. V. Apte, *Am J Pathol* **2010**, *177*, 2585.

[96] A. Ene-Obong, A. J. Clear, J. Watt, J. Wang, R. Fatah, J. C. Riches, J. F. Marshall, J. Chin-Aleong, C. Chelala, J. G. Gribben, A. G. Ramsay, H. M. Kocher, *Gastroenterology* **2013**, *145*, 1121.

[97] Y. Ma, R. F. Hwang, C. D. Logsdon, S. E. Ullrich, *Cancer Res* **2013**, *73*, 3927.

[98] T. A. Mace, M. Bloomston, G. B. Lesinski, *OncoImmunology* **2013**, *2*, e24891.

[99] M. F. B. Nielsen, M. B. Mortensen, S. Detlefsen, *WJG* **2016**, *22*, 2678.

[100] E. Sahai, I. Astsaturov, E. Cukierman, D. G. DeNardo, M. Egeblad, R. M. Evans, D. Fearon, F. R. Greten, S. R. Hingorani, T. Hunter, R. O. Hynes, R. K. Jain, T. Janowitz, C. Jorgensen, A. C. Kimmelman, M. G. Kolonin, R. G. Maki, R. S. Powers, E. Puré, D. C. Ramirez, R. Scherz-Shouval, M. H. Sherman, S. Stewart, T. D. Tlsty, D. A. Tuveson, F. M. Watt, V. Weaver, A. T. Weeraratna, Z. Werb, *Nat Rev Cancer* **2020**, *20*, 174.

[101] E. Helms, M. K. Onate, M. H. Sherman, *Cancer Discov* **2020**, *10*, 648.

[102] C. C. M. Neumann, E. von Hörschelmann, A. Reutzel-Selke, E. Seidel, I. M. Sauer, J. Pratschke, M. Bahra, R. B. Schmuck, *Hepatobiliary & Pancreatic Diseases International* **2018**, *17*, 461.

[103] D. Öhlund, A. Handly-Santana, G. Biffi, E. Elyada, A. S. Almeida, M. Ponz-Sarvise, V. Corbo, T. E. Oni, S. A. Hearn, E. J. Lee, I. I. C. Chio, C.-I. Hwang, H. Tiriac, L. A. Baker, D. D. Engle, C. Feig, A. Kultti, M. Egeblad, D. T. Fearon, J. M. Crawford, H. Clevers, Y. Park, D. A. Tuveson, *Journal of Experimental Medicine* **2017**, *214*, 579.

[104] E. Elyada, M. Bolisetty, P. Laise, W. F. Flynn, E. T. Courtois, R. A. Burkhart, J. A. Teinor, P. Belleau, G. Biffi, M. S. Lucito, S. Sivajothi, T. D. Armstrong, D. D. Engle, K. H. Yu, Y. Hao, C. L. Wolfgang, Y. Park, J. Preall, E. M. Jaffee, A. Califano, P. Robson, D. A. Tuveson, *Cancer Discov* **2019**, *9*, 1102.

[105] X. Geng, H. Chen, L. Zhao, J. Hu, W. Yang, G. Li, C. Cheng, Z. Zhao, T. Zhang, L. Li, B. Sun, *Frontiers in Cell and Developmental Biology* **2021**, *9*.

[106] G. Biondani, K. Zeeberg, M. R. Greco, S. Cannone, I. Dando, E. Dalla Pozza, M. Mastrodonato, S. Forciniti, V. Casavola, M. Palmieri, S. J. Reshkin, R. A. Cardone, *FEBS J* **2018**, *285*, 2104.

[107] X. Ning, Y. Du, Q. Ben, L. Huang, X. He, Y. Gong, J. Gao, H. Wu, X. Man, J. Jin, M. Xu, Z. Li, *Cell Cycle* **2016**, *15*, 403.

[108] A. Van den broeck, H. Vankelecom, W. Van Delm, L. Gremeaux, J. Wouters, J. Allemeersch, O. Govaere, T. Roskams, B. Topal, *PLoS ONE* **2013**, *8*, e73968.

[109] Z. Zhang, Q. Duan, H. Zhao, T. Liu, H. Wu, Q. Shen, C. Wang, T. Yin, *Cancer Letters* **2016**, *382*, 53.

[110] Y. Jia, Y. Wang, J. Xie, *Arch Toxicol* **2015**, *89*, 179.

[111] J.-Y. Zeng, S. Sharma, Y.-Q. Zhou, H.-P. Yao, X. Hu, R. Zhang, M.-H. Wang, *Molecular Cancer Therapeutics* **2014**, *13*, 37.

[112] S. Heiler, Z. Wang, M. Zöller, *WJG* **2016**, *22*, 5971.

[113] M. Cioffi, S. Trabulo, M. Hidalgo, E. Costello, W. Greenhalf, M. Erkan, J. Kleeff, B. Sainz, C. Heeschen, *Clin Cancer Res* **2015**, *21*, 2325.

[114] T. Yin, P. Shi, S. Gou, Q. Shen, C. Wang, *PLoS ONE* **2014**, *9*, e114581.

[115] G. van Duijneveldt, M. D. W. Griffin, T. L. Putoczki, *Clinical Science* **2020**, *134*, 2091.

[116] C. Minici, E. Rigamonti, M. Lanzillotta, A. Monno, L. Rovati, T. Maehara, N. Kaneko, V. Deshpande, M. P. Protti, L. De Monte, C. Scielzo, S. Crippa, P. G. Arcidiacono, E. Dugnani, L. Piemonti, M. Falconi, S. Pillai, A. A. Manfredi, E. Della-Torre, *OncoImmunology* **2020**, *9*, 1794359.

[117] S. Yang, Q. Liu, Q. Liao, *Front. Cell Dev. Biol.* **2021**, *8*, 607209.

[118] A. Thyagarajan, M. S. A. Alshehri, K. L. R. Miller, C. M. Sherwin, J. B. Travers, R. P. Sahu, *Cancers* **2019**, *11*, 1627.

[119] T. Lianyuan, L. Gang, T. Ming, X. Dianrong, Y. Chunhui, M. Zhaolai, J. Bin, *Cancer Biology & Therapy* **2020**, *21*, 937.

[120] R. R. Malla, S. Kumari, K. G. K. Deepak, M. M. Gavara, S. Guganavath, P. Rokkam, in *Theranostic Approach for Pancreatic Cancer*, Elsevier, **2019**, pp. 81–96.

[121] S. Tetik, N. Tekkesin, in *Theranostic Approach for Pancreatic Cancer*, Elsevier, **2019**, pp. 97–110.

[122] F. Marcon, J. Zuo, H. Pearce, S. Nicol, S. Margielewska-Davies, M. Farhat, B. Mahon, G. Middleton, R. Brown, K. J. Roberts, P. Moss, *Oncoimmunology* **2020**, *9*, 1845424.

[123] J. King, M. Bouvet, G. Singh, J. Williams, *J Surg Oncol* **2017**, *116*, 104.

[124] L. Feng, Q. Qi, P. Wang, H. Chen, Z. Chen, Z. Meng, L. Liu, *J Int Med Res* **2018**, *46*, 5228.

[125] H. Dong, D. Qian, Y. Wang, L. Meng, D. Chen, X. Ji, W. Feng, *World J Surg Onc* **2015**, *13*, 189.

[126] R. Hassan, A. Thomas, C. Alewine, D. T. Le, E. M. Jaffee, I. Pastan, *JCO* **2016**, *34*, 4171.

[127] R. Sawada, S.-M. Sun, X. Wu, F. Hong, G. Ragupathi, P. O. Livingston, W. W. Scholz, *Clin Cancer Res* **2011**, *17*, 1024.

[128] T. Tanaka, H. Kitamura, R. Inoue, S. Nishida, A. Takahashi-Takaya, S. Kawami, T. Torigoe, Y. Hirohashi, T. Tsukamoto, N. Sato, N. Masumori, *Clinical and Developmental Immunology* **2013**, *2013*, 1.

[129] Mayo Clinic, *Phase I/II Study of the Human Anti-Mesothelin Antibody Drug Conjugate Anetumab Ravtansine (AR), Combined With the PD-L1 Inhibitor Atezolizumab in Non-Small Cell Lung Cancer*, Clinicaltrials.Gov, **2020**.

[130] H. Y. Tanaka, K. Kitahara, N. Sasaki, N. Nakao, K. Sato, H. Narita, H. Shimoda, M. Matsusaki, H. Nishihara, A. Masamune, M. R. Kano, *Biomaterials* **2019**, *192*, 355.

[131] N. Sato, S. Kohi, K. Hirata, M. Goggins, *Cancer Sci* **2016**, *107*, 569.

[132] M. A. Jacobetz, D. S. Chan, A. Neesse, T. E. Bapiro, N. Cook, K. K. Frese, C. Feig, T. Nakagawa, M. E. Caldwell, H. I. Zecchini, M. P. Lolkema, P. Jiang, A. Kultti, C. B. Thompson, D. C. Maneval, D. I. Jodrell, G. I. Frost, H. M. Shepard, J. N. Skepper, D. A. Tuveson, *Gut* **2013**, *62*, 112.

[133] C. B. Thompson, H. M. Shepard, P. M. O'Connor, S. Kadhim, P. Jiang, R. J. Osgood, L. H. Bookbinder, X. Li, B. J. Sugarman, R. J. Connor, S. Nadjsombati, G. I. Frost, *Mol Cancer Ther* **2010**, *9*, 3052.

[134] R. Bhatia, S. K. Gautam, A. Cannon, C. Thompson, B. R. Hall, A. Aithal, K. Banerjee, M. Jain, J. C. Solheim, S. Kumar, S. K. Batra, *Cancer Metastasis Rev* **2019**, *38*, 223.

[135] D. Liu, C.-H. Chang, D. V. Gold, D. M. Goldenberg, *Oncotarget* **2015**, *6*, 4274.

[136] S. Naito, T. Takahashi, J. Onoda, S. Uemura, N. Ohyabu, H. Takemoto, S. Yamane, I. Fujii, S.-I. Nishimura, Y. Numata, *ACS Omega* **2017**, *2*, 7493.

[137] S. P. Hong, J. Wen, S. Bang, S. Park, S. Y. Song, *International Journal of Cancer* **2009**, *125*, 2323.

[138] Z. Li, K. Chen, P. Jiang, X. Zhang, X. Li, Z. Li, *Diagn Pathol* **2014**, *9*, 79.

[139] X.-P. Li, X.-W. Zhang, L.-Z. Zheng, W.-J. Guo, *Int J Clin Exp Pathol* **2015**, *8*, 6724.

[140] T. L. Fitzgerald, J. A. McCubrey, *Advances in Biological Regulation* **2014**, *56*, 45.

[141] K. Chen, Z. Li, P. Jiang, X. Zhang, Y. Zhang, Y. Jiang, Y. He, X. Li, *Oncol Rep* **2014**, *32*, 755.

[142] C.-C. Weng, K.-K. Kuo, H.-T. Su, P.-J. Hsiao, Y.-W. Chen, D.-C. Wu, W.-C. Hung, K.-H. Cheng, *Pancreas* **2016**, *45*, 443.

[143] J. Jacob, J. Bellach, R. Grützmann, I. Alldinger, C. Pilarsky, M. Dietel, G. Kristiansen, *Pancreatology* **2004**, *4*, 454.

[144] N. Ikenaga, K. Ohuchida, K. Mizumoto, J. Yu, T. Kayashima, A. Hayashi, K. Nakata, M. Tanaka, *Human Pathology* **2010**, *41*, 1466.

[145] J. A. Burger, T. J. Kipps, *Blood* **2006**, *107*, 1761.

[146] R. L. Sleightholm, B. K. Neilsen, J. Li, M. M. Steele, R. K. Singh, M. A. Hollingsworth, D. Oupicky, *Pharmacology & Therapeutics* **2017**, *179*, 158.

[147] M.-H. Wang, R. Sun, X.-M. Zhou, M.-Y. Zhang, J.-B. Lu, Y. Yang, L.-S. Zeng, X.-Z. Yang, L. Shi, R.-W. Xiao, H.-Y. Wang, S.-J. Mai, *Cell Death Dis* **2018**, *9*, 2.

[148] Y. Lu, H. Zhu, H. Shan, J. Lu, X. Chang, X. Li, J. Lu, X. Fan, S. Zhu, Y. Wang, Q. Guo, L. Wang, Y. Huang, M. Zhu, Z. Wang, *Cancer Letters* **2013**, *340*, 113.

[149] A. Gzil, I. Zarębska, W. Bursiewicz, P. Antosik, D. Grzanka, Ł. Szylberg, *Mol Biol Rep* **2019**, *46*, 6629.

[150] I. Tremblay, E. Paré, D. Arsenault, M. Douziech, M.-J. Boucher, *PLoS ONE* **2013**, *8*, e85502.

[151] Z. Wang, Y. Li, D. Kong, F. H. Sarkar, *CDT* **2010**, *11*, 745.

[152] C. Sahlgren, M. V. Gustafsson, S. Jin, L. Poellinger, U. Lendahl, *Proceedings of the National Academy of Sciences* **2008**, *105*, 6392.

[153] C. Güngör, H. Zander, K. E. Effenberger, Y. K. Vashist, T. Kalinina, J. R. Izbicki, E. Yekebas, M. Bockhorn, *Cancer Res* **2011**, *71*, 5009.

[154] B. Bournet, F. Muscari, C. Buscail, E. Assenat, M. Barthet, P. Hammel, J. Selves, R. Guimbaud, P. Cordelier, L. Buscail, *Clinical and Translational Gastroenterology* **2016**, *7*, e157.

[155] C. Chapouly, S. Guimbal, P.-L. Hollier, M.-A. Renault, *IJMS* **2019**, *20*, 3076.

[156] K. P. Olive, M. A. Jacobetz, C. J. Davidson, A. Gopinathan, D. McIntyre, D. Honess, B. Madhu, M. A. Goldgraben, M. E. Caldwell, D. Allard, K. K. Frese, G. DeNicola, C. Feig, C. Combs, S. P. Winter, H. Ireland-Zecchini, S. Reichelt, W. J. Howat, A. Chang, M. Dhara, L. Wang, F. Ruckert, R. Grutzmann, C. Pilarsky, K. Izeradjene, S. R. Hingorani, P. Huang, S. E. Davies, W. Plunkett, M. Egorin, R. H. Hruban, N. Whitebread, K. McGovern, J. Adams, C. Iacobuzio-Donahue, J. Griffiths, D. A. Tuveson, *Science* **2009**, *324*, 1457.

[157] H. Yu, R. Jove, *Nat Rev Cancer* **2004**, *4*, 97.

[158] K. Polireddy, Q. Chen, *J. Cancer* **2016**, *7*, 1497.

[159] C. Huang, R. Huang, W. Chang, T. Jiang, K. Huang, J. Cao, X. Sun, Z. Qiu, *neo* **2012**, *59*, 52.

[160] O. J. Buckens, B. El Hassouni, E. Giovannetti, G. J. Peters, *Expert Opinion on Investigational Drugs* **2020**, *29*, 567.

[161] E. B. Pasquale, *Nat Rev Cancer* **2010**, *10*, 165.

[162] S. V. Mudali, B. Fu, S. S. Lakkur, M. Luo, E. E. Embuscado, C. A. Iacobuzio-Donahue, *Clin Exp Metastasis* **2006**, *23*, 357.

[163] M. S. Duxbury, H. Ito, M. J. Zinner, S. W. Ashley, E. E. Whang, *Biochemical and Biophysical Research Communications* **2004**, *320*, 1096.

[164] N. Koshikawa, T. Minegishi, H. Kiyokawa, M. Seiki, *Cell Death Dis* **2017**, *8*, e3134.

[165] B. A. Quinn, S. Wang, E. Barile, S. K. Das, L. Emdad, D. Sarkar, S. K. De, S. M. Kharagh, J. L. Stebbins, S. J. Pandol, P. B. Fisher, M. Pellecchia, *Oncotarget* **2016**, *7*, 17103.

[166] A. F. Salem, L. Gambini, P. Udompholkul, C. Baggio, M. Pellecchia, *Pharmaceuticals* **2020**, *13*, 90.

[167] T. Annese, R. Tamma, S. Ruggieri, D. Ribatti, *Cancers* **2019**, *11*, 381.

[168] E. A. Kuczynski, P. B. Vermeulen, F. Pezzella, R. S. Kerbel, A. R. Reynolds, *Nat Rev Clin Oncol* **2019**, *16*, 469.

[169] R. Folberg, M. J. C. Hendrix, A. J. Maniotis, *The American Journal of Pathology* **2000**, *156*, 361.

[170] S. Li, H.-X. Xu, C.-T. Wu, W.-Q. Wang, W. Jin, H.-L. Gao, H. Li, S.-R. Zhang, J.-Z. Xu, Z.-H. Qi, Q.-X. Ni, X.-J. Yu, L. Liu, *Angiogenesis* **2019**, *22*, 15.

[171] P. A. Netti, D. A. Berk, M. A. Swartz, A. J. Grodzinsky, R. K. Jain, *Cancer Res* **2000**, *60*, 2497.

[172] A. Barău, A. Ruiz-Sauri, G. Valencia, M. del C. Gómez-Mateo, L. Sabater, A. Ferrandez, A. Llombart-Bosch, *Virchows Arch* **2013**, *462*, 541.

[173] H. Saiyin, C. M. Ardito-Abraham, Y. Wu, Y. Wei, Y. Fang, X. Han, J. Li, P. Zhou, Q. Yi, A. Maitra, J. O. Liu, D. A. Tuveson, W. Lou, L. Yu, *The Journal of Pathology* **2015**, *236*, 142.

[174] A. Caporali, A. Martello, V. Miscianinov, D. Maselli, R. Vono, G. Spinetti, *Pharmacol Ther* **2017**, *171*, 56.

[175] F. Maione, F. Molla, C. Meda, R. Latini, L. Zentilin, M. Giacca, G. Seano, G. Serini, F. Bussolino, E. Giraudo, *J. Clin. Invest.* **2009**, JCI36308.

[176] M.-E. Gilles, F. Maione, M. Cossutta, G. Carpentier, L. Caruana, S. D. Maria, C. Houppe, D. Destouches, K. Shchors, C. Prochasson, F. Mongelard, S. Lamba, A. Bardelli, P. Bouvet, A. Couvelard, J. Courty, E. Giraudo, I. Cascone, *Cancer Res* **2016**, *76*, 7181.

[177] R. K. Jain, *JCO* **2013**, *31*, 2205.

[178] K. Mallya, S. K. Gautam, A. Aithal, S. K. Batra, M. Jain, *Biochimica et Biophysica Acta (BBA) - Reviews on Cancer* **2021**, *1876*, 188554.

[179] J. A. Rivera, F. Graeme-Cook, J. Werner, K. Z'graggen, A. K. Rustgi, D. W. Rattner, A. L. Warshaw, C. F. Castillo, *Surgery* **1997**, *122*, 82.

[180] S. Yamamura, M. Onda, E. Uchida, *Journal of Nippon Medical School* **1999**, *66*, 253.

[181] S. R. Hingorani, E. F. Petricoin, A. Maitra, V. Rajapakse, C. King, M. A. Jacobetz, S. Ross, T. P. Conrads, T. D. Veenstra, B. A. Hitt, Y. Kawaguchi, D. Johann, L. A. Liotta, H. C. Crawford, M. E. Putt, T. Jacks, C. V. E. Wright, R. H. Hruban, A. M. Lowy, D. A. Tuveson, *Cancer Cell* **2003**, *4*, 437.

[182] C. Guerra, A. J. Schuhmacher, M. Cañamero, P. J. Grippo, L. Verdaguer, L. Pérez-Gallego, P. Dubus, E. P. Sandgren, M. Barbacid, *Cancer Cell* **2007**, *11*, 291.

[183] J. L. Kopp, G. von Figura, E. Mayes, F.-F. Liu, C. L. Dubois, J. P. Morris, F. C. Pan, H. Akiyama, C. V. E. Wright, K. Jensen, M. Hebrok, M. Sander, *Cancer Cell* **2012**, *22*, 737.

[184] J. P. M. IV, D. A. Cano, S. Sekine, S. C. Wang, M. Hebrok, "β-catenin blocks Kras-dependent reprogramming of acini into pancreatic cancer precursor lesions in mice," DOI 10.1172/JCI40045can be found under https://www.jci.org/articles/view/40045/pdf, **2010**.

[185] C. Guerra, M. Collado, C. Navas, A. J. Schuhmacher, I. Hernández-Porras, M. Cañamero, M. Rodriguez-Justo, M. Serrano, M. Barbacid, *Cancer Cell* **2011**, *19*, 728.

[186] M. Lesina, M. U. Kurkowski, K. Ludes, S. Rose-John, M. Treiber, G. Klöppel, A. Yoshimura, W. Reindl, B. Sipos, S. Akira, R. M. Schmid, H. Algül, *Cancer Cell* **2011**, *19*, 456.

[187] E. K. Colvin, C. J. Scarlett, *Semin Cell Dev Biol* **2014**, *27*, 96.

[188] S. R. Hingorani, L. Wang, A. S. Multani, C. Combs, T. B. Deramaudt, R. H. Hruban, A. K. Rustgi, S. Chang, D. A. Tuveson, *Cancer Cell* **2005**, *7*, 469.

[189] K. K. Frese, A. Neesse, N. Cook, T. E. Bapiro, M. P. Lolkema, D. I. Jodrell, D. A. Tuveson, *Cancer Discov* **2012**, *2*, 260.

[190] N. Bardeesy, K. -h. Cheng, J. H. Berger, G. C. Chu, J. Pahler, P. Olson, A. F. Hezel, J. Horner, G. Y. Lauwers, D. Hanahan, R. A. DePinho, *Genes & Development* **2006**, *20*, 3130.

[191] J. T. Siveke, H. Einwächter, B. Sipos, C. Lubeseder-Martellato, G. Klöppel, R. M. Schmid, *Cancer Cell* **2007**, *12*, 266.

[192] K. Izeradjene, C. Combs, M. Best, A. Gopinathan, A. Wagner, W. M. Grady, C.-X. Deng, R. H. Hruban, N. V. Adsay, D. A. Tuveson, S. R. Hingorani, *Cancer Cell* **2007**, *11*, 229.

[193] M. Pasca di Magliano, S. Sekine, A. Ermilov, J. Ferris, A. A. Dlugosz, M. Hebrok, *Genes Dev* **2006**, *20*, 3161.

[194] R. F. Hwang, T. Moore, T. Arumugam, V. Ramachandran, K. D. Amos, A. Rivera, B. Ji, D. B. Evans, C. D. Logsdon, *Cancer Res* **2008**, *68*, 918.

[195] M. J. Moore, D. Goldstein, J. Hamm, A. Figer, J. R. Hecht, S. Gallinger, H. J. Au, P. Murawa, D. Walde, R. A. Wolff, D. Campos, R. Lim, K. Ding, G. Clark, T. Voskoglou-Nomikos, M. Ptasynski, W. Parulekar, National Cancer Institute of Canada Clinical Trials Group, *J Clin Oncol* **2007**, *25*, 1960.

[196] C. Navas, I. Hernández-Porras, A. J. Schuhmacher, M. Sibilia, C. Guerra, M. Barbacid, *Cancer Cell* **2012**, *22*, 318.

[197] N. Cook, K. K. Frese, T. E. Bapiro, M. A. Jacobetz, A. Gopinathan, J. L. Miller, S. S. Rao, T. Demuth, W. J. Howat, D. I. Jodrell, D. A. Tuveson, *J Exp Med* **2012**, *209*, 437.

[198] L. Hanlon, J. L. Avila, R. M. Demarest, S. Troutman, M. Allen, F. Ratti, A. K. Rustgi, B. Z. Stanger, F. Radtke, V. Adsay, F. Long, A. J. Capobianco, J. L. Kissil, *Cancer Research* **2010**, *70*, 4280.

[199] P. K. Mazur, H. Einwächter, M. Lee, B. Sipos, H. Nakhai, R. Rad, U. Zimber-Strobl, L. J. Strobl, F. Radtke, G. Klöppel, R. M. Schmid, J. T. Siveke, *Proc Natl Acad Sci U S A* **2010**, *107*, 13438.

[200] E. A. Collisson, C. L. Trejo, J. M. Silva, S. Gu, J. E. Korkola, L. M. Heiser, R.-P. Charles, B. A. Rabinovich, B. Hann, D. Dankort, P. T. Spellman, W. A. Phillips, J. W. Gray, M. McMahon, *Cancer Discovery* **2012**, *2*, 685.

[201] M. V. Apte, J. S. Wilson, *Journal of Gastroenterology and Hepatology* **2012**, *27*, 69.

[202] R. F. Hwang, T. T. Moore, M. M. Hattersley, M. Scarpitti, B. Yang, E. Devereaux, V. Ramachandran, T. Arumugam, B. Ji, C. D. Logsdon, J. L. Brown, R. Godin, *Mol Cancer Res* **2012**, *10*, 1147.

[203] L. J. Bayne, G. L. Beatty, N. Jhala, C. E. Clark, A. D. Rhim, B. Z. Stanger, R. H. Vonderheide, *Cancer Cell* **2012**, *21*, 822.

[204] Y. Pylayeva-Gupta, K. E. Lee, C. H. Hajdu, G. Miller, D. Bar-Sagi, *Cancer Cell* **2012**, *21*, 836.

[205] C. Feig, J. O. Jones, M. Kraman, R. J. B. Wells, A. Deonarine, D. S. Chan, C. M. Connell, E. W. Roberts, Q. Zhao, O. L. Caballero, S. A. Teichmann, T. Janowitz, D. I. Jodrell, D. A. Tuveson, D. T. Fearon, *PNAS* **2013**, *110*, 20212.

[206] A. Neesse, K. K. Frese, T. E. Bapiro, T. Nakagawa, M. D. Sternlicht, T. W. Seeley, C. Pilarsky, D. I. Jodrell, S. M. Spong, D. A. Tuveson, *PNAS* **2013**, *110*, 12325.

[207] R. Winograd, K. T. Byrne, R. A. Evans, P. M. Odorizzi, A. R. L. Meyer, D. L. Bajor, C. Clendenin, B. Z. Stanger, E. E. Furth, E. J. Wherry, R. H. Vonderheide, *Cancer Immunol Res* **2015**, *3*, 399.

[208] R. H. Hruban, M. I. Canto, M. Goggins, R. Schulick, A. P. Klein, *Advances in Surgery* **2010**, *44*, 293.

[209] F. Skoulidis, L. D. Cassidy, V. Pisupati, J. G. Jonasson, H. Bjarnason, J. E. Eyfjord, F. A. Karreth, M. Lim, L. M. Barber, S. A. Clatworthy, S. E. Davies, K. P. Olive, D. A. Tuveson, A. R. Venkitaraman, *Cancer Cell* **2010**, *18*, 499.

[210] S. Kumar, M. P. Torres, S. Kaur, S. Rachagani, S. Joshi, S. L. Johansson, N. Momi, M. J. Baine, C. E. Gilling, L. M. Smith, T. A. Wyatt, M. Jain, S. S. Joshi, S. K. Batra, *Oncogene* **2015**, *34*, 2052.

[211] M. Edderkaoui, S. Xu, C. Chheda, S. Morvaridi, R. W. Hu, P. J. Grippo, E. Mascariñas, D. R. Principe, B. Knudsen, J. Xue, A. Habtezion, D. Uyeminami, K. E. Pinkerton, S. J. Pandol, *Oncotarget* **2016**, *7*, 7747.

[212] S. Xu, C. Chheda, Y. Ouhaddi, H. Benhaddou, M. Bourhim, P. J. Grippo, D. R. Principe, E. Mascariñas, B. DeCant, H. Tsukamoto, S. J. Pandol, M. Edderkaoui, *Pancreas* **2015**, *44*, 882.

[213] L. Wang, Y.-Y. Bai, Y. Yang, F. Hu, Y. Wang, Z. Yu, Z. Cheng, J. Zhou, *Oncotarget* **2016**, *7*, 38539.

[214] K. Kersten, K. E. de Visser, M. H. van Miltenburg, J. Jonkers, *EMBO Mol Med* **2017**, *9*, 137.

[215] K. Kong, M. Guo, Y. Liu, J. Zheng, *J Cancer* **2020**, *11*, 1555.

[216] M. Hidalgo, F. Amant, A. V. Biankin, E. Budinská, A. T. Byrne, C. Caldas, R. B. Clarke, S. de Jong, J. Jonkers, G. M. Mælandsmo, S. Roman-Roman, J. Seoane, L. Trusolino, A. Villanueva, for the EurOPDX Consortium, *Cancer Discovery* **2014**, *4*, 998.

[217] D. Delitto, K. Pham, A. C. Vlada, G. A. Sarosi, R. M. Thomas, K. E. Behrns, C. Liu, S. J. Hughes, S. M. Wallet, J. G. Trevino, *The American Journal of Pathology* **2015**, *185*, 1297.

[218] S. Aparicio, M. Hidalgo, A. L. Kung, *Nat Rev Cancer* **2015**, *15*, 311.

[219] A. F. Labrijn, J. I. Meesters, M. Bunce, A. A. Armstrong, S. Somani, T. C. Nesspor, M. L. Chiu, I. Altintaş, S. Verploegen, J. Schuurman, P. W. H. I. Parren, *Sci Rep* **2017**, *7*, 2476.

[220] B. N. Mills, K. A. Connolly, J. Ye, J. D. Murphy, T. P. Uccello, B. J. Han, T. Zhao, M. G. Drage, A. Murthy, H. Qiu, A. Patel, N. M. Figueroa, C. J. Johnston, P. A. Prieto, N. K. Egilmez, B. A. Belt, E. M. Lord, D. C. Linehan, S. A. Gerber, *Cell Rep* **2019**, *29*, 406.

[221] A. J. Rech, H. Dada, J. J. Kotzin, J. Henao-Mejia, A. J. Minn, C. Twyman-Saint Victor, R. H. Vonderheide, *Cancer Res* **2018**, *78*, 4282.

[222] P. A. Philip, J. Benedetti, C. L. Corless, R. Wong, E. M. O'Reilly, P. J. Flynn, K. M. Rowland, J. N. Atkins, B. C. Mirtsching, S. E. Rivkin, A. A. Khorana, B. Goldman, C. M. Fenoglio-Preiser, J. L. Abbruzzese, C. D. Blanke, *Journal of Clinical Oncology* **2010**, DOI 10.1200/JCO.2009.25.7550.

[223] H. Oettle, S. Post, P. Neuhaus, K. Gellert, J. Langrehr, K. Ridwelski, H. Schramm, J. Fahlke, C. Zuelke, C. Burkart, K. Gutberlet, E. Kettner, H. Schmalenberg, K. Weigang-Koehler, W.-O. Bechstein, M. Niedergethmann, I. Schmidt-Wolf, L. Roll, B. Doerken, H. Riess, *JAMA* **2007**, *297*, 267.

[224] E. P. Balaban, P. B. Mangu, N. S. Yee, *Journal of Oncology Practice* **2016**, DOI 10.1200/JOP.2016.017376.

[225] A. M. Nagrial, V. T. Chin, K. M. Sjoquist, M. Pajic, L. G. Horvath, A. V. Biankin, D. Yip, *Crit Rev Oncol Hematol* **2015**, *96*, 483.

[226] M. Ducreux, A. Sa. Cuhna, C. Caramella, A. Hollebecque, P. Burtin, D. Goéré, T. Seufferlein, K. Haustermans, J. L. Van Laethem, T. Conroy, D. Arnold, *Annals of Oncology* **2015**, *26*, v56.

[227] M. A. Tempero, M. P. Malafa, M. Al-Hawary, S. W. Behrman, A. B. Benson, D. B. Cardin, E. G. Chiorean, V. Chung, B. Czito, M. D. Chiaro, M. Dillhoff, T. R. Donahue, E. Dotan, C. R. Ferrone, C. Fountzilas, J. Hardacre, W. G. Hawkins, K. Klute, A. H. Ko, J. W. Kunstman, N. LoConte, A. M. Lowy, C. Moravek, E. K. Nakakura, A. K. Narang, J. Obando, P. M. Polanco, S. Reddy, M. Reyngold, C. Scaife, J. Shen, C. Vollmer, R. A. Wolff, B. M. Wolpin, B. Lynn, G. V. George, *Journal of the National Comprehensive Cancer Network* **2021**, *19*, 439.

[228] "ECOG Performance Status Scale," **n.d.**

[229] "Pancreatic Cancer Stages," can be found under https://www.cancer.org/cancer/pancreatic-cancer/detection-diagnosis-staging/staging.html, **n.d.**

[230] "Surgery for Pancreatic Cancer," can be found under https://www.cancer.org/cancer/pancreatic-cancer/treating/surgery.html, **n.d.**

[231] W. S. Tummers, J. V. Groen, B. G. Sibinga Mulder, A. Farina-Sarasqueta, J. Morreau, H. Putter, C. J. van de Velde, A. L. Vahrmeijer, B. A. Bonsing, J. S. Mieog, R. J. Swijnenburg, *British Journal of Surgery* **2019**, *106*, 1055.

[232] H. J. Yoo, M.-W. You, D. Y. Han, J. H. Hwang, S. J. Park, *Cancer Imaging* **2020**, *20*, 1.

[233] M. Tanaka, A. L. Mihaljevic, P. Probst, M. Heckler, U. Klaiber, U. Heger, M. W. Büchler, T. Hackert, *British Journal of Surgery* **2019**, *106*, 1590.

[234] V. P. Groot, N. Rezaee, W. Wu, J. L. Cameron, E. K. Fishman, R. H. Hruban, M. J. Weiss, L. Zheng, C. L. Wolfgang, J. He, *Ann Surg* **2018**, *267*, 936.

[235] C. C. N. Chong, *J Vis Surg* **2018**, *4*, 106.

[236] S. Hishinuma, Y. Ogata, M. Tomikawa, I. Ozawa, K. Hirabayashi, S. Igarashi, *J Gastrointest Surg* **2006**, *10*, 511.

[237] A. Van den broeck, G. Sergeant, N. Ectors, W. Van Steenbergen, R. Aerts, B. Topal, *European Journal of Surgical Oncology (EJSO)* **2009**, *35*, 600.

[238] *Lancet* **1995**, *345*, 939.

[239] D. B. Longley, D. P. Harkin, P. G. Johnston, *Nat Rev Cancer* **2003**, *3*, 330.

[240] W.-B. Wang, Y. Yang, Y.-P. Zhao, T.-P. Zhang, Q. Liao, H. Shu, *World J Gastroenterol* **2014**, *20*, 15682.

[241] C. Sethy, C. N. Kundu, *Biomedicine & Pharmacotherapy* **2021**, *137*, 111285.

[242] L. W. Hertel, G. B. Boder, J. S. Kroin, S. M. Rinzel, G. A. Poore, G. C. Todd, G. B. Grindey, *Cancer Res* **1990**, *50*, 4417.

[243] H. A. Burris, M. J. Moore, J. Andersen, M. R. Green, M. L. Rothenberg, M. R. Modiano, M. C. Cripps, R. K. Portenoy, A. M. Storniolo, P. Tarassoff, R. Nelson, F. A. Dorr, C. D. Stephens, D. D. Von Hoff, *J Clin Oncol* **1997**, *15*, 2403.

[244] M. P. Kim, G. E. Gallick, *Clin Cancer Res* **2008**, *14*, 1284.

[245] N. Weizman, Y. Krelin, A. Shabtay-Orbach, M. Amit, Y. Binenbaum, R. J. Wong, Z. Gil, *Oncogene* **2014**, *33*, 3812.

[246] E. Poplin, H. Wasan, L. Rolfe, M. Raponi, T. Ikdahl, I. Bondarenko, I. Davidenko, V. Bondar, A. Garin, S. Boeck, S. Ormanns, V. Heinemann, C. Bassi, T. R. J. Evans, R. Andersson, H. Hahn, V. Picozzi, A. Dicker, E. Mann, C. Voong, P. Kaur, J. Isaacson, A. Allen, *Journal of Clinical Oncology* **2013**, DOI 10.1200/JCO.2013.51.0826.

[247] R. Herrmann, G. Bodoky, T. Ruhstaller, B. Glimelius, E. Bajetta, J. Schüller, P. Saletti, J. Bauer, A. Figer, B. Pestalozzi, C.-H. Köhne, W. Mingrone, S. M. Stemmer, K. Tàmas, G. V. Kornek, D. Koeberle, S. Cina, J. Bernhard, D.

Dietrich, W. Scheithauer, Swiss Group for Clinical Cancer Research, Central European Cooperative Oncology Group, *J Clin Oncol* **2007**, *25*, 2212.

[248] V. Heinemann, D. Quietzsch, F. Gieseler, M. Gonnermann, H. Schönekäs, A. Rost, H. Neuhaus, C. Haag, M. Clemens, B. Heinrich, U. Vehling-Kaiser, M. Fuchs, D. Fleckenstein, W. Gesierich, D. Uthgenannt, H. Einsele, A. Holstege, A. Hinke, A. Schalhorn, R. Wilkowski, *JCO* **2006**, *24*, 3946.

[249] C. Louvet, R. Labianca, P. Hammel, G. Lledo, M. G. Zampino, T. André, A. Zaniboni, M. Ducreux, E. Aitini, J. Taïeb, R. Faroux, C. Lepere, A. de Gramont, *Journal of Clinical Oncology* **2016**, DOI 10.1200/JCO.2005.06.023.

[250] E. Poplin, Y. Feng, J. Berlin, M. L. Rothenberg, H. Hochster, E. Mitchell, S. Alberts, P. O'Dwyer, D. Haller, P. Catalano, D. Cella, A. B. Benson, *J Clin Oncol* **2009**, *27*, 3778.

[251] C. M. R. Lima, M. R. Green, R. Rotche, W. H. M. Jr, G. M. Jeffrey, L. A. Cisar, A. Morganti, N. Orlando, G. Gruia, L. L. Miller, *Journal of Clinical Oncology* **2016**, DOI 10.1200/JCO.2004.12.082.

[252] M. Suker, B. R. Beumer, E. Sadot, L. Marthey, J. E. Faris, E. A. Mellon, B. F. El-Rayes, A. Wang-Gillam, J. Lacy, P. J. Hosein, S. Y. Moorcraft, T. Conroy, F. Hohla, P. Allen, J. Taieb, T. S. Hong, R. Shridhar, I. Chau, C. H. van Eijck, B. G. Koerkamp, *Lancet Oncol* **2016**, *17*, 801.

[253] T. Conroy, F. Desseigne, M. Ychou, O. Bouché, R. Guimbaud, Y. Bécouarn, A. Adenis, J.-L. Raoul, S. Gourgou-Bourgade, C. de la Fouchardière, J. Bennouna, J.-B. Bachet, F. Khemissa-Akouz, D. Péré-Vergé, C. Delbaldo, E. Assenat, B. Chauffert, P. Michel, C. Montoto-Grillot, M. Ducreux, Groupe Tumeurs Digestives of Unicancer, PRODIGE Intergroup, *N Engl J Med* **2011**, *364*, 1817.

[254] B. A. Boone, J. Steve, A. M. Krasinskas, A. H. Zureikat, B. C. Lembersky, M. K. Gibson, R. G. Stoller, H. J. Zeh, N. Bahary, *J Surg Oncol* **2013**, *108*, 236.

[255] D. D. V. Hoff, R. K. Ramanathan, M. J. Borad, D. A. Laheru, L. S. Smith, T. E. Wood, R. L. Korn, N. Desai, V. Trieu, J. L. Iglesias, H. Zhang, P. Soon-Shiong, T. Shi, N. V. Rajeshkumar, A. Maitra, M. Hidalgo, *Journal of Clinical Oncology* **2011**, DOI 10.1200/JCO.2011.36.5742.

[256] C. Weekes, V. Narayanan, *GICTT* **2015**, 11.

[257] D. D. Von Hoff, T. Ervin, F. P. Arena, E. G. Chiorean, J. Infante, M. Moore, T. Seay, S. A. Tjulandin, W. W. Ma, M. N. Saleh, M. Harris, M. Reni, S. Dowden, D. Laheru, N. Bahary, R. K. Ramanathan, J. Tabernero, M. Hidalgo, D. Goldstein, E. Van Cutsem, X. Wei, J. Iglesias, M. F. Renschler, *N Engl J Med* **2013**, *369*, 1691.

[258] A. Wang-Gillam, C.-P. Li, G. Bodoky, A. Dean, Y.-S. Shan, G. Jameson, T. Macarulla, K.-H. Lee, D. Cunningham, J. F. Blanc, R. A. Hubner, C.-F. Chiu, G. Schwartsmann, J. T. Siveke, F. Braiteh, V. Moyo, B. Belanger, N. Dhindsa, E. Bayever, D. D. Von Hoff, L.-T. Chen, NAPOLI-1 Study Group, *Lancet* **2016**, *387*, 545.

[259] V. Muralidharan-Chari, H. G. Kohan, A. G. Asimakopoulos, T. Sudha, S. Sell, K. Kannan, M. Boroujerdi, P. J. Davis, S. A. Mousa, *Oncotarget* **2016**, *7*, 50365.

[260] A. Adamska, O. Elaskalani, A. Emmanouilidi, M. Kim, N. B. Abdol Razak, P. Metharom, M. Falasca, *Advances in Biological Regulation* **2018**, *68*, 77.

[261] X. Zheng, J. L. Carstens, J. Kim, M. Scheible, J. Kaye, H. Sugimoto, C.-C. Wu, V. S. LeBleu, R. Kalluri, *Nature* **2015**, *527*, 525.

[262] B. C. Özdemir, T. Pentcheva-Hoang, J. L. Carstens, X. Zheng, C.-C. Wu, T. R. Simpson, H. Laklai, H. Sugimoto, C. Kahlert, S. V. Novitskiy, A. De Jesus-Acosta, P. Sharma, P. Heidari, U. Mahmood, L. Chin, H. L. Moses, V. M. Weaver, A. Maitra, J. P. Allison, V. S. LeBleu, R. Kalluri, *Cancer Cell* **2014**, *25*, 719.

[263] S. Wang, Y. Li, C. Xing, C. Ding, H. Zhang, L. Chen, L. You, M. Dai, Y. Zhao, *Am J Cancer Res* **2020**, *10*, 1937.

[264] S. Yachida, C. A. Iacobuzio-Donahue, *Oncogene* **2013**, *32*, 5253.

[265] D. F. Quail, J. A. Joyce, *Nat Med* **2013**, *19*, 1423.

[266] G. Fountzilas, M. Bobos, A. Kalogera-Fountzila, N. Xiros, S. Murray, H. Linardou, G. Karayannopoulou, A. K. Koutras, D. Bafaloukos, E. Samantas, C. Christodoulou, T. Economopoulos, K. T. Kalogeras, P. Kosmidis, *Cancer Investigation* **2008**, *26*, 784.

[267] J. Harder, G. Ihorst, V. Heinemann, R. Hofheinz, M. Moehler, P. Buechler, G. Kloeppel, C. Röcken, M. Bitzer, S. Boeck, E. Endlicher, A. Reinacher-Schick, C. Schmoor, M. Geissler, *Br J Cancer* **2012**, *106*, 1033.

[268] Z. Wu, A. Gabrielson, J. J. Hwang, M. J. Pishvaian, L. M. Weiner, T. Zhuang, L. Ley, J. L. Marshall, A. R. He, *Cancer Chemother Pharmacol* **2015**, *76*, 1309.

[269] P. A. Philip, B. Goldman, R. K. Ramanathan, H.-J. Lenz, A. M. Lowy, R. P. Whitehead, T. Wakatsuki, S. Iqbal, R. Gaur, J. K. Benedetti, C. D. Blanke, *Cancer* **2014**, *120*, 2980.

[270] C. S. Fuchs, S. Azevedo, T. Okusaka, J.-L. V. Laethem, L. R. Lipton, H. Riess, C. Szczylik, M. J. Moore, M. Peeters, G. Bodoky, M. Ikeda, B. Melichar, R. Nemecek, S. Ohkawa, A. Świeboda-Sadlej, S. A. Tjulandin, E. V. Cutsem, R. Loberg, V. Haddad, J. L. Gansert, B. A. Bach, A. Carrato, *Annals of Oncology* **2015**, *26*, 921.

[271] E. V. Cutsem, H. van de Velde, P. Karasek, H. Oettle, W. L. Vervenne, A. Szawlowski, P. Schoffski, S. Post, C. Verslype, H. Neumann, H. Safran, Y. Humblet, J. P. Ruixo, Y. Ma, D. V. Hoff, *Journal of Clinical Oncology* **2016**, DOI 10.1200/JCO.2004.10.112.

[272] G. Bodoky, C. Timcheva, D. R. Spigel, P. J. La Stella, T. E. Ciuleanu, G. Pover, N. C. Tebbutt, *Invest New Drugs* **2012**, *30*, 1216.

[273] Washington University School of Medicine, *Phase Ib Study of BVD-523 Plus Nab-Paclitaxel and Gemcitabine in Patients With Metastatic Pancreatic Cancer*, Clinicaltrials.Gov, **2021**.

[274] B. H. O'Neil, A. J. Scott, W. W. Ma, S. J. Cohen, D. L. Aisner, A. R. Menter, M. A. Tejani, J. K. Cho, J. Granfortuna, L. Coveler, O. O. Olowokure, J. C. Baranda, M. Cusnir, P. Phillip, J. Boles, R. Nazemzadeh, M. Rarick, D. J. Cohen, J. Radford, L. Fehrenbacher, R. Bajaj, V. Bathini, P. Fanta, J. Berlin, A. J. McRee, R. Maguire, F. Wilhelm, M. Maniar, A. Jimeno, C. L. Gomes, W. A. Messersmith, *Ann Oncol* **2015**, *26*, 1923.

[275] E. Liu, P. Marincola, K. Öberg, *Therap Adv Gastroenterol* **2013**, *6*, 412.

[276] S. Kordes, H. J. Klümpen, M. J. Weterman, J. H. M. Schellens, D. J. Richel, J. W. Wilmink, *Cancer Chemother Pharmacol* **2015**, *75*, 1135.

[277] E. Jokinen, J. P. Koivunen, *Ther Adv Med Oncol* **2015**, *7*, 170.

[278] W.-C. Yen, M. M. Fischer, M. Hynes, J. Wu, E. Kim, L. Beviglia, V. P. Yeung, X. Song, A. M. Kapoun, J. Lewicki, A. Gurney, D. M. Simeone, T. Hoey, *Clin Cancer Res* **2012**, *18*, 5374.

[279] A. De Jesus-Acosta, D. Laheru, A. Maitra, J. Arcaroli, M. A. Rudek, A. Dasari, P. J. Blatchford, K. Quackenbush, W. Messersmith, *Invest New Drugs* **2014**, *32*, 739.

[280] H. I. Hurwitz, N. Uppal, S. A. Wagner, J. C. Bendell, J. T. Beck, S. M. Wade, J. J. Nemunaitis, P. J. Stella, J. M. Pipas, Z. A. Wainberg, R. Manges, W. M. Garrett, D. S. Hunter, J. Clark, L. Leopold, V. Sandor, R. S. Levy, *J Clin Oncol* **2015**, *33*, 4039.

[281] National Cancer Institute (NCI), *A Randomized Phase II Study of Gemcitabine, Cisplatin +/- Veliparib in Patients With Pancreas Adenocarcinoma and a Known BRCA/ PALB2 Mutation (Part I) and a Phase II Single Arm Study of Single-Agent Veliparib in Previously Treated Pancreas Adenocarcinoma (Part II)*, Clinicaltrials.Gov, **2021**.

[282] "Study of Combined SGT-53 Plus Gemcitabine/Nab-Paclitaxel for Metastatic Pancreatic Cancer - No Study Results Posted - ClinicalTrials.gov," can be found under https://clinicaltrials.gov/ct2/show/results/NCT02340117, **n.d.**

[283] M. Pàez-Ribes, E. Allen, J. Hudock, T. Takeda, H. Okuyama, F. Viñals, M. Inoue, G. Bergers, D. Hanahan, O. Casanovas, *Cancer Cell* **2009**, *15*, 220.

[284] H. L. Kindler, G. Friberg, D. A. Singh, G. Locker, S. Nattam, M. Kozloff, D. A. Taber, T. Karrison, A. Dachman, W. M. Stadler, E. E. Vokes, *J Clin Oncol* **2005**, *23*, 8033.

[285] H. L. Kindler, T. Ioka, D. J. Richel, J. Bennouna, R. Létourneau, T. Okusaka, A. Funakoshi, J. Furuse, Y. S. Park, S. Ohkawa, G. M. Springett, H. S. Wasan, P. C. Trask, P. Bycott, A. D. Ricart, S. Kim, E. Van Cutsem, *The Lancet Oncology* **2011**, *12*, 256.

[286] H. L. Kindler, K. Wroblewski, J. A. Wallace, M. J. Hall, G. Locker, S. Nattam, E. Agamah, W. M. Stadler, E. E. Vokes, *Invest New Drugs* **2012**, *30*, 382.

[287] P. Rougier, H. Riess, R. Manges, P. Karasek, Y. Humblet, C. Barone, A. Santoro, S. Assadourian, L. Hatteville, P. A. Philip, *Eur J Cancer* **2013**, *49*, 2633.

[288] S. M. Taylor, K. R. Nevis, H. L. Park, G. C. Rogers, S. L. Rogers, J. G. Cook, V. L. Bautch, *Blood* **2010**, *116*, 3108.

[289] H. Maes, D. Olmeda, M. S. Soengas, P. Agostinis, *The FEBS Journal* **2016**, *283*, 25.

[290] A. N. Hosein, R. A. Brekken, A. Maitra, *Nat Rev Gastroenterol Hepatol* **2020**, *17*, 487.

[291] J. Kota, J. Hancock, J. Kwon, M. Korc, *Cancer Letters* **2017**, *391*, 38.

[292] M. Hidalgo, C. Plaza, M. Musteanu, P. Illei, C. B. Brachmann, C. Heise, D. Pierce, P. P. Lopez-Casas, C. Menendez, J. Tabernero, A. Romano, X. Wei, F. Lopez-Rios, D. D. Von Hoff, *Clinical Cancer Research* **2015**, *21*, 4811.

[293] H. Kim, S. Samuel, P. Lopez-Casas, W. Grizzle, M. Hidalgo, J. Kovar, D. Oelschlager, K. Zinn, J. Warram, D. Buchsbaum, *Molecular Cancer Therapeutics* **2016**, *15*, 680.

[294] A. D. Rhim, P. E. Oberstein, D. H. Thomas, E. T. Mirek, C. F. Palermo, S. A. Sastra, E. N. Dekleva, T. Saunders, C. P. Becerra, I. W. Tattersall, C. B. Westphalen, J. Kitajewski, M. G. Fernandez-Barrena, M. E. Fernandez-Zapico, C. Iacobuzio-Donahue, K. P. Olive, B. Z. Stanger, *Cancer Cell* **2014**, *25*, 735.

[295] T. Stylianopoulos, R. K. Jain, *Proceedings of the National Academy of Sciences* **2013**, *110*, 18632.

[296] A. L. McCleary-Wheeler, R. M. Carr, S. R. Palmer, T. C. Smyrk, J. B. Allred, L. L. Almada, E. J. Tolosa, M. J. Lamberti, D. L. Marks, M. J. Borad, J. R. Molina, Y. Qi, W. L. Lingle, A. Grothey, H. C. Pitot, A. Jatoi, D. W.

Northfelt, A. H. Bryce, R. R. McWilliams, S. H. Okuno, P. Haluska, G. P. Kim, G. Colon-Otero, V. J. Lowe, M. R. Callstrom, W. W. Ma, T. Bekaii-Saab, M.-C. Hung, C. Erlichman, M. E. Fernandez-Zapico, *Pancreatology* **2020**, *20*, 101.

[297] A. De Jesus-Acosta, E. A. Sugar, P. J. O'Dwyer, R. K. Ramanathan, D. D. Von Hoff, Z. Rasheed, L. Zheng, A. Begum, R. Anders, A. Maitra, F. McAllister, N. V. Rajeshkumar, S. Yabuuchi, R. F. de Wilde, B. Batukbhai, I. Sahin, D. A. Laheru, *Br J Cancer* **2020**, *122*, 498.

[298] R. K. Ramanathan, S. L. McDonough, P. A. Philip, S. R. Hingorani, J. Lacy, J. S. Kortmansky, J. Thumar, E. G. Chiorean, A. F. Shields, D. Behl, P. T. Mehan, R. Gaur, T. Seery, K. A. Guthrie, H. S. Hochster, *J Clin Oncol* **2019**, *37*, 1062.

[299] E. Van Cutsem, M. A. Tempero, D. Sigal, D.-Y. Oh, N. Fazio, T. Macarulla, E. Hitre, P. Hammel, A. E. Hendifar, S. E. Bates, C.-P. Li, S. R. Hingorani, C. de la Fouchardiere, A. Kasi, V. Heinemann, A. Maraveyas, N. Bahary, L. Layos, V. Sahai, L. Zheng, J. Lacy, J. O. Park, F. Portales, P. Oberstein, W. Wu, D. Chondros, A. J. Bullock, HALO 109-301 Investigators, *J Clin Oncol* **2020**, *38*, 3185.

[300] Pancreatic Cancer Research Team, *Phase II Study of PEGPH20 and Pembrolizumab (MK-3475) for Patients With Previously Treated Hyaluronan High (HA-High) Metastatic Pancreatic Ductal Adenocarcinoma*, Clinicaltrials.Gov, **2019**.

[301] G. Manji, *A Phase 2, Open-Label, Multicenter, Randomized Study Evaluating NEOadjuvant Immunotherapy Based Combinations in Patients With Resectable PANCreatic Ductal Adenocarcinoma*, Clinicaltrials.Gov, **2020**.

[302] J. Lee, G. A. Wilkinson, T. Kimbler, B. Blouw, C. B. Thompson, *Cancer Research* **2020**, *80*, 2206.

[303] N. C. Singha, T. Nekoroski, C. Zhao, R. Symons, P. Jiang, G. I. Frost, Z. Huang, H. M. Shepard, *Molecular Cancer Therapeutics* **2015**, *14*, 523.

[304] R. Gao, D. R. Brigstock, *Gut* **2006**, *55*, 856.

[305] V. J. Picozzi, J. M. Pipas, A. Koong, A. Giaccia, N. Bahary, S. S. Krishnamurthi, C. D. Lopez, P. J. O'Dwyer, K. Modelska, M. Carney, H. Hernandez, J. Chou, T. Lee, M. Zhong, S. Porter, T. Neff, F. Valone, *JCO* **2014**, *32*, 4138.

[306] V. J. Picozzi, M. J. Pishvaian, K. Mody, J. M. Winter, J. A. Glaspy, T. Larson, M. R. Matrana, K. Saikali, M. Carney, S. Porter, P. Yu, E. Kouchakji, E. Carrier, *JCO* **2018**, *36*, 4016.

[307] FibroGen, *A Phase 3, Randomized, Double-Blind Study of Pamrevlumab or Placebo in Combination With Either Gemcitabine Plus Nab-Paclitaxel or FOLFIRINOX as Neoadjuvant Treatment in Patients With Locally Advanced, Unresectable Pancreatic Cancer*, Clinicaltrials.Gov, **2021**.

[308] N. Rath, J. P. Morton, L. Julian, L. Helbig, S. Kadir, E. J. McGhee, K. I. Anderson, G. Kalna, M. Mullin, A. V. Pinho, I. Rooman, M. S. Samuel, M. F. Olson, *EMBO Mol Med* **2017**, *9*, 198.

[309] C. Vennin, V. T. Chin, S. C. Warren, M. C. Lucas, D. Herrmann, A. Magenau, P. Melenec, S. N. Walters, G. Del Monte-Nieto, J. R. W. Conway, M. Nobis, A. H. Allam, R. A. McCloy, N. Currey, M. Pinese, A. Boulghourjian, A. Zaratzian, A. A. S. Adam, C. Heu, A. M. Nagrial, A. Chou, A. Steinmann, A. Drury, D. Froio, M. Giry-Laterriere, N. L. E. Harris, T. Phan, R. Jain, W. Weninger, E. J. McGhee, R. Whan, A. L. Johns, J. S. Samra, L. Chantrill, A. J. Gill, M. Kohonen-Corish, R. P. Harvey, A. V. Biankin, Australian Pancreatic Cancer Genome Initiative (APGI), T. R. J. Evans, K. I. Anderson, S. T. Grey, C. J. Ormandy, D. Gallego-Ortega, Y. Wang, M. S. Samuel, O. J. Sansom, A. Burgess, T. R. Cox, J. P. Morton, M. Pajic, P. Timpson, *Sci Transl Med* **2017**, *9*, eaai8504.

[310] H. Jiang, S. Hegde, B. L. Knolhoff, Y. Zhu, J. M. Herndon, M. A. Meyer, T. M. Nywening, W. G. Hawkins, I. M. Shapiro, D. T. Weaver, J. A. Pachter, A. Wang-Gillam, D. G. DeNardo, *Nat Med* **2016**, *22*, 851.

[311] M. H. Sherman, R. T. Yu, D. D. Engle, N. Ding, A. R. Atkins, H. Tiriac, E. A. Collisson, F. Connor, T. Van Dyke, S. Kozlov, P. Martin, T. W. Tseng, D. W. Dawson, T. R. Donahue, A. Masamune, T. Shimosegawa, M. V. Apte, J. S. Wilson, B. Ng, S. L. Lau, J. E. Gunton, G. M. Wahl, T. Hunter, J. A. Drebin, P. J. O'Dwyer, C. Liddle, D. A. Tuveson, M. Downes, R. M. Evans, *Cell* **2014**, *159*, 80.

[312] P. Edwards, B. W. Kang, I. Chau, *Frontiers in Oncology* **2021**, *11*.

[313] P. Sharma, J. P. Allison, *Science* **2015**, *348*, 56.

[314] B. Alberts, A. Johnson, J. Lewis, M. Raff, K. Roberts, P. Walter, *Molecular Biology of the Cell. 4th edition* **2002**.

[315] B. Alberts, A. Johnson, J. Lewis, M. Raff, K. Roberts, P. Walter, *Molecular Biology of the Cell. 4th edition* **2002**.

[316] C. Boutros, A. Tarhini, E. Routier, O. Lambotte, F. L. Ladurie, F. Carbonnel, H. Izzeddine, A. Marabelle, S. Champiat, A. Berdelou, E. Lanoy, M. Texier, C. Libenciuc, A. M. M. Eggermont, J.-C. Soria, C. Mateus, C. Robert, *Nat Rev Clin Oncol* **2016**, *13*, 473.

[317] C. Robert, *Nat Commun* **2020**, *11*, 3801.

[318] C. U. Blank, J. B. Haanen, A. Ribas, T. N. Schumacher, *Science* **2016**, DOI 10.1126/science.aaf2834.

[319] L. H. Schwartz, S. Litière, E. de Vries, R. Ford, S. Gwyther, S. Mandrekar, L. Shankar, J. Bogaerts, A. Chen, J. Dancey, W. Hayes, F. S. Hodi, O. S. Hoekstra, E. P. Huang, N. Lin, Y. Liu, P. Therasse, J. D. Wolchok, L. Seymour, *Eur J Cancer* **2016**, *62*, 132.

[320] L. Seymour, J. Bogaerts, A. Perrone, R. Ford, L. H. Schwartz, S. Mandrekar, N. U. Lin, S. Litière, J. Dancey, A. Chen, F. S. Hodi, P. Therasse, O. S. Hoekstra, L. K. Shankar, J. D. Wolchok, M. Ballinger, C. Caramella, E. G. E. de Vries, RECIST working group, *Lancet Oncol* **2017**, *18*, e143.

[321] C. Robert, A. Ribas, O. Hamid, A. Daud, J. D. Wolchok, A. M. Joshua, W.-J. Hwu, J. S. Weber, T. C. Gangadhar, R. W. Joseph, R. Dronca, A. Patnaik, H. Zarour, R. Kefford, P. Hersey, J. Zhang, J. Anderson, S. J. Diede, S. Ebbinghaus, F. S. Hodi, *J Clin Oncol* **2018**, *36*, 1668.

[322] D. Kabacaoglu, K. J. Ciecielski, D. A. Ruess, H. Algül, *Front Immunol* **2018**, *9*, 1878.

[323] K. Yamamoto, A. Venida, J. Yano, D. E. Biancur, M. Kakiuchi, S. Gupta, A. S. W. Sohn, S. Mukhopadhyay, E. Y. Lin, S. J. Parker, R. S. Banh, J. A. Paulo, K. W. Wen, J. Debnath, G. E. Kim, J. D. Mancias, D. T. Fearon, R. M. Perera, A. C. Kimmelman, *Nature* **2020**, *581*, 100.

[324] C. E. Clark, S. R. Hingorani, R. Mick, C. Combs, D. A. Tuveson, R. H. Vonderheide, *Cancer Res* **2007**, *67*, 9518.

[325] L. Zheng, *J Natl Cancer Inst* **2017**, *109*, DOI 10.1093/jnci/djw304.

[326] J. Blando, A. Sharma, M. G. Higa, H. Zhao, L. Vence, S. S. Yadav, J. Kim, A. M. Sepulveda, M. Sharp, A. Maitra, J. Wargo, M. Tetzlaff, R. Broaddus, M. H. G. Katz, G. R. Varadhachary, M. Overman, H. Wang, C. Yee, C. Bernatchez, C. Iacobuzio-Donahue, S. Basu, J. P. Allison, P. Sharma, *Proc Natl Acad Sci U S A* **2019**, *116*, 1692.

[327] Janssen Research & Development, LLC, *An Open-Label, First-in-Human, Phase 1 Study of the Safety, Pharmacokinetics, and Pharmacodynamics of JNJ-61610588, a Fully Human IgG1 Kappa Anti-VISTA (V-Domain Ig Suppressor of T-Cell Activation) Monoclonal Antibody, in Subjects With Advanced Cancer*, Clinicaltrials.Gov, **2018**.

[328] S. K. Gautam, S. Kumar, V. Dam, D. Ghersi, M. Jain, S. K. Batra, *Seminars in Immunology* **2020**, *47*, 101391.

[329] N. Tekkesin, S. Tetik, in *Theranostic Approach for Pancreatic Cancer*, Elsevier, **2019**, pp. 275–294.

[330] M. Miyazawa, M. Katsuda, H. Maguchi, A. Katanuma, H. Ishii, M. Ozaka, K. Yamao, H. Imaoka, M. Kawai, S. Hirono, K.-I. Okada, H. Yamaue, *Int J Cancer* **2017**, *140*, 973.

[331] K. C. Soares, A. A. Rucki, A. A. Wu, K. Olino, Q. Xiao, Y. Chai, A. Wamwea, E. Bigelow, E. Lutz, L. Liu, S. Yao, R. A. Anders, D. Laheru, C. L. Wolfgang, B. H. Edil, R. D. Schulick, E. M. Jaffee, L. Zheng, *J Immunother* **2015**, *38*, 1.

[332] Sidney Kimmel Comprehensive Cancer Center at Johns Hopkins, *A Platform Study of Combination Immunotherapy for the Neoadjuvant and Adjuvant Treatment of Patients With Surgically Resectable Adenocarcinoma of the Pancreas*, Clinicaltrials.Gov, **2021**.

[333] Sidney Kimmel Comprehensive Cancer Center at Johns Hopkins, *A Pilot Study of a GVAX Pancreas Vaccine (With Cyclophosphamide) in Combination With a PD-1 Blockade Antibody (Pembrolizumab) and a Macrophage Targeting Agent (CSF1R Inhibitor) for the Treatment of Patients With Borderline Resectable Adenocarcinoma of the Pancreas*, Clinicaltrials.Gov, **2022**.

[334] Centre Leon Berard, *A Dose Escalation Phase I Study With an Extension Part Evaluating the Safety and Activity of an Anti-PDL1 Antibody (DURVALUMAB) Combined With a Small Molecule CSF-1R Tyrosine Kinase Inhibitor (PEXIDARTINIB) in Patients With Metastatic/Advanced Pancreatic or Colorectal Cancers*, Clinicaltrials.Gov, **2021**.

[335] Weill Medical College of Cornell University, *To Assess the Safety of Continuous IV Administration of the CXCR4 Antagonist, Plerixafor at Potentially Active Plasma Concentrations and Assess Its Impact on the Immune Microenvironment in Patients With Advanced Pancreatic, High Grade Serous Ovarian and Colorectal Adenocarcinomas*, Clinicaltrials.Gov, **2020**.

[336] Abramson Cancer Center of the University of Pennsylvania, *Phase I Study of Neo-Adjuvant RO7009789 Alone or Neo-Adjuvant RO7009789 Plus Nab-Paclitaxel and Gemcitabine Followed by Adjuvant RO7009789 Plus Nab-Paclitaxel and Gemcitabine for Patients With Newly Diagnosed Resectable Pancreatic Carcinoma*, Clinicaltrials.Gov, **2019**.

[337] R. H. Vonderheide, D. L. Bajor, R. Winograd, R. A. Evans, L. J. Bayne, G. L. Beatty, *Cancer Immunol Immunother* **2013**, *62*, 949.

[338] S. F. Ngiow, A. Young, S. J. Blake, G. R. Hill, H. Yagita, M. W. L. Teng, A. J. Korman, M. J. Smyth, *Cancer Res* **2016**, *76*, 6266.

[339] G. L. Beatty, D. A. Torigian, E. G. Chiorean, B. Saboury, A. Brothers, A. Alavi, A. B. Troxel, W. Sun, U. R. Teitelbaum, R. H. Vonderheide, P. J. O'Dwyer, *Clin Cancer Res* **2013**, *19*, 6286.

[340] J. Li, K. T. Byrne, F. Yan, T. Yamazoe, Z. Chen, T. Baslan, L. P. Richman, J. H. Lin, Y. H. Sun, A. J. Rech, D. Balli, C. A. Hay, Y. Sela, A. J. Merrell, S. M. Liudahl, N. Gordon, R. J. Norgard, S. Yuan, S. Yu, T. Chao, S. Ye, T. S. K. Eisinger-Mathason, R. B. Faryabi, J. W. Tobias, S. W. Lowe, L. M. Coussens, E. J. Wherry, R. H. Vonderheide, B. Z. Stanger, *Immunity* **2018**, *49*, 178.

[341] M. H. O'Hara, E. M. O'Reilly, G. Varadhachary, R. A. Wolff, Z. A. Wainberg, A. H. Ko, G. Fisher, O. Rahma, J. P. Lyman, C. R. Cabanski, R. Mick, P. F. Gherardini, L. J. Kitch, J. Xu, T. Samuel, J. Karakunnel, J. Fairchild, S. Bucktrout, T. M. LaVallee, C. Selinsky, J. E. Till, E. L. Carpenter, C. Alanio, K. T. Byrne, R. O. Chen, O. C. Trifan, U. Dugan, C. Horak, V. M. Hubbard-Lucey, E. J. Wherry, R. Ibrahim, R. H. Vonderheide, *The Lancet Oncology* **2021**, *22*, 118.

[342] A. M. McDonnell, A. Cook, B. W. S. Robinson, R. A. Lake, A. K. Nowak, *BMC Cancer* **2017**, *17*, 417.

[343] J. R. Van Audenaerde, E. Marcq, B. von Scheidt, A. S. Davey, A. J. Oliver, J. De Waele, D. Quatannens, J. Van Loenhout, P. Pauwels, G. Roeyen, F. Lardon, C. Y. Slaney, M. Peeters, M. H. Kershaw, P. K. Darcy, E. L. Smits, *Clin Transl Immunology* **2020**, *9*, e1165.

[344] R. H. Vonderheide, *Annu Rev Med* **2020**, *71*, 47.

[345] F. Susa, T. Limongi, B. Dumontel, V. Vighetto, V. Cauda, *Cancers* **2019**, *11*, 1979.

[346] C. Théry, K. W. Witwer, E. Aikawa, M. J. Alcaraz, J. D. Anderson, R. Andriantsitohaina, A. Antoniou, T. Arab, F. Archer, G. K. Atkin-Smith, D. C. Ayre, J.-M. Bach, D. Bachurski, H. Baharvand, L. Balaj, S. Baldacchino, N. N. Bauer, A. A. Baxter, M. Bebawy, C. Beckham, A. Bedina Zavec, A. Benmoussa, A. C. Berardi, P. Bergese, E. Bielska, C. Blenkiron, S. Bobis-Wozowicz, E. Boilard, W. Boireau, A. Bongiovanni, F. E. Borràs, S. Bosch, C. M. Boulanger, X. Breakefield, A. M. Breglio, M. Á. Brennan, D. R. Brigstock, A. Brisson, M. L. Broekman, J. F. Bromberg, P. Bryl-Górecka, S. Buch, A. H. Buck, D. Burger, S. Busatto, D. Buschmann, B. Bussolati, E. I. Buzás, J. B. Byrd, G. Camussi, D. R. Carter, S. Caruso, L. W. Chamley, Y.-T. Chang, C. Chen, S. Chen, L. Cheng, A. R. Chin, A. Clayton, S. P. Clerici, A. Cocks, E. Cocucci, R. J. Coffey, A. Cordeiro-da-Silva, Y. Couch, F. A. Coumans, B. Coyle, R. Crescitelli, M. F. Criado, C. D'Souza-Schorey, S. Das, A. Datta Chaudhuri, P. de Candia, E. F. De Santana, O. De Wever, H. A. del Portillo, T. Demaret, S. Deville, A. Devitt, B. Dhondt, D. Di Vizio, L. C. Dieterich, V. Dolo, A. P. Dominguez Rubio, M. Dominici, M. R. Dourado, T. A. Driedonks, F. V. Duarte, H. M. Duncan, R. M. Eichenberger, K. Ekström, S. EL Andaloussi, C. Elie-Caille, U. Erdbrügger, J. M. Falcón-Pérez, F. Fatima, J. E. Fish, M. Flores-Bellver, A. Försönits, A. Frelet-

Barrand, F. Fricke, G. Fuhrmann, S. Gabrielsson, A. Gámez-Valero, C. Gardiner, K. Gärtner, R. Gaudin, Y. S. Gho, B. Giebel, C. Gilbert, M. Gimona, I. Giusti, D. C. Goberdhan, A. Görgens, S. M. Gorski, D. W. Greening, J. C. Gross, A. Gualerzi, G. N. Gupta, D. Gustafson, A. Handberg, R. A. Haraszti, P. Harrison, H. Hegyesi, A. Hendrix, A. F. Hill, F. H. Hochberg, K. F. Hoffmann, B. Holder, H. Holthofer, B. Hosseinkhani, G. Hu, Y. Huang, V. Huber, S. Hunt, A. G.-E. Ibrahim, T. Ikezu, J. M. Inal, M. Isin, A. Ivanova, H. K. Jackson, S. Jacobsen, S. M. Jay, M. Jayachandran, G. Jenster, L. Jiang, S. M. Johnson, J. C. Jones, A. Jong, T. Jovanovic-Talisman, S. Jung, R. Kalluri, S. Kano, S. Kaur, Y. Kawamura, E. T. Keller, D. Khamari, E. Khomyakova, A. Khvorova, P. Kierulf, K. P. Kim, T. Kislinger, M. Klingeborn, D. J. Klinke, M. Kornek, M. M. Kosanović, Á. F. Kovács, E.-M. Krämer-Albers, S. Krasemann, M. Krause, I. V. Kurochkin, G. D. Kusuma, S. Kuypers, S. Laitinen, S. M. Langevin, L. R. Languino, J. Lannigan, C. Lässer, L. C. Laurent, G. Lavieu, E. Lázaro-Ibáñez, S. Le Lay, M.-S. Lee, Y. X. F. Lee, D. S. Lemos, M. Lenassi, A. Leszczynska, I. T. Li, K. Liao, S. F. Libregts, E. Ligeti, R. Lim, S. K. Lim, A. Linē, K. Linnemannstöns, A. Llorente, C. A. Lombard, M. J. Lorenowicz, Á. M. Lörincz, J. Lötvall, J. Lovett, M. C. Lowry, X. Loyer, Q. Lu, B. Lukomska, T. R. Lunavat, S. L. Maas, H. Malhi, A. Marcilla, J. Mariani, J. Mariscal, E. S. Martens-Uzunova, L. Martin-Jaular, M. C. Martinez, V. R. Martins, M. Mathieu, S. Mathivanan, M. Maugeri, L. K. McGinnis, M. J. McVey, D. G. Meckes, K. L. Meehan, I. Mertens, V. R. Minciacchi, A. Möller, M. Møller Jørgensen, A. Morales-Kastresana, J. Morhayim, F. Mullier, M. Muraca, L. Musante, V. Mussack, D. C. Muth, K. H. Myburgh, T. Najrana, M. Nawaz, I. Nazarenko, P. Nejsum, C. Neri, T. Neri, R. Nieuwland, L. Nimrichter, J. P. Nolan, E. N. Nolte-'t Hoen, N. Noren Hooten, L. O'Driscoll, T. O'Grady, A. O'Loghlen, T. Ochiya, M. Olivier, A. Ortiz, L. A. Ortiz, X. Osteikoetxea, O. Østergaard, M. Ostrowski, J. Park, D. M. Pegtel, H. Peinado, F. Perut, M. W. Pfaffl, D. G. Phinney, B. C. Pieters, R. C. Pink, D. S. Pisetsky, E. Pogge von Strandmann, I. Polakovicova, I. K. Poon, B. H. Powell, I. Prada, L. Pulliam, P. Quesenberry, A. Radeghieri, R. L. Raffai, S. Raimondo, J. Rak, M. I. Ramirez, G. Raposo, M. S. Rayyan, N. Regev-Rudzki, F. L. Ricklefs, P. D. Robbins, D. D. Roberts, S. C. Rodrigues, E. Rohde, S. Rome, K. M. Rouschop, A. Rughetti, A. E. Russell, P. Saá, S. Sahoo, E. Salas-Huenuleo, C. Sánchez, J. A. Saugstad, M. J. Saul, R. M. Schiffelers, R. Schneider, T. H. Schøyen, A. Scott, E. Shahaj, S. Sharma, O. Shatnyeva, F. Shekari, G. V. Shelke, A. K. Shetty, K. Shiba, P. R.-M. Siljander, A. M. Silva, A. Skowronek, O. L. Snyder, R. P. Soares, B. W. Sódar, C. Soekmadji, J. Sotillo, P. D. Stahl, W. Stoorvogel, S. L. Stott, E. F. Strasser, S. Swift, H. Tahara, M. Tewari, K. Timms, S. Tiwari, R. Tixeira, M. Tkach, W. S. Toh, R. Tomasini, A. C. Torrecilhas, J. P. Tosar, V. Toxavidis, L. Urbanelli, P. Vader, B. W. van Balkom, S. G. van der Grein, J. Van Deun, M. J. van Herwijnen, K. Van Keuren-Jensen, G. van Niel, M. E. van Royen, A. J. van

Wijnen, M. H. Vasconcelos, I. J. Vechetti, T. D. Veit, L. J. Vella, É. Velot, F. J. Verweij, B. Vestad, J. L. Viñas, T. Visnovitz, K. V. Vukman, J. Wahlgren, D. C. Watson, M. H. Wauben, A. Weaver, J. P. Webber, V. Weber, A. M. Wehman, D. J. Weiss, J. A. Welsh, S. Wendt, A. M. Wheelock, Z. Wiener, L. Witte, J. Wolfram, A. Xagorari, P. Xander, J. Xu, X. Yan, M. Yáñez-Mó, H. Yin, Y. Yuana, V. Zappulli, J. Zarubova, V. Žėkas, J. Zhang, Z. Zhao, L. Zheng, A. R. Zheutlin, A. M. Zickler, P. Zimmermann, A. M. Zivkovic, D. Zocco, E. K. Zuba-Surma, *Journal of Extracellular Vesicles* **2018**, *7*, 1535750.

[347] Y.-L. Tai, K.-C. Chen, J.-T. Hsieh, T.-L. Shen, *Cancer Science* **2018**, *109*, 2364.

[348] F. G. Kugeratski, R. Kalluri, *The FEBS Journal* **2021**, *288*, 10.

[349] S. M. Patil, S. S. Sawant, N. K. Kunda, *European Journal of Pharmaceutics and Biopharmaceutics* **2020**, *154*, 259.

[350] O. Markov, A. Oshchepkova, N. Mironova, *Frontiers in Pharmacology* **2019**, *10*.

[351] A. Clayton, C. L. Harris, J. Court, M. D. Mason, B. P. Morgan, *European Journal of Immunology* **2003**, *33*, 522.

[352] C. Giacobino, M. Canta, C. Fornaguera, S. Borrós, V. Cauda, *Cancers (Basel)* **2021**, *13*, 2280.

[353] J. M. Pitt, M. Charrier, S. Viaud, F. André, B. Besse, N. Chaput, L. Zitvogel, *The Journal of Immunology* **2014**, *193*, 1006.

[354] X. Shi, J. Sun, H. Li, H. Lin, W. Xie, J. Li, W. Tan, *The Prostate* **2020**, *80*, 811.

[355] S. Hao, O. Bai, F. Li, J. Yuan, S. Laferte, J. Xiang, *Immunology* **2007**, *120*, 90.

[356] C. D. Phung, T. T. Pham, H. T. Nguyen, T. T. Nguyen, W. Ou, J.-H. Jeong, H.-G. Choi, S. K. Ku, C. S. Yong, J. O. Kim, *Acta Biomaterialia* **2020**, *115*, 371.

[357] L. Pascucci, V. Coccè, A. Bonomi, D. Ami, P. Ceccarelli, E. Ciusani, L. Viganò, A. Locatelli, F. Sisto, S. M. Doglia, E. Parati, M. E. Bernardo, M. Muraca, G. Alessandri, G. Bondiolotti, A. Pessina, *Journal of Controlled Release* **2014**, *192*, 262.

[358] J. R. Aspe, C. J. Diaz Osterman, J. M. S. Jutzy, S. Deshields, S. Whang, N. R. Wall, *Journal of Extracellular Vesicles* **2014**, *3*, 23244.

[359] L. Xiao, U. Erb, K. Zhao, T. Hackert, M. Zöller, *OncoImmunology* **2017**, *6*, e1319044.

[360] Z. Li, Y. Tao, X. Wang, P. Jiang, J. Li, M. Peng, X. Zhang, K. Chen, H. Liu, P. Zhen, J. Zhu, X. Liu, X. Liu, *CPB* **2018**, *51*, 610.

[361] B. Costa-Silva, N. M. Aiello, A. J. Ocean, S. Singh, H. Zhang, B. K. Thakur, A. Becker, A. Hoshino, M. T. Mark, H. Molina, J. Xiang, T. Zhang, T.-M. Theilen, G. García-Santos, C. Williams, Y. Ararso, Y. Huang, G. Rodrigues, T.-L. Shen, K. J. Labori, I. M. B. Lothe, E. H. Kure, J. Hernandez, A. Doussot, S. H. Ebbesen, P. M. Grandgenett, M. A. Hollingsworth, M. Jain, K. Mallya, S. K. Batra, W. R. Jarnagin, R. E. Schwartz, I. Matei, H. Peinado, B. Z. Stanger, J. Bromberg, D. Lyden, *Nat Cell Biol* **2015**, *17*, 816.

[362] X. Wang, G. Luo, K. Zhang, J. Cao, C. Huang, T. Jiang, B. Liu, L. Su, Z. Qiu, *Cancer Res* **2018**, *78*, 4586.

[363] H. Sun, K. Shi, K. Qi, H. Kong, J. Zhang, S. Dai, W. Ye, T. Deng, Q. He, M. Zhou, *Frontiers in Immunology* **2019**, *10*.

[364] Y. Fang, W. Zhou, Y. Rong, T. Kuang, X. Xu, W. Wu, D. Wang, W. Lou, *Exp Cell Res* **2019**, *383*, 111543.

[365] Z. Yang, N. Zhao, J. Cui, H. Wu, J. Xiong, T. Peng, *Cell Oncol.* **2020**, *43*, 123.

[366] Q. Ma, H. Wu, Y. Xiao, Z. Liang, T. Liu, *International Journal of Oncology* **2020**, *56*, 1025.

[367] A. N. Ariston Gabriel, F. Wang, Q. Jiao, U. Yvette, X. Yang, S. A. Al-Ameri, L. Du, Y. Wang, C. Wang, *Mol Cancer* **2020**, *19*, 132.

[368] S. A. Melo, L. B. Luecke, C. Kahlert, A. F. Fernandez, S. T. Gammon, J. Kaye, V. S. LeBleu, E. A. Mittendorf, J. Weitz, N. Rahbari, C. Reissfelder, C. Pilarsky, M. F. Fraga, D. Piwnica-Worms, R. Kalluri, *Nature* **2015**, *523*, 177.

[369] K. Valencia, L. M. Montuenga, *Cancers* **2021**, *13*, 2147.

[370] H. Ye, H. Wang, P. Wang, C.-H. Song, K.-J. Wang, L.-P. Dai, J.-X. Shi, X.-X. Liu, C.-Q. Sun, X. Wang, Y. Peng, X.-B. Chen, J.-Y. Zhang, *Eur Rev Med Pharmacol Sci* **2019**, *23*, 9351.

[371] Q. Liu, S. Li, A. Dupuy, H. le Mai, N. Sailliet, C. Logé, J.-M. H. Robert, S. Brouard, *International Journal of Molecular Sciences* **2021**, *22*, 7763.

[372] J. E. Pullan, M. I. Confeld, J. K. Osborn, J. Kim, K. Sarkar, S. Mallik, *Mol. Pharmaceutics* **2019**, *16*, 1789.

[373] S. Kamerkar, V. S. LeBleu, H. Sugimoto, S. Yang, C. F. Ruivo, S. A. Melo, J. J. Lee, R. Kalluri, *Nature* **2017**, *546*, 498.

[374] M.D. Anderson Cancer Center, *Phase I Study of Mesenchymal Stromal Cells-Derived Exosomes With KrasG12D siRNA for Metastatic Pancreas Cancer Patients Harboring KrasG12D Mutation*, Clinicaltrials.Gov, **2021**.

[375] V. Longo, O. Brunetti, A. Gnoni, S. Cascinu, G. Gasparini, V. Lorusso, D. Ribatti, N. Silvestris, *Oncotarget* **2016**, *7*, 58649.

[376] K. Chen, Q. Wang, M. Kornmann, X. Tian, Y. Yang, *Frontiers in Oncology* **2021**, *11*.

[377] J. M. Winter, M. F. Brennan, L. H. Tang, M. I. D'Angelica, R. P. DeMatteo, Y. Fong, D. S. Klimstra, W. R. Jarnagin, P. J. Allen, *Ann Surg Oncol* **2012**, *19*, 169.

[378] M. Sinn, M. Bahra, T. Denecke, S. Travis, U. Pelzer, H. Riess, *World J Gastrointest Oncol* **2016**, *8*, 248.

[379] E. A. Asare, D. B. Evans, B. A. Erickson, M. Aburajab, P. Tolat, S. Tsai, *J Surg Oncol* **2016**, *114*, 291.

[380] H. Haeno, M. Gonen, M. B. Davis, J. M. Herman, C. A. Iacobuzio-Donahue, F. Michor, *Cell* **2012**, *148*, 362.

[381] G. Perri, L. R. Prakash, M. H. G. Katz, *Frontiers in Oncology* **2020**, *10*.

[382] C. L. Roland, A. D. Yang, M. H. G. Katz, D. Chatterjee, H. Wang, H. Lin, J. N. Vauthey, P. W. Pisters, G. R. Varadhachary, R. A. Wolff, C. H. Crane, J. E. Lee, J. B. Fleming, *Ann Surg Oncol* **2015**, *22*, 1168.

[383] A. A. Mokdad, R. M. Minter, H. Zhu, M. M. Augustine, M. R. Porembka, S. C. Wang, A. C. Yopp, J. C. Mansour, M. A. Choti, P. M. Polanco, *JCO* **2017**, *35*, 515.

[384] Q. P. Janssen, S. Buettner, M. Suker, B. R. Beumer, P. Addeo, P. Bachellier, N. Bahary, T. Bekaii-Saab, M. A. Bali, M. G. Besselink, B. A. Boone, I. Chau, S. Clarke, M. Dillhoff, B. F. El-Rayes, J. M. Frakes, D. Grose, P. J. Hosein, N. B. Jamieson, A. A. Javed, K. Khan, K.-P. Kim, S. C. Kim, S. S. Kim, A. H. Ko, J. Lacy, G. A. Margonis, M. D. McCarter, C. J. McKay, E. A. Mellon, S. Y. Moorcraft, K.-I. Okada, A. Paniccia, P. J. Parikh, N. A. Peters, H. Rabl, J. Samra, C. Tinchon, G. van Tienhoven, E. van Veldhuisen, A. Wang-Gillam, M. J. Weiss, J. W. Wilmink, H. Yamaue, M. Y. V. Homs, C. H. J. van Eijck, M. H. G. Katz, B. Groot Koerkamp, *JNCI: Journal of the National Cancer Institute* **2019**, *111*, 782.

[385] S. Park, S. C. Kim, S.-M. Hong, Y.-J. Lee, K.-M. Park, D. W. Hwang, J. H. Lee, K.-B. Song, B.-Y. Ryoo, H.-M. Jang, K.-P. Kim, C. Yu, E. K. Choi, S. D. Ahn, S.-W. Lee, S. M. Yoon, J.-H. Park, J. H. Kim, *AR* **2017**, *37*, 755.

[386] J. P. Neoptolemos, D. D. Stocken, C. Bassi, P. Ghaneh, D. Cunningham, D. Goldstein, R. Padbury, M. J. Moore, S. Gallinger, C. Mariette, M. N. Wente, J. R. Izbicki, H. Friess, M. M. Lerch, C. Dervenis, A. Oláh, G. Butturini, R. Doi, P. A. Lind, D. Smith, J. W. Valle, D. H. Palmer, J. A. Buckels, J. Thompson, C. J. McKay, C. L. Rawcliffe, M. W. Büchler, for the European Study Group for Pancreatic Cancer, *JAMA* **2010**, *304*, 1073.

[387] J. P. Neoptolemos, D. H. Palmer, P. Ghaneh, E. E. Psarelli, J. W. Valle, C. M. Halloran, O. Faluyi, D. A. O'Reilly, D. Cunningham, J. Wadsley, S. Darby, T. Meyer, R. Gillmore, A. Anthoney, P. Lind, B. Glimelius, S. Falk, J. R. Izbicki, G. W. Middleton, S. Cummins, P. J. Ross, H. Wasan, A. McDonald, T. Crosby, Y. T. Ma, K. Patel, D. Sherriff, R. Soomal, D. Borg, S. Sothi, P. Hammel, T. Hackert, R. Jackson, M. W. Büchler, *The Lancet* **2017**, *389*, 1011.

[388] A. A. Khorana, P. B. Mangu, J. Berlin, A. Engebretson, T. S. Hong, A. Maitra, S. G. Mohile, M. Mumber, R. Schulick, M. Shapiro, S. Urba, H. J. Zeh, M. H. G. Katz, *Journal of Clinical Oncology* **2017**, DOI 10.1200/JCO.2017.72.4948.

[389] "ISRCTN - ISRCTN89500674: ESPAC-5F: European Study group for Pancreatic Cancer - Trial 5F," DOI 10.1186/ISRCTN89500674can be found under https://www.isrctn.com/ISRCTN89500674, **n.d.**

[390] D. Sohal, S. L. McDonough, S. A. Ahmad, N. Gandhi, M. S. Beg, A. Wang-Gillam, K. Guthrie, A. M. Lowy, P. A. Philip, H. S. Hochster, *JCO* **2017**, *35*, TPS4152.

[391] K. J. Labori, K. Lassen, D. Hoem, J. E. Grønbech, J. A. Søreide, K. Mortensen, R. Smaaland, H. Sorbye, C. Verbeke, S. Dueland, *BMC Surgery* **2017**, *17*, 94.

[392] S. Heinrich, B. Pestalozzi, M. Lesurtel, F. Berrevoet, S. Laurent, J.-R. Delpero, J.-L. Raoul, P. Bachellier, P. Dufour, M. Moehler, A. Weber, H. Lang, X. Rogiers, P.-A. Clavien, *BMC Cancer* **2011**, *11*, 346.

[393] A. Oba, F. Ho, Q. R. Bao, M. H. Al-Musawi, R. D. Schulick, M. Del Chiaro, *Front Oncol* **2020**, *10*, 245.

[394] D. Barrak, A. M. Villano, N. Villafane-Ferriol, L. G. Stockton, M. V. Hill, M. Deng, E. A. Handorf, S. S. Reddy, *European Journal of Surgical Oncology* **2022**, DOI 10.1016/j.ejso.2021.12.473.

[395] E. Oneda, A. Zaniboni, *Journal of Clinical Medicine* **2019**, *8*, 1922.

[396] J. S. Peng, J. Wey, S. Chalikonda, D. S. Allende, R. M. Walsh, G. Morris-Stiff, *Hepatobiliary & Pancreatic Diseases International* **2019**, *18*, 373.

[397] N. H. Tran, V. Sahai, K. A. Griffith, H. Nathan, R. Kaza, K. C. Cuneo, J. Shi, E. Kim, C. J. Sonnenday, C. S. Cho, T. S. Lawrence, M. M. Zalupski, *International Journal of Radiation Oncology, Biology, Physics* **2020**, *106*, 124.

[398] J. Li, L. Li, L. Yang, J. Yuan, B. Lv, Y. Yao, S. Xing, *Oncotarget* **2016**, *7*, 44857.

[399] E. A. Collisson, P. Bailey, D. K. Chang, A. V. Biankin, *Nat Rev Gastroenterol Hepatol* **2019**, *16*, 207.

[400] R. Casolino, C. Braconi, G. Malleo, S. Paiella, C. Bassi, M. Milella, S. B. Dreyer, F. E. M. Froeling, D. K. Chang, A. V. Biankin, T. Golan, *Annals of Oncology* **2021**, *32*, 183.

[401] C. M. Kang, Y. E. Chung, J. Y. Park, J. S. Sung, H. K. Hwang, H. J. Choi, H. Kim, S. Y. Song, W. J. Lee, *J Gastrointest Surg* **2012**, *16*, 509.

[402] S. Satoi, H. Toyokawa, H. Yanagimoto, T. Yamamoto, M. Kamata, C. Ohe, N. Sakaida, Y. Uemura, H. Kitade, N. Tanigawa, K. Inoue, Y. Matsui, A.-H. Kwon, *J Gastrointest Surg* **2012**, *16*, 784.

[403] N. E. Lopez, C. Prendergast, A. M. Lowy, *World Journal of Gastroenterology* **2014**, *20*, 10740.

[404] E. Versteijne, M. Suker, K. Groothuis, J. M. Akkermans-Vogelaar, M. G. Besselink, B. A. Bonsing, J. Buijsen, O. R. Busch, G.-J. M. Creemers, R. M. van Dam, F. A. L. M. Eskens, S. Festen, J. W. B. de Groot, B. G. Koerkamp, I. H. de Hingh, M. Y. V. Homs, J. E. van Hooft, E. D. Kerver, S. A. C. Luelmo, K. J. Neelis, J. Nuyttens, G. M. R. M. Paardekooper, G. A. Patijn, M. J. C. van der Sangen, J. de Vos-Geelen, J. W. Wilmink, A. H. Zwinderman, C. J. Punt, C. H. van Eijck, G. van Tienhoven, for the D. P. C. Group, *Journal of Clinical Oncology* **2020**, DOI 10.1200/JCO.19.02274.

[405] O. Turrini, M. Ychou, L. Moureau-Zabotto, P. Rouanet, M. Giovannini, V. Moutardier, D. Azria, J.-R. Delpero, F. Viret, *European Journal of Surgical Oncology* **2010**, *36*, 987.

[406] E. J. Kim, E. Ben-Josef, J. M. Herman, T. Bekaii-Saab, L. A. Dawson, K. A. Griffith, I. R. Francis, J. K. Greenson, D. M. Simeone, T. S. Lawrence, D. Laheru, C. L. Wolfgang, T. Williams, M. Bloomston, M. J. Moore, A. Wei, M. M. Zalupski, *Cancer* **2013**, *119*, 2692.

[407] R. J. Vidri, A. O. Vogt, D. C. Macgillivray, I. J. Bristol, T. L. Fitzgerald, *Ann Surg Oncol* **2019**, *26*, 3701.

[408] S. Rudra, N. Jiang, S. A. Rosenberg, J. R. Olsen, M. C. Roach, L. Wan, L. Portelance, E. A. Mellon, A. Bruynzeel, F. Lagerwaard, M. F. Bassetti, P. J. Parikh, P. P. Lee, *Cancer Medicine* **2019**, *8*, 2123.

[409] W. A. Hall, K. A. Goodman, *Radiation Oncology* **2019**, *14*, 114.

[410] E. W. Lee, S. Thai, S. T. Kee, *Gut Liver* **2010**, *4 Suppl 1*, S99.

[411] M. Linecker, T. Pfammatter, P. Kambakamba, M. L. DeOliveira, *DSU* **2016**, *33*, 351.

[412] I. Frigerio, R. Girelli, A. Giardino, P. Regi, R. Salvia, C. Bassi, *J Hepatobiliary Pancreat Sci* **2013**, *20*, 574.

[413] M. P. Belfiore, F. M. Ronza, F. Romano, G. P. Ianniello, G. De Lucia, C. Gallo, C. Marsicano, T. L. Di Gennaro, G. Belfiore, *Int J Surg* **2015**, *21 Suppl 1*, S34.

[414] Y. Wu, Z. Tang, H. Fang, S. Gao, J. Chen, Y. Wang, H. Yan, *J Surg Oncol* **2006**, *94*, 392.

[415] R. Girelli, I. Frigerio, A. Giardino, P. Regi, S. Gobbo, G. Malleo, R. Salvia, C. Bassi, *Langenbecks Arch Surg* **2013**, *398*, 63.

[416] V. Granata, R. Grassi, R. Fusco, S. V. Setola, R. Palaia, A. Belli, V. Miele, L. Brunese, R. Grassi, A. Petrillo, F. Izzo, *Frontiers in Oncology* **2020**, *10*.

[417] V. Granata, R. Fusco, O. Catalano, S. V. Setola, E. de Lutio di Castelguidone, M. Piccirillo, R. Palaia, R. Grassi, F. Granata, F. Izzo, A. Petrillo, *Infect Agent Cancer* **2016**, *11*, 57.

[418] M. N. Yousaf, H. Ehsan, A. Muneeb, A. Wahab, M. K. Sana, K. Neupane, F. S. Chaudhary, *Frontiers in Medicine* **2021**, *7*.

[419] J. Jung, S. M. Yoon, J.-H. Park, D.-W. Seo, S. S. Lee, M.-H. Kim, S. K. Lee, D. H. Park, T. J. Song, B.-Y. Ryoo, H.-M. Chang, K.-P. Kim, C. Yoo, J. H. Jeong, S. C. Kim, D. W. Hwang, J. H. Lee, K. B. Song, Y. Y. Jo, J. Park, J. H. Kim, *PLoS One* **2019**, *14*, e0214970.

[420] K. Goyal, D. Einstein, R. A. Ibarra, M. Yao, C. Kunos, R. Ellis, J. Brindle, D. Singh, J. Hardacre, Y. Zhang, J. Fabians, G. Funkhouser, M. Machtay, J. R. Sanabria, *J Surg Res* **2012**, *174*, 319.

[421] Z. Izadifar, Z. Izadifar, D. Chapman, P. Babyn, *J Clin Med* **2020**, *9*, 460.

[422] T. Yamaguchi, S. Kitahara, K. Kusuda, J. Okamoto, Y. Horise, K. Masamune, Y. Muragaki, *Cancers (Basel)* **2021**, *13*, 6184.

[423] H.-Y. Ge, L.-Y. Miao, L.-L. Xiong, F. Yan, C.-S. Zheng, J.-R. Wang, J.-W. Jia, L.-G. Cui, W. Chen, *Ultrasound in Medicine & Biology* **2014**, *40*, 947.

[424] S. E. Jung, S. H. Cho, J. H. Jang, J.-Y. Han, *Abdom Imaging* **2011**, *36*, 185.

[425] Z. Ning, J. Xie, Q. Chen, C. Zhang, L. Xu, L. Song, Z. Meng, *OTT* **2019**, *12*, 1021.

[426] S. G. G. Testoni, A. J. Healey, C. F. Dietrich, P. G. Arcidiacono, *Endosc Ultrasound* **2020**, *9*, 83.

[427] C. Bastianpillai, N. Petrides, T. Shah, S. Guillaumier, H. U. Ahmed, M. Arya, *Tumor Biol.* **2015**, *36*, 9137.

[428] A. Mehta, R. Oklu, R. A. Sheth, *Gastroenterol Res Pract* **2016**, *2016*, 9251375.

[429] T. A. Ferguson, J. Choi, D. R. Green, *Immunological Reviews* **2011**, *241*, 77.

[430] K. F. Chu, D. E. Dupuy, *Nat Rev Cancer* **2014**, *14*, 199.

[431] A. Giardino, G. Innamorati, S. Ugel, O. Perbellini, R. Girelli, I. Frigerio, P. Regi, F. Scopelliti, G. Butturini, S. Paiella, M. Bacchion, C. Bassi, *Pancreatology* **2017**, *17*, 962.

[432] A. M. Fietta, M. Morosini, I. Passadore, A. Cascina, P. Draghi, R. Dore, S. Rossi, E. Pozzi, F. Meloni, *Hum Immunol* **2009**, *70*, 477.

[433] M. Widenmeyer, Y. Shebzukhov, S. P. Haen, D. Schmidt, S. Clasen, A. Boss, D. V. Kuprash, S. A. Nedospasov, A. Stenzl, H. Aebert, D. Wernet, S. Stevanović, P. L. Pereira, H.-G. Rammensee, C. Gouttefangeas, *Int. J. Cancer* **2011**, *128*, 2653.

[434] M. Ahmed, G. Kumar, M. Moussa, Y. Wang, N. Rozenblum, E. Galun, S. N. Goldberg, *Radiology* **2016**, *279*, 103.

[435] Q. Pan, C. Hu, Y. Fan, Y. Wang, R. Li, X. Hu, *J BUON* **2020**, *25*, 1643.

[436] M. Lin, X. Zhang, S. Liang, H. Luo, M. Alnaggar, A. Liu, Z. Yin, J. Chen, L. Niu, Y. Jiang, *Signal Transduct Target Ther* **2020**, *5*, 215.

[437] X.-M. Luo, L.-Z. Niu, J.-B. Chen, K.-C. Xu, *World J Gastroenterol* **2016**, *22*, 790.

[438] D. M. R. Meijerink, *Irreversible Electroporation and Nivolumab Combined With Intratumoral Administration of a Toll-like Receptor Ligand as a Means of in Vivo Vaccination for Oligometastatic Pancreatic Ductal Adenocarcinoma*, Clinicaltrials.Gov, **2020**.

[439] M. S. Baptista, J. Cadet, P. Di Mascio, A. A. Ghogare, A. Greer, M. R. Hamblin, C. Lorente, S. C. Nunez, M. S. Ribeiro, A. H. Thomas, M. Vignoni, T. M. Yoshimura, *Photochemistry and Photobiology* **2017**, *93*, 912.

[440] C. C. Winterbourn, *Nat Chem Biol* **2008**, *4*, 278.

[441] Y. Nosaka, A. Y. Nosaka, *Chem. Rev.* **2017**, *117*, 11302.

[442] D. Trachootham, J. Alexandre, P. Huang, *Nat Rev Drug Discov* **2009**, *8*, 579.

[443] K. Ishikawa, K. Takenaga, M. Akimoto, N. Koshikawa, A. Yamaguchi, H. Imanishi, K. Nakada, Y. Honma, J.-I. Hayashi, *Science* **2008**, DOI 10.1126/science.1156906.

[444] C. Gorrini, I. S. Harris, T. W. Mak, *Nat Rev Drug Discov* **2013**, *12*, 931.

[445] J. P. Celli, B. Q. Spring, I. Rizvi, C. L. Evans, K. S. Samkoe, S. Verma, B. W. Pogue, T. Hasan, *Chem. Rev.* **2010**, *110*, 2795.

[446] M. T. Huggett, M. Jermyn, A. Gillams, R. Illing, S. Mosse, M. Novelli, E. Kent, S. G. Bown, T. Hasan, B. W. Pogue, S. P. Pereira, *Br J Cancer* **2014**, *110*, 1698.

[447] J. M. DeWitt, K. Sandrasegaran, B. O'Neil, M. G. House, N. J. Zyromski, A. Sehdev, S. M. Perkins, J. Flynn, L. McCranor, S. Shahda, *Gastrointestinal Endoscopy* **2019**, *89*, 390.

[448] Y. Hanada, S. P. Pereira, B. Pogue, E. V. Maytin, T. Hasan, B. Linn, T. Mangels-Dick, K. K. Wang, *Gastrointestinal Endoscopy* **2021**, *94*, 179.

[449] C. McEwan, J. Owen, E. Stride, C. Fowley, H. Nesbitt, D. Cochrane, Constantin. C. Coussios, M. Borden, N. Nomikou, A. P. McHale, J. F. Callan, *Journal of Controlled Release* **2015**, *203*, 51.

[450] A. J. Sorrin, M. Kemal Ruhi, N. A. Ferlic, V. Karimnia, W. J. Polacheck, J. P. Celli, H.-C. Huang, I. Rizvi, *Photochem Photobiol* **2020**, *96*, 232.

[451] M. Broekgaarden, I. Rizvi, A.-L. Bulin, L. Petrovic, R. Goldschmidt, J. P. Celli, T. Hasan, *Oncotarget* **2018**, *9*, 13009.

[452] K. Wang, Y. Zhang, J. Wang, A. Yuan, M. Sun, J. Wu, Y. Hu, *Sci Rep* **2016**, *6*, 27421.

[453] H. Li, P. Wang, Y. Deng, M. Zeng, Y. Tang, W.-H. Zhu, Y. Cheng, *Biomaterials* **2017**, *139*, 30.

[454] K. C. Sadanala, P. K. Chaturvedi, Y. M. Seo, J. M. Kim, Y. S. Jo, Y. K. Lee, W. S. Ahn, *Anticancer Research* **2014**, *34*, 4657.

[455] D. Costley, C. Mc Ewan, C. Fowley, A. P. McHale, J. Atchison, N. Nomikou, J. F. Callan, *International Journal of Hyperthermia* **2015**, *31*, 107.

[456] S. Mitragotri, *Nat Rev Drug Discov* **2005**, *4*, 255.

[457] P. Tharkar, R. Varanasi, W. S. F. Wong, C. T. Jin, W. Chrzanowski, *Frontiers in Bioengineering and Biotechnology* **2019**, *7*.

[458] D. Li, Y. Yang, D. Li, J. Pan, C. Chu, G. Liu, *Small* **2021**, *17*, 2101976.

[459] X. Qian, Y. Zheng, Y. Chen, *Advanced Materials* **2016**, *28*, 8097.

[460] N. Tsolekile, S. Nelana, O. S. Oluwafemi, *Molecules* **2019**, *24*, 2669.

[461] X. Xue, A. Lindstrom, Y. Li, *Bioconjugate Chem.* **2019**, *30*, 1585.

[462] Y.-S. Kim, V. Rubio, J. Qi, R. Xia, Z.-Z. Shi, L. Peterson, C.-H. Tung, B. E. O'Neill, *J Control Release* **2011**, *156*, 315.

[463] R. Teranishi, T. Matsuda, E. Yuba, K. Kono, A. Harada, *Macromolecular Bioscience* **2019**, *19*, 1800365.

[464] Y. Li, Q. Zhou, Z. Deng, M. Pan, X. Liu, J. Wu, F. Yan, H. Zheng, *Sci Rep* **2016**, *6*, 25968.

[465] M. Xu, L. Zhou, L. Zheng, Q. Zhou, K. Liu, Y. Mao, S. Song, *Cancer Lett* **2021**, *497*, 229.

[466] X. Xing, S. Zhao, T. Xu, L. Huang, Y. Zhang, M. Lan, C. Lin, X. Zheng, P. Wang, *Coordination Chemistry Reviews* **2021**, *445*, 214087.

[467] D. G. You, V. G. Deepagan, W. Um, S. Jeon, S. Son, H. Chang, H. I. Yoon, Y. W. Cho, M. Swierczewska, S. Lee, M. G. Pomper, I. C. Kwon, K. Kim, J. H. Park, *Sci Rep* **2016**, *6*, 23200.

[468] G. Dimcevski, S. Kotopoulis, T. Bjånes, D. Hoem, J. Schjøtt, B. T. Gjertsen, M. Biermann, A. Molven, H. Sorbye, E. McCormack, M. Postema, O. H. Gilja, *J Control Release* **2016**, *243*, 172.

[469] Q. Zhang, C. Bao, X. Cai, L. Jin, L. Sun, Y. Lang, L. Li, *Cancer Science* **2018**, *109*, 1330.

[470] P. Huang, X. Qian, Y. Chen, L. Yu, H. Lin, L. Wang, Y. Zhu, J. Shi, *J. Am. Chem. Soc.* **2017**, *139*, 1275.

[471] P. Zhao, Y. Deng, G. Xiang, Y. Liu, *Int J Nanomedicine* **2021**, *16*, 4615.

[472] Y. J. Li, P. Huang, C. L. Jiang, D. X. Jia, X. X. Du, J. H. Zhou, Y. Han, H. Sui, X. L. Wei, L. Liu, H. H. Yuan, T. T. Zhang, W. J. Zhang, R. Xie, X. H. Lang, L. Y. Wang, T. Liu, Y. X. Bai, Y. Tian, *Ultrasound in Medicine & Biology* **2014**, *40*, 2671.

[473] M. Maeda, Y. Muragaki, J. Okamoto, S. Yoshizawa, N. Abe, H. Nakamoto, H. Ishii, K. Kawabata, S. Umemura, N. Nishiyama, K. Kataoka, H. Iseki, *Ultrasound Med Biol* **2017**, *43*, 2295.

[474] S. Tinkle, S. E. McNeil, S. Mühlebach, R. Bawa, G. Borchard, Y. (Chezy) Barenholz, L. Tamarkin, N. Desai, *Annals of the New York Academy of Sciences* **2014**, *1313*, 35.

[475] D. R. Boverhof, C. M. Bramante, J. H. Butala, S. F. Clancy, M. Lafranconi, J. West, S. C. Gordon, *Regulatory Toxicology and Pharmacology* **2015**, *73*, 137.

[476] K. H. Bae, H. J. Chung, T. G. Park, *Mol Cells* **2011**, *31*, 295.

[477] Z. Cheng, M. Li, R. Dey, Y. Chen, *Journal of Hematology & Oncology* **2021**, *14*, 85.

[478] A. Cafarelli, A. Marino, L. Vannozzi, J. Puigmartí-Luis, S. Pané, G. Ciofani, L. Ricotti, *ACS Nano* **2021**, *15*, 11066.

[479] P. Gao, Y. Chen, W. Pan, N. Li, Z. Liu, B. Tang, *Angew Chem Int Ed Engl* **2021**, *60*, 16763.

[480] C. Buzea, I. I. Pacheco, K. Robbie, *Biointerphases* **2007**, *2*, MR17.

[481] R. van der Meel, E. Sulheim, Y. Shi, F. Kiessling, W. J. M. Mulder, T. Lammers, *Nat. Nanotechnol.* **2019**, *14*, 1007.

[482] B. Xie, J. Wan, X. Chen, W. Han, H. Wang, *Mol Cancer Ther* **2020**, *19*, 822.

[483] Y. Wang, H. Xie, K. Ying, B. Xie, X. Chen, B. Yang, J. Jin, J. Wan, T. Li, W. Han, S. Fang, H. Wang, *Biomaterials* **2021**, *270*, 120705.

[484] S. Sindhwani, A. M. Syed, J. Ngai, B. R. Kingston, L. Maiorino, J. Rothschild, P. MacMillan, Y. Zhang, N. U. Rajesh, T. Hoang, J. L. Y. Wu, S. Wilhelm, A. Zilman, S. Gadde, A. Sulaiman, B. Ouyang, Z. Lin, L. Wang, M. Egeblad, W. C. W. Chan, *Nat. Mater.* **2020**, *19*, 566.

[485] E. Ruoslahti, S. N. Bhatia, M. J. Sailor, *Journal of Cell Biology* **2010**, *188*, 759.

[486] Y. Yao, Y. Zhou, L. Liu, Y. Xu, Q. Chen, Y. Wang, S. Wu, Y. Deng, J. Zhang, A. Shao, *Frontiers in Molecular Biosciences* **2020**, *7*.

[487] H. Wang, Z. Lu, L. Wang, T. Guo, J. Wu, J. Wan, L. Zhou, H. Li, Z. Li, D. Jiang, P. Song, H. Xie, L. Zhou, X. Xu, S. Zheng, *Cancer Res* **2017**, *77*, 6963.

[488] Z. Shi, Y. Zhou, T. Fan, Y. Lin, H. Zhang, L. Mei, *Smart Materials in Medicine* **2020**, *1*, 32.

[489] L. Sercombe, T. Veerati, F. Moheimani, S. Y. Wu, A. K. Sood, S. Hua, *Frontiers in Pharmacology* **2015**, *6*.

[490] O. Veiseh, J. W. Gunn, M. Zhang, *Advanced Drug Delivery Reviews* **2010**, *62*, 284.

[491] M. J. Mitchell, M. M. Billingsley, R. M. Haley, M. E. Wechsler, N. A. Peppas, R. Langer, *Nat Rev Drug Discov* **2021**, *20*, 101.

[492] S. Tenzer, D. Docter, J. Kuharev, A. Musyanovych, V. Fetz, R. Hecht, F. Schlenk, D. Fischer, K. Kiouptsi, C. Reinhardt, K. Landfester, H. Schild, M. Maskos, S. K. Knauer, R. H. Stauber, *Nature Nanotech* **2013**, *8*, 772.

[493] E. Papini, R. Tavano, F. Mancin, *Frontiers in Immunology* **2020**, *11*.

[494] S. Gavas, S. Quazi, T. Karpiński, **2021**, DOI 10.20944/preprints202108.0218.v1.

[495] N. Shreyash, M. Sonker, S. Bajpai, S. K. Tiwary, *ACS Appl. Bio Mater.* **2021**, *4*, 2307.

[496] A. Alhussan, K. Bromma, E. P. D. Bozdoğan, A. Metcalfe, J. Karasinska, W. Beckham, A. S. Alexander, D. J. Renouf, D. F. Schaeffer, D. B. Chithrani, *Curr Oncol* **2021**, *28*, 1962.

[497] T. T. Hoang Thi, E. H. Pilkington, D. H. Nguyen, J. S. Lee, K. D. Park, N. P. Truong, *Polymers (Basel)* **2020**, *12*, E298.

[498] S. Schöttler, G. Becker, S. Winzen, T. Steinbach, K. Mohr, K. Landfester, V. Mailänder, F. R. Wurm, *Nature Nanotech* **2016**, *11*, 372.

[499] C.-M. J. Hu, L. Zhang, S. Aryal, C. Cheung, R. H. Fang, L. Zhang, *Proceedings of the National Academy of Sciences* **2011**, *108*, 10980.

[500] Z. Chen, P. Zhao, Z. Luo, M. Zheng, H. Tian, P. Gong, G. Gao, H. Pan, L. Liu, A. Ma, H. Cui, Y. Ma, L. Cai, *ACS Nano* **2016**, *10*, 10049.

[501] D. Kalyane, N. Raval, R. Maheshwari, V. Tambe, K. Kalia, R. K. Tekade, *Materials Science and Engineering: C* **2019**, *98*, 1252.

[502] K. N. Sugahara, T. Teesalu, P. P. Karmali, V. R. Kotamraju, L. Agemy, O. M. Girard, D. Hanahan, R. F. Mattrey, E. Ruoslahti, *Cancer Cell* **2009**, *16*, 510.

[503] X. Liu, J. Jiang, H. Meng, *Theranostics* **2019**, *9*, 8018.

[504] X. Liu, P. Lin, I. Perrett, J. Lin, Y.-P. Liao, C. H. Chang, J. Jiang, N. Wu, T. Donahue, Z. Wainberg, A. E. Nel, H. Meng, *Journal of Clinical Investigation* **2017**, *127*, 2007.

[505] Q. Sun, T. Ojha, F. Kiessling, T. Lammers, Y. Shi, *Biomacromolecules* **2017**, *18*, 1449.

[506] J. Ye, E. Liu, Z. Yu, X. Pei, S. Chen, P. Zhang, M.-C. Shin, J. Gong, H. He, V. C. Yang, *Int J Mol Sci* **2016**, *17*, E1892.

[507] T. Lu, J. Prakash, *Int J Nanomedicine* **2021**, *16*, 6313.

[508] D. Caputo, D. Pozzi, T. Farolfi, R. Passa, R. Coppola, G. Caracciolo, *World J Gastrointest Oncol* **2021**, *13*, 231.

[509] J. F. Finks, N. H. Osborne, J. D. Birkmeyer, *N Engl J Med* **2011**, *364*, 2128.

[510] J. E. Murphy, J. Y. Wo, D. P. Ryan, J. W. Clark, W. Jiang, B. Y. Yeap, L. C. Drapek, L. Ly, C. V. Baglini, L. S. Blaszkowsky, C. R. Ferrone, A. R. Parikh, C. D. Weekes, R. D. Nipp, E. L. Kwak, J. N. Allen, R. B. Corcoran, D. T. Ting, J. E. Faris, A. X. Zhu, L. Goyal, D. L. Berger, M. Qadan, K. D. Lillemoe, N. Talele, R. K. Jain, T. F. DeLaney, D. G. Duda, Y. Boucher, C. Fernández-Del Castillo, T. S. Hong, *JAMA Oncology* **2019**, *5*, 1020.

[511] A. L. Vahrmeijer, M. Hutteman, J. R. van der Vorst, C. J. H. van de Velde, J. V. Frangioni, *Nat Rev Clin Oncol* **2013**, *10*, 507.

[512] B. Qi, A. J. Crawford, N. E. Wojtynek, M. B. Holmes, J. J. Souchek, G. Almeida-Porada, Q. P. Ly, S. M. Cohen, M. A. Hollingsworth, A. M. Mohs, *Nanomedicine: Nanotechnology, Biology and Medicine* **2018**, *14*, 769.

[513] C. E. S. Hoogstins, L. S. F. Boogerd, B. G. Sibinga Mulder, J. S. D. Mieog, R. J. Swijnenburg, C. J. H. van de Velde, A. Farina Sarasqueta, B. A. Bonsing, B. Framery, A. Pèlegrin, M. Gutowski, F. Cailler, J. Burggraaf, A. L. Vahrmeijer, *Ann Surg Oncol* **2018**, *25*, 3350.

[514] W. S. Tummers, S. E. Miller, N. T. Teraphongphom, A. Gomez, I. Steinberg, D. M. Huland, S. Hong, S.-R. Kothapalli, A. Hasan, R. Ertsey, B. A. Bonsing, A. L. Vahrmeijer, R.-J. Swijnenburg, T. A. Longacre, G. A. Fisher, S. S. Gambhir, G. A. Poultsides, E. L. Rosenthal, *Ann Surg Oncol* **2018**, *25*, 1880.

[515] I. Rosenberger, A. Strauss, S. Dobiasch, C. Weis, S. Szanyi, L. Gil-Iceta, E. Alonso, M. González Esparza, V. Gómez-Vallejo, B. Szczupak, S. Plaza-García, S. Mirzaei, L. L. Israel, S. Bianchessi, E. Scanziani, J.-P. Lellouche, P. Knoll, J. Werner, K. Felix, L. Grenacher, T. Reese, J. Kreuter, M. Jiménez-González, *Journal of Controlled Release* **2015**, *214*, 76.

[516] H. J. M. Handgraaf, M. C. Boonstra, A. R. Van Erkel, B. A. Bonsing, H. Putter, C. J. H. Van De Velde, A. L. Vahrmeijer, J. S. D. Mieog, *BioMed Research International* **2014**, *2014*, e890230.

[517] L. Zhu, C. Staley, D. Kooby, B. El-Rays, H. Mao, L. Yang, *Cancer Letters* **2017**, *388*, 139.

[518] C. W. Kuo, D.-Y. Chueh, P. Chen, *Journal of Nanobiotechnology* **2019**, *17*, 26.

[519] D. G. Haller, *International Journal of Radiation Oncology*Biology*Physics* **2003**, *56*, 16.

[520] A. Wang-Gillam, R. A. Hubner, J. T. Siveke, D. D. Von Hoff, B. Belanger, F. A. de Jong, B. Mirakhur, L.-T. Chen, *European Journal of Cancer* **2019**, *108*, 78.

[521] A. Oluwasanmi, W. Al-Shakarchi, A. Manzur, M. H. Aldebasi, R. S. Elsini, M. K. Albusair, K. J. Haxton, A. D. M. Curtis, C. Hoskins, *Journal of Controlled Release* **2017**, *266*, 355.

[522] P. Ray, M. Confeld, P. Borowicz, T. Wang, S. Mallik, M. Quadir, *Colloids and Surfaces B: Biointerfaces* **2019**, *174*, 126.

[523] H. Zhou, W. Qian, F. M. Uckun, L. Wang, Y. A. Wang, H. Chen, D. Kooby, Q. Yu, M. Lipowska, C. A. Staley, H. Mao, L. Yang, *ACS Nano* **2015**, *9*, 7976.

[524] K. Samanta, S. Setua, S. Kumari, M. Jaggi, M. M. Yallapu, S. C. Chauhan, *Pharmaceutics* **2019**, *11*, 574.

[525] X. Pu, G. Ding, M. Wu, S. Zhou, S. Jia, L. Cao, *Oncology Letters* **2020**, *19*, 2062.

[526] M. S. Wason, J. Colon, S. Das, S. Seal, J. Turkson, J. Zhao, C. H. Baker, *Nanomedicine: Nanotechnology, Biology and Medicine* **2013**, *9*, 558.

[527] A. Yoshida, Y. Kitayama, K. Kiguchi, T. Yamada, H. Akasaka, R. Sasaki, T. Takeuchi, *ACS Appl. Bio Mater.* **2019**, *2*, 1177.

[528] M. Nakayama, R. Sasaki, C. Ogino, T. Tanaka, K. Morita, M. Umetsu, S. Ohara, Z. Tan, Y. Nishimura, H. Akasaka, K. Sato, C. Numako, S. Takami, A. Kondo, *Radiat Oncol* **2016**, *11*, 91.

[529] Y. Chen, P. Gao, T. Wu, W. Pan, N. Li, B. Tang, *Chem. Commun.* **2020**, *56*, 10621.

[530] X. Zhao, F. Li, Y. Li, H. Wang, H. Ren, J. Chen, G. Nie, J. Hao, *Biomaterials* **2015**, *46*, 13.

[531] H. Gibori, S. Eliyahu, A. Krivitsky, D. Ben-Shushan, Y. Epshtein, G. Tiram, R. Blau, P. Ofek, J. S. Lee, E. Ruppin, L. Landsman, I. Barshack, T. Golan, E. Merquiol, G. Blum, R. Satchi-Fainaro, *Nat Commun* **2018**, *9*, 16.

[532] X. Han, Y. Li, Y. Xu, X. Zhao, Y. Zhang, X. Yang, Y. Wang, R. Zhao, G. J. Anderson, Y. Zhao, G. Nie, *Nat Commun* **2018**, *9*, 3390.

[533] W. Chen, Y. Zhou, X. Zhi, T. Ma, H. Liu, B. W. Chen, X. Zheng, S. Xie, B. Zhao, X. Feng, X. Dang, T. Liang, *Biomaterials* **2019**, *192*, 590.

[534] P. Yang, D. Li, S. Jin, J. Ding, J. Guo, W. Shi, C. Wang, *Biomaterials* **2014**, *35*, 2079.

[535] T. Anajafi, M. D. Scott, S. You, X. Yang, Y. Choi, S. Y. Qian, S. Mallik, *Bioconjugate Chem.* **2016**, *27*, 762.

[536] F. Susa, T. Limongi, B. Dumontel, V. Vighetto, V. Cauda, *Cancers* **2019**, *11*, 1979.

[537] W. Zhou, Y. Zhou, X. Chen, T. Ning, H. Chen, Q. Guo, Y. Zhang, P. Liu, Y. Zhang, C. Li, Y. Chu, T. Sun, C. Jiang, *Biomaterials* **2021**, *268*, 120546.

[538] Y. Choi, U. Park, H.-J. Koo, J.-S. Park, D. H. Lee, K. Kim, J. Choi, *Biosens Bioelectron* **2021**, *177*, 112980.

[539] H. Qi, C. Liu, L. Long, Y. Ren, S. Zhang, X. Chang, X. Qian, H. Jia, J. Zhao, J. Sun, X. Hou, X. Yuan, C. Kang, *ACS Nano* **2016**, *10*, 3323.

[540] Y. Liu, L. Bai, K. Guo, Y. Jia, K. Zhang, Q. Liu, P. Wang, X. Wang, *Theranostics* **2019**, *9*, 5261.

[541] C. S. Mundry, K. C. Eberle, P. K. Singh, M. A. Hollingsworth, K. Mehla, *Biochimica et Biophysica Acta (BBA) - Reviews on Cancer* **2020**, *1874*, 188387.

[542] Y. Ino, R. Yamazaki-Itoh, K. Shimada, M. Iwasaki, T. Kosuge, Y. Kanai, N. Hiraoka, *Br J Cancer* **2013**, *108*, 914.

[543] M. E. Lorkowski, P. U. Atukorale, P. A. Bielecki, K. H. Tong, G. Covarrubias, Y. Zhang, G. Loutrianakis, T. J. Moon, A. R. Santulli, W. M. Becicka, E. Karathanasis, *Journal of Controlled Release* **2021**, *330*, 1095.

[544] X. Zhao, K. Yang, R. Zhao, T. Ji, X. Wang, X. Yang, Y. Zhang, K. Cheng, S. Liu, J. Hao, H. Ren, K. W. Leong, G. Nie, *Biomaterials* **2016**, *102*, 187.

[545] J. Lu, X. Liu, Y.-P. Liao, F. Salazar, B. Sun, W. Jiang, C. H. Chang, J. Jiang, X. Wang, A. M. Wu, H. Meng, A. E. Nel, *Nat Commun* **2017**, *8*, 1811.

[546] L. Shen, J. Li, Q. Liu, W. Song, X. Zhang, K. Tiruthani, H. Hu, M. Das, T. J. Goodwin, R. Liu, L. Huang, *ACS Nano* **2018**, *12*, 9830.

[547] Y. Xie, Y. Hang, Y. Wang, R. Sleightholm, D. R. Prajapati, J. Bader, A. Yu, W. Tang, L. Jaramillo, J. Li, R. K. Singh, D. Oupický, *ACS Nano* **2020**, *14*, 255.

[548] M. Li, M. Li, Y. Yang, Y. Liu, H. Xie, Q. Yu, L. Tian, X. Tang, K. Ren, J. Li, Z. Zhang, Q. He, *Journal of Controlled Release* **2020**, *321*, 23.

[549] Z. Lu, Y. Long, Y. Wang, X. Wang, C. Xia, M. Li, Z. Zhang, Q. He, *European Journal of Pharmaceutics and Biopharmaceutics* **2021**, *165*, 164.

[550] E. S. Glazer, C. Zhu, K. L. Massey, C. S. Thompson, W. D. Kaluarachchi, A. N. Hamir, S. A. Curley, *Clinical Cancer Research* **2010**, *16*, 5712.

[551] L. R. Jaidev, D. R. Chellappan, D. V. Bhavsar, R. Ranganathan, B. Sivanantham, A. Subramanian, U. Sharma, N. R. Jagannathan, U. M. Krishnan, S. Sethuraman, *Acta Biomaterialia* **2017**, *49*, 422.

[552] F. Brero, M. Albino, A. Antoccia, P. Arosio, M. Avolio, F. Berardinelli, D. Bettega, P. Calzolari, M. Ciocca, M. Corti, A. Facoetti, S. Gallo, F. Groppi, A. Guerrini, C. Innocenti, C. Lenardi, S. Locarno, S. Manenti, R. Marchesini, M. Mariani, F. Orsini, E. Pignoli, C. Sangregorio, I. Veronese, A. Lascialfari, *Nanomaterials* **2020**, *10*, 1919.

[553] Y. Luo, Y. Li, J. Li, C. Fu, X. Yu, L. Wu, *RSC Adv.* **2019**, *9*, 10486.

[554] Y. J. Roh, J. H. Kim, I.-W. Kim, K. Na, J. M. Park, M.-G. Choi, *Mol Cancer Ther* **2017**, *16*, 1487.

[555] S. Kirar, D. Chaudhari, N. S. Thakur, S. Jain, J. Bhaumik, J. K. Laha, U. C. Banerjee, *Journal of Photochemistry and Photobiology B: Biology* **2021**, *220*, 112209.

[556] H. Yang, R. Liu, Y. Xu, L. Qian, Z. Dai, *Nano-Micro Lett.* **2021**, *13*, 35.

[557] L. Huang, J. Wan, H. Wu, X. Chen, Q. Bian, L. Shi, X. Jiang, A. Yuan, J. Gao, H. Wang, *Nano Today* **2021**, *36*, 101030.

[558] S. Kang, Y.-G. Gil, D.-H. Min, H. Jang, *ACS Nano* **2020**, *14*, 4383.

[559] L. B. Silva, K. A. D. F. Castro, C. E. A. Botteon, C. L. P. Oliveira, R. S. da Silva, P. D. Marcato, *Front Bioeng Biotechnol* **2021**, *9*, 679128.

[560] C. Dong, H. Hu, L. Sun, Y. Chen, *Biomed. Mater.* **2021**, *16*, 032006.

[561] V. G. Deepagan, D. G. You, W. Um, H. Ko, S. Kwon, K. Y. Choi, G.-R. Yi, J. Y. Lee, D. S. Lee, K. Kim, I. C. Kwon, J. H. Park, *Nano Lett.* **2016**, *16*, 6257.

[562] L. Yu, P. Hu, Y. Chen, *Advanced Materials* **2018**, *30*, 1801964.

[563] M. D. Girgis, N. Federman, M. M. Rochefort, K. E. McCabe, A. M. Wu, J. O. Nagy, C. Denny, J. S. Tomlinson, *J Surg Res* **2013**, *185*, 45.

[564] H. Meng, M. Wang, H. Liu, X. Liu, A. Situ, B. Wu, Z. Ji, C. H. Chang, A. E. Nel, *ACS Nano* **2015**, *9*, 3540.

[565] X. Liu, A. Situ, Y. Kang, K. R. Villabroza, Y. Liao, C. H. Chang, T. Donahue, A. E. Nel, H. Meng, *ACS Nano* **2016**, *10*, 2702.

[566] S. Trabulo, A. Aires, A. Aicher, C. Heeschen, A. L. Cortajarena, *Biochimica et Biophysica Acta (BBA) - General Subjects* **2017**, *1861*, 1597.

[567] Y. T. Tam, C. Huang, M. Poellmann, G. S. Kwon, *ACS Nano* **2018**, *12*, 7406.

[568] L. Wu, F. Zhang, X. Chen, J. Wan, Y. Wang, T. Li, H. Wang, *ACS Appl. Mater. Interfaces* **2020**, *12*, 3327.

[569] M. Das, J. Li, M. Bao, L. Huang, *AAPS J* **2020**, *22*, 88.

[570] X. Chen, W. Zhou, C. Liang, S. Shi, X. Yu, Q. Chen, T. Sun, Y. Lu, Y. Zhang, Q. Guo, C. Li, Y. Zhang, C. Jiang, *Nano Lett.* **2019**, *19*, 3527.

[571] H. Han, D. Valdepérez, Q. Jin, B. Yang, Z. Li, Y. Wu, B. Pelaz, W. J. Parak, J. Ji, *ACS Nano* **2017**, *11*, 1281.

[572] M. Uz, M. Kalaga, R. Pothuraju, J. Ju, W. M. Junker, S. K. Batra, S. Mallapragada, S. Rachagani, *Journal of Controlled Release* **2019**, *294*, 237.

[573] S. Khan, S. Setua, S. Kumari, N. Dan, A. Massey, B. B. Hafeez, M. M. Yallapu, Z. E. Stiles, A. Alabkaa, J. Yue, A. Ganju, S. Behrman, M. Jaggi, S. C. Chauhan, *Biomaterials* **2019**, *208*, 83.

[574] C. K. Elechalawar, M. N. Hossen, P. Shankarappa, C. J. Peer, W. D. Figg, J. D. Robertson, R. Bhattacharya, P. Mukherjee, *IJN* **2020**, *Volume 15*, 991.

[575] Z. Kuncic, S. Lacombe, *Phys. Med. Biol.* **2018**, *63*, 02TR01.

[576] J. Zhao, H. Wang, C.-H. Hsiao, D. S.-L. Chow, E. J. Koay, Y. Kang, X. Wen, Q. Huang, Y. Ma, J. A. Bankson, S. E. Ullrich, W. Overwijk, A. Maitra, D. Piwnica-Worms, J. B. Fleming, C. Li, *Biomaterials* **2018**, *159*, 215.

[577] H. Meng, Y. Zhao, J. Dong, M. Xue, Y.-S. Lin, Z. Ji, W. X. Mai, H. Zhang, C. H. Chang, C. J. Brinker, J. I. Zink, A. E. Nel, *ACS Nano* **2013**, *7*, 10048.

[578] J. Norton, D. Foster, M. Chinta, A. Titan, M. Longaker, *Cancers (Basel)* **2020**, *12*, 1347.

[579] F. Mpekris, P. Papageorgis, C. Polydorou, C. Voutouri, M. Kalli, A. P. Pirentis, T. Stylianopoulos, *Journal of Controlled Release* **2017**, *261*, 105.

[580] D. Goehrig, J. Nigri, R. Samain, Z. Wu, P. Cappello, G. Gabiane, X. Zhang, Y. Zhao, I.-S. Kim, M. Chanal, R. Curto, V. Hervieu, C. de L. Fouchardière, F. Novelli, P. Milani, R. Tomasini, C. Bousquet, P. Bertolino, A. Hennino, *Gut* **2019**, *68*, 693.

[581] J. Zhao, Z. Xiao, T. Li, H. Chen, Y. Yuan, Y. A. Wang, C.-H. Hsiao, D. S.-L. Chow, W. W. Overwijk, C. Li, *ACS Nano* **2018**, *12*, 9881.

[582] U. Vaish, T. Jain, A. C. Are, V. Dudeja, *Int J Mol Sci* **2021**, *22*, 13408.

[583] J. Vaz, D. Ansari, A. Sasor, R. Andersson, *Pancreas* **2015**, *44*, 1024.

[584] Z. V. Diaz-Riascos, M. M. Ginesta, J. Fabregat, T. Serrano, J. Busquets, L. Buscail, P. Cordelier, G. Capellá, *Molecular Therapy - Nucleic Acids* **2019**, *17*, 491.

[585] J. Schnittert, P. R. Kuninty, T. F. Bystry, R. Brock, G. Storm, J. Prakash, *Nanomedicine* **2017**, *12*, 1369.

[586] H. Y. Tanaka, M. R. Kano, *Cancer Science* **2018**, *109*, 2085.

[587] S. A. El-Zahaby, Y. S. R. Elnaggar, O. Y. Abdallah, *Journal of Controlled Release* **2019**, *293*, 21.

[588] X. Chen, F. Jia, Y. Li, Y. Deng, Y. Huang, W. Liu, Q. Jin, J. Ji, *Biomaterials* **2020**, *246*, 119999.

[589] S. Matsumoto, K. Nakata, A. Sagara, W. Guan, N. Ikenaga, K. Ohuchida, M. Nakamura, *Oncology Letters* **2021**, *22*, 1.

[590] Y. T. Sato, K. Umezaki, S. Sawada, S. Mukai, Y. Sasaki, N. Harada, H. Shiku, K. Akiyoshi, *Sci Rep* **2016**, *6*, 21933.

[591] M.-J. Su, H. Aldawsari, M. Amiji, *Sci Rep* **2016**, *6*, 30110.

[592] B. Dumontel, F. Susa, T. Limongi, M. Canta, L. Racca, A. Chiodoni, N. Garino, G. Chiabotto, M. L. Centomo, Y. Pignochino, V. Cauda, *Nanomedicine* **2019**, *14*, 2815.

[593] A. Ancona, B. Dumontel, N. Garino, B. Demarco, D. Chatzitheodoridou, W. Fazzini, H. Engelke, V. Cauda, *Nanomaterials (Basel)* **2018**, *8*, E143.

[594] S. Tangutoori, B. Q. Spring, Z. Mai, A. Palanisami, L. B. Mensah, T. Hasan, *Nanomedicine* **2016**, *12*, 223.

[595] B. Q. Spring, R. Bryan Sears, L. Z. Zheng, Z. Mai, R. Watanabe, M. E. Sherwood, D. A. Schoenfeld, B. W. Pogue, S. P. Pereira, E. Villa, T. Hasan, *Nature Nanotech* **2016**, *11*, 378.

[596] T. Zhang, Z. Jiang, L. Chen, C. Pan, S. Sun, C. Liu, Z. Li, W. Ren, A. Wu, P. Huang, *Nano Res.* **2020**, *13*, 273.

[597] Z. Wang, X. Gong, J. Li, H. Wang, X. Xu, Y. Li, X. Sha, Z. Zhang, *ACS Nano* **2021**, *15*, 5405.

[598] A. Harada, M. Ono, E. Yuba, K. Kono, *Biomater. Sci.* **2012**, *1*, 65.

[599] X. Han, J. Huang, X. Jing, D. Yang, H. Lin, Z. Wang, P. Li, Y. Chen, *ACS Nano* **2018**, *12*, 4545.

[600] A. P. Sviridov, V. G. Andreev, E. M. Ivanova, L. A. Osminkina, K. P. Tamarov, V. Yu. Timoshenko, *Appl. Phys. Lett.* **2013**, *103*, 193110.

[601] L. A. Osminkina, V. A. Sivakov, G. A. Mysov, V. A. Georgobiani, U. A. Natashina, F. Talkenberg, V. V. Solovyev, A. A. Kudryavtsev, V. Y. Timoshenko, *Nanoscale Research Letters* **2014**, *9*, 463.

[602] N. Yumita, Y. Iwase, T. Imaizumi, A. Sakurazawa, Y. Kaya, K. Nishi, T. Ikeda, S.-I. Umemura, F.-S. Chen, Y. Momose, *Anticancer Research* **2013**, *33*, 3145.

[603] Y.-W. Chen, T.-Y. Liu, P.-H. Chang, P.-H. Hsu, H.-L. Liu, H.-C. Lin, S.-Y. Chen, *Nanoscale* **2016**, *8*, 12648.

[604] A. Sazgarnia, A. Shanei, N. T. Meibodi, H. Eshghi, H. Nassirli, *J Ultrasound Med* **2011**, *30*, 1321.

[605] A. Ma, H. Ran, J. Wang, R. Ding, C. Lu, L. Liu, Y. Luo, H. Chen, T. Yin, *Nanomaterials* **2022**, *12*, 209.

[606] V. Vighetto, A. Ancona, L. Racca, T. Limongi, A. Troia, G. Canavese, V. Cauda, *Frontiers in Bioengineering and Biotechnology* **2019**, *7*.

[607] A. Ancona, A. Troia, N. Garino, B. Dumontel, V. Cauda, G. Canavese, *Ultrasonics Sonochemistry* **2020**, *67*, 105132.

[608] J. C. Matos, M. Laurenti, V. Vighetto, L. C. J. Pereira, J. C. Waerenborgh, M. C. Gonçalves, V. Cauda, *Applied Sciences* **2020**, *10*, 8479.

[609] M. Carofiglio, M. Laurenti, V. Vighetto, L. Racca, S. Barui, N. Garino, R. Gerbaldo, F. Laviano, V. Cauda, *Nanomaterials* **2021**, *11*, 2628.

[610] L. Racca, T. Limongi, V. Vighetto, B. Dumontel, A. Ancona, M. Canta, G. Canavese, N. Garino, V. Cauda, *Frontiers in Bioengineering and Biotechnology* **2020**, *8*.

[611] V. Vighetto, L. Racca, M. Canta, J. C. Matos, B. Dumontel, M. C. Gonçalves, V. Cauda, *Pharmaceutics* **2021**, *13*, 1423.

[612] K. Zhang, H. Xu, H. Chen, X. Jia, S. Zheng, X. Cai, R. Wang, J. Mou, Y. Zheng, J. Shi, *Theranostics* **2015**, *5*, 1291.

[613] C. McEwan, C. Fowley, N. Nomikou, B. McCaughan, A. P. McHale, J. F. Callan, *Langmuir* **2014**, *30*, 14926.

[614] C. McEwan, S. Kamila, J. Owen, H. Nesbitt, B. Callan, M. Borden, N. Nomikou, R. A. Hamoudi, M. A. Taylor, E. Stride, A. P. McHale, J. F. Callan, *Biomaterials* **2016**, *80*, 20.

[615] Y. Sheng, E. Beguin, H. Nesbitt, S. Kamila, J. Owen, L. C. Barnsley, B. Callan, C. O'Kane, N. Nomikou, R. Hamoudi, M. A. Taylor, M. Love, P. Kelly, D. O'Rourke, E. Stride, A. P. McHale, J. F. Callan, *Journal of Controlled Release* **2017**, *262*, 192.

[616] H. Nesbitt, Y. Sheng, S. Kamila, K. Logan, K. Thomas, B. Callan, M. A. Taylor, M. Love, D. O'Rourke, P. Kelly, E. Beguin, E. Stride, A. P. McHale, J. F. Callan, *Journal of Controlled Release* **2018**, *279*, 8.

[617] J. Chen, H. Luo, Y. Liu, W. Zhang, H. Li, T. Luo, K. Zhang, Y. Zhao, J. Liu, *ACS Nano* **2017**, *11*, 12849.

[618] D.-B. Cheng, X.-H. Zhang, Y. Chen, H. Chen, Z.-Y. Qiao, H. Wang, *iScience* **2020**, *23*, 101144.

[619] P. Nasirmoghadas, A. Mousakhani, F. Behzad, N. Beheshtkhoo, A. Hassanzadeh, M. Nikoo, M. Mehrabi, M. A. J. Kouhbanani, *Biotechnology Progress* **2021**, *37*, e3070.

[620] Y. Li, X. Zhang, X. Liu, W. Pan, N. Li, B. Tang, *Chem. Sci.* **2021**, *12*, 3130.

[621] F. E. F. Timmer, B. Geboers, S. Nieuwenhuizen, E. A. C. Schouten, M. Dijkstra, J. J. J. de Vries, M. P. van den Tol, T. D. de Gruijl, H. J. Scheffer, M. R. Meijerink, *Curr Oncol Rep* **2021**, *23*, 68.

[622] J. Zhao, X. Wen, L. Tian, T. Li, C. Xu, X. Wen, M. P. Melancon, S. Gupta, B. Shen, W. Peng, C. Li, *Nat Commun* **2019**, *10*, 899.

[623] J. S. S. Narayanan, P. Ray, T. Hayashi, T. C. Whisenant, D. Vicente, D. A. Carson, A. M. Miller, S. P. Schoenberger, R. R. White, *Cancer Immunol Res* **2019**, *7*, 1714.

[624] J. W. Kleinovink, P. B. van Driel, T. J. Snoeks, N. Prokopi, M. F. Fransen, L. J. Cruz, L. Mezzanotte, A. Chan, C. W. Löwik, F. Ossendorp, *Clinical Cancer Research* **2016**, *22*, 1459.

[625] A. P. Castano, P. Mroz, M. R. Hamblin, *Nat Rev Cancer* **2006**, *6*, 535.

[626] Y. Zheng, G. Yin, V. Le, A. Zhang, S. Chen, X. Liang, J. Liu, *Int J Biol Sci* **2016**, *12*, 120.

[627] F. Sun, Q. Zhu, T. Li, M. Saeed, Z. Xu, F. Zhong, R. Song, M. Huai, M. Zheng, C. Xie, L. Xu, H. Yu, *Advanced Science* **2021**, *8*, 2002746.

[628] X. Wang, W. Zhang, Z. Xu, Y. Luo, D. Mitchell, R. W. Moss, *Integr Cancer Ther* **2009**, *8*, 283.

[629] X. Lin, R. Huang, Y. Huang, K. Wang, H. Li, Y. Bao, C. Wu, Y. Zhang, X. Tian, X. Wang, *Int J Nanomedicine* **2021**, *16*, 1889.

[630] H. Nesbitt, K. Logan, K. Thomas, B. Callan, J. Gao, T. McKaig, M. Taylor, M. Love, E. Stride, A. P. McHale, J. F. Callan, *Cancer Lett* **2021**, *517*, 88.

[631] T. R. Abreu, N. A. Fonseca, N. Gonçalves, J. N. Moreira, *Journal of Controlled Release* **2020**, *319*, 246.

[632] X. Ma, P. Shou, C. Smith, Y. Chen, H. Du, C. Sun, N. Porterfield Kren, D. Michaud, S. Ahn, B. Vincent, B. Savoldo, Y. Pylayeva-Gupta, S. Zhang, G. Dotti, Y. Xu, *Nat Biotechnol* **2020**, *38*, 448.

[633] K. Watanabe, Y. Luo, T. Da, S. Guedan, M. Ruella, J. Scholler, B. Keith, R. M. Young, B. Engels, S. Sorsa, M. Siurala, R. Havunen, S. Tähtinen, A. Hemminki, C. H. June, *JCI Insight* **2018**, *3*, DOI 10.1172/jci.insight.99573.

[634] D. Yeo, C. Giardina, P. Saxena, J. E. J. Rasko, *Mol Ther Oncolytics* **2022**, *24*, 561.

[635] F. Zhang, S. B. Stephan, C. I. Ene, T. T. Smith, E. C. Holland, M. T. Stephan, *Cancer Research* **2018**, *78*, 3718.

[636] Q. Chen, Q. Hu, E. Dukhovlinova, G. Chen, S. Ahn, C. Wang, E. A. Ogunnaike, F. S. Ligler, G. Dotti, Z. Gu, *Advanced Materials* **2019**, *31*, 1900192.

[637] Q. Yu, X. Tang, W. Zhao, Y. Qiu, J. He, D. Wan, J. Li, X. Wang, X. He, Y. Liu, M. Li, Z. Zhang, Q. He, *Acta Biomaterialia* **2021**, *133*, 244.

[638] T. T. Smith, S. B. Stephan, H. F. Moffett, L. E. McKnight, W. Ji, D. Reiman, E. Bonagofski, M. E. Wohlfahrt, S. P. S. Pillai, M. T. Stephan, *Nature Nanotech* **2017**, *12*, 813.

[639] J. Liu, Q. Liu, X. Zhang, M. Cui, T. Li, Y. Zhang, Q. Liao, *Cancer Cell International* **2021**, *21*, 137.

[640] H. He, L. Liu, E. E. Morin, M. Liu, A. Schwendeman, *Acc. Chem. Res.* **2019**, *52*, 2445.

[641] Samyang Biopharmaceuticals Corporation, *Phase II Study of Weekly Genexol®-PM Plus Gemcitabine in Subjects With Recurrent and Metastatic Adenocarcinoma of the Pancreas*, Clinicaltrials.Gov, **2018**.

[642] "Combination Therapy With NC-6004 and Gemcitabine Versus Gemcitabine Alone in Pancreatic Cancer - No Study Results Posted - ClinicalTrials.gov," can be found under https://clinicaltrials.gov/ct2/show/results/NCT02043288, **n.d.**

[643] Silence Therapeutics GmbH, *A PHASE Ib/IIa STUDY OF COMBINATION THERAPY WITH GEMCITABINE AND ATU027 IN SUBJECTS WITH LOCALLY ADVANCED OR METASTATIC PANCREATIC ADENOCARCINOMA*, Clinicaltrials.Gov, **2016**.

[644] J. L. MD, *Nano-SMART: An Adaptive Phase I-II Trial of AGuIX Gadolinium-Based Nanoparticles With Stereotactic Magnetic Resonance-Guided Adaptive Radiation Therapy for Centrally Located Lung Tumors and Locally Advanced Unresectable Pancreatic Ductal Adenocarcinoma*, Clinicaltrials.Gov, **2021**.

[645] M.D. Anderson Cancer Center, *Phase I Study of NBTXR3 Activated by Radiotherapy for Locally Advanced or Borderline Resectable Pancreatic Ductal Adenocarcinoma*, Clinicaltrials.Gov, **2020**.

[646] E. Tomás-Bort, M. Kieler, S. Sharma, J. B. Candido, D. Loessner, *Theranostics* **2020**, *10*, 5074.

[647] J. Drost, H. Clevers, *Nat Rev Cancer* **2018**, *18*, 407.

[648] K. Kretzschmar, *J Mol Med (Berl)* **2021**, *99*, 501.

[649] S. F. Boj, C.-I. Hwang, L. A. Baker, I. I. C. Chio, D. D. Engle, V. Corbo, M. Jager, M. Ponz-Sarvise, H. Tiriac, M. S. Spector, A. Gracanin, T. Oni, K. H. Yu, R. van Boxtel, M. Huch, K. D. Rivera, J. P. Wilson, M. E. Feigin, D. Öhlund, A. Handly-Santana, C. M. Ardito-Abraham, M. Ludwig, E. Elyada, B. Alagesan, G. Biffi, G. N. Yordanov, B. Delcuze, B. Creighton, K. Wright, Y. Park, F. H. M. Morsink, I. Q. Molenaar, I. H. Borel Rinkes, E. Cuppen, Y. Hao, Y. Jin, I. J. Nijman, C. Iacobuzio-Donahue, S. D. Leach, D. J. Pappin, M. Hammell, D. S. Klimstra, O. Basturk, R. H. Hruban, G. J. Offerhaus, R. G. J. Vries, H. Clevers, D. A. Tuveson, *Cell* **2015**, *160*, 324.

[650] L. Huang, A. Holtzinger, I. Jagan, M. BeGora, I. Lohse, N. Ngai, C. Nostro, R. Wang, L. B. Muthuswamy, H. C. Crawford, C. Arrowsmith, S. E. Kalloger, D. J. Renouf, A. A. Connor, S. Cleary, D. F. Schaeffer, M. Roehrl, M.-S. Tsao, S. Gallinger, G. Keller, S. K. Muthuswamy, *Nat Med* **2015**, *21*, 1364.

[651] K. Y. Aguilera, D. W. Dawson, *Frontiers in Cell and Developmental Biology* **2021**, *9*.

[652] T. Seino, S. Kawasaki, M. Shimokawa, H. Tamagawa, K. Toshimitsu, M. Fujii, Y. Ohta, M. Matano, K. Nanki, K. Kawasaki, S. Takahashi, S. Sugimoto, E. Iwasaki, J. Takagi, T. Itoi, M. Kitago, Y. Kitagawa, T. Kanai, T. Sato, *Cell Stem Cell* **2018**, *22*, 454.

[653] H. Tiriac, P. Belleau, D. D. Engle, D. Plenker, A. Deschênes, T. D. D. Somerville, F. E. M. Froeling, R. A. Burkhart, R. E. Denroche, G.-H. Jang, K. Miyabayashi, C. M. Young, H. Patel, M. Ma, J. F. LaComb, R. L. D. Palmaira, A. A. Javed, J. C. Huynh, M. Johnson, K. Arora, N. Robine, M. Shah, R. Sanghvi, A. B. Goetz, C. Y. Lowder, L. Martello, E. Driehuis, N. LeComte, G. Askan, C. A. Iacobuzio-Donahue, H. Clevers, L. D. Wood, R. H. Hruban, E. Thompson, A. J. Aguirre, B. M. Wolpin, A. Sasson, J. Kim, M. Wu, J. C. Bucobo, P. Allen, D. V. Sejpal, W. Nealon, J. D. Sullivan, J. M. Winter, P. A. Gimotty, J. L. Grem, D. J. DiMaio, J. M. Buscaglia, P. M. Grandgenett, J. R. Brody, M. A. Hollingsworth, G. M. O'Kane, F. Notta, E. Kim, J. M. Crawford, C. Devoe, A. Ocean, C. L. Wolfgang, K. H. Yu, E. Li, C. R. Vakoc, B. Hubert, S. E. Fischer, J. M. Wilson, R. Moffitt, J. Knox, A. Krasnitz, S. Gallinger, D. A. Tuveson, *Cancer Discovery* **2018**, *8*, 1112.

[654] E. Driehuis, A. van Hoeck, K. Moore, S. Kolders, H. E. Francies, M. C. Gulersonmez, E. C. A. Stigter, B. Burgering, V. Geurts, A. Gracanin, G. Bounova, F. H. Morsink, R. Vries, S. Boj, J. van Es, G. J. A. Offerhaus, O. Kranenburg, M. J. Garnett, L. Wessels, E. Cuppen, L. A. A. Brosens, H. Clevers, *PNAS* **2019**, *116*, 26580.

[655] L. Moreira, B. Bakir, P. Chatterji, Z. Dantes, M. Reichert, A. K. Rustgi, *Cellular and Molecular Gastroenterology and Hepatology* **2018**, *5*, 289.

[656] S. Tsai, L. McOlash, K. Palen, B. Johnson, C. Duris, Q. Yang, M. B. Dwinell, B. Hunt, D. B. Evans, J. Gershan, M. A. James, *BMC Cancer* **2018**, *18*, 335.

[657] M. Swayden, P. Soubeyran, J. Iovanna, *Frontiers in Oncology* **2020**, *9*.

[658] M. J. Ware, K. Colbert, V. Keshishian, J. Ho, S. J. Corr, S. A. Curley, B. Godin, *Tissue Eng Part C Methods* **2016**, *22*, 312.

[659] A. M. Bejoy, K. N. Makkithaya, B. B. Hunakunti, A. Hegde, K. Krishnamurthy, A. Sarkar, C. F. Lobo, D. V. S. Keshav, D. G, D. D. S, S. Mascarenhas, S. Chakrabarti, S. R. R. D. Kalepu, B. Paul, N. Mazumder, *Bioprinting* **2021**, *24*, e00176.

[660] P. Datta, M. Dey, Z. Ataie, D. Unutmaz, I. T. Ozbolat, *npj Precis. Onc.* **2020**, *4*, 1.

[661] R. Augustine, S. N. Kalva, R. Ahmad, A. A. Zahid, S. Hasan, A. Nayeem, L. McClements, A. Hasan, *Translational Oncology* **2021**, *14*, 101015.

[662] S. Hou, H. Tiriac, B. P. Sridharan, L. Scampavia, F. Madoux, J. Seldin, G. R. Souza, D. Watson, D. Tuveson, T. P. Spicer, *SLAS DISCOVERY: Advancing the Science of Drug Discovery* **2018**, *23*, 574.

[663] E. M. Langer, B. L. Allen-Petersen, S. M. King, N. D. Kendsersky, M. A. Turnidge, G. M. Kuziel, R. Riggers, R. Samatham, T. S. Amery, S. L. Jacques, B. C. Sheppard, J. E. Korkola, J. L. Muschler, G. Thibault, Y. H. Chang, J. W. Gray, S. C. Presnell, D. G. Nguyen, R. C. Sears, *Cell Rep* **2019**, *26*, 608.

[664] D. Hakobyan, C. Médina, N. Dusserre, M.-L. Stachowicz, C. Handschin, J.-C. Fricain, J. Guillermet-Guibert, H. Oliveira, *Biofabrication* **2020**, *12*, 035001.

[665] K. Unnikrishnan, L. V. Thomas, R. M. Ram Kumar, *Frontiers in Oncology* **2021**, *11*.

[666] C. Ricci, C. Mota, S. Moscato, D. D'Alessandro, S. Ugel, S. Sartoris, V. Bronte, U. Boggi, D. Campani, N. Funel, L. Moroni, S. Danti, *Biomatter* **2014**, *4*, e955386.

[667] S. Totti, M. C. Allenby, S. B. D. Santos, A. Mantalaris, E. G. Velliou, *RSC Adv.* **2018**, *8*, 20928.

[668] P. Gupta, P. A. Pérez-Mancera, H. Kocher, A. Nisbet, G. Schettino, E. G. Velliou, *Front Bioeng Biotechnol* **2020**, *8*, 290.

[669] M. R. Haque, T. H. Rempert, T. A. Al-Hilal, C. Wang, A. Bhushan, F. Bishehsari, *Cancers* **2021**, *13*, 4487.

[670] C. R. Drifka, K. W. Eliceiri, S. M. Weber, W. J. Kao, *Lab Chip* **2013**, *13*, 3965.

[671] M. Beer, N. Kuppalu, M. Stefanini, H. Becker, I. Schulz, S. Manoli, J. Schuette, C. Schmees, A. Casazza, M. Stelzle, A. Arcangeli, *Sci Rep* **2017**, *7*, 1325.

[672] D.-H. T. Nguyen, E. Lee, S. Alimperti, R. J. Norgard, A. Wong, J. J.-K. Lee, J. Eyckmans, B. Z. Stanger, C. S. Chen, *Science Advances* **2019**, *5*, eaav6789.

[673] M. J. Bradney, S. M. Venis, Y. Yang, S. F. Konieczny, B. Han, *Small* **2020**, *16*, 1905500.

[674] B. F. L. Lai, R. X. Z. Lu, Y. Hu, L. Davenport Huyer, W. Dou, E. Y. Wang, N. Radulovich, M. S. Tsao, Y. Sun, M. Radisic, *Advanced Functional Materials* **2020**, *30*, 2000545.

[675] S. A. Moosavian, V. Bianconi, M. Pirro, A. Sahebkar, *Seminars in Cancer Biology* **2021**, *69*, 337.

[676] N. M. Percivalle, M. Carofiglio, M. Conte, G. Rosso, A. Bentivogli, G. Mesiano, V. Vighetto, V. Cauda, *International Journal of Molecular Sciences* **2022**, *23*, 15815.

[677] *Nat Rev Mater* **2021**, *6*, 1071.

[678] R. Verbeke, I. Lentacker, S. C. De Smedt, H. Dewitte, *Journal of Controlled Release* **2021**, *333*, 511.

[679] M. Kim, M. Jeong, S. Hur, Y. Cho, J. Park, H. Jung, Y. Seo, H. A. Woo, K. T. Nam, K. Lee, H. Lee, *Sci Adv* **2021**, *7*, eabf4398.

[680] A. B. Vogel, I. Kanevsky, Y. Che, K. A. Swanson, A. Muik, M. Vormehr, L. M. Kranz, K. C. Walzer, S. Hein, A. Güler, J. Loschko, M. S. Maddur, A. Ota-Setlik, K. Tompkins, J. Cole, B. G. Lui, T. Ziegenhals, A. Plaschke, D. Eisel, S. C. Dany, S. Fesser, S. Erbar, F. Bates, D. Schneider, B. Jesionek, B. Sänger, A.-K. Wallisch, Y. Feuchter, H. Junginger, S. A. Krumm, A. P. Heinen, P. Adams-Quack, J. Schlereth, S. Schille, C. Kröner, R. de la Caridad Güimil Garcia, T. Hiller, L. Fischer, R. S. Sellers, S. Choudhary, O. Gonzalez, F. Vascotto, M. R. Gutman, J. A. Fontenot, S. Hall-Ursone, K. Brasky, M. C. Griffor, S. Han, A. A. H. Su, J. A. Lees, N. L. Nedoma, E. H. Mashalidis, P. V. Sahasrabudhe, C. Y. Tan, D. Pavliakova, G. Singh, C. Fontes-Garfias, M. Pride, I. L. Scully, T. Ciolino, J. Obregon, M. Gazi, R. Carrion, K. J. Alfson, W. V. Kalina, D. Kaushal, P.-Y. Shi, T. Klamp, C.

Rosenbaum, A. N. Kuhn, Ö. Türeci, P. R. Dormitzer, K. U. Jansen, U. Sahin, *Nature* **2021**, *592*, 283.

[681] P. R. Krause, M. F. Gruber, *New England Journal of Medicine* **2020**, *383*, e107.

[682] E. J. Sayers, S. E. Peel, A. Schantz, R. M. England, M. Beano, S. M. Bates, A. S. Desai, S. Puri, M. B. Ashford, A. T. Jones, *Molecular Therapy* **2019**, *27*, 1950.

[683] A. Thess, S. Grund, B. L. Mui, M. J. Hope, P. Baumhof, M. Fotin-Mleczek, T. Schlake, *Molecular Therapy* **2015**, *23*, 1456.

[684] K. J. Hassett, K. E. Benenato, E. Jacquinet, A. Lee, A. Woods, O. Yuzhakov, S. Himansu, J. Deterling, B. M. Geilich, T. Ketova, C. Mihai, A. Lynn, I. McFadyen, M. J. Moore, J. J. Senn, M. G. Stanton, Ö. Almarsson, G. Ciaramella, L. A. Brito, *Molecular Therapy - Nucleic Acids* **2019**, *15*, 1.

[685] N. Pardi, M. J. Hogan, R. S. Pelc, H. Muramatsu, H. Andersen, C. R. DeMaso, K. A. Dowd, L. L. Sutherland, R. M. Scearce, R. Parks, W. Wagner, A. Granados, J. Greenhouse, M. Walker, E. Willis, J.-S. Yu, C. E. McGee, G. D. Sempowski, B. L. Mui, Y. K. Tam, Y.-J. Huang, D. Vanlandingham, V. M. Holmes, H. Balachandran, S. Sahu, M. Lifton, S. Higgs, S. E. Hensley, T. D. Madden, M. J. Hope, K. Karikó, S. Santra, B. S. Graham, M. G. Lewis, T. C. Pierson, B. F. Haynes, D. Weissman, *Nature* **2017**, *543*, 248.

[686] E. J. Anderson, N. G. Rouphael, A. T. Widge, L. A. Jackson, P. C. Roberts, M. Makhene, J. D. Chappell, M. R. Denison, L. J. Stevens, A. J. Pruijssers, A. B. McDermott, B. Flach, B. C. Lin, N. A. Doria-Rose, S. O'Dell, S. D. Schmidt, K. S. Corbett, P. A. Swanson, M. Padilla, K. M. Neuzil, H. Bennett, B. Leav, M. Makowski, J. Albert, K. Cross, V. V. Edara, K. Floyd, M. S. Suthar, D. R. Martinez, R. Baric, W. Buchanan, C. J. Luke, V. K. Phadke, C. A. Rostad, J. E. Ledgerwood, B. S. Graham, J. H. Beigel, *N Engl J Med* **2020**, *383*, 2427.

[687] **N.d.**

[688] **N.d.**

[689] J. A. Kulkarni, M. M. Darjuan, J. E. Mercer, S. Chen, R. van der Meel, J. L. Thewalt, Y. Y. C. Tam, P. R. Cullis, *ACS Nano* **2018**, *12*, 4787.

[690] L. Schoenmaker, D. Witzigmann, J. A. Kulkarni, R. Verbeke, G. Kersten, W. Jiskoot, D. J. A. Crommelin, *International Journal of Pharmaceutics* **2021**, *601*, 120586.

[691] L. A. Brito, M. Chan, C. A. Shaw, A. Hekele, T. Carsillo, M. Schaefer, J. Archer, A. Seubert, G. R. Otten, C. W. Beard, A. K. Dey, A. Lilja, N. M. Valiante, P. W. Mason, C. W. Mandl, S. W. Barnett, P. R. Dormitzer, J. B.

Ulmer, M. Singh, D. T. O'Hagan, A. J. Geall, *Molecular Therapy* **2014**, *22*, 2118.

[692] J. H. Erasmus, A. P. Khandhar, J. Guderian, B. Granger, J. Archer, M. Archer, E. Gage, J. Fuerte-Stone, E. Larson, S. Lin, R. Kramer, R. N. Coler, C. B. Fox, D. T. Stinchcomb, S. G. Reed, N. Van Hoeven, *Molecular Therapy* **2018**, *26*, 2507.

[693] J. C. Kaczmarek, A. K. Patel, K. J. Kauffman, O. S. Fenton, M. J. Webber, M. W. Heartlein, F. DeRosa, D. G. Anderson, *Angew Chem Int Ed Engl* **2016**, *55*, 13808.

[694] L. Van Hoecke, R. Verbeke, D. De Vlieger, H. Dewitte, K. Roose, S. Van Nevel, O. Krysko, C. Bachert, B. Schepens, I. Lentacker, X. Saelens, *Molecular Therapy - Nucleic Acids* **2020**, *20*, 777.

[695] A. Luchini, G. Vitiello, *Frontiers in Chemistry* **2019**, *7*.

[696] **N.d.**

[697] H. Meng, M. Wang, H. Liu, X. Liu, A. Situ, B. Wu, Z. Ji, C. H. Chang, A. E. Nel, *ACS Nano* **2015**, *9*, 3540.

[698] P. N. Durfee, Y.-S. Lin, D. R. Dunphy, A. J. Muñiz, K. S. Butler, K. R. Humphrey, A. J. Lokke, J. O. Agola, S. S. Chou, I.-M. Chen, W. Wharton, J. L. Townson, C. L. Willman, C. J. Brinker, *ACS Nano* **2016**, *10*, 8325.

[699] B. Dumontel, M. Canta, H. Engelke, A. Chiodoni, L. Racca, A. Ancona, T. Limongi, G. Canavese, V. Cauda, *J. Mater. Chem. B* **2017**, *5*, 8799.

[700] D. Cao, X. Shu, D. Zhu, S. Liang, M. Hasan, S. Gong, *Nano Convergence* **2020**, *7*, 14.

[701] K. S. Butler, P. N. Durfee, C. Theron, C. E. Ashley, E. C. Carnes, C. J. Brinker, *Small* **2016**, *12*, 2173.

[702] M. Carofiglio, M. Laurenti, V. Vighetto, L. Racca, S. Barui, N. Garino, R. Gerbaldo, F. Laviano, V. Cauda, *Nanomaterials* **2021**, *11*, 2628.

[703] S. Barui, N. M. Percivalle, M. Conte, B. Dumontel, L. Racca, M. Carofiglio, V. Cauda, *Development of doped ZnO-based biomimicking and tumor targeted nanotheranostics to improve pancreatic cancer treatment* **2022**.

[704] R. Tavano, D. Segat, E. Reddi, J. Kos, M. Rojnik, P. Kocbek, S. Iratni, D. Scheglmann, M. Colucci, I. M. R. Echevarria, F. Selvestrel, F. Mancin, E. Papini, *Nanomedicine (Lond)* **2010**, *5*, 881.

[705] L. Bircher, O. M. Theusinger, S. Locher, P. Eugster, B. Roth-Z'graggen, C. M. Schumacher, J.-D. Studt, W. J. Stark, B. Beck-Schimmer, I. K. Herrmann, *J. Mater. Chem. B* **2014**, *2*, 3753.

[706] C. Santos, S. Turiel, P. Sousa Gomes, E. Costa, A. Santos-Silva, P. Quadros, J. Duarte, S. Battistuzzo, M. H. Fernandes, *Journal of Nanobiotechnology* **2018**, *16*, 27.

[707] V. Cauda, T. T. Xu, I. Nunes, E. Mereu, S. Villata, E. Bergaggio, M. Labrador, T. Limongi, F. Susa, A. Chiodoni, M. Cumerlato, G. Rosso, R. Stefania, R. Piva, *Microporous and Mesoporous Materials* **2021**, *325*, 111320.

[708] S. G. M. Ong, M. Chitneni, K. S. Lee, L. C. Ming, K. H. Yuen, *Pharmaceutics* **2016**, *8*, 36.

[709] S. R. Tabaei, J. A. Jackman, S.-O. Kim, V. P. Zhdanov, N.-J. Cho, *Langmuir* **2015**, *31*, 3125.

[710] A. O. Hohner, M. P. C. David, J. O. Rädler, *Biointerphases* **2010**, *5*, 1.

[711] J. A. Jackman, S. R. Tabaei, Z. Zhao, S. Yorulmaz, N.-J. Cho, *ACS Appl. Mater. Interfaces* **2015**, *7*, 959.

[712] H. Xu, H. Tae, N.-J. Cho, C. Huang, K. J. Hsia, *Micromachines (Basel)* **2022**, *13*, 134.

[713] D. J. Pochapski, C. Carvalho dos Santos, G. W. Leite, S. H. Pulcinelli, C. V. Santilli, *Langmuir* **2021**, *37*, 13379.

[714] Y. Zhang, Y. Chen, P. Westerhoff, K. Hristovski, J. C. Crittenden, *Water Research* **2008**, *42*, 2204.

[715] M. Weber, H. Steinle, S. Golombek, L. Hann, C. Schlensak, H. P. Wendel, M. Avci-Adali, *Frontiers in Bioengineering and Biotechnology* **2018**, *6*.

[716] L. Chen, J. J. Glass, R. De Rose, C. Sperling, S. J. Kent, Z. H. Houston, N. L. Fletcher, B. E. Rolfe, K. J. Thurecht, *ACS Appl. Bio Mater.* **2018**, *1*, 756.

[717] K. M. de la Harpe, P. P. D. Kondiah, Y. E. Choonara, T. Marimuthu, L. C. du Toit, V. Pillay, *Cells* **2019**, *8*, 1209.

[718] F. Barbero, L. Russo, M. Vitali, J. Piella, I. Salvo, M. L. Borrajo, M. Busquets-Fité, R. Grandori, N. G. Bastús, E. Casals, V. Puntes, *Semin Immunol* **2017**, *34*, 52.

[719] M. P. Nikolova, M. S. Chavali, *Biomimetics* **2020**, *5*, 27.

[720] Y. Yan, H. Ding, *Nanomaterials* **2020**, *10*, 1613.

[721] M. Canta, V. Cauda, *Biomater Sci* **2020**, *8*, 6157.

[722] L. Racca, M. Canta, B. Dumontel, A. Ancona, T. Limongi, N. Garino, M. Laurenti, G. Canavese, V. Cauda, **2018**.

[723] T. Xia, Y. Zhao, T. Sager, S. George, S. Pokhrel, N. Li, D. Schoenfeld, H. Meng, S. Lin, X. Wang, M. Wang, Z. Ji, J. I. Zink, L. Mädler, V. Castranova, S. Lin, A. E. Nel, *ACS Nano* **2011**, *5*, 1223.

[724] M. Carofiglio, S. Barui, V. Cauda, M. Laurenti, *Applied Sciences* **2020**, *10*, 5194.

[725] M. Muller, V. Haghnejad, M. Schaefer, G. Gauchotte, B. Caron, L. Peyrin-Biroulet, J.-P. Bronowicki, C. Neuzillet, A. Lopez, *Cancers* **2022**, *14*, 995.

[726] M. Geyer, L.-M. Gaul, S. L. D`Agosto, V. Corbo, K. Queiroz, *Front. Immunol.* **2023**, *14*, DOI 10.3389/fimmu.2023.1155085.

[727] M. Conte, V. Cauda, *Advanced Therapeutics* **n.d.**, 2200079.

[728] W.-P. Li, C.-J. Yen, B.-S. Wu, T.-W. Wong, *Biomedicines* **2021**, *9*, 69.

[729] Y. Wang, H. Wang, L. Zhou, J. Lu, B. Jiang, C. Liu, J. Guo, *Photodiagnosis and Photodynamic Therapy* **2020**, *31*, 101876.

[730] S. Siva, M. P. MacManus, R. F. Martin, O. A. Martin, *Cancer Lett* **2015**, *356*, 82.

[731] Y. Hu, C. Chi, S. Wang, L. Wang, P. Liang, F. Liu, W. Shang, W. Wang, F. Zhang, S. Li, H. Shen, X. Yu, H. Liu, J. Tian, *Advanced Materials* **2017**, *29*, 1700448.

[732] Y. Yang, J. Huang, M. Liu, Y. Qiu, Q. Chen, T. Zhao, Z. Xiao, Y. Yang, Y. Jiang, Q. Huang, K. Ai, *Advanced Science* **2023**, *10*, 2204365.

[733] T. Wang, W. Peng, M. Du, Z. Chen, *Front Oncol* **2023**, *13*, 1167105.

[734] X. Liu, X. Pan, C. Wang, H. Liu, *Particuology* **2023**, *75*, 199.

[735] V. Vighetto, E. Pascucci, G. Savino, G. Rosso, N. M. Percivalle, M. Conte, B. Dumontel, A. Balboni, G. Mesiano, A. Masoero, V. Cauda, *Advanced Therapeutics* **n.d.**, *n/a*, 2400161.

[736] S. Wang, Z. Hu, X. Wang, C. Gu, Z. Gao, W. Cao, J. Zheng, *Ultrasound in Medicine and Biology* **2014**, *40*, 2125.

[737] C.-Y. Lin, H.-C. Tseng, H.-R. Shiu, M.-F. Wu, C.-Y. Chou, W.-L. Lin, *International Journal of Nanomedicine* **2012**, *7*, 2143.

[738] J. Chen, H. Luo, Y. Liu, W. Zhang, H. Li, T. Luo, K. Zhang, Y. Zhao, J. Liu, *ACS Nano* **2017**, *11*, 12849.

[739] M. Xu, P. Wang, S. Sun, L. Gao, L. Sun, L. Zhang, J. Zhang, S. Wang, X. Liang, *Nanoscale* **2020**, *12*, 21519.

[740] B. Huang, S. Chen, W. Pei, Y. Xu, Z. Jiang, C. Niu, L. Wang, *Front. Chem.* **2020**, *8*, DOI 10.3389/fchem.2020.00358.

[741] D. Cheng, X. Wang, X. Zhou, J. Li, *Front Bioeng Biotechnol* **2021**, *9*, 761218.

[742] S. George, S. Pokhrel, T. Xia, B. Gilbert, Z. Ji, M. Schowalter, A. Rosenauer, R. Damoiseaux, K. A. Bradley, L. Mädler, A. E. Nel, *ACS Nano* **2010**, *4*, 15.

[743] M. Conte, M. Carofiglio, G. Rosso, V. Cauda, *Nanomaterials* **2023**, *13*, 2250.

[744] C. Zhang, S. Wang, J. Xiao, X. Tan, Y. Zhu, Y. Su, T. Cheng, C. Shi, *Biomaterials* **2010**, *31*, 1911.

[745] C. Zhang, T. Liu, Y. Su, S. Luo, Y. Zhu, X. Tan, S. Fan, L. Zhang, Y. Zhou, T. Cheng, C. Shi, *Biomaterials* **2010**, *31*, 6612.

[746] E. Zhang, S. Luo, X. Tan, C. Shi, *Biomaterials* **2014**, *35*, 771.

[747] Y. Liu, Y. Wang, W. Zhen, Y. Wang, S. Zhang, Y. Zhao, S. Song, Z. Wu, H. Zhang, *Biomaterials* **2020**, *251*, 120075.

[748] Q. Sun, B. Zhang, Q. Hu, Y. Qin, W. Xu, W. Liu, X. Yu, J. Xu, *Theranostics* **2018**, *8*, 5072.

[749] C. Y. X. Chua, J. Ho, S. Demaria, M. Ferrari, A. Grattoni, *Adv Ther (Weinh)* **2020**, *3*, 2000027.

[750] M. Carofiglio, M. Conte, L. Racca, V. Cauda, *ACS Appl. Nano Mater.* **2022**, *5*, 17212.

[751] L. Racca, G. Rosso, M. Carofiglio, S. Fagoonee, G. Mesiano, F. Altruda, V. Cauda, *Cancer Nanotechnology* **2023**, *14*, 37.

[752] V. Vighetto, M. Conte, G. Rosso, M. Carofiglio, F. Sidoti Abate, L. Racca, G. Mesiano, V. Cauda, *Discover Nano* **2024**, *19*, 28.

[753] F. Giordano, S. Lenna, G. Baudo, R. Rampado, M. Massaro, E. De Rosa, A. Ewing, L. Kurenbekova, M. Agostini, J. T. Yustein, F. Taraballi, *Cancer Nano* **2022**, *13*, 40.

[754] Y. Liu, D. Yu, X. Ge, L. Huang, P.-Y. Pan, H. Shen, R. I. Pettigrew, S.-H. Chen, J. Mai, *Biomaterials* **2025**, *314*, 122835.

[755] M. Miquel, S. Zhang, C. Pilarsky, *Front. Cell Dev. Biol.* **2021**, *9*, DOI 10.3389/fcell.2021.748631.

[756] D. P. Ferrari, F. Ramos-Gomes, F. Alves, M. A. Markus, *Sci Rep* **2024**, *14*, 13602.

[757] A. N. Ariston Gabriel, Q. Jiao, U. Yvette, X. Yang, S. A. Al-Ameri, L. Du, Y. Wang, C. Wang, *Pancreatology* **2020**, *20*, 79.

[758] N. Mathuria, A. L. R. Royal, J. Enterría-Rosales, Y. Carcamo-Bahena, R. Terracciano, A. Dave, M. Valderrabano, C. S. Filgueira, *Heart Rhythm* **2022**, *19*, 1550.

[759] R. Terracciano, A. Zhang, E. B. Butler, D. Demarchi, J. H. Hafner, A. Grattoni, C. S. Filgueira, *Pharmaceutics* **2021**, *13*, 216.

[760] R. Podgórski, M. Wojasiński, T. Ciach, *Sci Rep* **2022**, *12*, 9047.

[761] F. L. Tansi, R. Rüger, M. Rabenhold, F. Steiniger, A. Fahr, W. A. Kaiser, I. Hilger, *Small* **2013**, *9*, 3659.

[762] Y. Xiao, T. Qin, L. Sun, W. Qian, J. Li, W. Duan, J. Lei, Z. Wang, J. Ma, X. Li, Q. Ma, Q. Xu, *Cell Transplant* **2020**, *29*, 0963689720929987.

[763] X. Cao, S. Zhu, G. Luo, G. Huang, *Asian Journal of Surgery* **2021**, *44*, 421.

[764] E. Vernucci, J. Abrego, V. Gunda, S. K. Shukla, A. Dasgupta, V. Rai, N. Chaika, K. Buettner, A. Illies, F. Yu, A. J. Lazenby, B. J. Swanson, P. K. Singh, *Cancers* **2020**, *12*, 2.

[765] C. M. Neophytou, C. Pierides, M.-I. Christodoulou, P. Costeas, T.-C. Kyriakou, P. Papageorgis, *Front. Oncol.* **2020**, *10*, DOI 10.3389/fonc.2020.00899.

[766] H.-Y. Tan, N. Wang, S. Li, M. Hong, X. Wang, Y. Feng, *Oxid Med Cell Longev* **2016**, *2016*, 2795090.

[767] A. Kotsafti, M. Scarpa, I. Castagliuolo, M. Scarpa, *Cancers (Basel)* **2020**, *12*, 1748.

Appendix A

List of publications

Conte, M., Cauda, V., **Multimodal Therapies against Pancreatic Ductal Adenocarcinoma: A Review on Synergistic Approaches toward Ultimate Nanomedicine Treatments**. Adv. Therap. 2022, 2200079. https://doi.org/10.1002/adtp.202200079. Review Article.

Barui S., Percivalle N. M., **Conte M.**, Dumontel B., Racca L., Carofiglio M. and Cauda V., **Development of doped ZnO-based biomimicking and tumor-targeted nanotheranostics to improve pancreatic cancer treatment**. Cancer Nanotechnology (2022) 13:37. https://doi.org/10.1186/s12645-022-00140-z. Research Article

Carofiglio M., **Conte M.**, Racca L. and Cauda V., **Synergistic Phenomena between Iron-Doped ZnO Nanoparticles and Shock Waves Exploited against Pancreatic Cancer Cells**. *ACS Appl. Nano Mater 2022, 5, 11, 17212–17225.* https://doi.org/10.1021/acsanm.2c04211. Research Article

Percivalle, N.M.; Carofiglio, M.; **Conte, M.**; Rosso, G.; Bentivogli, A.; Mesiano, G.; Vighetto, V.; Cauda, V. **Artificial and Naturally Derived Phospholipidic Bilayers as Smart Coatings of Solid-State Nanoparticles: Current Works and Perspectives in Cancer Thera**py. Int. J. Mol. Sci. 2022, 23, 15815. https://doi.org/10.3390/ijms232415815. Review Article

Barui, S., **Conte, M.**, Percivalle, N. M., Montero, R. M. G., Racca, L., Allione, M., Cauda, V., **Dual Drug Loaded Nanotheranostic Platforms as a Novel Synergistic Approach to Improve Pancreatic Cancer Treatment**. *Part. Part. Syst. Charact.* 2023, 40, 2200138. https://doi.org/10.1002/ppsc.202200138. Research Article

Conte, M.; Carofiglio, M.; Rosso, G.; Cauda, V., **Lipidic Formulations Inspired by COVID Vaccines as Smart Coatings to Enhance Nanoparticle-Based Cancer Therapy**. Nanomaterials 2023, 13, 2250. https://doi.org/10.3390/nano13152250. Research Article

Vighetto V, **Conte M**, Rosso G, Carofiglio M, Sidoti Abate F, Racca L, Mesiano G, Cauda V. **Anti-CD38 targeted nanotrojan horses stimulated by acoustic waves as therapeutic nanotools selectively against Burkitt's lymphoma cells**. Discov Nano. 2024 Feb 14;19(1):28. https://doi.org/10.1186/s11671-024-03976-z Research Article

Hsuan-Chen Liu, H., Di Trani, N., **Conte, M.**, Nguyen, D.C., Jokonya, S., Wu, A., Vander Pol, R., Joubert, A, Facchi, I., Wood A., Ho, J., Pesaresi, F., Cauda, V., Chen, S., Liu, X., Stayton, P., Chua C.Y.X., Grattoni, A., **Nanofluidic delivery implant sustains localization and maximizes efficacy of intratumoral immunotherapy**, Nano Today, Volume 56, 2024, 102258, https://doi.org/10.1016/j.nantod.2024.102258. Research Article

Vighetto, V., Pascucci, E., Savino, G., Rosso, G., Percivalle, N.M., **Conte, M.**, Dumontel, B., Balboni, A., Mesiano, G., Masoero, A., Cauda, V., **The multifunctional Purposes of Ultrasound in 3D models**. Adv. Therap. 2400161. https://doi.org/10.1002/adtp.202400161. Review Article.

Carofiglio, M., Mesiano, G., Rosso, G., **Conte, M.**, Zuccheri, M., Pignochino, Y., Cauda, V., **Targeted lipid-coated ZnO nanoparticles coupled with ultrasound: A sonodynamic approach for the treatment of osteosarcoma as 3D spheroid models**. Materials Today Communications, Volume 40, August 2024, 109826. https://doi.org/10.1016/j.mtcomm.2024.109826. Research Article

Rosso, G., Mesiano, G., Dumontel, B., Carofiglio, M., **Conte, M.**, Grattoni, A., Cauda, V., **Acoustic waves and smart biomimetic nanoparticles: combination treatment from 2D to 3D colorectal cancer models**. Cancer Nanotechnology 15, 42 (2024). https://doi.org/10.1186/s12645-024-00281-3. Research Article

Conte, M., Carofiglio, M., Vander Pol, R., Wood, A., Hernandez, N., Joubert, A., Cauda, V., Grattoni A. **Acoustically-driven Zinc Oxide Nanoparticles for In Vivo Pancreatic Cancer Treatment**. ACS Applied Materials & Interfaces, 2025. https://doi.org/10.1021/acsami.4c21975. Research Article

Abroad Experience

December 2022 - April 2024: Research conducted at the **Houston Methodist Research Institute**, Department of Nanomedicine, GrattoniLab, Houston, Texas.

Attended conferences and symposia, awards

Elevator Pitch Workshop Series and Competition. June 14, 2023. Houston, TX. **First Place Presentation**.

MAPTA 2023 Summer Science Symposium. August 3-4, 2023. Houston, TX. **Oral presentation**: **Conte, M.**, Carofiglio, M., Vander Pol, R., Wood, A., Hernandez, N., Joubert, A., Cauda, V., Grattoni A. Ultrasound-stimulated Zinc Oxide Nanoconstructs as a Novel Pancreatic Cancer Treatment. **Second Place Presentation.**

MIRABILIS (MIraculous RAnge of Beauty ILlustrations In Science) **scientific image contest**. Consulate General of Italy in Houston. November 1st, 2023. **Second Place.**

Nanomedicine 2023 Symposium. November 15, 2023. Houston, TX. **Oral presentation**: **Conte, M.**, Carofiglio, M., Vander Pol, R., Wood, A., Hernandez, N., Joubert A., Chua, C.Y.X., Cauda, V., Grattoni A. Ultrasound-stimulated Zinc Oxide Nanoconstructs as a Novel Pancreatic Cancer Treatment.

MD Anderson 2023 Leading Edge of Cancer Research Symposium. November 16, 2023. Houston, TX. **Poster presentation**: **Conte, M.**, Carofiglio, M., Vander Pol, R., Wood, A., Hernandez, N., Joubert A., Chua, C.Y.X., Cauda, V.**,** Grattoni A. Ultrasound-stimulated Zinc Oxide Nanoconstructs as a Novel Pancreatic Cancer Treatment.

FlowTex 2024 Cytometry Conference. March 26-28, 2024. UTHealth IMM, Houston, TX.

DISAT Research Days Conference 2024, Politecnico di Torino, Torino, November 13 and 14, 2024. **Best Poster Award**.

Patents

"**Nanoparticelle rivestite e loro uso per il trasporto di agenti terapeutici e diagnostici**" Italian Patent Application N. 102023000015396 of 21th July 2023, Inventors: V. Cauda, G. Rosso, **M. Conte**, L. DeCola, M. Sancho Albero.